EXAMINATION OF A MOUSE MODEL LACKING THE ENGULFMENT RECEPTOR JEDI

By

Alexandra J. Trevisan

Dissertation

Submitted to the Faculty of the

Graduate School of Vanderbilt University

in partial fulfillment of the requirements

for the degree of

DOCTOR OF PHILOSOPHY

in

Biochemistry

May 8, 2020

Nashville, TN

Approved:

Bruce D. Carter, Ph.D.

Scott W. Hiebert, Ph.D.

John D. York, Ph.D.

Manuel Ascano, Ph.D.

Kevin P.M. Currie, Ph.D.

TABLE OF CONTENTS

LIST OF TABLES

Table Page

LIST OF FIGURES

LIST OF ABBREVIATIONS

12-HETE	12-hydroxyeicosatetraenoic acid
15-HETE	15-hydroxyeicosatetraenoic acid
AA	Arachidonic acid
ABCA1	ATP binding cassette subfamily A member 1
ADP	Adenosine diphosphate
AITC	Allyl isothiocyanate
AKT	AKT serine/threonine kinase 1 also known as protein kinase B
Ang1	Angiopoietin-1
AP	Action potential
Apaf-1	Apoptosome complex with apoptotic protease activating factor-1
APC	Antigen presenting cell
ATF3	Activating transcription factor 3
Atg7	Autophagy related 7
ATP	Adenosine TriPhosphate
ATP11A	ATPase phospholipid transporting 11A
ATP11C	ATPase phospholipid transporting 11C
BAI1	Brain specific angiogenesis inhibitor 1
BBB	Blood brain barrier
BDNF	Brain-derived neurotrophic factor
BFABP	Brain-type fatty acid-binding protein also known as FABP7
bFGF	Basic fibroblast growth factor
BH3	Bcl-3 homology

BioVU	Vanderbilt's repository of di-identified medical records linked to genotyping data
BNB	Blood nerve barrier
Brn2	Brain-2 also known as Oct7 and POU3F2
C	Celsius, degrees
C1q	Complement component C1q also known as C1q
C3/4R	Complement 3 or 4 Receptors
Ca^{2+}	Calcium ions
cAMP	Cyclic adenosine monophosphate
CAP	Capsaicin
CCL2	C-C motif chemokine ligand 2 also known as MCP-1
CED-1	Cell death abnormality protein 1
CGRP	Calcitonin gene-related peptide
CNS	Central nervous system
COPD	Chronic obstructive pulmonary disease
CpG	Cytosine-phosphate-guanine
Cre	Cre recombinase
CREB1	cAMP responsive element binding protein1
CreERT2	Cre fused to mutant estrogen ligand-binding domain
CrkII	CRK proto-oncogene adaptor protein
Cysltr2	CYSteinyl leukotriene receptor 2
DAMPs	Damage associated molecular patterns
DCC	Deleted in colorectal cancer
DHH	Desert hedgehog
DLK	Dual leucine zipper kinase
DNA	Deoxyribonucleic acid

DNAse	Deoxyribonuclease
DNGR-1	C type lectin domain containing 9A (CLEC9A)
Dock180	Dedicator of cytokines 1
DRG	Dorsal root ganglia
Dsarm	Drosophila sterile alpha/Armadillo/Toll-Interleukin receptor homology domain
ECM	Extracellular matrix
EGF	Epidermal Growth Factor
Egr-2	Early growth response 2 also known as Krox-20
ELMO	Engulfment and cell motility 1
EM	Electron microscopy
ER	Endoplasmic reticulum
erbB2/3	ERB-B2/3 receptor tyrosine kinase
ERK	Extracellular signal regulated kinase 2 also known as MAPK1
FcγR	Fcγ Receptor
FcεR1α	Fcε receptor subunit α
GABA	Gamma aminobutyric acid
GDNF	Glial cell line-derived neurotrophic factor
GEF	Guanine nucleotide exchange factor
GFAP	Glial fibrillary acidic protein
GFP	Green fluorescent protein
GLAST	Glutamate aspartate transporter
GLT1	Glutamate transporter 1
GM-CSF	Colony stimulating factor 2
GPCR	G Protein Coupled Receptor
GS	Glutamine synthetase

GTP	Guanosine triphosphate
GULP	GULP PTB domain containing engulfment adaptor 1
GWAS	Genome wide association studies
HDAC5	Histone deacetylase 5
HEK	Human embryonic kidney cells
Hiw	Highwire (Drosophila)
HIV	Human immunodeficiency virus
HMBG-1	High mobility group box 1
HTMR	High threshold mechanoreceptor
Htr1f	5-Hydroxytryptamine receptor 1F
ICAM-3	Intercellular cell adhesion molecule 3
IFNα	Interferon α
IGF-1	Insulin-like growth factor 1
IgE	Immunoglobin E
IgG	Immunoglobin G
IgM	Immunoglobin M
IgV	Immunoglobin V
IL-1α/β	Interleukin 1α or β
IL-31RA	Interleukin 31 receptor A
IL-6/10	Interleukin 6/10
IP	Immunoprecipitation
IP3R	Inositol (1,4,5) tri-phosphate receptors
ITAM	Immunoreceptor tyrosine-based activation motif
JIP3	JNK-interacting protein 3
JNK(3)	c-Jun n-terminal kinase (3)

K^+	Potassium ions
KD	Knock down
Kir4.1	Potassium inwardly rectifying channel 4.1
KO	Knock-out
KOMP	Knock-out mouse project (https://www.komp.org)
LAMP1	Lysosome-associated membrane glycoprotein 1
LC3	Autophagy related protein LC3 A
LOF	Loss of function
LPC	Lysophosphatidylcholine
LPS	Lipopolysaccharide
LRP1	LDL Receptor related Protein 1
LTMR	Low threshold mechanoreceptor
MAP3K	Mitogen activated protein kinase kinase kinase
MAPK	Mitogen activated protein kinase
MBP	Myelin basic protein
MCP-1	Monocyte chemoattractant protein-1 also known as CCL2
MEGF10-12	Multiple EGF like domains family member 10 or 12
MEK-1	Mitogen activated protein kinase kinase 1 also known as ERK activator kinase 1
MFG-E8	Milk fat globule-EGF factor 8 protein
mGluR	Metabotropic glutamate receptors
MHC-1	Major histocompatibility class 1 complex
MIP-1	Macrophage inflammatory protein-1
MKK-4	Mitogen activated protein kinase kinase 4
MMP	Matrix metalloproteases
MrgprA3/D	MAS related G-protein coupled receptor member A3/D

mRNA	Messenger RNA
mTOR	Mammalian target of rapamycin
mTorc1	Mammalian target of rapamycin complex 1
Na^+	Sodium ions
NAD^+	Nicotinamide adenine dinucleotide (reduced form)
NADH	Nicotinamide adenine dinucleotide (oxidized form)
NBF	Neutral buffered formalin
NFκB	Nuclear factor κ B subunit 1
NGF	Nerve growth factor
Nkx2.2	NK transcription factor related, locus 2
NLS	Nuclear localization signal
NMN	nicotinamide mononucleotide
Nmnat1	Nicotinamide nucleotide adenylyl transferase 1
NMDAR	N-methyl-D-aspartate receptors
NMJ	Neuromuscular junction
NO	Nitric oxide
NPPB	Natriuretic peptide B
NPY	Neuropeptide Y
Npy2R	Neuropeptide Y2 receptor
NRG	Neuregulin
NT3	Neurotrophin-3
Nts	Neurotensin
Oct6	Octamer binding protein 6 also known as POU3F1
OSMR	Oncostatin M receptor
P0	Myelin protein 0 also known as MPZ

P2X7R	Purinergic receptor P2X7
P2Y2	Purinergic receptor P2Y2
PAMPs	Pathogen associated molecular patterns
PBS	Phosphate buffered saline
PCD	Programmed cell death
PCR	Polymerase chain reaction
PD-L1	Program cell death ligand 1
PEAR1	Platelet endothelial aggregation receptor 1
PGD2	Prostaglandin D2
PGE2	Prostaglandin E2
Phr1	PAM/Highwire/Rpm-1 protein also known as MYCBP2, PAM, Highwire
PI	Propidium iodide
PKA	Protein kinase A
PKCμ	Protein kinase C μ
PLA_2	Phospholipase A2
PNS	Peripheral nervous system
PS	Phosphatidyl serine
PTEN	Phosphatase and tensin homolog
RA	Rapidly adapting
RAGE	Receptor for advanced glycoslyation end products
Rac1	Rac family small GTPase 1
Reg-2	Regenerating family member 2
RNA	Ribonucleic acid
RNAseq	RNA sequencing
ROCK1	RhO associated Coiled-coil containing protein Kinase 1

ROS	Reactive oxygen species
RPE	Retinal pigment epithelium
RT-PCR	Reverse transcriptase polymerase chain reaction
qRT-PCR	Quantitative real time polymerase chain reaction
SA	Slowly adapting
Sarm1	Sterile alpha/Armadillo/Toll-Inter-leukin receptor homology domain (Mammalian)
SCARF1	Scavenger receptor class F member 1
scRNAseq	Single cell RNA sequencing
seq	Sequencing
SGC	Satellite glial cell
SH2	Src Homology domains
SHP-1	Protein tyrosine phosphatase SHP-1
shRNA	Small hairpin RNA
siRNA	Small interfering RNA
SIRPα	Signal regulatory protein α
SLE	Systemic lupus erythematosus
SMAD	Mothers against decapentaplegic homologs
SNP	Single nucleotide polymorphisms
Sox10	SRY-Box transcription factor 10
SST	Somatostatin
STAT3	Signal transducer and activator of transcription 3
Syk	Spleen tyrosine Kinase
Tac1	Tachykinin Precursor 1
TAM	Tyro1, Axl, and Mer
TEM	Transmission electron microscopy

TGFβ	Transforming growth factor β
TH	Tyrosine hydroxylase
TIM1/3/4	T cell immunoglobin and mucin domain containing 1/3/4
TIR	Toll-interleukin receptor domain
TLR	Toll like receptors
TMEM30A	Transmembrane protein 30A also known as CDC50A
TNFα	Tumor necrosis factor α
TrkB	Tyrosine receptor kinase B
TrkC	Tyrosine receptor kinase C
TrpA1	Transient receptor potential ankyrin 1
TREM2	Triggering receptor expressed on myeloid cells 2
TrpM2/3/8	Transient receptor potential menthol 2/3/8
TrpV1	Transient receptor potential vanilloid 1
TSP-1	Thrombospondin type 1
TUNEL	Terminal deoxynucleotidyl transferase dUTP nick end labeling
Ube4b	Ubiquitination factor E4B
Unc5A-D	Uncoordinated 5A-D
UTP	Uridine triphosphate
UV	Ultraviolet
VCP	Valosin-containing protein
VEGF	Vascular endothelial growth factor
vGLUT1	Vesicular gluamate transporter
vGLUT2	Vesicular glutamate transporter 2
vGLUT3	Vesicular glutamate transporter 3
WASP	Wiskott-Aldrich Syndrome Protein

Wld^S	Wallerian degeneration slow
WT	Wild type
Xkr8	XK-Related protein 8
ZO	Zonula occludens

CHAPTER 1

INTRODUCTION

Section 1.1: The importance of the somatosensory nervous system

The term somatosensory derives from the Greek words “soma” meaning body and “sensation” meaning perception[1]. As such, the somatosensory nervous system is responsible for detecting all of our bodily senses, including proprioception (spatial awareness of one’s body in space), mechanoreception (this itself is extremely complex and includes touch sensations such as vibration, indentation, pressure, size, etc.), thermosensation, nociception (pain is multi-modal and includes noxious mechanical, thermal, and chemical stimulation), and pruriception (itch). The somatosensory nervous system innervates the skin, muscles, joints, bones, tendons, and all visceral organs. Somatosensation is essential for the survival of multicellular organisms (and, depending on your perspective, even single celled organisms), especially in relation to nociception. Pain allows us to avoid harmful stimuli that causes tissue damage – probably the best example of this are congenital abnormalities that cause pain insensitivity in humans. These patients accumulate severe life-threatening injuries, partake in self-mutilation, and have a decreased life expectancy[2–4]. While acute pain sensation clearly is advantageous for survival, the cellular and molecular (mal)adaptations that occur in chronic pain situations have dubious evolutionary benefits.

A similar argument can be made for acute versus chronic itch. For example, a mosquito carrying malaria lands on an animal and an acute itch sensation elicits a subsequent scratching behavior to remove the bug and prevent infection. Chronic pruriception, ironically one of the most common side effects of malaria treatment as well as many other disorders, occurs perpetually without a causative external stimulus. The result of both chronic pain and itch, which

collectively affects over 500 million Americans, is an extremely poor quality of life for which current treatments are either ineffective, unsuitable for long-term use, or accompanied by severe side effects including dependency/addiction/overdose[5,6].

Although chronic itch and pain are extremely important topics in human health, the importance of somatosensation goes far beyond just aversion to dangerous stimuli. For example, goal-directed motor tasks - including mobility and handling tools - requires precise proprioception and mechanoperception[7]. Regulation of blood pressure, tissue turgor, voluntary urination, and peristalsis occurs through mechanoreceptive somatosensory neurons, which perceive force and movement in the vasculature, lymph vessels, bladder and the gut[8–11]. Body temperature homeostasis also relies on temperature receptors in the somatosensory system[12]. These examples clearly illustrate the absolute necessity of somatosensation for life in multicellular organisms. But beyond basic survival, more recent literature has shown the importance of touch, a major component of somatosensation, for cognitive development worms, rats, and humans[13,14]. In fact, several neurodevelopmental disorders including autism, are characterized by tactile hyper- or hypo-sensitivity[15–17]. The importance of mechanosensory stimulation has become a major concern for orphaned or institutionalized children and babies in incubators in the NICU in regard to their growth rate, motor function, immune strength, and social interactions[14,18,19]. The unexpected role of touch in social and emotional development illustrates the far-reaching effects of somatosensation and its fundamental importance not only in sustaining life but also in generating the rich human experience and perception of the world. Undoubtably as we understand more about this system, new and surprising roles for somatosensation will become apparent.

Section 1.2: The peripheral neurons of somatosensation

Introduction

The contents of this dissertation will focus almost exclusively on the peripheral nervous system (PNS), so I will limit my discussion to the peripheral somatosensory neurons and reference the central nervous system (CNS) only as synaptic targets of the peripheral neurons. As previously mentioned, the somatosensory system is responsible for detecting a very diverse array of sensations, and each of these has unique upstream circuitry. For reviews on the various CNS somatosensory circuits see these references: For pain circuits[20–22], for touch circuits[23], for itch circuits[24,25].

The primary peripheral somatosensory neurons are called the dorsal root ganglia (DRG) neurons, aptly named after the anatomical location of their cell bodies in the dorsal projection of the spinal cord. Humans possess 31 pairs of DRGs that innervate the left and right sides of the body on their respective ipsilateral sides (crossover does not occur until higher level processing in the CNS)[26]. In mice, each ganglia contains about 10,000-20,000 individual neurons depending on the spinal level (cervical, thoracic, lumbar, or sacral), but humans possess many more neurons per ganglia, roughly 60,000-100,000[27,28]. DRG neurons are pseudounipolar, meaning that they have one continuous axon that emanates from the cell body with a proximal end that synapses in the dorsal horn of the spinal cord and a distal end that innervates peripheral target tissues including skin, muscles, bones, joints, tendon, and all visceral organs[29]. The proximal branch of the axon synapses in the spinal cord in a somatotopic manner, meaning that the proximal-distal location of the target organ corresponds to the location of synaptic integration into the medial-lateral axis of the spinal cord. The dorsal-ventral axis of the spinal cord (i.e. which laminae) corresponds to modality of the input neuron. For example, nociceptors tend to synapse in the most dorsal laminae layers 1 and II, Low threshold mechanoreceptors

(LTMRs) in more ventral laminae III and IV, and proprioceptors in even more ventral layers V to VII[30]. The site of synaptic connection also varies along the rostral-caudal axis depending on modality, and for some non-noxious touch detectors, this occurs at a very distant location from the DRG soma itself[23,31]. In humans, the farthest peripheral target DRG axons are the feet. Given that these cells may synapse rostrally many spinal levels, the total length of an individual neuron will reach over 1.5 meters[32]. Even more impressive is the blue whale, the largest animal known to inhabit Earth, whose DRG axon length is estimated at over 30 meters[33]. Of course embryonic axonal pathfinding to distant target organs does not quite occur on the same scale as an adult animal, but it still presents a significant spatial challenge for which only 50% of DRG neurons are successful[34] (see further discussion below in *Section 1.4: Phagocytosis).*

The large physical distances traversed by the DRG neurons present other challenges, especially the fast transmission of key sensory information in a timely manner. There are generally two factors that influence conduction velocity of peripheral neurons – diameter of the axon and the presence of an electrically insulating sheath of fatty myelin produced by Schwann cells (See *Section 1.3: Non-neuronal cells in the peripheral somatosensory nervous system* for more details on Schwann cells). DRG neurons exhibit an extremely large range of axon/soma diameters. Generally, small sensory neurons are less than 20 microns in soma diameter and large axons are greater than 20 microns in diameter, with the largest exceeding an impressive 150 microns in diameter[35,36]. The large, myelinated cells are referred to as A fibers and they have a conduction velocity of 30-120 m/s, while small unmyelinated DRG neurons are called C fibers and exhibit conduction velocities between 0.3-1.2 m/s[37]. The A classification is further broken down into three subcategories: Aα and Aβ fibers are the largest and most heavily myelinated, while Aδ neurons are medium in size with only a thin layer of myelin. It is important to keep in mind that the proportion of A versus C neurons varies depending on the species,

spinal level of the ganglia, age, and disease/injury state of the animal, but C fibers generally outnumber A fibers roughly 4:1[38].

As previously mentioned, DRG neurons are able to recognize an incredibly diverse array of somatosensory input including proprioception, mechanoreception, thermosensation, nociception, and pruriception. The ability of these cells to detect so many different inputs results from highly specialized nerve endings in the periphery. These specialized nerve endings have been extensively reviewed elsewhere, so they will not be discussed in detail here (see[23,39,40]).

Each type of DRG neuron also has unique electrophysiological properties that encode sensory information. Many features of the action potential (AP), such as the amplitude, duration, shape, firing frequency, conduction velocity, and adaptation rates are used to convey information about the type of stimulus and its location, intensity, and duration. These variables depend on specific ion channel properties whose expression and activity vary between DRG subtypes. The sensitization of AP firing in response to a sustained stimulus is often used to distinguish different types of sensory cells. Rapidly adapting (RA) cells fire action potentials only during dynamic input, while slowly adapting (SA) cells exhibit a tonic firing pattern throughout a sustained stimulus[41]. The combination of these signals from different DRG neurons are locally processed in the spinal cord to discriminate between transient or persistent environmental cues. The stratification of DRG neurons into RA or SA is often used to discriminate between subtypes, as described below.

There are several historical and biological reasons why DRG neuron subtype specification is complicated. First, various groups have studied different aspects of somatosensory biology and chose to categorize their cells by either their conduction velocity, size, specialized end organ, myelin status, AP firing properties, rates of adaptation, spinal cord patterning, expression of various markers, etc., but the relation of one of these to another is not always clear. Second, many DRG neurons are multi-modal (meaning that, for example, a single

cell can respond to both heat and touch). This feature of many sensory neurons not only makes their classification more difficult, but raises interesting biological questions as how these sensations are discriminated by the organism as either a heat or a touch stimulus in order to elicit the proper behavioral response. Third, DRG neurons are plastic in their identity – this is one mechanism of chronic pain maladaptation that causes non-nociceptive neurons to become sensitized to pain[37]. Lastly, the use of single markers to delineate subtypes is becoming obsolete with the advent of single cell ribonucleic acid sequencing (scRNAseq) techniques. The most recent data obtained from three recent scRNAseq analyses of DRG neurons revealed 18 clusters[42–45]. The following summary of this data combines some groups of cells where possible for the sake of simplicity.

Cold sensing neurons

Cold-sensitive neurons constitute about 20% of cultured DRG neurons *in vitro*[46]. All of them express Transient Receptor Potential cation channel subfamily M member 8 (TrpM8), which opens and depolarizes the cell at temperatures less than 28°C[47]. While TrpM8 knock-out (KO) mice show reduced sensitivity to cool temperatures, they maintain noxious cold sensation, indicating another, yet unknown, channel is involved in painful cold sensation[48,49]. Cold-sensitive DRG neurons include both C and Aδ fibers[45,50]. Interestingly, nearly all DRG neurons respond to extremely cold temperatures less than -18°C, which most likely reflects cellular damage rather than the specific response of an ion channel[51].

Mechano-heat neurons

Mechano-heat neurons are polymodal nociceptors because they respond to noxious heat and injurious mechanical force. They consist mostly of unmyelinated C fibers but also some myelinated Aδ and Aβ fibers[52,53]. All of mechano-heat neurons are peptidergic: The C

fibers express Tachykinin Precursor 1 (Tac1), the gene that produces Substance P, while the A fibers express Calca, the gene that encodes Calcitonin Gene-Related Peptide 1 (CGRP)[54,55]. There are three known ion channels that directly respond to noxious heat above 43°C: Transient Receptor Potential Vanilloid 1 (TrpV1), TrpM3, and Transient Receptor Potential Ankyrin 1 (TrpA1). These heat-sensitive TRP channels are heterologously expressed amongst the mechano-heat neurons. All three must be knocked-out in order to completely eliminate heat-induced pain in mice[56]. The mechano-heat DRG neurons also express the bona fide mechanically activated channel Piezo2[57]. Although this channel is directly activated by force *in vitro*, Piezo2 KO mice only have deficits in light touch sensation but normal noxious touch responses[58]. The molecular identity of high threshold mechanoreceptor(s) (HTMRs) remains unknown.

A fiber LTMRs

A fiber LTMRs detect non-noxious mechanical stimuli and include several subtypes: Aα proprioceptors, Aδ LTMRs, Aβ RA LTMRs, and Aβ SA LTMRs. Proprioceptors are Aα LTMRs with terminal nerve endings located in muscle spindles and Golgi tendon organs that express the Neurotrophin-3 (NT3) receptor Tyrosine Receptor Kinase C (TrkC) and parvalbumin[59]. Proprioceptors detect muscle tension and joint position required for proper movement. Aδ LTMRs innervate Zigzag and Awl/Auchene hairs via longitudinal lanceolate structures that are important for detecting direction of movement and light touch[60]. Aδ hair follicle afferents are identified by high expression of TrkB lack of Ret[31,61]. Aβ RA LTMRs innervate guard hairs, Meissner corpuscles, and Pacinian corpuscles where they detect vibration, movement, and indentation of the skin. The combination of these features allows us to recognize the shape and texture of objects. All Aβ RA LTMRs express Ret, calbindin, low levels of TrkB, but do not express TrkC[62]. While the combination of these proteins uniquely identifies Aβ RA LTMRs from

other types of DRG neurons, within this group the individual fiber types that innervate guard hairs, D hairs, or Meissner/Pacinian corpuscles are molecularly indistinguishable and can only be discerned from one another by the structure of the specialized end organ itself. Aβ SA LTMRs innervate circumferential lanceolate endings in all types of hair follicles as well as Merkel disks. They respond to skin movement, static indentation, gentle stroking, and pressure which is important to recognize the shape and texture of objects[63]. All Aβ SA LTMRs express TrkC and the ones innervating hair follicles are TrkC+ and Ret+[64].

C fiber LTMRs

These non-nociceptive C fibers detect pleasurable touch via longitudinal lanceolate nerve endings in zigzag and Awl/Auchene hair follicles[31,65]. They are the only DRG neurons to express tyrosine hydroxylase (TH) and vesicular glutamate transporter 3 (vGlut3, gene name SLC17A8) and are believed to convey the affective attributes of touch[66].

Itch-mechano-heat neurons

This class of polymodal neurons are all unmyelinated C fibers that only innervate the skin, which anecdotally corresponds with our own experience of itch as a skin-specific sensation (we do not feel the need to scratch our visceral organs). They include three subsets of cells demarcated by the expression of MAS Related G-Protein coupled Receptor member D (MrgprD), MAS Related G-Protein coupled Receptor member A3 (Mrgpra3), or any of the following uniquely-expressed genes in the final subset: somatostatin (Sst), neurotensin (Nts), natriuretic peptide B (NPPB), interleukin 31 receptor A (IL-31RA), oncostatin M receptor (Osmr), cysteinyl leukotriene receptor 2 (Cysltr2), 5-hydroxytryptamine receptor 1F (Htr1f), TrpM2, and neuropeptide Y2 receptor (Npy2r). MrgprD+ cells are important for non-histaminergic itch, as MrgprD is a receptor for the itch-inducing compound β-alanine. Additionally, all MrgprD+ cells

respond to noxious mechanical stimulation and about half also respond to high heat through Trpm3 or Trpa1 – they do not express TrpV1 and are therefore not sensitive to capsaicin. MrgprD+ cells are the only known non-peptidergic nociceptors. Mrgpra3 is the chloroquine receptor; these cells respond to histamine-dependent and histamine independent itch, noxious heat, noxious cold, and mechanical pain. The final subset of this group of polymodal nociceptors can be identified by their unique expression of any of the genes listed above, which confer mechanical pain, warm temperature, hot temperature, and itch sensitivity to the cells. For example, Npy2r+ cells were previously shown to be imperative for pin-prick pain[67]. The TrpM2 channel directly responds to warmth but not hot temperatures[68]. Il-31ra, its co-receptor Osmr, and Cysltr2 make this subset of cells imperative for allergy-induced itch[69,70]. Sst and NPPB neuropeptides are essential for itch sensation elicited from a number of compounds[71,72]. These cells also (not uniquely) express TrpV1, conferring the ability to detect noxious heat.

Summary

Even this simplified view of DRG neuron diversity clearly demonstrates that somatosensory neurons are extremely heterogeneous and somewhat overlapping in function. For the sake of simplicity, we often separate subtypes of DRG neurons into ‘labeled lines’, a theory first proposed by Blix, Goldscheider, and Donaldson in the late 1800s and later endorsed by von Frey, which states that each sensory modality has a unique and specific line of communication to the brain[73]. While there are certainly examples of labeled line DRGs that are solely dedicated to detecting one and only one input, such as cold-sensing neurons, there are also many examples of poly-modal neurons such as the itch-mechano-heat sensitive cells. Pattern theory, or population coding, proposes that a particular sensation results from the integration of multiple inputs[74]. Traditionally this higher level processing was thought to occur in higher brain regions such as the somatosensory cortex, but recent research indicates that local

processing of somatosensory input occurs through complicated networks of interneurons in the dorsal horn of the spinal cord[75]. Many properties of DRG neuron APs, such as the amplitude, duration, shape, firing frequency, conduction velocity, and adaptation rates are integrated in the dorsal horn to determine information about the type of stimulus and its location, intensity, and duration. Further characterization of the spinal cord circuits will help us better understand the central processing of itch and nociception which may identify novel clinical treatments for chronic pruritus and pain.

Section 1.3: Non-neuronal cells in the peripheral somatosensory nervous system

Introduction

DRG neurons have been studied in great depth due to their fundamental role in somatosensory perception. However, glial cells in the CNS and PNS play an integral part in neuron function and provide much more than just a 'supportive' role as they were traditionally seen. "Simply stated, glia tell neurons what to do."[76] PNS glia includes Schwann cells, satellite cells, and perineurial glia. These cell types are generally far less understood than their CNS counterparts. Endothelial cells also play a significant role in modulating DRG neuron activity and will also be briefly reviewed here.

Schwann cells

Schwann cells constitute about 90% of all nucleated cells in a healthy adult nerve and are by far the best-understood peripheral glial cell. They play essential roles in neuron development, survival, function, metabolism, and repair, but are best known for their role in peripheral myelin production[77,78]. Myelinating Schwann cells associate with large and medium diameter axons in a 1:1 relationship. The abaxonal (outermost) surface of the Schwann cell

contains the cell body, while the adaxonal (innermost) surface of the Schwann cell circumferentially spirals around the associated axon in up to 100 layers of lamellae[79]. Myelin is a high-resistance, low-capacitance sheath of insulation required for impulse propagation by saltatory conduction that is essential for fast transmission of electrical signals across the long distances traversed by peripheral nerves. The periaxonal space is about 12-14 nm, a distance small enough to allow cell-cell receptor ligand cross-talk between axons and Schwann cells. Schwann cell differentiation into myelinating or non-myelinating status depends on axonal cues, especially neuregulin (NRG). NRG1 is a member of the epidermal growth factor (EGF) superfamily with at least six different alternatively spliced isoforms, with type III being the major peripheral axon isoform[80]. NRG1 is a ligand for the ERB-B2 (erbB) receptor tyrosine kinase family. Schwann cells predominantly express erbB2 and erbB3[81]. Axon diameter correlates with levels of NRG1 type III, i.e. large axons express high levels and small axons express low levels of neuregulin[82]. Ectopic expression of NRG1 type III in non-myelinated sympathetic fibers results in their myelination[82]. Inactivation of NRG1 type III results in fewer axons and thinner myelin, while its overexpression results in hypermyelination[82–84]. These studies indicate that neuregulin signaling is an instructive cue for myelin formation, however, it is not required for its maintenance once established[85,86]. Downstream of ErbB activation, the transcription factor Krox-20, also known as Early Growth Response 2 (Egr-2), is a master regulator of Schwann cell myelination, along with Octamer binding protein 6 (Oct6) and Brain-2 (Brn2)[87–94].

While myelinating Schwann cells are essential for saltatory conduction, not all peripheral axons are myelinated. In fact, in a typical cutaneous nerve there are approximately fourfold more unmyelinated fibers compared to myelinated ones[95,96]. This is in direct contrast to the CNS, where nearly all axons are myelinated regardless of size. Even small diameter, peripherally unmyelinated DRG neurons become myelinated by oligodendrocytes when they enter the CNS. In the periphery though, non-myelinating Schwann cells vastly outnumber

myelinating Schwann cells. Unlike myelinating Schwann cells, a single non-myelinating Schwann cell ensheaths multiple axons in a structure called the Remak bundle. The exact number of axons in a single Remak bundle varies on type of neuron and proximo-distal location[97]. Considering the clear benefits of myelination on conduction velocity, metabolic efficiency, and protection from axonal degeneration, it is interesting to consider why so many axons have evolved myelin-free in peripheral nerves[98]. In the absence of myelin, axons have enhanced ability to sprout and grow making them more suitable for dynamic environmental changes that would typically occur in epithelial tissues that constantly turnover and are subject to frequent injury and chemical insult. In support of this hypothesis, mature non-myelinating Schwann cells retain proliferative ability while myelinating Schwann cells do not (however, as discussed later, both types of Schwann cells reprogram after injury and are able to proliferate under these conditions)[99].

While an extremely fascinating cell type of utmost importance in the PNS, Schwann cells are not the primary focus of this dissertation. For more information on Schwann cell biology please see these reviews[100–104].

Satellite glia

Satellite glia are neural crest-derived cells that form a multi-cellular sheath that enshrouds DRG cell bodies. Due to their specific location only at the somas of the neurons, these cells are only found in peripheral ganglia and not the nerves. The number of satellite glia surrounding each individual cell body depends on a number of factors including species, age, size of the neuron, infection, inflammation, and chronic pain, but an average ratio of satellite cells to DRG neurons is about 10:1[105,106]. The satellite glia connect to one another through adhesion molecules and their cytoplasm is contiguous due to gap junctions not only between all the satellite glia surrounding one neuron soma but also with adjacent satellite glia ensheathing

neighboring neurons[107–109]. This network of interconnected satellite cells is thought to contribute to cross excitation of neurons not directly activated by environmental stimuli[110,111]. Unlike the perineurial glia described below, satellite glia are not connected by tight junctions and therefore do not contribute to barrier function – even cells such as macrophages can penetrate between them[112–115]. The intercellular distance between the DRG neuron cell body and it satellite glia sheath is only 20nm, placing satellite glia in an ideal location to modulate neuron function either through modulating extracellular ion concentrations and/or communicating via soluble compounds across this small distance[116]. Microvilli protrude from DRG neuron somas into invaginations of the satellite cells, but the function of these microvilli are unknown. Interestingly though, the microvilli increase the surface area of the neuron by 30-40%[107].

Satellite glia play numerous roles in the DRG, especially in the potentiation of DRG neuron activity during chronic pain. I will only relay some specific mechanisms of satellite glial control of DRG neuron function. For reviews that outline the many other mechanisms please see[105,116,117]. AP dynamics are critically determined by the electrochemical gradient between the inside and outside of the cell membrane, such that the regulation of extracellular ion concentrations greatly affects AP firing properties[118]. When a neuron fires an AP, potassium ions (K^+) exit the cell. Since the extracellular volume around the DRG soma is very small due to the intimate physical location of the satellite glia, even small amounts of K^+ can increase the extracellular potassium concentration. Excess K^+ outside the cell leads to depolarization and increased neuron excitability, which for DRGs, has been linked to chronic pain. Satellite glia, but not DRG neurons, express the Potassium Inwardly Rectifying 4.1 (Kir4.1) channel that removes excess K^+ from the space in a similar manner to CNS astrocytes[119,120]. After nerve injury or inflammation, Kir4.1 expression decreases and K^+ current is reduced in satellite cells, a change that predicts an increase in neuron excitability[121]. Vit et al. used *in vivo* delivery of small interfering RNA (siRNA) into the DRG to down-regulate Kir4.1 in the absence of a nerve injury

and observed excessive nocifensive behaviors in the mouse above control siRNA levels, providing the most definitive evidence to date that satellite glia can directly modulate neuron activity[121].

Satellite glia are also responsible for recycling neurotransmitters in the DRG. All of the typical machinery is present in the ganglia for non-synaptic glutamate signaling including the amidohydrolase enzyme, glutaminase, vesicular glutamate transporters (vGLUT1, 2, and 3), the glutamate aspartate transporter (GLAST), glutamate transporter (GLT1), and the recycling enzyme glutamine synthetase (GS)[122–127]. Recall that satellite glia do not have tight junctions, so neurotransmitters released from one cell body can diffuse to surrounding cells within the ganglia. To regulate potential cross-excitation of neighboring neurons, satellite glia express both GLT1 and GLAST, allowing them to uptake extracellular glutamate, and GS, which converts glutamate to glutamine. The non-neuroactive glutamine is then release from satellite glia and re-uptaken by neurons where glutaminase converts it back to glutamate. This is the typical glutamate-glutamine recycling pathway typically observed in CNS astrocytes[128]. It will be interesting to find if the endogenous expression of GLT1 and GLAST changes in satellite glia following chronic pain conditions, but we do know that knock-down (KD) of these proteins does induce painful behaviors in mice[117,129].

There is still much to learn about glutamate signaling between DRG neurons and glia – recently, satellite glia were also found to express functional N-methyl-D-aspartate receptors (NMDAR) and metabotropic glutamate receptors (mGluRs)[123,130,131]. Astrocytic mGluR8 responds to neuronal-derived glutamate in the CNS, which contributes to astrocyte activation including up-regulation of glial fibrillary acidic protein (GFAP)[132]. GFAP is an intermediate filament protein that anchors GLAST to the plasma membrane[133]. It is also a marker of satellite glial activation, so presumably mGluRs in satellite glia follow a similar mechanism to astrocytes and contribute to satellite cell activation.

The two examples I have provided above demonstrate that satellite glia and neurons communicate with one another by releasing soluble factors into the intracellular space between. There are several other examples of small molecules, lipid second messengers, and cytokines that participate in this bi-directional communication. For example, neurons release adenosine triphosphate (ATP)[134,135], CGRP[136], matrix metalloproteases (MMP2 and MMP9)[137], nitric oxide (NO)[138,139]and Substance P[140]. Satellite glia release ATP[134], prostaglandin E2 (PGE2), interleukin-1β (IL-1β)[141,142], and tumor necrosis factor a (TNFα)[143]. Most of these signaling mechanisms were discovered while looking for peripheral mechanisms of chronic pain potentiation. Satellite glia have a well-documented role in undergoing 'activation,' which often leads to a maladaptive response in potentiating DRG neuron activity. A commonly used marker for satellite glial activation is GFAP, but there is also an increase in the release of cytokines and pro-inflammatory lipid species, gap junction connections, and proliferation[144–147]. Many of these changes in activated satellite glia will be evaluated in the experimental chapters of this thesis.

Epineurial and perineurial glia

Glial cells in peripheral nerves consist of Schwann cells, endoneurial fibroblasts (which will not be discussed here), perineurial glia, and the epineurium. The outermost barrier of peripheral nerves is the epineurium, which is mostly composed of adipocytes, lymph vessels, and extracellular matrix (ECM). It groups individual fascicles together and contributes mostly to the tensile and torsional strength of the nerve[148].

The inner layer of the nerve barrier is comprised of perineurial glia, a multi-layered sheet of cells connected by tight junctions that bundle axons into fascicles. Depending on the size and proximal-distal distance of the nerve, perineurial thickness varies between one and fifteen concentric layers of cells[149]. Due to its production of a thick basal lamina and network of cells connected by claudins, occludins, zonula occludens (ZO), and junctional adhesion molecules,

the perineurium is the primary barrier between axons and external interstitial fluid. Therefore the perineurium, along with special adaptations to nerve endothelial cells (discussed below), is a major constituent of the blood-nerve-barrier (BNB), the peripheral equivalent to the blood-brain-barrier (BBB) in the CNS that protects neurons from toxins, pathogens, and drastic changes in extracellular ion concentration. Both the BNB and BBB are extremely clinically relevant as they present a major barrier to drug delivery and their breakdown is associated with neurodegenerative diseases, neuropathies, autoimmune dysfunction[150,151]. Selective transport across the perineurium is evident, however, in electron microscopy (EM) studies showing extensive transcytosis across it, although we know virtually nothing about the molecular mechanisms or regulation of this transport[152,153]. The perineurium plays a significant role in pressure homeostasis of the nerve, which can have severe consequences on axonal health and degeneration[154–157].

Vascular cells of DRGs and nerves

Besides the perineurium, the endoneurial vascular cells also contribute to the BNB. This includes the endothelial cells of the blood vessel wall and the pericytes around them which share basement membrane[158]. Tight junctions connect these cells to one another in order to prevent free passage of molecules into the axonal space. Pericytes are known to release a number of soluble factors like transforming growth factor β (TGFβ), vascular endothelial growth factor (VEGF), angiopoietin-1 (Ang1), and basic fibroblast growth factor (bFGF), that maintain endothelial tight junctions[159,160]. Interestingly, only the axon-containing nerves and not the soma-containing ganglia are protected by the BNB. The density of capillaries is much higher in the DRG than in nerves, which is similar to the CNS where grey matter vascularization greater than white matter[161]. Ganglia endothelial cells are fenestrated and therefore extremely permeable to blood-borne molecules of varying sizes[162–165]. It is unknown why peripheral nerves are shielded

from blood constituents but sensory ganglia are not. Anti-human immunodeficiency virus (HIV) drugs, chemotherapy, heavy metal poisoning, and other pharmacologicals that typically cause pain and neuropathy likely gain access to sensory neurons via the ganglia rather than the nerve due to these differences in permeability[166,167]. In support of this hypothesis, many of these drugs preferentially cause sensory rather than motor neuropathies, the latter of which are protected by BBB in the spinal cord. Evolutionarily, perhaps ganglia permeability confers some advantage to sampling blood contents or it is required due to high metabolic demand of sensory neuron cell bodies.

The mechanisms by which endothelial cells can modulate neuron function are primarily through changes in blood vessel permeability or paracrine signaling. BNB breakdown occurs in chronic pain conditions including diabetes[168,169], peripheral nerve injury[170,171], various neuropathies[172,173], or inflammatory disease[174]. Resident macrophages in nerves will increase BNB permeability injury by releasing VEGF[175]. Delivery of exogenous VEGF into nerves will open the BNB and induce neuropathic pain even in the absence of an injury for extended periods of time[176]. VEGF opens the BNB by down-regulating the expression of the tight junction protein ZO-1 in the endothelium and perineurium, and promoting the growth of new and leaky blood vessels in the nerve and ganglia[163,175,177]. Upon breakdown of the BNB, nerves become permeable to leukocytes and pronociceptive molecules in the blood such as fibrinogen and cytokines[176,178,179]. Some, but not all reports indicate that the loss of pericytes contributes to the decline BNB integrity in several disorders[180]. Endothelial cells themselves also produce factors that act in paracrine and autocrine signaling to increase permeability of nerve blood vessels, attract white blood cells, and directly activate DRG neurons. These endothelial derived pain-promoting molecules include NO[181], TNFα, IL-1β, and interleukin 6 (IL-6)[182]. In short, endothelial cells play a vital role in a number of painful disorders and peripheral neurodegenerative diseases.

Summary

Here I have demonstrated that a number of non-neuronal cells play crucial roles in DRG neuron development, function, and repair. Their importance in homeostatic and pathological somatosensation cannot be overstated. Unlike DRG neurons, whose subtypes have been extensively studied, peripheral glia heterogeneity investigations are still in their infancy. Single cell analyses will undoubtedly improve our knowledge of this diversity. How all of these cell types coordinate with one another is also quite complicated. For example, it seems clear that Schwann cells and perineurial glia communicate with one another during development, but these signals remain a mystery. A better understanding of these molecular mechanisms may have profound clinical implications for the treatment of chronic pain and itch, because, as discussed above, modulation of glia can affect nociceptor activity. Given the problems with current analgesic treatments of anti-inflammatories and opioids, peripheral glia are an attractive alternative target for decreasing DRG neuron AP firing patterns.

Section 1.4: Phagocytosis

Introduction

DRGs, like the rest of the nervous system, undergo massive waves of programmed cell death (PCD) during embryonic development such that 50-70% of the cells die, including neurons and glia.[34] It is interesting to speculate why more than twice the number of necessary cells are initially generated only to commit suicide a short time later. Explanations include regulation of cell number/size, negative selection of mis-specified cells, morphogenesis, removal of damaged or diseased cells, proper cell positioning, remodeling, and removal of inappropriately targeting axons[183]. The discovery of endogenous apoptosis of peripheral ganglia was made by Rita Levi-Montalcini and Viktor Hamburger in the 1940s, and nerve growth factor

(NGF) was later identified and characterized by Rita Levi-Montalcini and Stanley Cohen at Washington University in the 1950s[184–189]. These discoveries are actually two sides of the same coin, though at the time they were not recognized as such[189–193]. Originally the neurotrophin NGF was identified from tumors that caused excessive survival and growth of sensory and sympathetic neurons, but it is the *lack* of target-derived NGF and other neurotrophins and growth factors that cause massive cell death in developing DRGs in utero[194,195]. An excess of neurons competing for limited survival factors secreted by synaptic targets ensures proper innervation of peripheral tissues – this is the basis of trophic theory, a term originally coined by the prolific neuroscientist Ramon y Cajal in 1928[196,197]. Rita Levi-Montalcini and Stanley Cohen would later go on to win the Nobel Prize in Physiology or Medicine in 1986 for their discovery of NGF, but Victor Hamburger was not awarded with the prize despite his participation in the initial experiments. However, Rita-Montalcini dedicated her Nobel Prize acceptance speech to Hamburger and declared that the discovery would not have been possible without him[198]. During the writing of this dissertation, Dr. Cohen sadly passed away at the age of 97.

The details of neurotrophin signaling have been a major area of study in the Carter lab, however, the primary focus of my work has been its aftermath – what happens to the cellular corpses that result from 50% of DRG cells dying? The same question applies not only to embryonic development but also to universal tissue homeostasis, as billions of cells turnover daily in a healthy adult human[199]. Although oft overlooked by researchers, the logical final stage of cell death must be a mechanism to remove the ensuing cellular corpses. Many epithelial cells, including denucleated keratinocytes in the outermost layer of the skin, are simply sloughed off into the external environment[200]. However, the removal of dead cells typically occurs through the process of phagocytosis, defined as the cellular internalization of any object greater than 0.5 microns in diameter[201]. Phagocytosis is distinguished from endocytosis or pinocytosis by the large size of the ingested material, which requires extension of filopodia for

internalization rather than invagination of the plasma membrane[202,203]. As such, phagocytosis is not a passive, continuous process – it requires receptor engagement with specific ligands for initiation[201]. Elie Metchnikoff was the first person to observe phagocytosis by placing wooden thorns into starfish and observing special cells attacking these foreign particles. He fathered the concept of cellular immunity and received the Nobel Prize in 1908[204]. Metchnikoff's work demonstrates that phagocytosis is not only utilized for the clearance of 'self' dying cells, but also used for the elimination of 'non-self' foreign invaders including bacteria, viruses, and, as described below, 'self' cells that are no longer recognized as such. The ligands, receptors, and other downstream signaling events are fundamentally different depending on whether the phagocytic target is recognized as 'self' or 'non-self'. Efferocytosis, a Greek term meaning "to carry the corpse to the grave", technically refers to the engulfment of 'self' cells, but often 'phagocytosis' and 'efferocytosis' are interchanged in the literature[205]. Morphologically, the process of internalization of both types of prey ('self' or 'non-self' phagocytic targets) appears similar, but the cellular machinery underlying these processes is fundamentally different and has extremely important consequences for human health. Before discussing the implications of these different forms of engulfment, I will describe the normal molecular signals used to remove apoptotic cells that occurs in the pruning of embryonic DRG neurons.

Apoptotic 'find me' signals

During early stages of apoptosis, dying cells attract phagocytes by releasing soluble factors, or 'find me' signals. 'Find me' signals include lysophosphatidylcholine (LPC)[206], sphingosine-1-phosphate[207], fractalkine[208], and nucleotides adenosine triphosphate (ATP) and uridine triphosphate (UTP)[209]. These factors are intentionally released by apoptotic cells before loss of plasma membrane integrity and are therefore not a byproduct simply of leakage of intracellular contents. Although they were first characterized as chemoattractants, 'find me'

signals also prime phagocytes for anti-inflammatory engulfment characteristic of efferocytosis. It is unclear whether a single apoptotic cell releases all of these 'find me' factors simultaneously or if it is dependent on the type of apoptosis (for example, extrinsic versus intrinsic initiation), and whether different 'find me' molecules preferentially attract a particular type of phagocyte. The range of 'find me' signals and physiological concentrations are difficult to measure and also require further study. I will use the best-studied example of ATP to demonstrate the principles of 'find me' signals, but for details regarding the others please see[210]. ATP is released from apoptotic cells prior to degradation of the plasma membrane through Pannexin-1 channels[211]. Normally these channels are closed by an autoinhibitory C terminal domain that gets cleaved by caspase 3 and 7 to allow nucleotide transport outside the cell. While there are a variety of both ionotropic and metabotropic purinergic receptors, the low concentrations of ATP released from Pannexin-1 channels (100–200 nM) specifically activates the purinergic receptor P2Y2 on the surface of phagocytic cells and does not activate purinergic receptor P2X7R, which requires high ATP concentrations (more than 100 μM)[212,213]. The distinction is important because P2Y2 activation is anti-inflammatory while P2X7R is pro-inflammatory[214–216]. P2Y2 is heavily expressed in monocytes and macrophages and P2Y2 KO mice have deficiencies in apoptotic cell clearance, although they have not been reported to acquire autoimmune disease[209].

Apoptotic 'eat me' and 'don't eat me' signals

In order to be recognized by phagocytes, apoptotic cells upregulate surface expression of 'eat me' signals on their surface and downregulate the opposing 'don't eat me' signals. Both types of positive and negative cues are recognized by their cognate receptors on phagocytic cells and their balance determines whether internalization will occur or not. 'Eat me' signals include phosphatidyl serine (PS), intercellular cell adhesion molecule 3 (ICAM-3)[217], and modified carbohydrates[218]. By far the best studied of these is PS.

Eukaryotic cells display asymmetric distribution of lipids across the inner and outer leaflets of their plasma membrane, with PS predominantly localized to the inner leaflet in healthy cells[219]. Flippases ATPase phospholipid transporting 11C (ATP11C), ATPase phospholipid transporting 11A (ATP11A), and their chaperone protein CDC50A (also known as TMEM30A) contribute to this asymmetry by translocating PS specifically from the outer to inner leaflet of the plasma membrane[220]. During apoptosis, these flippases are inactivated by caspase activity[220]. When the cleavage sites in ATP11C and ATP11A are mutated, dying cells fail to expose PS to the outer leaflet and do not get phagocytosed[220]. However, inactivation of flippases alone is not sufficient for PS exposure, given the pre-established asymmetry and extremely rare occurrence of spontaneous lipid transfer between leaflets[221,222]. Scramblases such as Xk-related protein 8 (Xkr8), which non-specifically transfer lipids between the inner and outer bilayer, must also be activated by caspase-dependent cleavage[223]. Mutations in Xkr8 also fail to expose PS and do not get phagocytosed. In conclusion, the display of the ubiquitous ‘eat me’ signal PS requires both the caspase dependent inactivation of flippases and the caspase dependent activation of scramblases. This mechanism of PS exposure was only recently discovered by Shigekazy Nagata’s lab in Japan within the past decade.

Another hallmark of apoptosis is the blebbing of the plasma membrane. These small, round spherical fractions of cells are dynamically extended and retracted during apoptosis though actin-myosin interactions[224,225]. Apoptosis is well known to induce caspase activity, and caspase-dependent cleavage of the actomyosin regulator Rho associated coiled-coil containing protein Kinase 1 (ROCK1) is required for bleb formation and packaging[226–228]. Inhibiting apoptotic blebbing decreases phagocytosis of apoptotic cells, but can be rescued by adding excess PS-recognizing proteins[229]. Therefore, blebbing is thought to abet efferocytosis by concentrating ‘eat me’ signals in high concentration focal points easily engaged by phagocytic receptors[230].

There are always counter mechanisms in place that positively and negatively regulate virtually every biological activity, the metaphorical sword and shield of mother nature. For efferocytosis, if the 'eat me' signal is the phagocytic sword, then the 'don't eat me' signal is the shield. Examples of 'don't eat me' signals include CD47[231], CD24[232], programmed cell death ligand 1 (PD-L1)[233], and a subunit of the major histocompatibility class 1 complex (MHC-1)[234]. Most of these 'don't eat me signals' were discovered due to their overexpression in cancer cells in order to avoid immune system surveillance. Of them, we know the most about CD47. The importance of CD47 ligand and its receptor signal regulatory protein a (SIRPa) is demonstrated by inhibiting their interaction or knocking out CD47: This causes aberrant efferocytosis of live cells that are not normally engulfed[235,236]. SIRPa prevents formation of the phagocytic cup by activating the protein tyrosine phosphatase SHP1/2 (SHP1/2) and inhibiting Rac family small guanosine triphosphate (GTP)ase 1 (Rac1), a critical regulator for cytoskeletal rearrangements that are fundamental to efferocytosis[237]. We know that CD47 is downregulated in apoptotic cells to promote their own clearance, but the mechanism is currently unknown[238].

Recognition and internalization of apoptotic cells

The cells actually responsible for efferocytosis are incredibly diverse. "Professional" phagocytes are myeloid-derived cells such as macrophages, immature dendritic cells, and neutrophils, but emerging evidence shows more and more "non-professional" phagocytic cells including endothelial cells, several types of epithelial cells, and fibroblasts are also capable of efferocytosis under the right circumstances[239]. While professional phagocytes perform the task faster and more efficiently (they are 'primed' for phagocytosis) non-professional phagocytes can compensate for the loss of macrophages *in vivo* quite well by removing troves of dead cells during development[240]. How dead cell clearance is coordinated by professional versus non-professional phagocytes is not well understood, however, recent work by Kodi Ravichandran's lab at University of Virginia showed that macrophages regulate the phagocytic activity of lung

epithelial cells by releasing insulin-like growth factor-1 (IGF1)[241]. IGF-1 promoted epithelial cell uptake of small extracellular vesicles, which also have externally exposed PS, and discouraged epithelial cell efferocytosis. Using *in vivo* models of lung irritation, they showed negative regulation of epithelial cell phagocytosis by macrophages was important for dead cell clearance in an anti-inflammatory rather than pro-inflammatory manner. While these results suggest that profession phagocytes are important for setting the inflammatory tone of dead cell inflammation, there remains much to be explored regarding the bi-directional communication between these cell types.

There are a plethora of engulfment receptors that recognize 'eat me' signals on the surface of apoptotic cells. These include the TAM family (Tyro1, Axl, and Mer), brain specific angiogenesis inhibitor 1 (BAI1), T cell Immunoglobin and Mucin domain containing 1/3/4 (TIM1/3/4), CD14, integrins $\alpha_v\beta_3$ and $\alpha_v\beta_5$, LDL receptor related protein 1 (LRP1), CD14, Stabilin1/2, CD36, CD91, multiple EGF like domains 10/12 (MEGF10/12 see also *Section 1.5 Background on the Jedi receptor*), scavenger receptor class F member 1 (SCARF1), lectin receptors, receptor for advanced glycoslyation end products (RAGE), triggering receptor expressed on myeloid cells 2 (TREM2), and CD300. They may directly engage PS, as is the case with the TIM[242] and Stabilin family members[243], or they may indirectly bind PS using a bridging molecule such as milk fat globule EGF factor 8 protein (MFG-E8)[244], Gas6, and protein S[245], which is how the integrin receptor a_vb_3 and TAM family members initiate efferocytosis. TAM receptors themselves are kinases, while other engulfment receptors do not possess any enzymatic activity[246]. BAI1 is the only engulfment receptor that is a G protein coupled receptor (GPCR); most others are single pass transmembrane proteins[247]. The engulfment receptors also do not share common protein motifs despite multiple of them recognizing the same ligand, PS. For example, MFG-E8 binds PS with its C1 and C2 domains[244,248]. BAI1 directly interacts with PS via thrombospondin type 1 (TSP-1) repeats[247]. TIM1 and TIM4 recognize PS through

immunoglobin V (IgV) domains[242,249,250]. Stabilin-2 bind PS through EGF-like repeats[251]. It is not precisely known why so much redundancy and diversity has evolved in mammalian efferocytosis receptors, however, it appears that professional and non-professional phagocytes simultaneously express overlapping sets of receptors. Although there is certainly a huge amount of redundancy in the system, KO mouse studies of various receptors exhibiting differing phenotypes indicate that not all phagocytic receptors can compensate for one another in various contexts. Often a number of different phagocytic receptors are expressed by the same cell and their clustering around a target is important for the initiation of internalization[252]. The focalization of phagocytic receptors with their targets is sometimes referred to as the “phagocytic synapse”[253].

Although there is wide diversity in efferocytosis receptors, they all lead to actin cytoskeletal rearrangement and vesicle fusion with the plasma membrane[254]. Downstream of engulfment receptor activation by ‘eat me’ ligands, usually one of two major downstream signaling complexes are activated, the CRK proto-oncogene adaptor protein/engulfment and cell motility 1/dedicator of cytokines 1 (CrkII/ELMO/Dock180) complex[255] or the ATP binding cassette subfamily A member 1/GULP PTB domain containing engulfment adaptor 1 (ABCA1/GULP) complex[202]. Both pathways activate the small GTPase Rac1, which initiates actin cytoskeleton rearrangement required for pseudopod extension[256,257]. Professional phagocytes are known to ingest 10–20 apoptotic cells as large or larger than themselves and can even internalize synthetic targets up to thirty microns in diameter[258–260]. This requires a 20-500% increase in surface area in a very short amount of time, in the range of minutes[261]. At least some of this membrane is provided by endosomes and the endoplasmic reticulum (ER)[262,263].

Apoptotic cell digestion and response

Once internalized, the apoptotic target cell undergoes a series of fusions with early endosomes, late endosomes, and finally lysosomes where it will eventually be degraded[264,265]. As the phagosome matures, the vesicle becomes increasingly acidic. This acidity activates various enzymes that degraded ingested cells into their amino acid, nucleotide, fatty acid, and monosaccharide components. Once such enzyme is deoxyribonuclease II (DNase II), deficiencies in which causes anemia and rheumatoid arthritis[266,267]. Disintegration of apoptotic cells into individual amino acids, nucleotides, and lipids prevents antigen presentation of self peptides[268–271].

The key conclusion that distinguishes efferocytosis of apoptotic cells from phagocytosis of invading pathogens is the anti-inflammatory response. Efferocytosis concludes with the release of anti-inflammatory molecules such as TGFβ, IL-10, and lactate, and the suppression of pro-inflammatory signaling including toll like receptor (TLR), nuclear factor κ B subunit 1 (NFκB), and interferon signaling[272]. The anti-inflammatory effect of efferocytosis is apparent in models of lipopolysaccharide (LPS)-induced lung inflammation, myocardial infarction, and murine skin edema, where professional phagocytes can quickly reduce inflammation in a TGFβ–dependent manner when stimulated to perform efferocytosis by exogenous deliver of PS-containing liposomes to mimic dead cells[273–276]. PS is becoming widely recognized as a universal immunosuppressive signal in many contexts including cancer and infectious disease[277]. In fact, its popularity has permeated into everyday use as you can buy PS as an over-the-counter supplement where it is advertised to reduce inflammation. The anti-inflammatory consequences of efferocytosis actively induce tolerance to self-antigens through a number of mechanisms, only some of which are mentioned here. For example, TGFβ induces regulatory T (T_{regs}) cells, a subset of inhibitory T cells that is critical for the prevention of autoimmunity[278–280]. Anti-inflammatory engulfment also leads to decreased antigen presentation

by down-regulating MHC molecules and co-stimulatory molecules CD40, CD86, and CD80[281,282]. These measures help to ensure that autoreactive adaptive immune cells are kept in check by either T_{regs}, anergy or depletion.

Unengulfed apoptotic cells undergo secondary necrosis

The release of 'find me' signals, exposure of PS, and membrane blebbing described above are examples of how apoptotic cells facilitate their own clearance in a timely and anti-inflammatory manner. These events start to occur within 2–4 hours after initiation of apoptosis, and generally will be cleared within 12 hours under basal conditions[211,283,284]. A recent report by the Kucenas lab showed that apoptotic cells injected intraperitoneally into mice were phagocytosed within 15–30 minutes[261]. The efficiency of this process is demonstrated by the lack of detectable dead cells in tissues with extremely high rates of turnover including testes, bone marrow, and thymus – the dead cells are removed so quickly that steady-state fixed sections are unable to accurately capture the extent of apoptosis occurring there[199,285].

There are two general categories of phagocytic cells, 'professional' or 'non-professional' phagocytes[239]. So called 'professional' phagocytes are myeloid-derived cells such as monocytes, macrophages, dendritic cells, and neutrophils[200,286]. These cells comprise 10-15% of total cells in a given organ and are able to engulf a larger quantity and diversity of targets in a faster time frame than 'non-professional' phagocytes[287]. A wide array of other cells are capable of phagocytosis under certain conditions, such as epithelial cells, fibroblasts, endothelial cells, stromal cells, and Sertoli cells[288,289]. These non-professional phagocytes can actually compensate for loss of macrophages during development[240]. How dead cell clearance is coordinated by professional versus non-professional phagocytes is not well understood, however, recent work by Kodi Ravichandran's lab at University of Virginia showed that macrophages regulate the phagocytic activity of lung epithelial cells by releasing insulin-like

growth factor-1 (IGF1)[241]. IGF-1 promoted epithelial cell uptake of small extracellular vesicles, which also have externally exposed PS, and discouraged epithelial cell efferocytosis. Using *in vivo* models of lung irritation, they showed negative regulation of epithelial cell phagocytosis by macrophages was important for dead cell clearance in an anti-inflammatory rather than pro-inflammatory manner. While these results suggest that professional phagocytes are important for setting the inflammatory tone of phagocytosis, there remains much to be explored regarding the bi-directional communication between these cell types. In conclusion, there are a multitude of professional and non-professional cell types capable of phagocytosing apoptotic dying cells prior to the completion of PCD.

Although there are multiple redundant mechanisms (as described above) in place to compensate for deficiencies in efferocytosis, the temporal coupling of apoptosis and phagocytosis may be disrupted by genetic mutations in the engulfment machinery or excessive numbers of dead cells caused through disease that overwhelm the phagocytic capacity of the organism. Estimations of the ratio of apoptotic cells to phagocytes at homeostasis indicate that dying cells vastly outnumber phagocytic cells by a factor of at least ten, so perturbations to the number or function of these cells leads to accumulation of uncleared dying cells[290]. Apoptotic cells that remain un-engulfed for more than twelve hours will then undergo secondary necrosis, which leads to loss of plasma membrane integrity and the un-regulated release of intracellular contents into the microenvironment that are potentially cytotoxic, immunogenic, and pro-inflammatory[291–293]. While they differ in their initiation either from external or internal stimuli, primary and secondary necrosis share similar features such as metabolic/mitochondrial failure, non-caspase protease activation, imbalance of the electrochemical gradient, and lysosome rupture[294]. The transition from apoptosis to necrosis involves several key steps. First, apoptosis requires energy in order to produce ‘find me’ and ‘eat me’ signal, undergo membrane blebbing, activate caspases, etc., and is characterized by high levels of ATP[295,296]. As apoptosis

progresses, ATP levels deplete and mitochondrial membrane potential dissipates – this energy depletion is considered a trigger for necrosis[297,298]. Second, the switch from apoptosis to secondary necrosis features a transition from caspase-only protease activation to caspase-independent proteases[299]. Caspases themselves trigger this switch by cleaving the sodium/calcium (Na^+/Ca^{2+}) exchanger, inositol 1,4,5-triphosphate receptors (IP3Rs), and calcium-dependent ATPases, leading to sharp increases in cytosolic calcium levels in later stages of apoptosis[300]. Calcium triggers calpain activation and subsequent lysosome rupture[301]. Calpain and the release of lysosomal enzymes contributes to plasma membrane damage observed in secondarily necrotic cells[302,303]. Reactive oxygen species (ROS) increase during apoptosis due to mitochondria break-down and play a role in secondary necrosis, as anti-oxidant treatment delays the transition from PCD to necrosis[304]. Unengulfed apoptotic cells that transition to secondary necrosis no longer are removed by the immunologically-silent mechanism of efferocytosis, but rather transition to pro-inflammatory clearance by phagocytosis, as described below.

Necrotic alarmin signals

When secondarily necrotic cells lose membrane integrity, they release their contents into the extracellular milieu. Because many of these are potentially cytotoxic, immunogenic, and pro-inflammatory, they are referred to as damage associated molecular patterns (DAMPs) or alarmins[305]. Some specific molecules released from secondarily necrotic cells in a non-controlled fashion include DNA, RNA, proteases, chromatin, high mobility group box-1 (HMBG-1), cytoskeletal proteins, and urate crystals[306–310]. While apoptotic 'find me' signals prime the phagocyte for non-inflammatory clearance, necrotic DAMPs alert phagocytes to enter a pro-inflammatory state by activating pattern recognition receptors such as TLRs, lectin receptors, and C type lectin domain containing 9A (CLEC9A/DNGR-1). TLR signaling activates NFκB signaling and the inflammasome, causing release of the pro-inflammatory cytokines TNFα, IL-6,

and interferon-α (IFNα)[311–313]. In other words, DAMPs are the sterile version pathogen-associated molecular patterns (PAMPs), which both activate pattern recognition receptors. The combination of these pro-inflammatory signals galvanize the phagocytes for antigen presentation by increasing the expression of MHCI and II, decreasing the degradation capability of the lysosome to preserve self-antigens for presentation, and increasing the expression of co-stimulatory receptors required to activate T cells[314,315]. The ability of DAMPs (and PAMPs) to activate the innate immune system's antigen presenting cells (APCs) in response to cellular damage, which subsequently drives the adaptive immune response, was famously first proposed by Dr. Polly Matzinger as the 'danger theory' in 1994[316]. DAMPs are often used as a non-microbial adjuvant for various treatments, including vaccines, for this reason.

'Eat me' signals and recognition of necrotic cells

DAMPs/alarmins released from necrotic cells activate TLRs. While TLRs facilitate engulfment of necrotic cells, TLRs themselves are not engulfment receptors per se[317]. The receptors specifically responsible for phagocytosis of necrotic cells is less understood relative to those responsible for efferocytosis of apoptotic cells. Some receptors recognize both apoptotic and necrotic prey, as PS is also available for binding of necrotic cells when the plasma membrane is destroyed[318,319]. One example of this are the integrins $\alpha_v\beta_3$ and $\alpha_v\beta_5$, which act on their own to efferocytose apoptotic cells, but act in a complex with CD36 to phagocytose necrotic cells. Integrin-mediated engulfment illustrates the importance of cellular context in phagocytosis, as the repertoire of receptors available is probably dynamic depending on the pro- or anti-inflammatory conditions[320]. The $\alpha_v\beta_{3/5}$-CD36 complex indirectly recognizes necrotic cells via the adaptor protein thrombospondin (TSP-1). Its endogenous target on necrotic cells is unknown, but interestingly, TSP-1 has been shown to bind to bacterial peptidoglycans and

facilitate their removal[321]. TSP-1 illustrates a recurring theme – necrotic cells and foreign pathogens are similarly recognized by the innate immune system.

Fcγ receptors (FcγR) also play a role in necrotic cell engulfment. FcγRs bind to immunoglobin G (IgG); in the case of necrotic cell phagocytosis a number of auto-reactive IgGs may opsonize the target. Clustering of the receptor leads to phosphorylation of its Fcγ immunoreceptor tyrosine-based activation motif (ITAM) repeats by Src family-kinases[322,323]. Phosphorylated FcγR recruits spleen tyrosine kinase (Syk) through its Src homology (SH2) domains, which phosphorylates and recruits several adaptor proteins[324,325]. The combination of Syk and other adaptor proteins leads to several downstream events in FcγR-mediated phagocytosis, including the dynamic regulation of phospholipids orchestrated by phosphatidylinositol kinases, phosphatases, and phosphoinositide-specific phospholipases[326]. Syk also activates the guanine nucleotide exchange factors (GEFs) Dock180-ELMO1 and Vav proteins, leading to Rho family GTPase activation[327]. Ultimately this leads to actin polymerization required for internalization through the Wiskott-Aldrich syndrome protein (WASP) family member Scar1/WAVE and Arp2/3 nucleation factors[328]. Much of the down-stream signaling in efferocytosis and pro-inflammatory phagocytosis is similar, which fits with the morphological similarity of both processes.

Complement-mediated phagocytosis also seems to play a role in necrotic rather than apoptotic cell removal[329]. As previously mentioned, necrotic cells extrude their intracellular contents, including proteases such as caspases and calpain. These molecules are thought to potentiate complement-mediated engulfment[330]. C1q binds to dead cells through myosin, LPC, and other autoreactive immunoglobin M (IgM) antibodies[331–333]. Recent studies show that C1q can also directly bind histones without the requirement for prior antibody opsonization[334]. The classical complement pathway may ensue with C3 and C4 deposition on the necrotic cell and

subsequent recognition with the C3 and C4 receptor (C3R and C4R) or C1q may directly activate internalization through calreticulin/CD91 complexes[335–337].

Chronic failure to efficiently clear apoptotic cells leads to autoimmune disease

Most professional phagocytes are also antigen presenting cells (APCs), which inform the adaptive immune system about potentially harmful material ingested material. When apoptotic cells undergo secondary necrosis, there are several key immunological responses from professional phagocytes that differ from efferocytosis of apoptotic cells: Enhanced antigen presentation, up-regulation of co-stimulatory molecules, and release of pro-inflammatory cytokines[338]. The Mellman lab was the first to show that antigen presentation of phagocytosed material does not occur in dendritic cells unless they were first stimulated with LPS[339]. Similarly, it was later shown that antigen presentation is enhanced specifically by the uptake of necrotic but not apoptotic cells[340]. These and other studies indicate that MHC binding alone is not sufficient to elicit a response from an adaptive immune cell. Co-stimulatory molecules are also required to activate lymphocytes. CD40, CD80, and CD86 are up-regulated in the pro-inflammatory environment of necrotic, but not apoptotic, cell clearance[341,342]. The release of pro-inflammatory cytokines by activated phagocytes, including IL-1, TNFα, IL-6, provides a third signal to adaptive B and T cells that causes their expansion and activation[343]. Many of these changes result from TLR signaling (mentioned previously) and other pattern recognition receptors including Nod-like receptors, lectin receptors, and C type lectin domain containing 9A (CLEC9A/DNGR-1)[344]. TLR activation preserves peptides (and other molecules) that will be used for antigen presentation by modulating phagosome acidity; this contrasts TLR-negative phagosomes whose contents are fully degraded[271,345]. The combination of these events leads to the activation of self-reactive adaptive immune cells, which over time may lead to loss of self-tolerance and autoimmune disease.

It has been well-established in the literature that defects in efferocytosis lead to autoimmune disorders in humans and mice such as systemic lupus erythematosus (SLE), rheumatoid arthritis, pulmonary diseases including asthma and chronic obstructive pulmonary disease (COPD), atherosclerosis, and type I diabetes[290]. Chapter 2 of this dissertation will focus on SLE. SLE is a pleiotropic, chronic autoimmune disease with wide-ranging symptoms that affect many organ systems and both the innate and adaptive immune systems exhibit dysregulation[346]. Characteristics of SLE include autoantibodies against nuclear components such as anti-double stranded DNA and anti-ribonucleoprotein, deposition of immune complexes, and upregulation of inflammatory responses and tissue damage[347]. Current SLE treatments include antimalarial drugs, steroids, nonsteroidal anti-inflammatory drugs (NSAIDs), and immunosuppressors, however, better targeted therapies with fewer side effects are needed[348].

Given the heterogeneity of SLE, there are probably multiple underlying causes for its development. However, a subset of cases arise from defective apoptotic cell clearance, causing apoptotic cells to undergo secondary necrosis. As described above, this leads to a shift from anti- to pro-inflammatory responses to cellular corpses, presentation of self-antigens, and stimulation of autoreactive lymphocytes. There are a number of observations that support defective apoptotic cell clearance as the etiology of lupus. SLE patients have higher than normal numbers of apoptotic cells and nucleosomes in circulating blood[349,350], there are decreased numbers of macrophages in germinal centers of SLE patients[351], professional phagocytic cells isolated from SLE patients have reduced phagocytic capabilities[352], there is an accumulation of dead cells in various organs of SLE patients[353,354], exogenous injection of apoptotic cells into mice results in SLE[355], blocking the ‘eat me’ signal PS results in SLE in mice[356], and genetic loss of function genetic variants in molecules involved in any stage of efferocytosis leads autoimmune disorders[290,357]. The loss of self-tolerance further propagates the disease by causing excessive cell death and organ damage, production of autoantibodies, and chronic

inflammation[310]. The precise molecular mechanisms leading to SLE are not fully understood and are probably pleiotropic, requiring more research to elucidate and potentially find new treatments.

Section 1.5: Background on the Jedi receptor

Summary of previous findings from the Carter lab

As previously mentioned, approximately 50% of DRG neurons die during embryonic development due to competition for peripheral target neurotrophins. The Carter lab discovered that satellite glia are non-professional phagocytes responsible for removing dying DRG neurons during this wave of developmental cell death[358]. Satellite-glia mediated internalization of sensory neurons was dependent on the Type I transmembrane protein Jedi (PEAR1/Megf12), a mammalian homolog of the *C. elegans* and Drosophila engulfment receptors CED-1 and Draper, respectively. Two later papers used culture systems to delineate downstream signaling of Jedi activation that ultimately causes internalization of dying cells[359,360]. Briefly, these papers revealed that Jedi signals through its ITAM repeats, the tyrosine kinase Sky, and the adaptor protein Gulp similar to its fly homolog Draper and other mammalian engulfment receptors. Nevertheless, the *in vivo* data presented in this dissertation do Jedi having a critical role in homeostatic efferocytosis. Therefore, it is useful to review some of the limitations of the original finding.

By far the strongest data presented by Wu et al. consists of all of the primary DRG cell culture work. These cultures require double axotomy of sensory ganglia and enzymatic digestion into single cells. Although enriched for neurons and satellite glia, these cultures will inevitably contain other cell types such as Schwann cells, fibroblasts, endothelial cells, and probably many others. As is the case with primary culture of any cell type, not just DRGs, the

harsh process of selecting cells to grow in a dish will undoubtedly change their behavior relative to an intact animal. With these caveats in mind, Wu et al. show S100+, brain-type fatty acid binding protein (BFABP+) glial precursor cells containing extra-nuclear DNA that co-localizes with the lysosomal marker lysosome-associated membrane glycoprotein 1 (LAMP1). This data indicates that S100+BFABP+ cells are phagocytic *in vitro*. To demonstrate that Jedi mediates this phenotype, the authors perform reverse-transcriptase polymerase chain reaction (RT-PCR) on cultures enriched for either neurons or glia, although the method of this enrichment and level of purity is not clearly indicated. Gels of RT-PCR product show Jedi RNA expression in both neurons and satellite glia, whereas my data presented in Chapter 3 is unable to detect Jedi protein expression using standard immunostaining techniques. This discrepancy may be a result of RNA and protein not correlating with one another, the relative insensitivity of immunostaining compared to PCR-based techniques, or cell type contamination that inevitably results from pooling samples to asses bulk RNA levels.

The authors modulated the expression of Jedi by overexpressing it in DRG cultures or knocking it down with two independent small hairpin RNAs (shRNAs). Validation of this knock-down was performed in a human embryonic kidney (HEK) cell line overexpressing Jedi but not confirmed in DRG cultures. While overexpression of Jedi did increase engulfment and its knock-down (KD) did decrease engulfment, the physiological relevance of Jedi overexpression and the lack of validation of the shRNA makes it impossible to rule out the possibility that other proteins involved in phagocytosis were affected.

The authors also looked *in vivo* for evidence of Jedi as an engulfment receptor. In sections of embryonic DRGs during maximal neuronal apoptosis, they do observe neuronal cells with pyknotic nuclei being enveloped by BFABP+ satellite glia. However, their basal morphology is to wrap around and enshroud sensory neuron cell bodies. Therefore, it is unclear whether apoptotic neurons are actually being internalized by satellite glia, or they surround the

neuron because that is their normal state. They follow up with EM studies showing apoptotic nuclei inside of other cells, but there no way of identifying the phagocytes as satellite glia or the bait as neurons. This assumption is made solely based on morphology and not immunogold labeling with markers. Another interesting *in vivo* experiment was performed in *C. elegans*, because as mentioned, Jedi shares homology with a well-characterized engulfment receptor in this model organism, CED-1. In these experiments, the endogenous ced-1 gene was deleted and replaced under the same promoter with mammalian full length Jedi or a chimeric extracellular Jedi-intracellular CED-1 protein in order to rescue ced-1 deletion at physiological levels. While the extracellular domain of Jedi did seem to accumulate around dead cells, full length Jedi was not well expressed in *C. elegans* and therefore could not be tested for phagocytic competence. Additionally, phagocytosis was evaluated in worm gonads, not DRGs like the other mouse experiments. Overall, while some of this data is certainly suggestive of satellite glia phagocytosis by means of Jedi, there is a dearth of *in vivo* data to support this hypothesis.

The role of Jedi in humans

A number of studies have used genome wide association studies (GWAS) to identify genetic components that may contribute to variability in platelet clotting at baseline and in response to anti-coagulation drugs, which has huge impacts on many aspects of cardiovascular health, including myocardial infarction, stroke, and peripheral artery disease ischemia. A number of these studies have identified single nucleotide polymorphisms (SNPs) of Jedi that are highly significant for changes in platelet aggregation[361–370]. An alternative name for Jedi is Platelet Endothelial Aggregation Receptor 1 (PEAR1), so named due to its expression by endothelial cells and platelets and role in platelet activation[371]. Most of the GWAS studies used peripheral blood collected from patients before and after anti-platelet therapy such as low dose

aspirin or clopidogrel. Although several SNPs fell out of these studies, there was one particular Jedi SNP that was repeatedly identified to be significantly associated with reduced clotting, rs12041331. rs12041331 is much more prevalent in African Americans compared to Caucasians with a minor allele frequency of 30% vs 10%[365,366]. At baseline, most papers show either no change or a slight reduction in blood clotting, but after low dose anticoagulant treatment homozygous rs12041331 carriers have a very pronounced decrease in clotting responses. Heterozygotes have an intermediate phenotype that in most reports does not reach statistical significance. Despite a reduction in clotting, rs12041331 carriers have a higher risk for adverse cardiovascular-related events including ischemic stroke, stent thrombosis, and heart attack[364]. It is unknown why reduced clotting in rs12041331 patients increases risk for a cardiovascular event, since the opposite would be predicted, but this data suggests that the standard of care antiplatelet therapy may not be an ideal choice for all patient populations. The current working hypothesis is that the thrombi formed in rs12041331 carriers are unstable and vulnerable to plaque rupture.

Because this particular Jedi SNP was identified in so many of the GWAS studies, rs12041331 has been particularly well characterized. rs12041331 is a G to A mutation located in the first intron of Jedi in a cytosine-phosphate-guanine (CpG) island upstream of the first coding exon. Methylation of CpG islands was traditionally viewed as a silencing mark for transcription, however, recent genome-wide mapping of DNA methylation reveals a more complex relationship that is highly context-dependent[372]. In the case of Jedi, CpG methylation in the first intron is associated with higher rates of transcription. When the methylation of this CpG island is disrupted by the G to A mutation in rs12041331, Jedi transcription decreases leading to a reduction in total protein levels[363,373,374]. In conclusion, the rs12041331 Jedi SNP essentially acts as a KD of Jedi for which the Jedi KO mouse presumably would serve as a good model.

Jedi studies in mice outside the somatosensory nervous system

Given the human data showing that a decrease in Jedi expression affect platelet function, a KO mouse of Jedi was used to evaluate murine platelet aggregation. Note that the Jedi KO mouse model used in the study is the same one used in this dissertation. However, with and without aspirin treatment, Jedi KO mice did not recapitulate the human clotting phenotype[375]. The reason for this discrepancy between *Mus musculus* and *Homo sapiens* remains unknown[376].

Despite finding no change in clotting in the absence of Jedi, the same lab did find other interesting phenotypes in the Jedi KO mouse model. For example, Jedi they found that Jedi negatively regulates proliferation by activating phosphatase and tensin homolog (PTEN), thus inhibiting AKT serine/threonine kinase 1 (AKT) signaling[377]. Jedi expression increases as megakaryoblasts differentiate into platelets, correlating with decreased proliferation[378]. High levels of Jedi expression has also been reported in endothelial cells, where it negatively regulates proliferation and migration[371,379]. Negative regulation of endothelial cell proliferation and migration causes Jedi KO mice to have severe defects in neoangiogenesis that ultimately resulted in enhanced healing in Jedi KO mice after either femoral artery ligation or cutaneous wounds [380]. It is unclear whether humans harboring SNP rs12041331 also heal faster than their wild type (WT) counterparts, although a positive benefit to rs12041331 may explain the high prevalence of this allele in the population.

Section 1.6: Nerve injury repair

Introduction

One scenario where phagocytic clearance of cellular debris plays a critical role in the nervous system is following a nerve injury. Twenty million Americans per year suffer from

peripheral nerve injuries caused by trauma or medical disorders, resulting in $150 billion annual costs[381]. As previously discussed, sensory and other types of PNS neurons have extremely long axons that traverse the length of the animal. A nerve injury occurs when a traumatic event separates the cell body from the terminal nerve ending structure. The PNS is often touted for its ability to heal after such injuries, whereas the CNS has almost no regenerative capacity[382]. Ramon y Cajal correctly observed that peripheral nerves regrow from the remaining proximal fibers still attached to their cell bodies[196]. Their successful reinnervation of target tissues requires the breakdown and removal of distally severed axons, which post-injury are no longer connected to the cell soma, and their associated myelin. While trauma to peripheral axons has a much better prognosis than a central spinal cord injury, epidemiological studies report that up to 50% of patients experience sub-par recovery and some studies indicate that only 10% of axons are able to regrow across a transected nerve[382–384]. Axon regeneration is affected by a number of factors, such as the type of injury, its proximal-distal location, age at time of injury, and type of surgical intervention. Improper fiber regeneration leads to severe defects in quality of life that include paralysis, severe pain, or loss of sensation[385]. Further research into peripheral nerve injury will benefit many other diseases, as the mechanisms of distal nerve degeneration and axon regeneration are similar in chemotherapy-induced peripheral neuropathies, Parkinson's disease, CNS injury, and glaucoma[167,386,387].

Molecular responses of the distal nerve stump to injury

The response of nerve cells distal to a nerve injury can be roughly separated into two distinct events. The first is degeneration and removal of pre-existing axon fiber structures (Wallerian degeneration) and the second is the creation of a pro-regenerative environment for new axon and myelin growth. Both topics will be discussed herein.

Wallerian degeneration, named after Augustus Waller who first described it in 1850, refers to all of the degenerative changes that occur in the distal stump of an injured nerve[388]. It really consists of two separate processes, the active disintegration of axons and myelin and the subsequent phagocytosis of the resulting debris[388]. Since Waller's discovery, it was believed for over 150 years that distal axons die because separation from their somas led to a lack of nutrients[389]. The serendipitous discovery of the 'Wallerian degeneration slow' (Wld^S) mouse model in 1989 challenged this assumption, as it showed that axons separated from their cell bodies could remain intact and electrically functional for weeks rather than the normal breakdown within ~1.5 days[390,391]. In the nearly 30 years since this discovery, the mechanism of Wld^S mice is still controversial. Despite the lack of consensus on its molecular underpinnings, Wld^S mice were the first indication that axon degeneration following injury is an *active* death process akin to apoptotic cell death.

Wld^S is a tandem triplication of a genetic fusion of the first 70 amino acids of the N terminus of the gene ubiquitination factor E4B (ube4b), followed by translation of 18 amino acids in the 5' UTR of the gene nicotinamide nucleotide adenylyl transferase 1 (nmnat1), and finally full length nmnat1. Ube4b is an E4 ubiquitin ligase, although the truncated region associated with Wld^S does not have enzymatic activity[392]. However, N terminal Ube4b is essential for the Wld^S phenotype, although it is unclear whether this is due to the presence of the 5' localization signal that drives the protein out of the nucleus or its binding to other proteins such as valosin-containing protein (VCP)[393,394]. NMNAT1 is an enzyme that converts nicotinamide mononucleotide (NMN) to nicotinamide adenine dinucleotide (NAD^+). NAD^+, the reduced form of NADH, plays a central role in cellular metabolism as a cofactor for glycolysis, oxidative phosphorylation, citric acid cycle, redox reactions, and post translational protein modifications[395]. Nmnat1 enzymatic activity is unequivocally required to confer the Wld^S phenotype, as enzymatically dead versions do not have neuroprotective properties in flies or

mice[396,397]. There are 3 NMNAT mammalian family members, Nmnat1/2/3 which localize to the nucleus, Golgi/cytoplasm, and mitochondria, respectively[398,399]. Nmnat2 is synthesized in the cell bodies and continuously anterogradely transported to axons due to a very short half-life of less than 4 hours[400]. Upon nerve injury, Nmnat2 can no longer be delivered to distal axons, causing an increase in its substrate NMN and a decrease in its product NAD+ within 2–4 hours[401,402]. It is unclear whether it is the loss of NAD^+, the gain of NMN, or the increased ratio of NMN to NAD^+ that leads to axonal fragmentation[401,403]. When ectopically expressed in WT axons, the Wld^S fusion protein phenocopies the axonal preservation phenotype observed in the original Wld^S mouse[404]. There is other evidence to show that the mechanism Wld^S prevention of axonal disintegration is more complex than the rescue of Nmnat2, however, this is beyond the scope of this work and is reviewed in[389]. Wld^S not only is protective for Wallerian degeneration but also improves the outcome of many CNS and PNS neurodegenerative diseases – suggesting that the mechanisms of axon death are shared in injury and disease[405]. However, Wld^S does not protect against neuronal cell body apoptosis or axon pruning, indicating these are distinct molecular pathways[406].

The discovery of the Wld^S mouse has had a tremendous influence on the field of axon biology, as it was the first indication that an active axon death pathway existed. However, since the Wld^S protein is a gain of function mutant, there has been considerable work in discovering the endogenous pathways for axon degradation. Like apoptosis, axon death probably has intrinsic and extrinsic initiation signals, but the relative contribution of these to Wallerian degeneration is difficult to quantify. Unlike apoptosis however, caspases are *not* required for axon fragmentation[407,408]. Rather, axon degeneration relies on a family of non-lysosomal, calcium-dependent proteases called calpains[409]. Following neve injury, the distal axons experience two waves of calcium influx – an short, rapid initial wave originating from the extracellular space and a long-term second wave from intracellular stores such as

mitochondria[410–412]. Wld^S zebrafish maintain the first but not the second wave of calcium influx in distal axons post injury, suggesting that the second round of calcium influx is important for calpain activation[410,412]. The Wld^S fusion protein localizes to axonal mitochondria, further supporting the role of late calcium released from intra-axonal stores in initiating axon death[411].

A forward genetic screen in Drosophila identified an endogenous mediator of distal axon degeneration activated by calcium called Drosophila sterile alpha/Armadillo/Toll-Interleukin receptor homology domain (dsarm) which was confirmed in mice where it is called Sarm1[408]. Dsarm/Sarm1 mutants phenocopy Wld^S, indicating that Dsarm activation is essential for injury induced axon degeneration[408,413–415]. The toll-interleukin receptor (TIR) domain of dsarm/Sarm1 contains NADase activity similar to Nmnat[416]. Aberrant Sarm1 activity causes axon degeneration in the absence of injury, suggesting that Sarm1 depletion of NAD^+ is an important mechanism of axonal death[413,417].

As previously mentioned, endogenous Nmnat2 has a very short half-life, so when axonal injury terminates anterograde delivery, local concentrations of its substrate NMN increase and its product NAD^+ decrease. Highwire (Hiw) in Drosophila or PAM/Highwire/RPM-1 (Phr1) in mammals is the E3 ubiquitin ligase responsible for such fast turnover of axonal Nmnat2[418,419]. Removal of Hiw or Phr sustains Nmnat2 levels in WT mice or flies and prevents axonal degeneration for 5–10 days in mice or up to two weeks in flies[420]. It is unclear whether there are other Hiw/Phr targets for ubiquitination that contribute to axon degeneration.

Thus far, I have provided several examples of intrinsic mediators of axonal degeneration that all affect a critical modulator in this process, the NMN/NAD^+ ratio. How these various proteins and signaling molecules, including Nmnat protein family members, calcium, Sarm1, and Phr, interface with one another is not entirely clear.

Wallerian degeneration includes not only to distal *axon* death but also distal myelin breakdown. Throughout development and maintenance of both myelinating and non-myelinating

Schwann cells, axon cues dictate Schwann cell phenotype[421]. When distal axons degenerate through the mechanisms described above, Schwann cells undergo a remarkable de-differentiation program and enter a 'repair' state, where they are sometimes called Bungner Schwann cells. The first stage of Schwann cell de-differentiation applies to both myelinating and non-myelinating Remark cells. Myelin associated genes including the transcription factor Krox20, cholesterol synthesis enzymes, and myelin proteins MPZ, MBP, MAG, and periaxin are down-regulated while genes more characteristic of immature and Remark Schwann cells are up-regulated such as NCAM, p75, GFAP, and L1[422,423]. However, de-differentiated Schwann cells are distinct from immature cells in their unique expression of Olig1 and Shh[424]. The known axonal cues that trigger Schwann cell response to injury and the downstream effectors of this process have yet to be fully elucidated.

Axonal Nrg-1 and Schwann cell ErbB2/3 signaling is probably one of the best understood relationships between axons and Schwann cells that plays an important role in myelination, differentiation, survival, and migration during development[82,83,425,426]. Despite its well-established role in Schwann cell differentiation, Nrg1-ErbB signaling after nerve injury is more controversial. Schwann cells lose contact with axons during Wallerian degeneration, therefore Nrg1 input is lost. Some studies have shown that both Nrg1 and ErbB2 are dispensable for the maintenance of axon and myelin in healthy adult animals and have no effect on de-myelination, Schwann cell proliferation, or macrophage recruitment after injury[85,427]. Therefore, loss of axonal Nrg1 does not play an essential role in Schwann cell de-differentiation, but what about re-myelination after Wallerian degeneration? Nrg-1 is surprisingly not essential for re-myelination after injury, although its absence does delay the process significantly[427,428]. This is quite different from initial development of myelin and contributes to a larger body of evidence showing that immature Schwann cells and repair Schwann cells are molecularly and functionally distinct from one another. Despite not being essential for re-myelination after injury,

Nrg1-ErbB signaling does accelerate the process and contribute to the thickness of the myelin sheath[86,427]. Additionally, exogenous application of soluble Nrg1 isoforms has beneficial effects on Schwann cell proliferation and migration[429–431]. The role of Nrg1-ErbB signaling is therefore complex – it seems that lack of axonal Nrg1 is not necessary for myelin breakdown and that there are alternative mechanisms for remyelination post injury, but axonal Nrg1 can have beneficial effects in recovery.

Axons release a number of factors after injury that may play a role in Schwann cell de-differentiation. These include mitochondrial DNA, cytochrome C, and hydrogen peroxide, which can all each lead to mitogen activated protein kinase (MAPK) signaling in Schwann cells within minutes[432]. Schwann cells express a number of TLR receptors, especially TLR3, 4 and 7, which may respond to these axonally-derived danger signals[433,434]. Activation of TLRs in Schwann cells causes up-regulation of pro-inflammatory signaling mediators such as TNFα, IL-1β, monocyte chemoattractant 1/C-C motif chemokine ligand 2 (MCP-1/CCL2), and nitric oxide, which are important for macrophage recruitment[435].

Another insight into Wallerian degeneration that the Wld^S mouse provided was that myelin disintegration is not totally dependent on axonal death. Takada et al. performed detailed studies of myelin in Wld^S mice and found that despite intact axons, there was evidence for myelin destruction, indicating that Schwann cell de-differentiation is at least partially independent of axons[436]. A similar observation was found in Death Receptor 6 (DR6) KO mice, where axons distal to nerve transection remained intact but myelin integrity was compromised[437]. Parsing out the temporal cues that coordinate degeneration of distal stump axon and myelin will require further studies, but regardless of the cues that initiate Schwann cell de-differentiation, many pathways (MAPK, Notch, mammalian target of rapamycin complex 1 [mTorc1]) activated in distal stump Schwann cells converge on activation of the master regulator of Schwann cell plasticity, c-Jun[438,439].

c-Jun is a transcription factor that is highly up-regulated in distal Schwann cells post injury. In Schwann cell conditional c-Jun KO mice, there is catastrophic failure to recover from nerve trauma[440]. c-Jun is not required for development of myelinating or Remak Schwann cells and is therefore unique to injury repair Schwann cells (although it is expressed at low levels in non-myelinating adult Schwann cells[441]), but is essential for de-differentiation of Schwann cells. In conjunction with other transcriptional regulators, c-Jun is responsible for down-regulating pro-myelinating genes (Krox20, myelin basic protein [MBP], and myelin protein 0 [P0] for example) post injury[423]. In addition to its suppressive role in myelinating genes, c-Jun also activates transcription of a number of repair genes in Schwann cells including trophic factors that are important for survival of neuron somas (glial cell line-derived neurotrophic factor [GDNF], artemin, brain-derived neurotrophic factor [BDNF]), axon growth (N-cadherin), myelinophagy (discussed below), and inflammation (TNFα, IL-1a, IL-1β, MCP-1, macrophage inflammatory protein 1 [MIP-1], IL-10, TGFβ, galectin-3)[442–444]. The importance of repair Schwann cells in axon regeneration is demonstrated by Schwann cell condition c-Jun KO mice, which after injury have substantial decrease in axon regeneration due to increased neuronal death[440]. There is a critical time after injury in which axon regeneration successfully occurs; 2-3 months after injury there is a precipitous decline in axon regeneration rates due to a drop in Schwann cell c-Jun levels. However, exogenous induction of c-Jun expression at later time points restores axon regeneration rates to their initial levels[445]. Additionally, aged animals are unable to induce c-Jun post injury and have corresponding poor outcomes, but their recovery can also be rescued by addition of c-Jun[446].

So far, I have discussed some of the molecular responses to peripheral nerve injury that occur in the distal stump that initiate axon death and myelin breakdown. As discussed in the *Section 1.4: Phagocytosis*, cellular debris is removed through the process of phagocytosis. In a nerve injury, this applies to the cells directly affected by the assault but also the axons and

myelin distal to it. If left uncleared, axonal and myelin debris inhibit axon regrowth[447–449]. Slower regeneration in older mice seems to be due to inefficient clearance of debris, not diminished neural regrowth capacity[450,451]. When Wallerian degeneration is impaired, as in the Wld^S mouse, axon regrowth is severely inhibited[452,453]. While there is general consensus in the field that myelin debris negatively affects regeneration, there are some reports to the contrary[454]. Experimental conditions such as the degree of myelin degeneration, growth factors, and adhesion factors present may explain this result.

50% of distal myelin is removed by Schwann cells themselves through a specialized autophagic process sometimes referred to as myelinophagy[455]. Myelinophagy occurs at early time points (3-5 days) post injury before immune cell migration[455]. Logically it makes sense that Schwann cells use autophagy to clear their own myelin debris since it is the typical mechanism for self-digestion of cellular organelles and there is no evidence that myelin actually separates from the Schwann cells during the *early* phases of Wallerian degeneration. However, Schwann cells may also utilize efferocytosis or phagocytosis to internalize extracellular debris at later time points after the injury. c-Jun reprogramming of Schwann cells is important for myelinophagy, as c-Jun induces IL-1β and TNFα production, which acts in an autocrine manner to activate both cytosolic and secreted forms of phospholipase A_2 (PLA_2)[456]. PLA2 hydrolyzes phosphatidylcholine, which is highly enriched in myelin, into LPC and arachidonic acid (AA) causing the myelin sheath to collapse into ovoid fragments within the cytoplasm[457,458]. This myelin debris is present in double membrane autophagosomes generated by classical autophagy related protein LC3 A/autophagy related 7 (LC-3/Atg7) autophagic signaling and eventually degraded in lysosomes[459]. In these early stages after the injury, other cell types like perineurial cells have also been shown to phagocytoses distal debris[460].

During the second phase of debris clearance, which occurs around 4-14 days after injury, the remaining 50% of distal myelin and axonal fragments are cleared by infiltrating

myeloid cells, namely neutrophils and macrophages (note that resident endoneurial macrophages, which constitute 2–9% of nucleated cells in the nerve at baseline, proliferate and contribute to the initial wave of engulfment along with Schwann cells, whereas the second wave of macrophages are monocyte derived and infiltrate from the blood[461–464]). In order for neutrophils and monocytes to enter the nerve and clean up the remaining axon and myelin remnants, the BNB must breakdown[465]. Initially the physical injury will compromise the BNB at the lesion itself, but distal to this the BNB will continue to be leaky for at least four weeks with maximal permeability after 4–7 days corresponding to myeloid infiltration[149,466,467]. Loss of BNB integrity is due to decreased expression of tight junction proteins and adhesion molecules in both the endoneurial vasculature and the perineurium[175,176]. Reprogrammed repair Schwann cells and resident macrophages produce VEGF, which when added exogenously in the absence of injury mimics the same leaky effects on the BNB[175].

Given the discussion in *Section 1.4: Phagocytosis* regarding the engulfment of dead cells and its relation to loss of self-tolerance that can lead to autoimmune disorders, it is worth considering whether Wallerian degeneration occurs under anti- or pro-inflammatory conditions. Schwann cells and macrophages both express MHCI and II and are capable of antigen presentation, most likely to T cells that enter the nerve approximately 3 weeks after injury[468]. In the first few days after the injury, there is an acute pro-inflammatory phase triggered by damage-induced necrosis and leakage of intracellular contents. This first phase of Wallerian degeneration is characterized by pro-inflammatory cytokine production by Schwann cells, typically TNFα, IL-1a, IL-1β, colony stimulating factor 2 (GM-CSF), and IL-6[469]. These cytokines/chemokines enhance the breakdown of distal axons and myelin, promote BNB breakdown, and recruit myeloid cells. However, entry of macrophages into the nerve marks the second phase of anti-inflammatory Wallerian degeneration characterized by the reduction of TNFα and IL-1β and production of IL-10, and IL-6[470]. The activation status of “pro-inflammatory”

M1 versus “anti-inflammatory” M2 macrophages within a damaged nerve is debated in the field, but in reality there are probably dynamic populations of both types of macrophages that depend on the physical and temporal proximity to the injury[471,472]. Our understanding of the ligands and receptors used to engulf axonal and myelin debris supports that both phagocytic and efferocytic mechanisms are involved in Wallerian degeneration. For example, some reports illustrate the use of classic efferocytosis anti-inflammatory engulfment machinery in Wallerian degeneration: PS serves as an important axonal ‘eat me’ signal and the TAM receptors Axl and MerTK mediate immunologically silent clearance[473–475]. On the other hand, damaged axons have also been shown to release classical ‘danger’ signals including hydrogen peroxide, DNA, and cytochrome c and pro-inflammatory receptors such as TLRs, complement, and FcγRs, are also important for debris clearance during Wallerian degeneration[432,434,435]. A more precise timeline that delineates when and where each of these clearance mechanisms occurs is needed to fully understand how the resolution of inflammation occurs in the PNS. Future studies will hopefully be able to apply lessons learned from PNS injury recovery to CNS regeneration, where the injury sight remains chronically inflamed, develops a glial scar, and currently has very poor prognostic recovery outcomes[476,477].

Molecular responses of the proximal nerve stump to injury

As previously mentioned, 50% of DRG neurons die during development due to neurotrophin deprivation. As the neurons age, however, they no longer require trophic support for survival[478–480], and the somatosensory neurons you are born with are the same cells you will die with. Reinnervation after a nerve injury can occur through two mechanisms: collateral branching of uninjured axons or regeneration of injured axons[481]. For the latter to occur, the proximal fibers and their somas must survive long enough to re-innervate their original targets. The resistance of adult versus early post-natal sensory neurons to programmed cell death is

readily apparent after axotomy. Approximately one third of adult versus two thirds of neonate DRG neurons will die following injury (note that the exact numbers depend on a number of other factors such as the type/size of injury, its proximal-distal location, and type of neuron)[478,482–485]. Loss of neurons after an injury is one of the most influential factors on functional recovery after nerve damage[486,487]. Therefore, preventing neuron cell death will greatly improve patient outcome.

There are a number of mechanisms by which adult neurons resist apoptosis, mostly by inhibiting machinery in the intrinsic mitochondrial apoptotic pathway. Embryonic DRGs undergoing trophic deprivation utilize the c-Jun N-terminal kinase (JNK) pathway to phosphorylate c-Jun. Phosphorylated c-Jun transcriptionally up-regulates expression of Bcl-2 homology (BH3)-only genes like Bim and Hrk. The BH3-only proteins inhibit pro-survival Bcl-2-like proteins and activate pro-survival Bax either directly or indirectly. Bax then oligomerizes and forms a pore in the mitochondrial membrane to release cytochrome c, which eventually forms the apoptosome along with scaffolding protein Apoptosome complex with apoptotic protease activating factor-1 (Apaf-1) and caspase-9. Eventually the apoptotosome activates effector caspases especially caspase-3[488]. Adult neurons resist programmed cell death by inhibiting multiple steps of this apoptotic process. For example, the expression of Bax decreases in DRG neurons with age and what little is left does not localize to the mitochondrial membrane even when the JNK pathway is experimentally activated[478,489,490]. microRNAs play a role in altering the expression of Bcl-2 family members with age[491]. Downstream of Bax, Apaf-1 and caspase-3 expression are also reduced with age due to epigenetic silencing[492]. Given the multiple fail-safes set in place by mature DRG neurons to avoid PCD, it is surprising that one third of them still die after peripheral nerve injury. This may be due to apoptosis-independent cell death mechanisms, or it may reflect injury-induced reprogramming of adult DRG neurons back to an immature state that is more permissive for axon outgrowth but simultaneously vulnerable to cell death [493,494].

Retrograde signaling from the site of injury to the cell soma must occur in order to facilitate transcriptional reprogramming of DRG neurons into a regenerative state. One of the most important signals that initiates this process in calcium influx into the cell following injury-induced breach of the plasma membrane. Intracellular calcium levels will reach millimolar levels at the site of the injury and will be propagated to the soma by L type voltage-gated calcium channels[495,496]. While this wave of calcium plays a critical role in membrane sealing, retrograde signaling, local translation, and growth cone assembly, excess intracellular calcium can lead to cell/axon death and therefore must be carefully regulated[497]. This initial calcium wave 'primes' retrograde axonal signaling by jump-starting a number of molecular events.

One mechanism by which intracellular calcium flux in the proximal neuron initiates regeneration is through epigenetic changes to nuclear histone modifications. Calcium activates serine/threonine protein kinase Cm (PKCm), which translocates to the nucleus and phosphorylates histone deacetylase 5 (HDAC5)[496]. phosphoHDAC5 then exits the nucleus allowing histone acetylation to accumulate on nucleosomes. Histone acetylation has beneficial effects on regeneration probably because it creates a more relaxed chromatin structure that can be readily accessed by transcription factors[498]. Cytoplasmic HDAC5 then deacetylates microtubules, allowing more dynamic microtubule assembly and disassembly which is important for extension of the growth cone and axon regrowth[499].

Calcium also activates dual leucine zipper kinase (DLK), a mitogen activated protein kinase kinase kinase (MAP3K) that plays multiple roles in axon regeneration. Calcium entry into the axon activates adenylyl cyclase and produces cyclic adenosine monophosphate (cAMP), which activates protein kinase A (PKA), which subsequently phosphorylates DLK[500]. phosphoDLK is responsible for dynein-dynactin mediated transport of itself, JNK-interacting protein 3 (JIP3), and JNK3 back to the nucleus[501]. DLK is not only responsible for JNK retrograde transport but also is upstream of JNK activation, as it phosphorylates mitogen

activated protein kinase kinase 1 (MEK-1)[502]. MEK-1 will subsequently phosphorylate JNK to activate it. Nuclear JNK signaling leads to phosphorylation of c-Jun, a transcription factor that, when bound to activating transcription factor 3 (ATF3), regulates regenerative reprogramming[503–505]. DLK also phosphorylates mitogen activated protein kinase kinase 4 (MKK-4), which subsequently phosphorylates p38[506]. Coordination of the JNK and p38 MAPK pathways by DLK is essential for proper axon regeneration[502].

Calcium entry into the proximal segment of injured axons also plays a role in the retrograde transport of locally translated transcription factors and other types of signaling proteins back to the nucleus. Proteomic studies have identified hundreds of proteins uniquely synthesized in the axon after injury, including cytoskeletal components, heat shock proteins, metabolic enzymes, and transcription factors[507]. p38 and mammalia target of rapamycin (mTOR) signaling are important regulators of local translation[508]. The importin family of nucleocytoplasmic transport factors containing a nuclear localization signal (NLS) are important for retrograde movement of these newly synthesized proteins via the dynein-dynactin motor complex. Calcium is important for regulating the translation of these proteins and their binding to importins and retrograde motor proteins. Some of the best studied of these targets includes signal transducer and activator of transcription 3 (STAT3), filamin A, phospho-extracellular signal regulated kinase 2 (phosphoERK), and vimentin[509,510].

These pathways are only a few of the interconnected array of signals that transmit to the DRG neuron nucleus that an injury has occurred to the axon. I have mentioned a few transcription factors that reprogram gene expression to favor regeneration, c-Jun, ATF3, and STAT3. There are a number of other transcription factors involved in this process as well, such as the mothers against decapentaplegic homolog (SMAD) family, cAMP responsive element binding protein 1 (CREB1), and p53. These transcription factors in combination with epigenetic changes alter the expression of over 1,000 genes after nerve injury[511]. scRNAseq of DRG

neurons after injury show that individual neurons respond differently to injury, which is not a surprise given their diversity described above[512]. Altered gene expression in DRG neurons following injury results in pro-regenerative changes but also influences pain, cell death/survival and inflammatory pathways. For example, c-Jun increases the transcription of integrins, galanin, and CD44[513], which play important roles in neurite outgrowth, while phospho-STAT3 upregulates Bcl-xl and regenerating family member 2 (Reg-2), which are pro-survival factors that prevent cell death[514]. I mentioned previously that the transcriptional reprogramming of DRG neurons mimics their developmental state where they initial grow out to their targets. This is true to some extent, for example, netrin signaling, which I will describe in more detail below is shared between embryonic and injured neurons. However, c-Jun is dispensable for axonal growth during development but is essential for regeneration after nerve injury[513].

Netrin signaling is one example of regenerative neurons repurposing a developmental program of axon pathfinding. Of the four known families of axon guidance cues, netrin-1 is the strongest chemoattractant for axon extension, depending on receptor expression[515]. Netrin-1 is a secreted, soluble laminin-like protein that is conserved in vertebrates, *C. elegans*, and Drosophila[516]. Netrin-1 receptors such as Deleted in Colorectal Cancer (DCC) and neogenin cause axon attraction, while Uncoordinated 5A-D (Unc5A-D) receptors facilitate axon repulsion[517]. In healthy adult DRG neurons, there are low levels of the attraction receptor DCC and high levels of repulsive receptors Unc5A-C[518,519]. Following a peripheral nerve injury, distal Schwann cells highly up-regulate Netrin-1 expression, while proximal axons up-regulate the attraction receptor DCC and down regulate repulsive receptors Unc5B and Unc5C[519–521]. These changes in gene expression reflect the reprogramming of Schwann cells and DRG neurons after injury, but the exact transcription factors responsible are unknown. Genetic studies show that heterozygous KO mice for Netrin-1 have impaired functional recovery and a decrease in regenerated fiber density[522]. Taken together, this data suggests that Netrin signaling plays a

significant role in axon regeneration after injury. There are significant differences between this repair signaling and development, however, as Netrin-1 cues during development are generated by target tissues or blood vessels, rather than repair Schwann cells[523]. Netrin signaling is only one example of many pathways that play a fundamental role in nerve injury repair, reviewed in[383,524,525].

Summary

Most of what we know about human peripheral nerve regeneration was initially found by Australian medical physician Dr. Sydney Sunderland in the aftermath of World War II. The war left many young soldiers with peripheral nerve injuries and Dr. Sunderland was fascinated by the spontaneous, full functional recovery of some patients but the utter lack of recovery in others[526]. Although the PNS is often touted for its regenerative capacity, even in modern times there is a significant need for improved clinical therapies for these types of injuries which preferentially affect young people like the WWII veterans[383,384,475]. Although Dr. Sunderland was not a molecular scientist per se, he is famous for recognizing the importance of fascicles in regeneration, which we now know are composed of perineurial glia. While it is clear that successful regeneration requires careful coordination of multiple cell types including neurons, satellite glia, Schwann cells, and macrophages, the molecular contribution of 'under-rated' perineurial glia and endothelial cells (and certain others) are only recently gaining recognition[460,527]. The third data chapter of this dissertation assesses the role of some of these non-neuronal cells in recovery after nerve injury. There are still many unanswered questions about the molecular machinery responsible for PNS regeneration, and these are still discussed today at the Sunderland Society meetings, founded in 1980 to honor Dr. Sunderland, "the father of modern nerve surgery." The primary goals of understanding these mechanisms are to improve the speed, frequency, and accuracy of re-innervating fibers

Section 1.7: Summary

The primary goal of this dissertation was to investigate the role of Jedi *in vivo* using a global, constitutive KO mouse model. Based on previous data in our lab, we hypothesized that Jedi was an engulfment receptor involved in the removal of dead cells. Loss of other engulfment receptors leads to accumulation of cellular corpses, constitutive inflammation, loss of self-tolerance, and eventually autoimmune disease. In Chapter 2 we assessed Jedi KO mice for lupus-like autoimmune disease. Given our previous knowledge of Jedi expression in the peripheral nervous system, we also investigated somatosensory phenotypes of KO mice *in vitro* and *in vivo* in Chapters 3 and 4.

CHAPTER 2

LOSS OF THE PHAGOCYTIC RECEPTOR JEDI DOES NOT LEAD TO LUPUS-LIKE AUTOIMMUNE DISEASE

Authors

Alexandra J. Trevisan, Ashley J. Wilhelm, Jillian P. Rhoads, Kristy R. Stengel, Scott W. Hiebert, Amy S. Major, and Bruce D. Carter

Section 2.1: Introduction

In a healthy adult human, more than ten billion cells turnover everyday just to maintain tissue homeostasis[357]. Proper organ function not only requires cell turnover but also a mechanism of disposal for these cellular corpses. In many epithelial cell types, such as the intestines and skin, 'old' cells are simply sloughed off into the extracellular milieu, but in many organs such as the spleen, testes, thymus, and lymph nodes, apoptotic cells are cleared by the immunologically inert process of efferocytosis, or phagocytosis of 'self' cells[528,529]. Efferocytosis must occur in a time efficient manner prior to loss of plasma membrane integrity of the target cell in order to avoid a pro-inflammatory phagocytotic response[530]. To this end, apoptosis and phagocytosis are highly coordinated processes that start with the release soluble "find me" chemokines (examples include fractaline, ATP, and UTP) from the dying cell that attract phagocytes to the vicinity of dying cells[531]. In turn, the apoptotic cells down-regulate cell surface expression of 'don't eat me' proteins (CD47, CD24, PD-L1) and increase cell surface exposure of 'eat me' signals like PS[232,234,532]. The phagocytic cell engages PS either directly or indirectly through various receptors, including BAI1, TIM4, members of the TAM family, SCARF1, and

integrin $\alpha_v\beta_3$, which initiate an intracellular signaling cascade that ultimately results in actin-dependent internalization of the dying cell. The contents of the resulting phagosome will eventually be degraded in the lysosomal compartment of the cell.

If, however, apoptosis and efferocytosis become temporally uncoupled, dead cells will no longer be recognized as 'self' and removed in an anti-inflammatory manner. Rather, the apoptotic cell will eventually undergo autolysis, leading to loss of plasma membrane integrity and extrusion of intracellular components, including nucleosomes, DNA, and RNA[530]. These molecules engage a different repertoire of receptors based on pattern-recognition that includes TLRs, complement, and FcRs; in other words, the secondarily necrotic cell is indistinguishable from foreign pathogens that initiate pro-inflammatory responses in the host immune system[248]. Chronic failure at any stage of efferocytosis leads to increased risk for a number of autoimmune diseases in humans and mice, including SLE[310]. Serum from mice and humans with SLE tests positive for autoantibodies that recognize all of the damage associated molecular patterns listed above, i.e. DNA, RNA, and nucleosomes. Further evidence for the role of defective dead cell clearance in SLE includes the following: SLE patients have higher than normal numbers of apoptotic cells in the blood, professional phagocytic cells isolated from SLE patients have reduced phagocytic capabilities, exogenous injection of apoptotic cells into mice results in SLE, blocking the 'eat me' signal PS results in SLE in mice, and genetic loss of function variants in molecules involved in any stage of efferocytosis leads autoimmune disorders[350,352,355–357].

Previously, our lab identified a novel mammalian engulfment receptor, Jedi (PEAR1/MEGF12) which is homologous to the *Drosophila* phagocytic receptor Draper and the *C. elegans* receptor CED1[358]. In non-phagocytic HeLa cells, exogenous Jedi expression is sufficient to confer phagocytic ability[359,360]. Based on *in vitro* studies, Jedi facilitates the engulfment of peripheral sensory neurons by satellite glial precursors during development of the dorsal root ganglia[358]. However, the role of Jedi in efferocytosis performed by professional

phagocytic cells such as monocytes, macrophages, dendritic cells, and neutrophils on a global scale remains unknown.

Literature from other labs has also identified Jedi expression in platelets in both humans and mice, where it plays a critical role in platelet activation[363,364,371,533]. While traditionally known for their role in clotting, emerging data also indicates that platelets play a significant role in the immune response by aggregating white blood cells at sites of infection or tissue damage, releasing cytokines and chemokines, and a controversial role as phagocytic cells themselves[534]. Platelets derived from SLE patients are hyperactive, and in mouse models the depletion of platelets improved diagnostic parameters while infusion of excess platelets exacerbated the disease[535]. Due to high Jedi expression in platelets, which tune the immune system's response to insult, and because KO mice of several other engulfment receptors leads lupus-like autoimmune disease, we wanted to investigate the role of Jedi in the context of autoimmune disease[536–538]. Since we found that Jedi acts as a phagocytic receptor *in vitro*, we predicted that if Jedi were important for efferocytosis, its absence in a KO mouse model would lead to similar phenotypes as knock-outs of other engulfment receptors, mainly, a deficiency in clearance of dead cells and subsequent SLE. In this study, we tested this hypothesis using a global Jedi KO mouse which we analyzed for defects in efferocytosis and signs of immune hypersensitivity.

Section 2.2: Results

Previously our lab published that HeLa cells overexpressing Jedi phagocytose inert carboxylated beads[359,360]. Here, we show that HeLa cells overexpressing Jedi also phagocytose apoptotic cells significantly more than controls, a much more physiologically relevant model for studying the clearance of apoptotic cells that occurs *in vivo* (Figure 1A). For this experiment, we

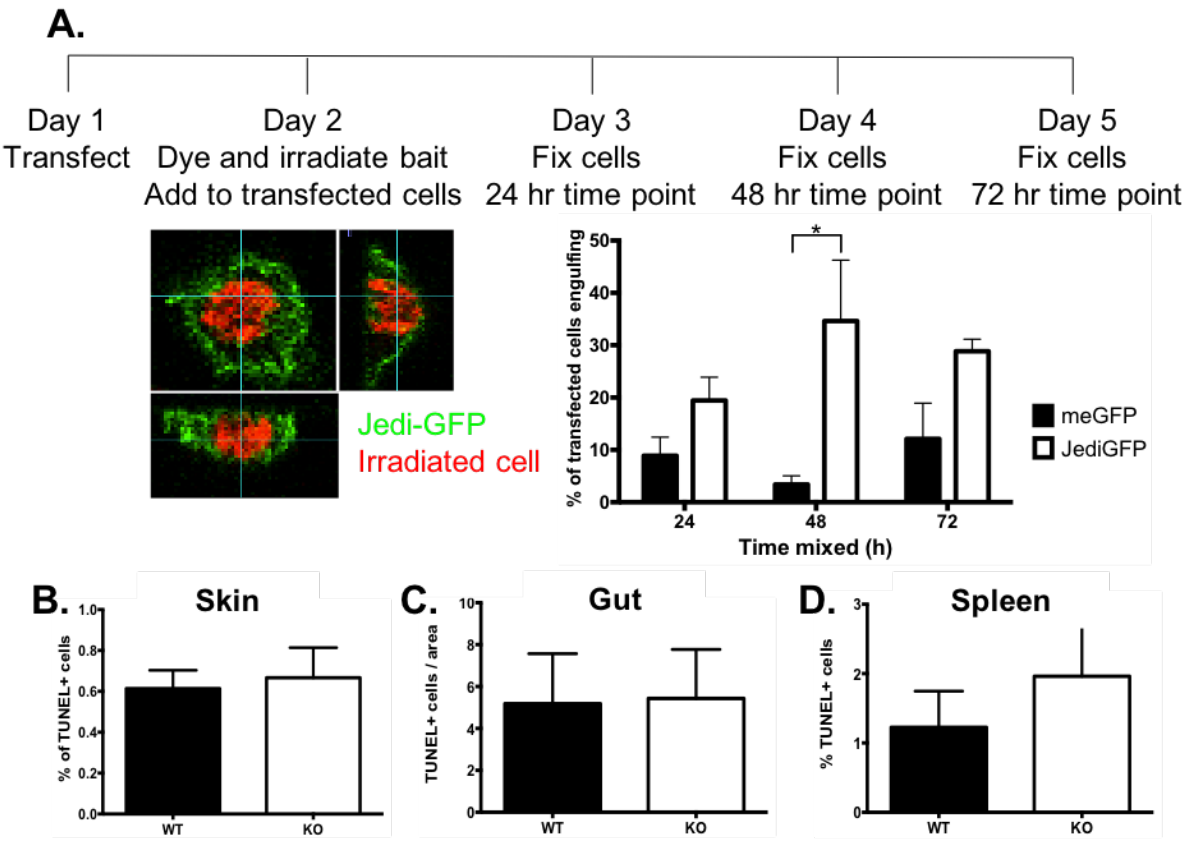

Figure 1: Overexpressed Jedi is an engulfment receptor *in vitro* but is dispensable for dead cell clearance *in vivo*. (A) HeLa cells overexpressing membrane bound GFP (meGFP) or JediGFP (green) were mixed with UV-irradiated HeLa cells (red) for various time points, fixed, and imaged by confocal microscopy. An orthogonal projection of an engulfing cell shown as an example. The percent of transfected cells containing a red cell is reported on the right. Error bars are SEM. 2 way ANOVA $p < 0.05$. (B-D) Adult WT and KO skin, ileum, and spleen were used for TUNEL staining. n=3 animals per genotype with at least 5 non-consecutive sections analyzed per animal. Error bars represent SEM. No statistically significant differences using student's t test in any group.

co-cultured HeLa cells overexpressing either a Jedi-green fluorescent protein (GFP) fusion protein[359] or GFP alone with HeLa cells that were fluorescently labeled (for the purpose of visualization) and then ultraviolet (UV)-irradiated to instigate cell death. Apoptosis in these UV-treated cells was confirmed using AnnexinV/propidium iodide (PI) staining (data not shown). We found that cells overexpressing JediGFP but not GFP alone had a statistically significant increase in engulfment 48 hours after co-culturing. At 24 and 72 hours there was a trend toward JediGFP increasing engulfment but it did not reach statistical significance. These new results

along with our prior work showing that Jedi is important for removing neuronal corpses during the development of DRG imply that Jedi is a bona fide engulfment receptor.

To test Jedi's role in the clearance of dead cells *in vivo*, we utilized global Jedi KO mice from the knock-out mouse project (KOMP) consortium. To see validation of this mouse model, please see Figure 7. If Jedi were important for removal of cellular corpses *in vivo*, we expected to see an accumulation of dead cells in tissues with high cell turnover, so, we performed Terminal deoxynucleotidyl transferase dUTP nick end labeling (TUNEL) staining in the skin, gut, and spleen. However, we did not observe a statistically significant increase in the number of dead cells in any of these tissues (Figure 1B-D). We also looked for dead cells in the DRG where we previously found Jedi to be important for phagocytosis, but did not find any changes their either (please see Figure 10 for this data).

Chronic failure to efficiently clear dying cells is one underlying causes for lupus like autoimmune disease, which is characterized by B and T cell dysfunction, autoantibody production, and end organ damage[539]. A previous graduate student in the lab preliminary found data to support this hypothesis[540]. We looked for overt problems in the mice by checking overall body weight, spleen weight, and kidney weight in mice 10–14 months old (Figure 2A-C), but we did not find statistically significant changes in any of these measures when stratified by sex. Additionally, we did not observe significant increases in the total number of spleenocytes or cells in lymph nodes (Figure 2D, 2E). We then went on to test for several diagnostic measures of SLE-like symptoms in the mice, such as the circulation of autoreactive antibodies (Figure 3A), proteinurea (Figure 3B), and dermatological symptoms such as scratching (Figure 3C and D) or leukocyte accumulation in the skin (Figure 2F). By all accounts, Jedi KO mice did not exhibit any characteristics of SLE-like disease. However, since these measures are late-stage readouts of severe autoimmunity, we performed flow cytometry analysis of lymphocyte populations because these cellular/molecular changes precede overt SLE symptoms[541,542].

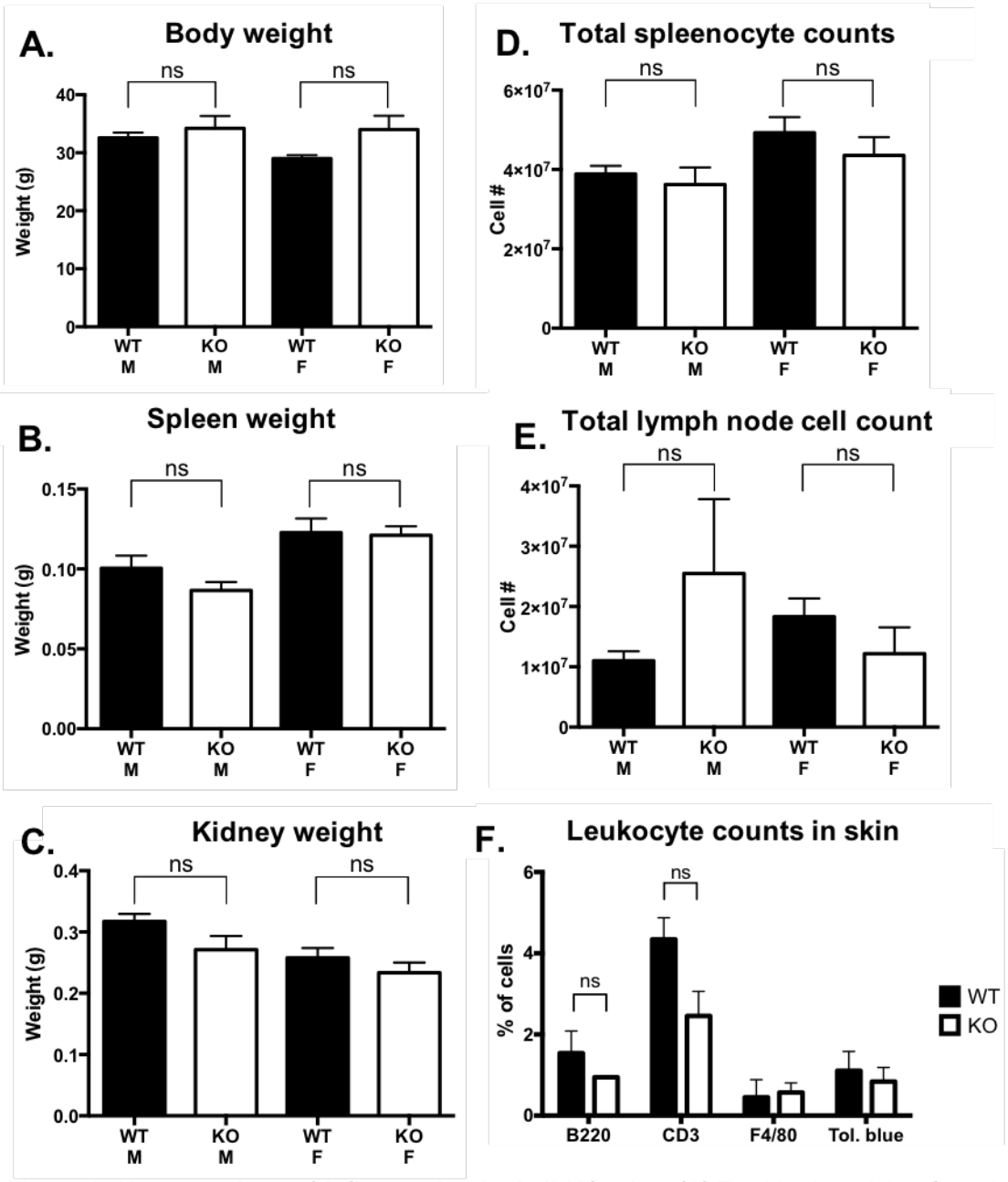

Figure 2: No overt signs of inflammation in Jedi KO mice. (A) Total body weight of aged mice 12–18 months old stratified by sex and genotype. n=3-7 animals per condition. No statistical differences as measured by Student's t test. (B) Total spleen weight of aged mice 12–18 months old stratified by sex and genotype. n=3-7 animals per condition. No statistical differences as measured by Student's t test. (C) Total spleen weight of aged mice 12–18 months old stratified by sex and genotype. n=3-7 animals per condition. No statistical differences as measured by Student's t test. (D) Total number of spleenocytes. n=3-7 animals per condition. No statistical differences as measured by Student's t test. (E) Total number of cells in lymph nodes. . n=3-7 animals per condition. No statistical differences as measured by Student's t test. (F) Percentage of B cells (B220+), T cells (CD3+), macrophages (F4/80+) and mast cells (Toluidine blue+) in the dermis and epidermis of adult mouse skin age 8-12 weeks old. n=3 animals per condition. No statistical differences as measured by Student's t test.

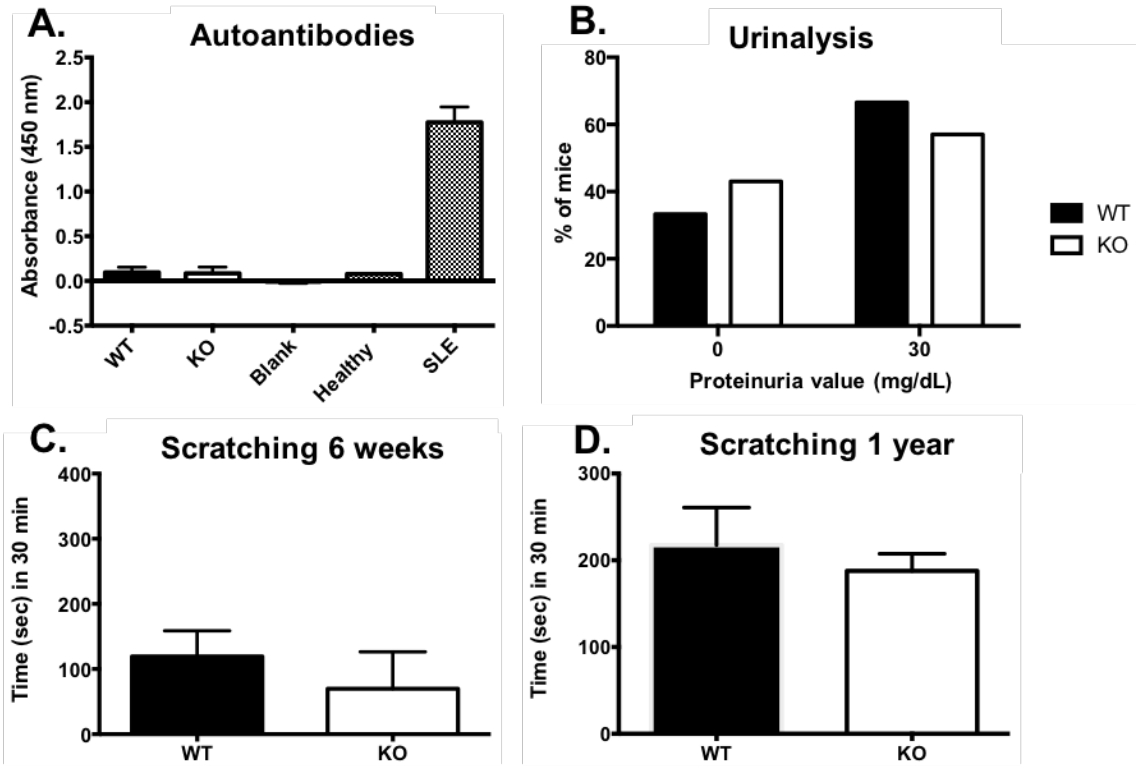

Figure 3: Jedi KO mice to not exhibit signs of lupus-like autoimmune disease. (A) ELISA of serum from mice age 12-18 m for anti-dsDNA antibodies. SLE mice were used as a positive control. n=7-10 mice per genotype. Error bars show SEM. No statistically significant difference found between WT and KO using student's t test. (B) Proportion of mice with proteinurea values of 0 or 30 mg/dL at age 12-18 m. No mice had values greater than 30. n=7-10 mice per genotype. No statistically significant difference using Fisher's exact test. (C and D) Mice were recorded for 30 minutes at 6 w or 1 y old. Videos were reviewed for hind limb scratching and back biting. Time spent performing these behaviors during the course of 30 min are shown for WT and KO animals. n=16-17 mice per genotype. Error bars show SEM. No statistically significant differences found using student's t test.

Since the dysregulation of autoreactive B cells is one of the most well-known characteristics of SLE, we first looked at various B cell types in the lymph nodes and spleen due to their role in antibody production. We used CD19+B220+(CD45R) to delineate mature B cells[543], but found no significant change in the percent of cells positive for these markers between genotypes in males or females (Figure 4A, 2B). Within this population of CD19+B220+ B cells, we looked at cell surface expression of surface MHCII due to its role in B cell activation, proliferation, and differentiation and its critical role in B-cell activation of CD4+ T cells[544] (Figure 4C, 4D). When stratified by sex, we did not observe statistically significant changes in MHCII expression in B cells between Jedi WT and KO mice. Finally, we evaluated the expression of another activation marker of B cells, the co-stimulatory molecule CD86, well known to be upregulated in SLE[545], but we did not find significant changes amongst genotypes in CD86 expression levels (Figure 4E and 4F). These results suggest that B cells are not intrinsically dysregulated in mice lacking the phagocytic receptor Jedi.

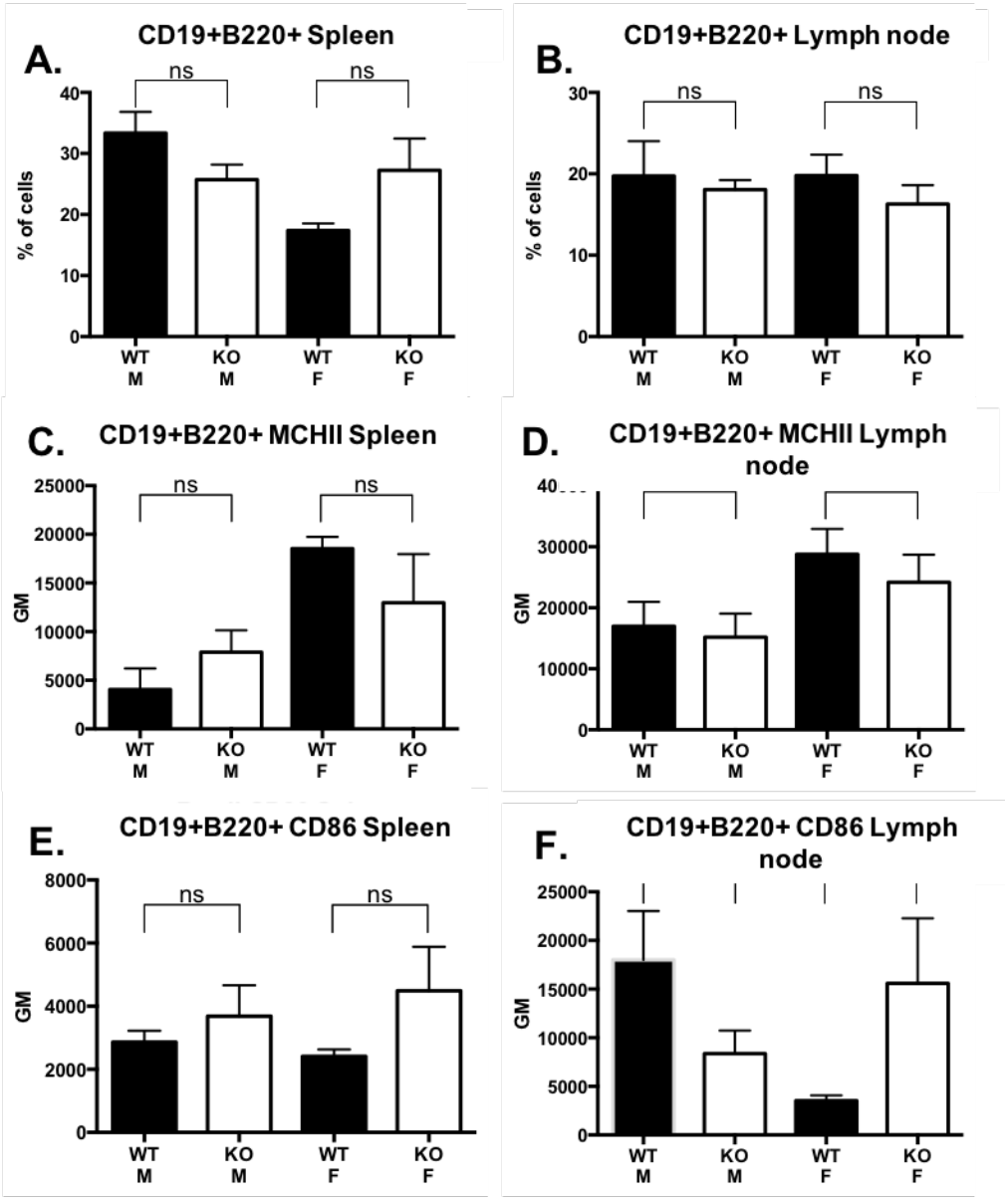

Figure 4: Aged Jedi KO B cells do not exhibit changes in number or activation status. (All) Spleens or lymph nodes from mice age 12–18 months old were dissociated and immunostained with antibodies against cell surface markers CD19, B220, MHCII, and CD86. (A-B) Proportion of CD19+B220+ mature, resting B cells in the spleen (A) or lymph nodes (B). No significant changes between genotypes within each sex. (C-D) Geometric mean (GM) of surface MHCII expression levels in CD19+B220+ B cells isolated from spleen (C) or lymph nodes (D). No significant changes between genotypes within each sex. (E-F) B cell activation status in spleen and lymph node was assessed by measuring surface expression of CD86. n=3-7 mice per genotype and sex. Error bars are SEM. No statistical significance using student's t test in any group.

T cells also play a critical role in the development and maintenance of SLE[546]; therefore, we assessed changes in the relative abundance of T cell subtypes and their activation status by flow cytometry in spleen and lymph nodes. The proportion of TCRβ+CD3+CD4+ T helper cells, which contribute to antibody production and tissue inflammation, were not significantly increased in Jedi KO mice (Figure 5A and 5B). Similarly, TCRβ+CD3+CD8+ cytotoxic T cells also did not have changes in cell number either in spleen or lymph nodes isolated from WT or Jedi KO mice (Figure 5C and 5D). T regulatory cells, identified by CD3+CD25+ are generally found in lower numbers in SLE patients and play an important role in the suppressing the activation and proliferation of self-recognizing lymphocytes[547], but we did not find a change in their numbers between sex-matched genotypes (Figure 5E and 5F). Lastly, we evaluated the percentage of double negative (DN) T cells by CD3+CD4-CD8- markers because they are often increased in SLE patients due to inactivation or exhaustion of autoreactive cytotoxic T cells[546] (Figure 5G and 5H). Again, however, we did not find changes to DN T cell numbers in the absence of Jedi.

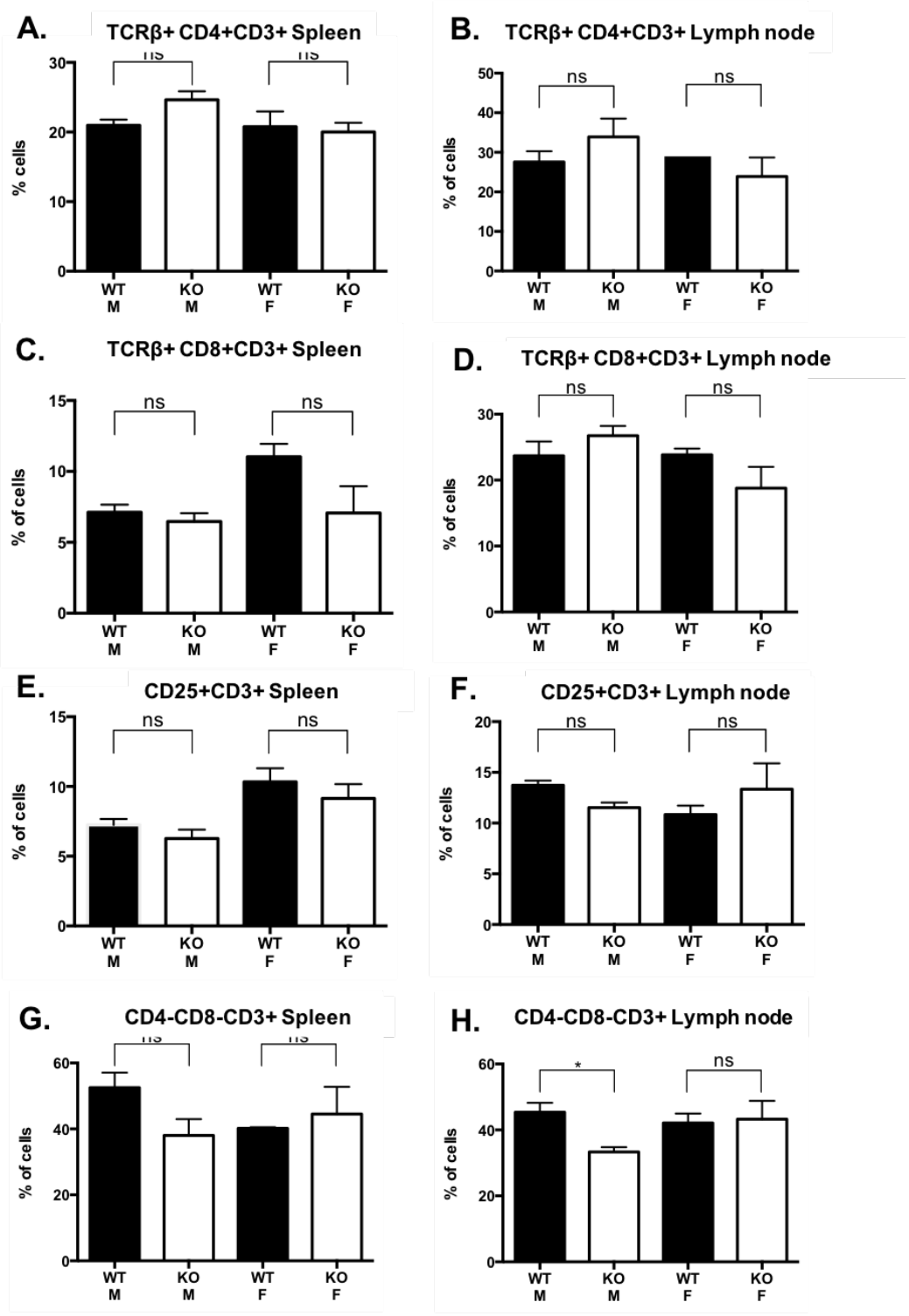

Figure 5: Aged Jedi KO mouse T cells do not exhibit changes in number or activation status. Spleens or lymph nodes from mice aged 12–18 months old were dissociated and stained for CD3, TCRβ, CD3, CD8, CD25. The percent of cells positive for each combination of markers is shown. (A and B) T helper cells. (C and D) Cytotoxic t cells. (E and F) T_{regs}. (G and H) Double negative (DN) T cells. n of 3-7 mice per genotype and sex. Error bars are SEM. No statistical significance using student's t test in any group.

Because we did not observe any changes in lymphocytes, autoantibody production, or organ damage in Jedi KO mice at baseline, we decided to immunologically challenge the mice to try to induce SLE. We used one of the most common inducible mouse models of SLE, intraperitoneal (i.p.) injection of the mineral oil pristane[548]. We monitored circulating anti-dsDNA antibodies for 6 months post injection, but did not observe pathological levels akin to positive-control SLE mice in our animals (Figure 6A). Due to the role of Jedi in the clearance of dying cells, we also instigated massive apoptosis in the animals by administering lethal doses of irradiation and performing a bone marrow transplant (data not shown). Despite stimulating cell death and the subsequent removal of these cellular corpses, we were still unable to detect changes in autoantibody production, changes to skin, or glomerular nephritis in Jedi KO mice. Several studies have shown a link between the western high fat diet and autoimmune prevalence which has also been validated in mouse models[549–552]. We transferred our Jedi WT and KO mice to a high fat diet for 8 months and measured autoantibodies but again found no statistically significant change (Figure 6B). Since diet profoundly influences the microbiome, which may have developmental effects on the tone of the immune system, we kept the mice on the high fat diet for 4 generations and evaluated scratching behavior (Figure 6C), proteinurea (Figure 6D), and autoantibodies in 12-month-old mice. None of these interventions triggered an immune response in the Jedi KO animals. This data along with the other negative data shown here, leads us to conclude that Jedi KO mice are not predisposed to autoimmune disorders.

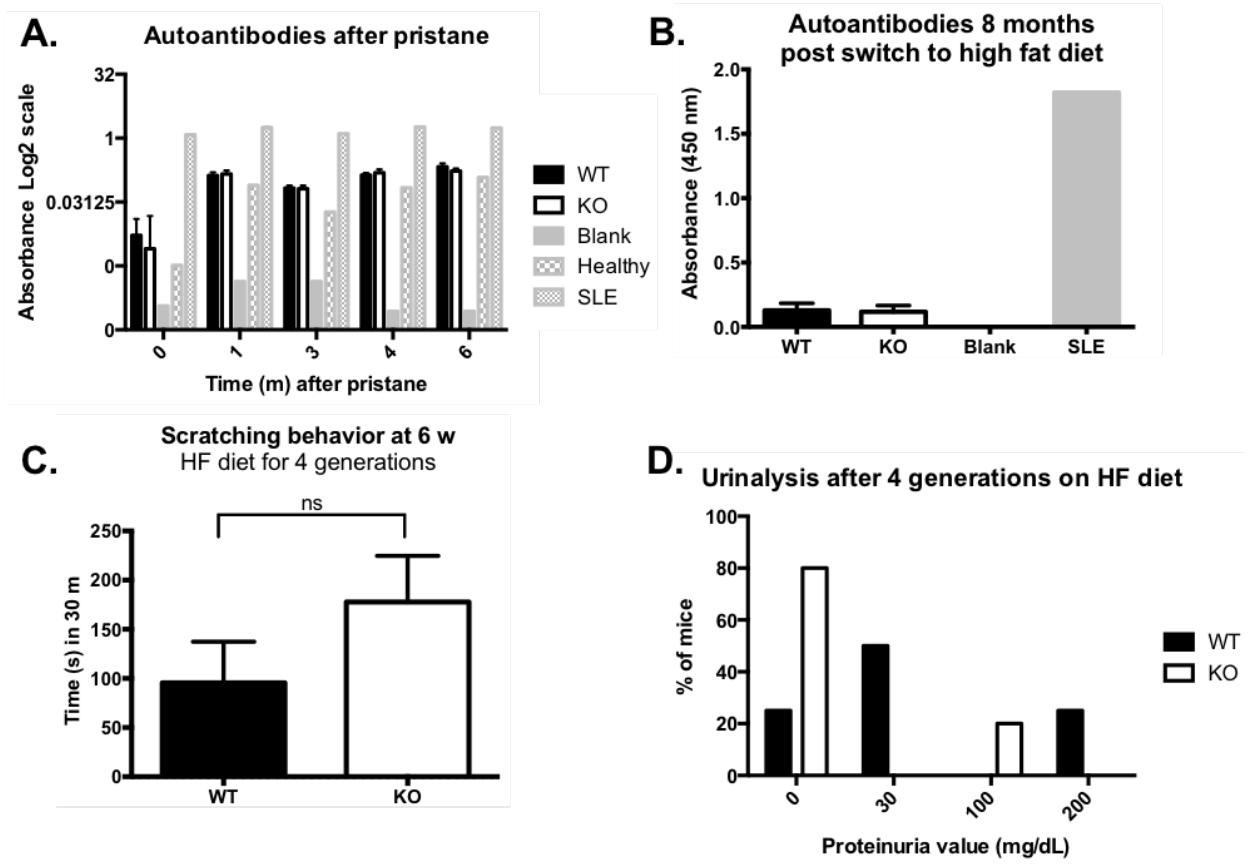

Figure 6: Jedi KO mice do not have autoimmune symptoms after inflammatory stimuli. (A) Mice were injected i.p. with pristane at at 6-8 w old and serum was tested monthly for 6 months for anti-dsDNA antibodies. No serum (blank) and serum from a healthy mouse were used as negative controls and aged female SLE mice used as a positive control. n=5 mice per genotype. Error bars represent SEM. (B) Mice were switched to a high fat breeder chow at 3 m old and autoantibodies tested 8 m post diet switch. n=8 mice per genotype. Error bars represent SEM. (C) Mice were bred for 4 generations on high fat breeder chow. F4 mice were monitored for scratching behavior at 6w old. n=6-10 mice per genotype. Error bars represent SEM. No statistically significant difference from student's t test. (D) Urinalysis was performed on the same mice shown in F4 mice when they were 1 y old. n=6-10 mice per genotype. Error bars represent SEM. No statistically difference by Fisher's exact test.

Section 2.3: Discussion

In this study, we have expanded upon our previous work to confirm that Jedi is sufficient to relay phagocytic capability to HeLa cells, not only of inert beads as previously published, but actual dying cells (Figure 1A). Despite this data, we provide a preponderance of evidence showing no significant effect of the loss of Jedi on dead cell removal, SLE diagnostic markers, or lymphocyte populations/function *in vivo* using a KO mouse model. We conclude that Jedi is dispensable for efferocytosis in an animal. Because our previously published work focused on the role of Jedi in phagocytosis specifically in the peripheral nervous system, we assessed clearance of dying cells and debris in the DRG during development (Please see Figure 10) and following a peripheral nerve injury (Figure 18B) in other chapters of this dissertation. In those assays as well, we did not find any deficit in phagocytosis when comparing Jedi KO mice to controls.

As mentioned earlier in the text, there are many engulfment receptors that are involved in dead cell clearance, including stabilin-1, BAI1, TIM4, SCARF1, LRP, and the TAM receptors to name a few[553]. For the studies throughout this dissertation, WT and Jedi KO mice were bred homozygously on the same background and then aged matched for experiments - therefore from 'half-cell' gametes the cells always lacked Jedi, allowing ample time for compensation by redundant receptor molecules. It is not surprising that the Jedi KO mice did not have an overt problem with dead cell clearance. Jedi, also known as MEGF12, actually belongs to a family of receptors that includes MEGF10 and MEGF11. MEGF10 is also a known phagocytic receptor that functions primarily in the nervous system[554]. Therefore, we are in the process of making isogenetic double KO mice of both Jedi and MEGF10. We have also created a floxed Jedi allele, which we can combine with a tamoxifen-inducible Cre to acutely delete Jedi in aged mice to avoid some of these potential compensation issues.

Autoimmune disorders, especially SLE, have complex genetic contributions attributed to combined effects of multiple genes. We used the C57BL/6 strain for the present study, however C57BL/6, C57BL/10, BALB/c, and DBA/2 mice are resistant to autoimmune disorders[555]. Perhaps on an autoimmune-prone strain, such as NZB/NZW, 129, SB/Le or BXSB mice, deletion of Jedi may have a more pronounced effect. Similarly, analysis of Vanderbilt University's biorepository of DNA genotyping data linked to de-identified medical records (BioVU) did not reveal and significant associations between Jedi SNPs and incidence of any autoimmune disorders (data not shown). However, a more complex analysis using the involvement of several genes may show that in combination with other genetic factors, Jedi may have an effect on lupus in humans.

In all of the experiments performed in this report, professional phagocytes, defined by their myeloid origin and efficiency of phagocytosis, contribute most to efferocytosis. These cell types include monocytes, macrophages, neutrophils, and osteoclasts, eosinophils, and dendritic cells. Given our negative results, we subsequently assessed Jedi expression in professional phagocytic cells using the Immunological Genome Project database (http://www.immgen.org/Databrowser19/DatabrowserPage.html). Relative to endothelial cells, which are known to express Jedi RNA and protein[379,380], there were very low levels of Jedi message in these professional phagocytes, with some being below background levels.

However, these results do not preclude the role of Jedi in non-professional phagocytic cells, such as endothelial cells, satellite glia, and meningeal cells, all of which express Jedi and are capable of engulfment[289,358,556]. In recent years, the literature shows more and more examples of non-canonical phagocytes, including but not limited to smooth muscle cells, renal cells, hepatocytes, and epithelial cells in the lung and gut[557–561]. So many diverse cell types are capable of efferocytosis, even in culture, that this phenomenon is now considered a general feature of normal tissue cells[562]. While non-professional phagocytes generally have a smaller

repertoire of ingestible targets and perform this process slower and less efficiently than their myeloid-derived professional counterparts, they can actually compensate for the loss of macrophages during developmental waves of programmed cell death by clearing out large numbers of dead cells[240].

It seems then, that professional phagocytes are 'primed' for efferocytosis compared to part-time phagocytes, which leads to a number of questions – is the molecular machinery of engulfment different between full and part-time phagocytes the same or different? Why are there so many types of these receptors, and related, how did the recognition of PS lead to so many diverse receptor protein structures? How is removal of apoptotic corpses coordinated by the vast number of cells capable of cleaning up the mess? As mentioned earlier in this text, there are many engulfment receptors, and interestingly, their structures are quite diverse and do not share any universal protein domain structures. Some of the phagocytic receptors (BAI1) traverse the plasma membrane seven times while others do so only once; some have enzymatic activity (TAM family) and others do not; some directly recognize PS (TIM4, Stabilin1/2) while others using bridging molecules to indirectly detect PS (TAM family, integrins)[199]. Most phagocytes express multiple engulfment receptors within the same cell, but amongst various cell types, this repertoire of receptors is not the same. Additionally, we know that these receptors cannot always compensate for one another and that the functional inactivation in mice and/or humans can lead to diverse phenotypes. For example, deletion of TIM4 in mice leads to lupus-like autoimmunity and it has high expression in macrophages and dendritic cells[563–565]. Mice lacking MerTK are blind due to its role in engulfment of rod outer segments by the retinal pigment epithelia (RPE), but only upon deletion of all three TAM family members does lupus-like autoimmune disease become apparent[246,566]. KO of another engulfment receptor, CD14, results in accumulation of dead cells but not signs of inflammation or autoimmune disease, as professional phagocytic macrophages retain their ability to secrete

anti-inflammatory factors in the presence of cell corpses[567]. Loss of function variants of MEGF10, a closely related gene to Jedi, are associated with schizophrenia in humans, probably due to its role in synaptic pruning by astrocytes[554,568]. The diversity of phenotypes associated with deletion or inactivation of these engulfment receptors shows that they have some non-overlapping function and expression across a diversity of professional and non-professional phagocytic cells. While the data presented here does not show overt signs of a chronic inflammatory condition in a mouse model lacking Jedi, it is possible that Jedi plays a niche role in engulfment in a non-professional phagocytic cell in a particular context, either in development or in an injury setting.

In order to narrow down where and when Jedi may function as an engulfment receptor *in vivo*, determining its ligand may help narrow down the suspects. Previous literature reports several ligands for Jedi that induce its activation as measured by phosphorylation : dextran sulfate[569], the high affinity immunoglobin E receptor subunit α (FcεR1α)[570], and Jedi itself[371]. While these studies did not consider the role of Jedi in engulfment, some of these results are intriguing. FcεR1α binds to IgE, which is canonically known for its role in allergic reactions, but recent data provides strong evidence for the role of IgE autoantibodies in many autoimmune diseases, including lupus[571,572]. In the phagocytic synapse, there is a high concentration of engulfment receptors that cluster together and ‘zipper’ around the target, so the prior finding that Jedi activation is amplified by close aggregation could also have important functional implications in the context of efferocytosis[573]. Our lab is currently testing an alternative hypothesis that, like other engulfment receptors, Jedi is activated by the classical ‘eat me’ signal PS.

In conclusion, our data illustrates that Jedi is dispensable for the removal of dying cells during development or normal tissue homeostasis *in vivo*, although we confirm our previous reports of its function as an engulfment receptor when overexpressed *in vitro*. We hypothesize

that compensation by other phagocytic receptors masks the role of Jedi in efferocytosis, or that the specific context in which Jedi plays an essential role has yet to be investigated. A more thorough analysis of Jedi expression in both professional and non-professional phagocytes may help unlock its role *in vivo*, as well as a more thorough understanding of its upstream activators. Future chapters in this dissertation will specifically address the role of Jedi in the peripheral nervous system.

Section 2.4: Materials and Methods

Mice

The Institutional Animal Care and Use Committee at Vanderbilt University approved all experimental procedures using animals. Mice were housed under a controlled 12-hour light/dark cycle. Standard laboratory rodent diet (*LabDiet* catalog no. 5001) was available *ad libitum* except where indicated in the text. Under high fat diet conditions, mice were given *ad libitum* access to standard breeder's chow (*LabDiet* catalog no. 5LJ5). All mice in this study were on a C57BL/6 background, which was originally obtained from Jackson labs and then maintained in our laboratory. Jedi KO (Pear1$^{tm1a(KOMP)Wtsi}$) mice were derived from the International Mouse Phenotype Consortium (IMPC, CSD31459_C05). Control mice were wild-type (WT) C57/BL6 mice obtained from Jackson Labs (Catalog no. 000664). Mice were genotyped with the following primers to distinguish WT and KO animals: Forward 5'-CTGCCACTGTCATAGCATTA-3', Reverse 5'-CACTTAATGACACTCCTTTC-3'. Wild type mice used in the bone marrow transplant study were B6 CD45.1 Pep Boy mice obtained from Jackson labs (catalog no. 002014).

Cell Culture

HeLa cells were culture in Gibco media (catalog no. 11995-065) with 10% serum under 5% CO_2 conditions. The membrane bound GFP (meGFP) plasmid was carried in the pCAG plasmid backbone. The JediGFP plasmid was carried in the pCMV backbone. Cells were transfected using Lipofectamine 2000 with the manufacturer's protocol (ThermoFisher Scientific catalog no. 11668027). Bait cells were dyed with Cell Tracker Orange (Life Technologies catalog no. C2927) according to the manufacturer's protocol. For UV irradiation, $5.5X10^6$ cells were plated in 10 cm plates, and the next day dosed with 200 J/m^2 of using a VWR UV crosslinker. Bait cells were trypsinized immediately after irradiation and added 10:1 to transfected HeLa cells. At 24, 48, and 72 hours after adding, the cells were rinsed with PBS and fixed with 10% neutral buffered formalin (NBF) for 15 minutes at room temperature. Immunocytochemistry was performed using a standard protocol with Abcam anti-GFP antibody catalog no. ab13970. Cells were imaged on a Leica SP5 confocal microscope and analyzed in ImageJ software. At least 50 transfected cells were analyzed per condition.

Flow Cytometry

Flow cytometry was performed as previously described[574–576]. Splenocytes and lymphocytes were prepared by crushing the organs through a 70 micron strainer followed by one wash and red blood cell (RBC) lysis. One million cells were incubated with the following anti-mouse antibodies for 30 minutes then fixed in 2% paraformaldehyde in phosphate buffered saline (PBS): CD4, CD25, CD4-PE, TCRb-PE, CD8-PerCP, B220-A450, CD119-PECy7, (BD Biosciences). T_{reg} staining was performed using the mouse regulatory T cell staining kit from eBioscience according to the manufacturer's instructions. All samples were acquired on a MACSQuant flow cytometer (Miltenyi Biotec) and data analyzed using FlowJo analysis software (Treestar).

Autoantibodies

At various ages delineated in the text, blood was collected from tail vein and allowed to clot at room temperature. Serum was isolated by spinning the samples at 16,000 rcf at 4°C for 20 min and stored at -80°C. IgG class antibodies against double stranded DNA (dsDNA) were measured by ELISA as follows: Immunlon2 Nunc plates (Fisher catalog no. 12-565-136) were pre-coated with methylated BSA (mBSA, Sigma catalog no. A1009) at a final concentration of 1 mg/mL diluted in PBS pH 7.4 for 30 min at 37°C. After removing mBSA, the wells were washed twice with PBS. The wells were then coated with calf thymus DNA (Sigma catalog no. D1501), which was pre-filtered through a 0.2 μm cellulose acetate filter to remove and single-stranded DNA (ssDNA), at a final concentration of 50 μg/mL diluted in PBS for 30 min at 37°C. After removing the dsDNA, the wells were washed twice with PBS. The plate was then blocked overnight at 4°C in 3% BSA, 3 mM EDTA in 0.1% porcine gelatin (Sigma catalog no. G1890). The next day, the plate was rinsed twice with PBS before adding the serum samples diluted 1:500 in 2% BSA, 3mM EDTA, 0.05% Tween-20 dissolved in 0.1% gelatin in triplicate or quadruplet replicates. Controls were the serum diluent solution alone, serum from a healthy young adult mouse, and serum from an aged female systemic lupus erythematosus (SLE) mouse model, B6.*Sle.1.2.*3. Serum from SLE mice was graciously provided by Amy Major's laboratory at Vanderbilt University. The serum samples were gently rocked on the plate for 2 hours at room temperature and then underwent two rounds of washing: twice with 0.05% PBS-Tween and twice with PBS. Bound antibodies were detected by adding an anti-mouse IgG secondary antibody conjugated to HRP (Promega catalog no. W4021) diluted 1:5000 in 1% BSA, 0.05% Tween-20 dissolved in PBS for 2 hours at 37°C. The plate was washed twice with 0.05% PBS-Tween and twice with PBS. HRP activity was detected using TMB substrate. Experimental replicates were averaged for each sample and reported as shown.

Urinalysis

At the ages specified, urine was collected from mice and immediately incubated on Siemens Multistix 10 SG for 1 minute. A user blinded to genotype determined a colorimetric score corresponding to 0, 30, 100, 200, or 300+ mg/dL of protein per volume of urine.

Scratching behavior

Mice at the indicated ages were habituated to individual cages in a quiet room for four days before collecting data. Ambient temperature in the room was generally 22-25°C. On the fifth day, mice were acclimated to the cages for 15 minutes and then their behavior was recorded for 10 or 30 minutes (as indicated in the text) in the absence of a human observer, except for brief periods when the camera was turned on or off. A blinded observer analyzed the videos for scratching behavior. Scratching behavior was categorized into two sub-categories: hind limb scratching and biting hairy skin. For hind limb scratching, one bout was considered to be lifting of the hind limb, scratching, and replacing the limb back to the floor, regardless of how many scratching strokes occurred. For biting, one bout was lowering the head to hairy skin only, biting, and returning the head to normal height. Bouts and time spent during each bout were both recorded, and the two behaviors were combined to monitor total scratching behavior.

Bone marrow (BM) transplant

The bone marrow (BM) transplant was performed as previously described[577]. Briefly, a single cell suspension of BM cells was obtained from the femur of Pep boy and Jedi KO mice. Red blood cells were lysed with hypotonic lysis Buffer EL (Qiagen). Recipient mice were lethally irradiated (900 rads) before donor BM was injected via tail vein. Transplant efficiency was evaluated 6 weeks and 11 months post transplant using flow cytometry of peripheral blood for

cell surface markers CD45.1 and CD45.2. Autoantibodies and urinalysis were performed before the transplant and every 1–2 months post BM transplant.

Pristane injections

Age matched WT and KO mice 6–8 weeks old were given either 500 uL of pristane (Sigma cat no. P2870) or 500 uL of 0.9% normal saline via intraperitoneal injection. Autoantibodies and urinalysis were performed before the injection and every 1–2 months post pristane injection.

Immunofluorescence

Ileum, spleen, and skin from 8 to 12-month old animals were fixed in 10% neutral buffered formalin (NBF) for 24 hours, dehydrated, and embedded in paraffin. 5 μm sections were cut and baked at 55°C for 1 hour. TUNEL was performed according to the manufacturer's protocol (Millipore catalog no. S7110) and is reported as percent of total cells, as measured by DAPI, or number of TUNEL-positive cells per area of tissue. Toluidine blue was performed by standard de-paraffinization followed by 10 minutes in 1 mg/mL toluidine blue dissolved in water. Slides were quickly re-dehydrated and mounted in DPX (VWR catalog no. 100504-938). Images were captured using a Zeiss Axioskop 2 and analyzed in ImageJ. Cells positive for these markers were counted and reported as percent of total cells or number of total cells per area of tissue.

Section 2.5: Acknowledgments

We acknowledge the Translational Pathology Shared Resource supported by NCI/NIH Cancer Center Support Grant 5P30 CA68485-19 and the Vanderbilt Mouse Metabolic

Phenotyping Center Grant 2 U24 DK059637-16 for performing immunohistochemistry (IHC) for B220, CD3, and F4/80 and toluidine blue staining.

CHAPTER 3

JEDI DEFICIENCY INCREASES SENSORY NEURON EXCITABILITY THROUGH A NON-CELL AUTONOMOUS MECHANISM

Authors

Alexandra J. Trevisan, Mary Beth Bauer, Rebecca L. Brindley, Kevin P.M. Currie, and Bruce D. Carter

Section 3.1: Introduction

The primary afferent somatosensory neurons are a heterogeneous population of peripheral neurons responsible for detecting and transmitting information about external stimuli such as temperature, proprioception, touch, pain, and itch to the CNS, where they are integrated and processed[578]. These pseudo-unipolar neuron cell bodies reside in the DRG and innervate peripheral tissues as well as extending axons into the CNS where they synapse in the dorsal horn of the spinal cord. Like the rest of the developing nervous system, approximately 50% of DRG neurons undergo normal developmental apoptosis[34]. The cellular corpses are efficiently removed through phagocytosis, which we previously demonstrated is carried out in the DRG by satellite glia, a specialized type of peripheral glial cell that enshrouds the sensory neuron somas[358]. This clearance process involves the phagocytic receptors MEGF10 and Jedi (MEGF12/PEAR1), homologs of the well-characterized engulfment receptors Draper in *Drosophila melanogaster* and CED1 in *Caenorhabditis elegans*[358–360].

Satellite glial cells (SGCs) envelop DRG neuron somas in very close proximity (~20 nm), an ideal anatomical position for their role in phagocytosis of apoptotic DRG neurons during embryogenesis. This close proximity also facilitates modulation of neuronal activity via several

mechanisms, including the regulation of extracellular ion concentrations, the release of paracrine signaling molecules, and the creation of SGC nets linked through gap junctions[105]. SGCs, therefore, contribute to neuronal sensitization and chronic pain when they enter an 'activated' state, characterized by an increase in their proliferation, up-regulation of the intermediate filament protein GFAP, and cytokine production[146].

The DRG and the associated peripheral nerves contain a host of other cell types required for efficient conduction of electrical signals across long distances in the organism, including perineurial cells. These cells encapsulate the DRG and bundle groups of axons into fascicles within the nerve[579]. The canonical function of perineurial glia is to establish the BNB through tight junctions that occlude ions, molecules, and cells from entering the nerve[580]. Additionally, it has been reported that the perineurium can modulate the development of the neuromuscular junction (NMJ), Schwann cell myelin production, and aid in phagocytosis and regeneration after nerve injury[460,581,582].

In the current study, we resolved to understand the role of Jedi in the peripheral somatosensory nervous system by analyzing a global Jedi KO mouse model. We first used WT mice to characterize Jedi expression in satellite glia and endothelial cells, where it has previously been detected[379,380] and report that Jedi is a novel marker for perineurial glia. We found no changes in morphology or function of peripheral glial cells in the absence of Jedi. Surprisingly, however, we did observe changes in DRG neuron activity, despite not detecting Jedi protein in the neurons themselves. Specifically, in Jedi KO neurons, there was an increase in the fraction of neurons responsive to capsaicin and patch-clamp electrophysiology revealed an increase in excitability, with a shift from phasic to tonic firing patterns in KO neurons. We also found alterations in the properties of voltage-gated sodium channel currents. These data indicate that Jedi acts in a non-cell autonomous manner to modulate sensory neuron function.

Section 3.2: Results

Validation of mouse model

In order to study the role of Jedi *in vivo*, we used a KO mouse model available through the KOMP repository (https://www.komp.org) (Figure 7A). Through PCR of genomic DNA, we verified the correct location and orientation of the KOMP construct (data not shown) and by RT-PCR, validated that full-length Jedi messenger RNA (mRNA) was not expressed in Jedi KO mice (Figure 7B). Using two antibodies against the intracellular domain of Jedi, we also confirmed that Jedi KO mice do not express Jedi protein (Figure 7C). Additionally, we did not detect the N-terminal fragment of Jedi using a polyclonal antibody generated against the entire extracellular domain (Figure 7D).

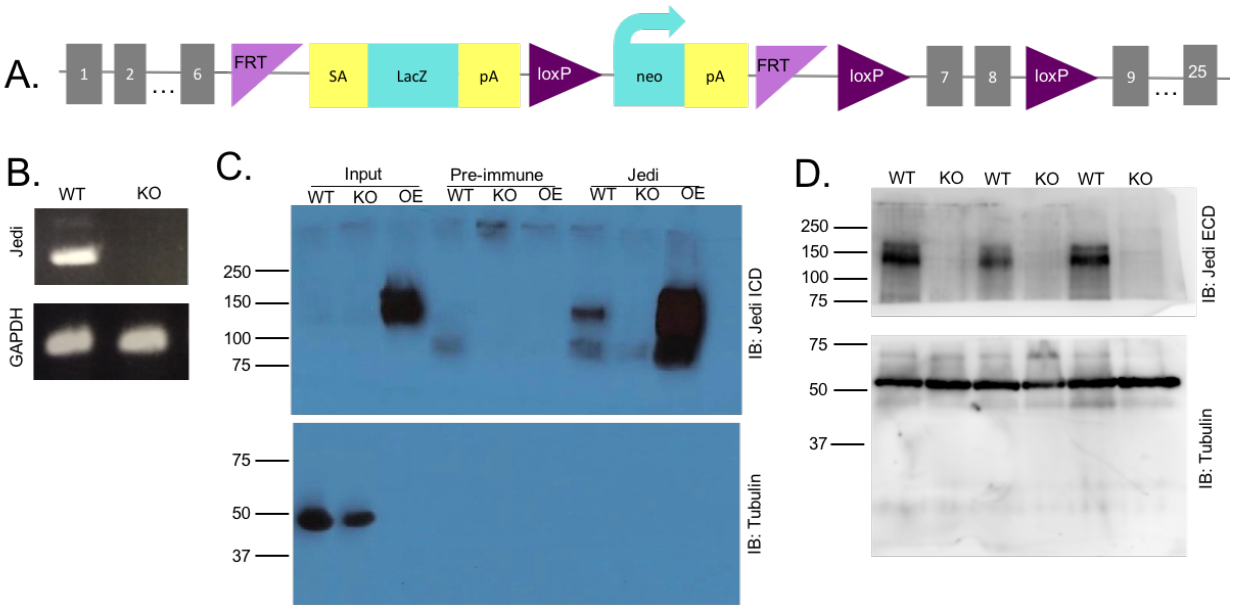

Figure 7: Mouse model validation. (A) Scheme of KOMP Jedi KO mouse model. SA = splice acceptor, pA = poly A tail. Exons numbered in grey boxes (not drawn to scale). (B) RT-PCR of WT and KO brain lysates using primers for Jedi that span the KOMP lacZ insertion. Control primers for GAPDH used. (C) IP-western using two different antibodies generated against the intracellular domain (ICD) of Jedi. Samples are adult whole brain lysates from WT or KO animals or HeLa cells overexpressing (OE) Jedi. Markers in kDa. The full length of the gels are shown. (D) Western blot using a polyclonal antibody generated against the entire extracellular domain (ECD) of Jedi using pooled DRGs from 3 replicate WT and KO adult mice. Markers in kDa. The full length of the gels are shown.

Jedi is expressed in peripheral nervous system glia

We previously reported that Jedi mRNA is expressed in the DRG both *in vivo* and in primary DRG mixed neuron-glia co-cultures[358]. According to the Broad Institute resource Genotype-Tissue Expression human RNAseq database, the highest level of Jedi expression is in peripheral nerves (https://gtexportal.org/home/), so we investigated Jedi protein expression in the context of the peripheral nervous system with a focus on the sciatic nerve. Consistent with previous reports[379,380], we confirmed Jedi expression in structures that appear to be blood vessels (Figure 8A insets). In addition, we detected Jedi expression in the perineurium of the nerve (Figure 8A and Figure 9). We confirmed Jedi expression in the perineurium by staining adjacent sections for Glut1, a marker for the perineurium as well as blood vessels[583] (co-staining was not possible due to antibody incompatibility) (Figure 9A). We further verified Jedi expression in perineurial cells using several other markers, including laminin, Claudin and ZO-1[584] in both the nerve and ganglia (Figure 9B and 9C). To our knowledge, this is the first report showing that Jedi is a perineurial marker.

In addition to nerve samples, we also stained DRGs for Jedi and again found the highest levels of expression in the perineurium (Figure 8B). Jedi was also expressed at lower levels in a subset of SGCs as detected by BFABP staining (Figure 8B). We also checked whether Jedi was expressed in DRG neurons by co-staining for Jedi and PGP9.5, a pan-neuronal marker, *in vivo* (Figure 8C) and *in vitro* by co-staining WT DRG cultures with Tuj1 (Figure 8D). However, we did not observe any Jedi signal in the neurons. In total, these results indicate that Jedi is expressed in peripheral glial and endothelial cells but not in DRG neurons.

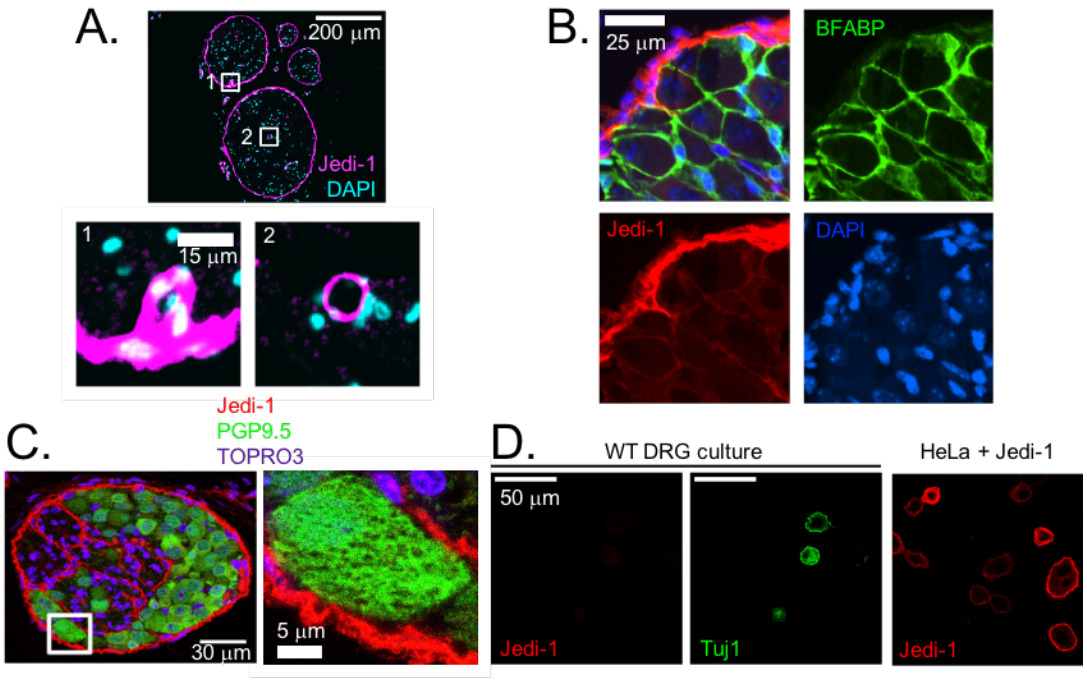

Figure 8: Jedi is expressed in peripheral glia and endothelium. (A) Cross section of adult (8-12 weeks old) WT sciatic nerve stained for Jedi-1 (magenta) and DAPI (blue). Insets 1 and 2 show Jedi expression in blood vessels. See Supplementary Figure S2 for validation of Jedi-1 expression in perineurial glial cells. (B) WT P0 DRG co-stained for Jedi-1 (red), satellite glial marker BFABP (green), and DAPI (blue). (C) WT DRG co-stained for Jedi-1 (red) and PGP9.5 (green) and TOPRO3 (blue). Right shows inset. (D) Right: Primary WT DRG cultures stained for neurons using Tuj1 (green) and Jedi-1 (red). Left: HeLa cells overexpressing mouse Jedi-1 were used as a positive control for Jedi-1 immunocytochemistry *in vitro*. All images were analyzed in ImageJ version 2.0.0-rc-69/1.52p.

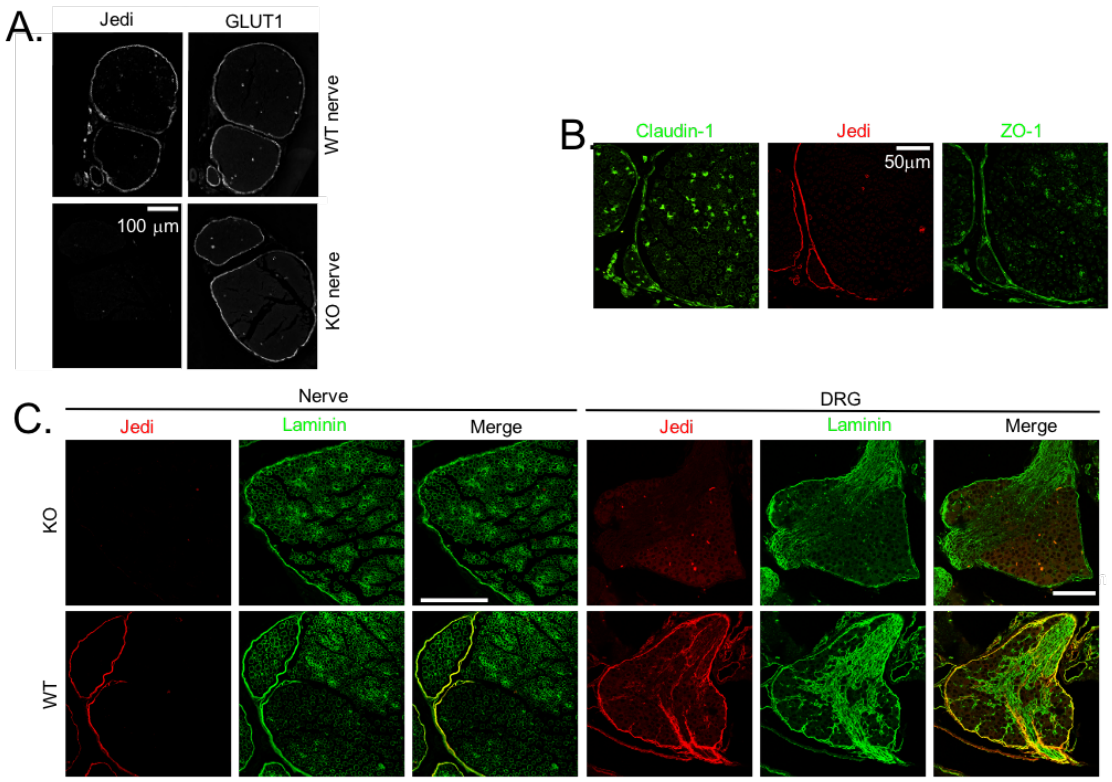

Figure 9: Jedi is a novel marker for perineurial glia. (A) Consecutive sciatic nerve cross sections stained for Jedi (left) and GLUT1 (right). These antibodies cannot be co-stained together, so consecutive sections were stained and rotated to show the nerve in the same orientation on a black background. Both Jedi and GLUT1 are expressed in perineurial glia and endothelial cells. (B) WT sciatic nerve was serially sectioned and consecutive cross sections were stained for Claudin-1 (green), Jedi (red), and ZO-1 (green). Antibodies are not compatible for co-staining. (C) WT and KO nerve cross sections or DRGs were co-stained for Jedi (cyan) and laminin (magenta). White shows co-localization.

Peripheral glial cell morphology and function are not altered in the absence of Jedi

Since we observed expression of Jedi in the perineurium and the SGCs, we investigated whether the KO animals exhibit changes in the development of these peripheral glia cell types. H&E staining of paraffin sections (Figure 10A) and transmission electron microscopy (TEM) of the sciatic nerve (Figure 11A) show normal morphology of the perineurial cell layer. In Jedi KO animals there was no sign of glial activation in the SGCs based on GS and GFAP staining in early post-natal animals (Figure 11B) and one-year-old animals (data not shown).

Previous reports indicate that Jedi is a negative regulator of proliferation in endothelial cells lines[380], bone marrow mononuclear cells[378], and megakaryocyte precursors[373]. However, we did not find any significant difference between genotypes in the proliferation rate of SGCs or perineurial cells based on Ki67 staining (Figure 11C). Because a change in perineurial proliferation might lead to thickening of the perineurial barrier around the nerve, we measured width of the perineurium (Figure 11D), but found no change in Jed-1 KO mice. The perineurium also produces ECM, which we measured by western blot for collagen IV (data not shown) and laminin (Figure 10B), but found no significant change in ECM levels at several developmental ages.

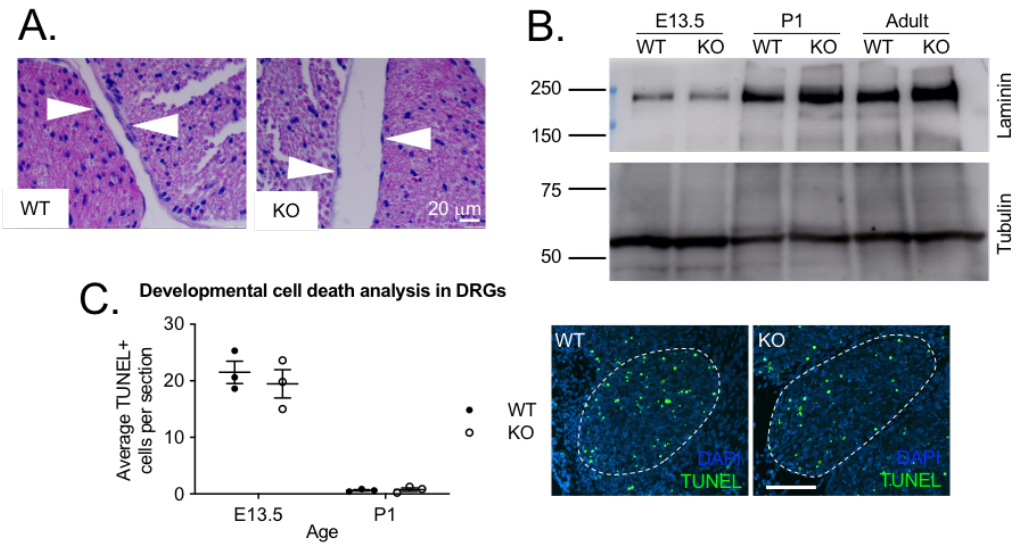

Figure 10: Peripheral glia are not altered in the absence of Jedi. (A) H&E of WT and KO adult sciatic nerves. Arrows point to the perineurial cell layer. (B) Western blot from DRG lysates collected at various developmental ages in WT and KO mice immunoblotted with a pan-laminin antibody and tubulin as a loading control. (C) Left shows the quantification of TUNEL staining at E13.5 or P1 in WT or KO mice. Serial sections were taken at 5 microns through all spinal levels of ganglia and every 12th section stained. Average number of TUNEL+ cells per section per ganglia were averaged for each animal and 3 animals analyzed per genotype and time point. Error bars represent SEM. No statistically significant differences between genotypes. Right shows representative picture of TUNEL staining (green) and DAPI (blue) of E13.5 DRGs, outlined in white dotted lines. Scale bar is 100 microns.

The perineurium and peripheral nerve endothelial cells both contribute to the blood nerve barrier, which shields the endoneurial space from extreme changes in solute concentration and protects axons from potentially cytotoxic substances[585]. Since both of these cell types express Jedi, we tested the integrity of the blood nerve barrier by measuring extravasation of Evan's Blue dye from the blood to the nerve and sensory ganglia, but we did not detect a significant difference in permeability between genotypes (Figure 11E). As a control for a tissue with limited permeability, we measured Evan's Blue in the brain, and as a positive control for tissue penetration of the dye, we measured kidney. In both cases, we found no change in Jedi KO mice relative to WT control animals (Figure 11E).

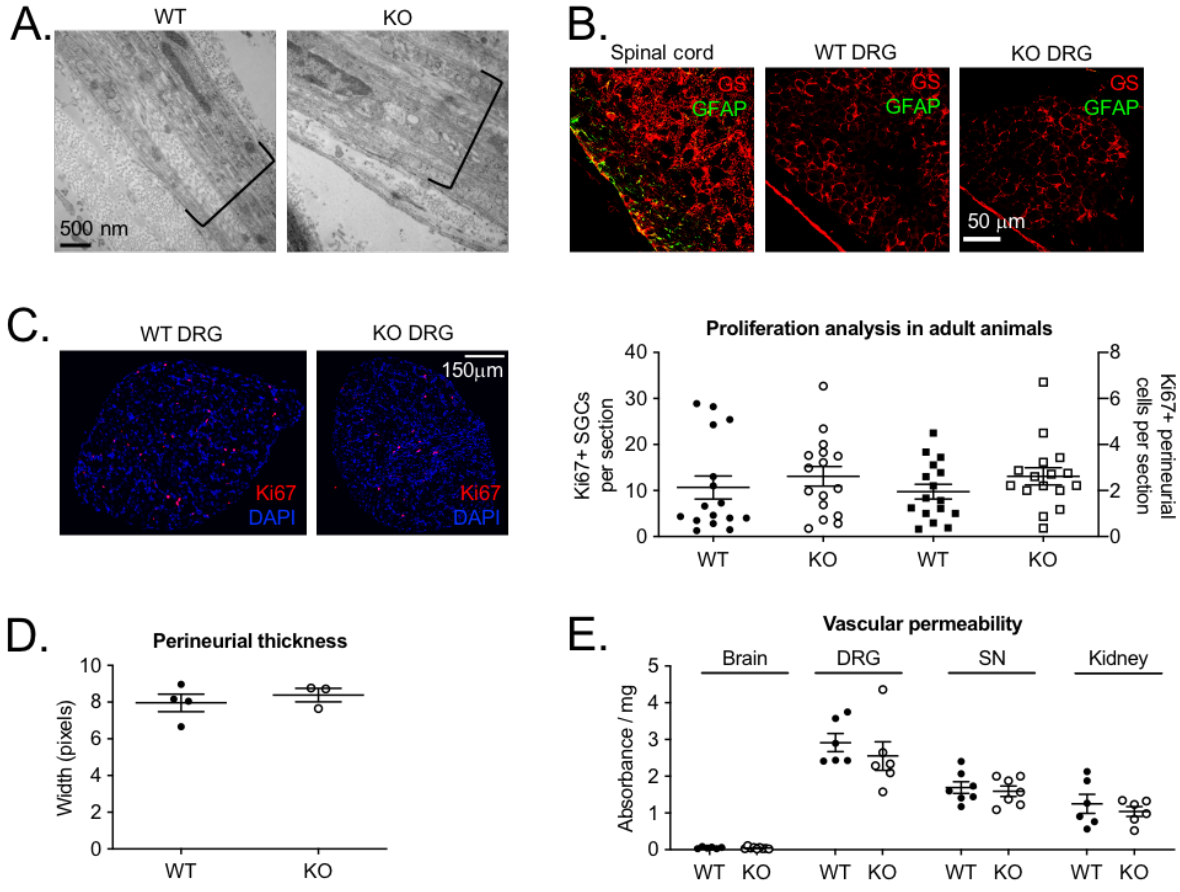

Figure 11: Peripheral glia are not altered in the absence of Jedi-1. (A) TEM images of WT and KO sciatic nerves showing the morphology of the perineurial cell layer, labeled in brackets. (B) Glutamine synthetase (GS, red) and glial fibrillary acidic protein (GFAP, green) immunostaining of spinal cord (positive control) or DRG of P1 mice from WT and KO animals. (C) Ki67 (red) and DAPI (blue) staining in adult WT or KO DRGs 8-12 weeks old. Circles (left axis) are Ki67+ SGCs while squares (right axis) are Ki67+ perineurial cells. 16 animals analyzed per genotype with a minimum of 5 sections 60 microns apart analyzed per animal. No statistical difference between genotypes. (D) Quantification of laminin IF pictures such as those shown in Supplementary Figure S2C. Thickness of the perineurial sheath measured in pixels. n=3 animals analyzed per genotype with a minimum of 8 sections analyzed per animal at least 60 microns apart. Error bars represent SEM. No statistically significant difference between genotypes. (E) Evan's blue dye extravasation from brain, DRG, sciatic nerve (SN), and kidney in adult WT and KO mice. Absorbance normalized to weight of tissue. No statistical difference between genotypes. All images were analyzed in ImageJ version 2.0.0-rc-69/1.52p.

Previous studies from our lab demonstrated that SGCs phagocytose apoptotic neurons during the development of the DRG and *in vitro* evidence indicated that this occurs via Jedi-dependent engulfment[359,360]. However, when we performed TUNEL staining at E13.5, during the peak of apoptosis, and P1, after the normal cell death period[586], we did not observe an accumulation of dead cells in Jedi KO DRGs relative to WT (Figure 10C). We propose that other phagocytic receptors may compensate for lack of Jedi such as MEGF10, Tyro3, Axl, or Mer. In summary, we did not detect any morphological or functional differences in the perineurium or SGCs in the absence of Jedi under basal conditions.

Altered functionality of sensory neurons from Jedi KO mice

Although we did not detect Jedi in DRG neurons, we considered the possibility that Jedi deficiency in glial cells could indirectly affect the neurons. The *Drosophila* homolog of Jedi, Draper, is expressed by glia - not neurons - yet deficiency in Draper leads to neurodegeneration[587]. In addition, SGCs and endothelial cells, where we detected Jedi expression, can release factors that affect sensory neuron function[105]. We also detected high levels of Jedi in perineurial cells, which have been shown to be important for axon regeneration in zebrafish and mammals[460,582]. Therefore, we investigated DRG neuron function in Jedi KO mice.

We did not find any loss of sensory neurons in the Jedi KO mice (Figure 12A & B) or alteration in size distribution, which correlates with sensory modality (Figure 12C). The number of neurons per ganglion varies with spinal level. Thus, to enable direct comparison between genotypes, we quantified cell number and size in thoracic level 13 (T13) ganglia as this spinal level is readily identifiable. We suggest our data from T13 is representative of all ganglia; however, it is possible that other DRGs may have differences not represented in T13.

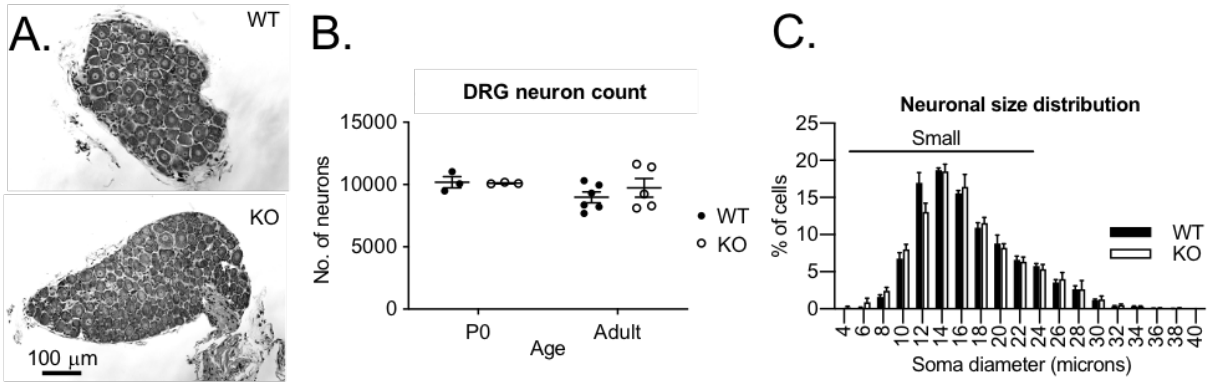

Figure 12: DRG neurons develop normally in the absence of Jedi-1. (A) Example pictures of toluidine blue staining of DRG sections from adult (8-12 weeks) WT and KO mice quantified in B and C. (B) Quantification of total DRG neuron counts from serially sectioned thoracic level 13 (T13) DRGs where every 12th section was counted, summed, and total neuron counts were estimated by multiplying by 12. Analysis was performed at two different developmental ages, P0 and adult animals 8–12 weeks old. Error bars indicated SEM. No statistically significant change between genotypes at either time point. (C) Frequency distribution of soma size measured from toluidine blue staining of adult DRGs WT n = 4 animals, KO n = 3 animals with a minimum of 500 cells analyzed per animal. Small DRGs less than 25 microns in diameter are indicated by the top horizontal bar. Error bars indicated SEM. No statistical difference between genotypes in any group using 2-way ANOVA. All images were analyzed in ImageJ version 2.0.0-rc-69/1.52p.

To assess neuronal function, we performed live cell imaging of cultured DRG neuron calcium responses to several chemical pruritogens and allogens including chloroquine, histamine, allyl isothiocyanate (AITC), or capsaicin (CAP) (Figure 13A). Although this group of compounds is not comprehensive for all DRG neuron subtypes, the vast majority of DRG neurons (70% by our measure) will respond to one or more of these drugs. We found that the percentage of cells that responded to chloroquine, histamine, and AITC were not statistically significant between genotypes. However, the proportion of cells that responded to capsaicin, a TrpV1 ion channel agonist, was increased in cells isolated from Jedi KO mice (Figure 13B and 13C). The baseline calcium concentration was not statistically different between genotypes, nor was the maximum intracellular calcium concentration following capsaicin treatment (Figure 13D).

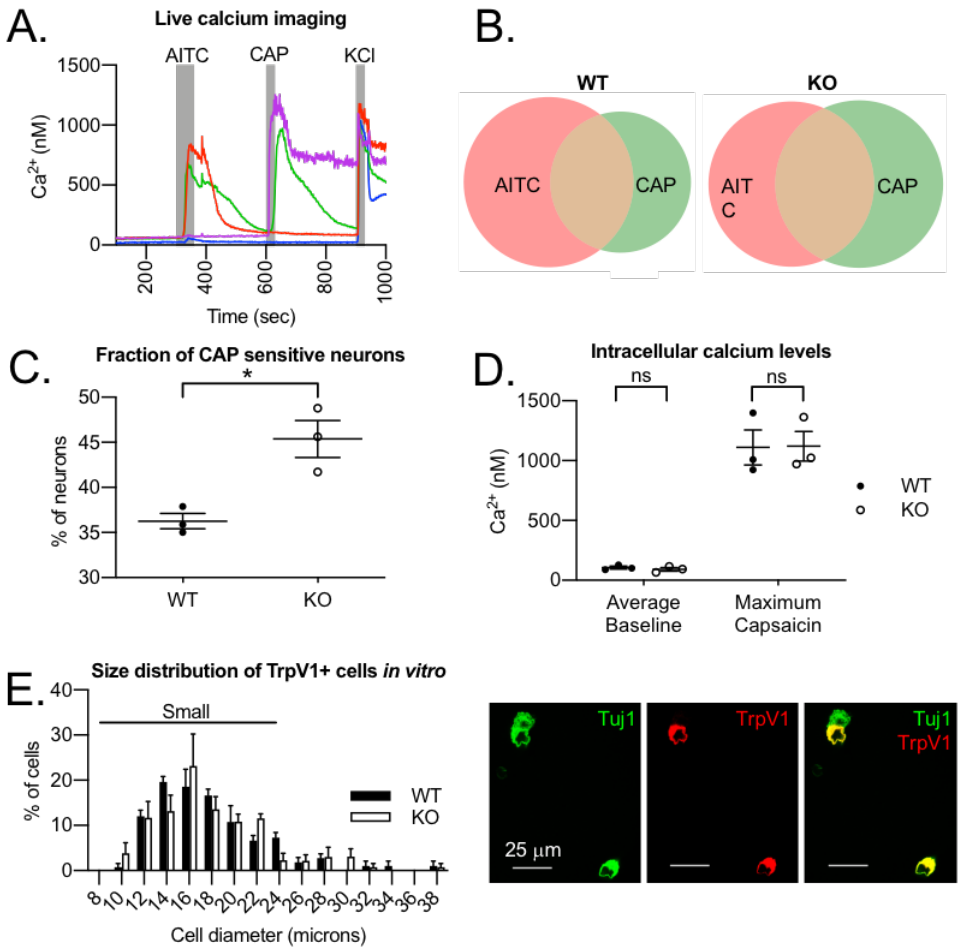

Figure 13: DRG neurons isolated from Jedi-1 KO mice are sensitized to capsaicin. (A) Representative trace of 4 cells used to obtain live cell calcium imaging data. Duration of treatment with allylisothiocyanate (AITC), capsaicin (CAP), and KCl is shown in grey boxes. Blue cell is a healthy neuron that responded to KCl but not AITC or CAP. Red cell responded to AITC and KCl. Purple cell responded to CAP and KCl. CAP responding cells often did not return to baseline. Green cell responded to AITC, CAP, and KCl. (B) Venn diagrams showing the proportions of cells that responded to AITC and CAP. t tests were used to compare overall responses to each drug. There was no statistical difference in AITC responses between genotypes. (C) Fraction of cells that responded to capsaicin over the course of 3 independent experiments with a minimum of 100 cells analyzed in each experiment. Two-tailed t test with Welch's correction p=0.03. (D) Intracellular calcium concentration measured by Fura-2AM. Baseline calcium concentration was averaged over the course of 1 minute before any drug treatment. Maximum calcium concentration is the peak calcium concentration during treatment with 500 nM capsaicin for 30 seconds. Each data point represents an independent experiment with a minimum of 100 cells analyzed in each. Students t test was used to compare calcium concentrations between genotypes at baseline and after CAP treatment. (E) Left: Quantification of the size of of TrpV1+ neurons *in vitro*. n=4 animals per genotype analyzed. Scale bars represent SEM. 2 way ANOVA used to compare genotypes across all size categories. No statistical differences between genotypes. Right: Representative image of TrpV1 staining in primary DRG cultures showing neurons in Tuj1 (green) and TrpV1 (red). All images were analyzed in ImageJ version 2.0.0-rc-69/1.52p.

These results indicate that loss of Jedi indirectly affects the fraction of DRG neurons responding to capsaicin, which suggests that either there is an alteration in the distribution of neuron subtypes or that TrpV1 is up-regulated or its activity sensitized. It is interesting to note that such up regulation and/or sensitization of TrpV1 occurs in inflammatory pain[588]. To investigate TrpV1 expression, we used immunostaining of both intact fixed ganglia and cultured DRG neurons (Figure 13E). We did not find a significant change in the fraction of cells that express TrpV1 in the intact ganglia (WT 29.6% $\pm$ 4.9 SD of HuC/D+ neurons stained positive for TrpV1 compared to KO 28.3% $\pm$ 2.0 SD, n=3 animals per genotype) or in isolated cells (WT was 32.5% $\pm$ 4.3 SD of Tuj1+ neurons compared to KO 29.2% $\pm$ 3, n=4 animals analyzed per genotype; no significant changes between genotypes using Student's t test for both data). The size distribution of TrpV1+ cells was also not significantly different between genotypes (Figure 13E). Note that the majority (90%) of TrpV1+ cells were small diameter, which we defined as <25 microns (Figure 13E). The analysis of TrpV1 expression suggests that Jedi KO neurons have not changed their subtype distribution or identity; rather, TrpV1 sensitivity is being modulated through a mechanism that does not involve an increase in total TrpV1 protein levels. There are a number of post-translational modifications that could account for this, such as phosphorylation or glycosylation [589].

Increased excitability of Jedi KO neurons

As another approach to assess alterations in neuronal activity, we used whole cell patch-clamp electrophysiology. We first compared the basic membrane properties and excitability of small diameter neurons (<25 microns, which are primarily nociceptors) isolated from WT and KO mice using current-clamp recording (Figure 14A). The membrane capacitance, which is directly proportional to the surface area of the cell, was not significantly different between genotypes, confirming neurons were of similar size (WT 19.9 ± 11.1 (SD) pF, n = 12; KO 18.4 ±

11 (SD) pF, n = 12, p = 0.75). Membrane resistance was slightly higher and resting membrane potential was slightly more depolarized in KO cells, but neither of these parameters were significantly different (Table 1). To test membrane excitability we applied a series of 100ms depolarizing current steps of increasing magnitude. Rheobase, defined as the smallest current step that evoked an action potential, was significantly less in KO neurons, indicating increased excitability compared to WT ($p = 0.03$) (Figure 14A, 14B). We compared various parameters of the evoked action potentials in KO and WT neurons (Table 1). The threshold potential was slightly more depolarized ($p = 0.048$), the after hyperpolarization was larger ($p = 0.009$), and the overall amplitude of the action potential was larger in KO compared to WT neurons ($p = 0.027$). There was no significant difference in the peak membrane voltage ($p = 0.065$), the rising slope ($p = 0.32$), or the duration at half maximal amplitude (half width) ($p = 0.48$) of the action potential (Table 1). The most overt difference between genotypes was the number and pattern of action potentials evoked when neurons were stimulated using a current step to twice rheobase for 1 second (Figure 14C, D). The KO neurons fired significantly more action potentials compared to WT neurons (Figure 14C, $p = 0.04$). Moreover, there was a significant ($p = 0.01$) shift in the firing pattern of KO neurons; 10 out 12 KO neurons displayed a tonic firing pattern with action potentials evoked throughout the duration of the stimulus. In contrast, only 3 out 12 WT neurons displayed tonic firing and the remaining 9 cells displayed phasic firing in which one or two action potentials were evoked at the start of the stimulus and the cell then remained quiescent (Figure 14D, E).

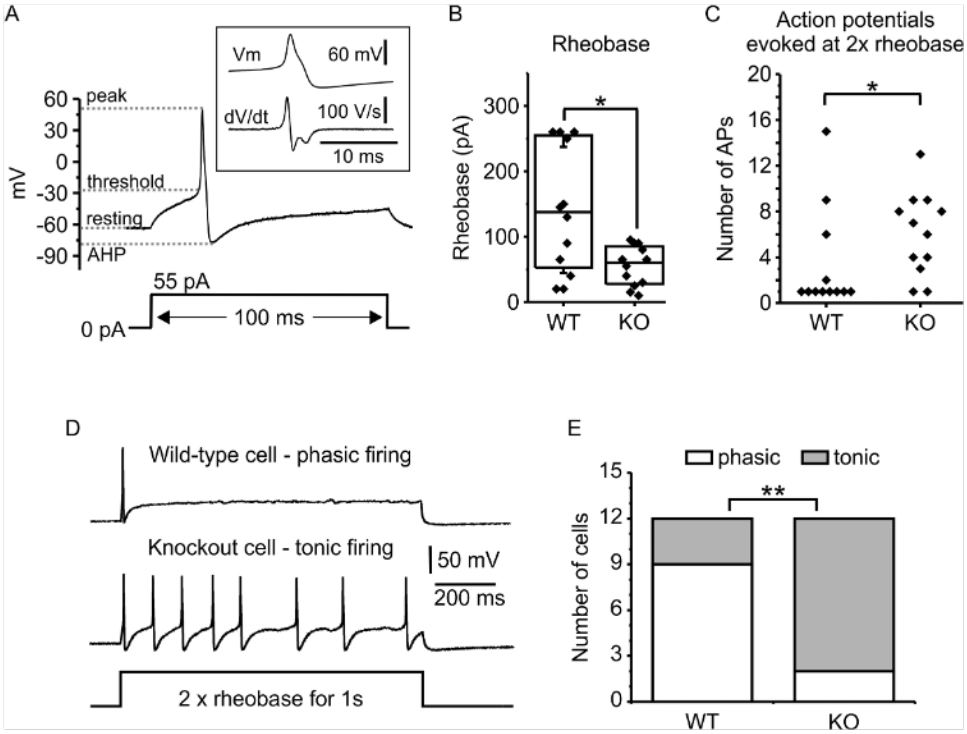

Figure 14: DRG neurons cultured from Jedi-1 KO mice are hyperexcitable. Patch clamp electrophysiology was used to record evoked action potentials from small diameter WT and KO DRG neurons. (A) Representative current-clamp recording from a Jedi-1 KO neuron. Stimulation with an excitatory current step (55 pA for 100 ms, lower trace) evoked a typical action potential (upper trace). The upper inset trace shows the action potential on an expanded time scale along with the 1st derivative of the trace. (B) Rheobase (defined as the smallest current step that evoked an action potential) was significantly smaller in Jedi-1 KO cells (*p = 0.03, Mann-Whitney test). Each point is from an individual cell and the box indicates median, 25% and 75% of the distribution. (C) Each point represents the number of action potentials evoked in an individual cell by a 1s current step at twice rheobase (see panel D). Significantly more action potentials were evoked in Jedi-1 KO neurons compared to WT (*p = 0.04, Mann-Whitney test). (D) Representative traces from a WT neuron (upper trace) and Jedi-1 KO neuron (lower trace) stimulated with a 1s current step at twice rheobase. The WT cell displayed phasic firing (a single action potential evoked at the onset of the stimulus) and the KO cell displayed tonic firing (8 action potentials evoked over the duration of the 1s stimulus). (E) The number of cells that displayed either phasic or tonic firing during a 1s stimulus (as in panel D) is shown. The proportion of Jedi-1 KO cells displaying tonic firing was significantly higher than WT (**p = 0.01, Fishers exact test).

	WT (n = 12)	KO (n = 12)	Statistical comparison
Membrane capacitance (pF) [mean (SD)]	19.9 (SD 11.1)	18.4 (SD 11)	p = 0.75 (t test)
Membrane resistance (MΩ) [median (1^{st}, 3^{rd} quartile)]	387 (168, 612)	576 (366, 820)	p = 0.24 (Mann-Whitney test)
Resting membrane potential (mV) [mean (SD)]	-61.5 (SD 6.9)	-57.2 (SD 4.2)	p = 0.08 (t test)
Rheobase (pA) [median (1^{st}, 3^{rd} quartile)]	138 (46, 258) *	60 (26, 88)	p = 0.03 (Mann-Whitney test)
AP threshold potential (mV) [mean (SD)]	-24.5 (SD 5.8)	-20 (SD 4.7) *	p = 0.048 (t test)
Membrane potential at peak (mV) [mean (SD)]	51 (SD 10)	57 (SD 5)	p = 0.065 (t test)
Maximal rising slope (V/s) [mean (SD)]	162 (SD 76)	138 (SD 30)	p = 0.32 (t test)
Membrane potential at peak of afterhyperpolarization (mV) [mean (SD)]	-73 (SD 5.4)	-77 (SD 3.5)	p = 0.056 (t test)
Amplitude of afterhyperpolarization (change from baseline) [mean (SD)]	11.8 (SD 8.3)	19.9 (SD 4.3) **	p = 0.009 (t test)
Action potential amplitude (peak to AHP) [mean (SD)]	124 (SD 12.6)	134 (SD 7) *	p = 0.027 (t test)
AP duration at half max (ms) [mean (SD)]	2.0 (SD 0.46)	1.9 (SD 0.3)	p = 0.48 (t test)

Table 1: Basic electrical properties and parameters of evoked action potentials from WT and Jedi KO neurons. Properties of WT neurons (n = 12 cells from 4 independent preparations) or Jedi KO neurons (n = 12 cells from 3 independent preparations) are shown along with results of statistical comparisons performed using Student's t-test or Mann-Whitney test for parametric and non-parametric datasets, respectively. Bold font indicates properties that were significantly different in Jedi cells compared for wild-type (* $p < 0.05$, ** $p < 0.01$).

These results indicate that Jedi KO neurons are hyper-excitable, suggesting there might be differences in the expression and/or function of ion channels. To investigate this further we used voltage clamp recording, focusing on voltage-gated sodium channel currents (I_{Na}). The peak sodium current density (evoked by a voltage step to 0mV) was not significantly different in KO neurons compared to WT neurons (Figure 15A). The current-voltage relationships (Figure 15B) were similar for the two genotypes, with a slight (4-5 mV) hyperpolarizing shift apparent in the KO neurons that was also apparent in the activation curves (plotting normalized conductance Vs voltage) (Figure 15C). However, the midpoint of activation (V_{50}) determined by fitting each individual cell was not significantly different (WT -12.8 ± 4.4 (SD) mV, n = 8; KO -17.5 ± 7.4 (SD) n = 7, p = 0.14). Steady state inactivation (Figure 15C) was best fit using a double Boltzman function and there was a significantly larger contribution of the more hyperpolarized component in KO compared to WT neurons (Table 2). The inactivation and activation curves are plotted together in Figure 15C showing the shifts in voltage-dependence of I_{Na} result in a slightly larger and hyperpolarized window current in KO neurons. Overall, these data support the idea that changes in the expression and/or function of voltage-gated sodium channels contribute to the increased excitability of KO neurons.

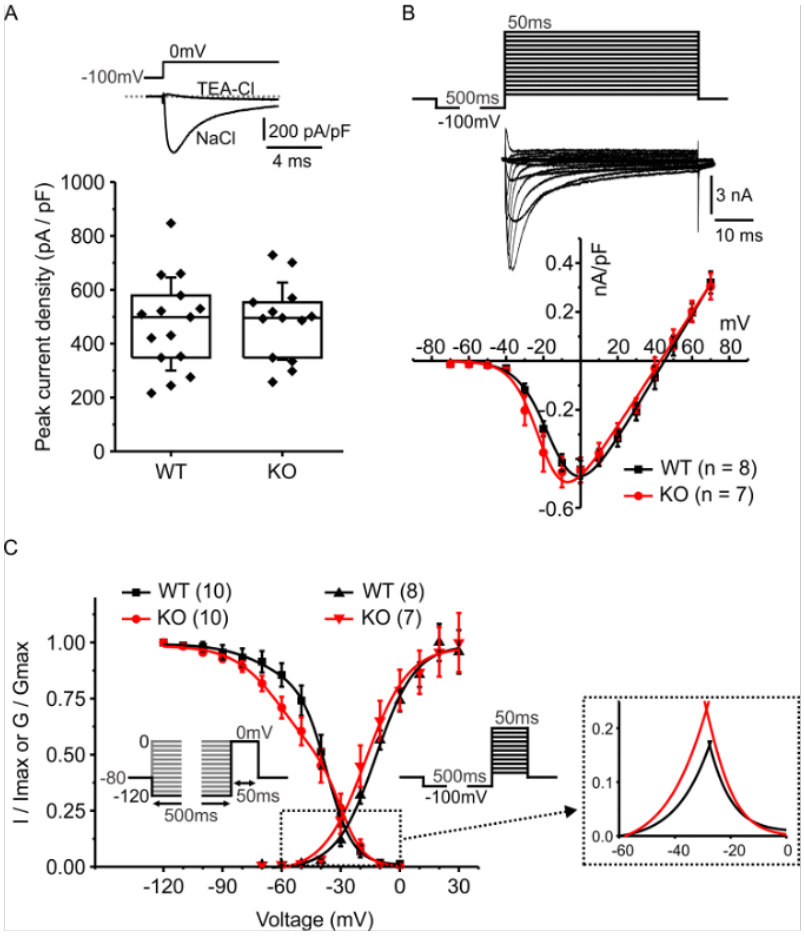

Figure 15: Voltage gated sodium channels have altered properties in DRG neurons isolated from Jedi-1 KO mice. Whole cell patch clamp electrophysiology was used to record voltage-gated sodium channel currents from small diameter wild-type (WT) and Jedi-1 knockout (KO) DRG neurons. (A) The upper trace shows two superimposed currents from the same cell evoked by a voltage step from -100mV to 0mV. Replacement of extracellular NaCl with TEA-Cl abolished the fast inward current confirming it was due to activation of voltage-gated sodium channels. The peak current density evoked by a voltage step to 0mV was not significantly different between genotypes. Each point is from an individual cell, box indicates median, 25% and 75% of the distribution, whisker indicate standard deviation of the mean. (B) Current-voltage relationship for wild type (WT) and knockout (KO) neurons. The upper panel shows an example of the stimulus protocol and sodium currents from a representative neuron. The lower panel plots mean peak current density against the test potential. (C) Normalized inactivation curves (left two curves) and activation curves (right two curves) for wild type and knockout neurons are superimposed. The inset cartoons depict the voltage protocols: inactivation was produced by a series of 500ms steps (-120mV to 0mV) prior to a 50ms test pulse to 0mV. Peak current amplitude produced by the test pulse was normalized to the largest current and plotted against the voltage of the 500ms conditioning pulse. Solid curves show the fit with a double Boltzmann function. Activation curves were derived from the same data used to produce the current voltage-relationship in panel B (see methods for more detail). Solid curves show the fit with a Boltzmann function. The “window current” is shown on an expanded scale in the dashed box to the right.

Activation	**WT (n = 8)**	**KO (n = 7)**	
V_{50} act (mV)	-12.8 (SD 4.4)	-17.5 (SD 7.4)	p = 0.15
Slope (activation) (mV)	9.6 (SD 1.4)	8.5 (SD 2.4)	p = 0.29
Inactivation	**WT (n = 10)**	**KO (n = 10)**	
V_{50} inact 1 (mV)	-68 (SD 13.5)	-70 (SD 10.7)	p = 0.77
V_{50} inact 2 (mV)	-38 (SD 7.8)	-33 (SD 10.1)	p = 0.24
Slope inact 1 (mV)	13.5 (SD 6.3)	15 (SD 7.8)	p = 0.69
Slope inact 2 (mV)	5.4 (SD 1.1)	5.6 (SD 1.6)	p = 0.71
Fractional contribution of component 1	0.17 (SD 0.17)	0.39 (SD 0.27)	* p = 0.046

Table 2: Activation and inactivation parameters of I_{Na}. Parameters of the Boltzman fits to the activation and inactivation curves. Each individual cell was fit with a single (activation) or double (inactivation) Boltzman function and the indicated parameters pooled for statistical comparison using Student's independent t-test. V_{50} act is the midpoint at which 50% of the channels were activated. V_{50} inact are the midpoints for the two components of the inactivation curve. * denotes statistically significant difference, $p < 0.05$.

Section 3.3: Discussion

DRG neuron hyperexcitability is correlated with chronic pain, a severe problem in our society that affects an estimated 50 million people in the United States alone[590]. Understanding the cellular and molecular mechanisms that regulate neuro-responsiveness is essential for improved treatment of chronic pain conditions. In the current study, we demonstrate that loss of the phagocytic receptor Jedi increases DRG neuronal excitability; however, Jedi was not detected in the neurons, but was expressed by endothelial cells, satellite glia and perineurial cells. These results indicate that deficiency in Jedi indirectly alters sensory neuron activity in a non-cell autonomous mechanism. Our findings contribute to the growing body of literature that suggests that neuron-glia interactions are essential for proper regulation of neuronal homeostasis.

We found that SGCs express low levels of Jedi, similar to previous results[358]. Satellite glial cells have a well-established role in augmenting DRG neuron activity through several mechanisms, including paracrine signaling and regulation of extracellular ion concentration[105]. SGCs release a number of soluble factors that contribute to the inflammatory milieu including PGE2[591], IL1-β[142], and TNFα[592]. Conversely, the SGCs respond to signals from the neurons including neurotransmitters and neuropeptides, which act in a feed forward mechanism to produce more inflammatory signals from the SGCs. SGCs typically exhibit canonical signs of activation when they enhance neuronal activity and potentiate chronic pain, which includes increased proliferation and up-regulation of GFAP. In the current study, we did not observe morphological changes or traditional activation markers to satellite glia. It is possible that Jedi KO SGCs operate through a novel mechanism independent of conventional activation pathways or that Jedi acts during a specific developmental window that was not observed in our analysis focused mostly on postnatal mice.

Surprisingly, loss of Jedi did not result in the accumulation of apoptotic neurons, despite

our previous *in vitro* findings that Jedi contributed to the phagocytosis of neuronal corpses by satellite glia[358]. We suggest that this is due to the presence of additional engulfment receptors; for example, MEGF10 is also expressed by satellite glia[358]. Recent findings suggest that satellite glia are developmentally arrested Schwann cells,[593] which also express multiple engulfment receptors[475]. Due to redundancy and compensation by other engulfment receptors, a defect in phagocytosis is unlikely to occur unless multiple receptors are deleted.

Jedi was also detected in endothelial cells, in agreement with previous studies[371,379,380]. The endothelium lies in very close proximity to the neurons and can influence their function directly by producing pro-nociceptive compounds or indirectly by attracting inflammatory cells such as macrophages and T cells[594–596]. In rodent models of chronic pain including nerve injury and chronic inflammation, the vasculature undergoes neoangiogenesis, increases in branching complexity, and has a distinct 'leakiness' believed to contribute to chronic pain[597,598]. In our Jedi KO animals, however, we did not find changes in vascularization in the ganglia or nerve (data not shown), nor did we observe differences in leakiness of the vessels (Figure 11E). Our results confirm a prior study that utilized the same Jedi KO mouse model to show no significant changes in baseline density of blood vessels in muscle and skin[380]. Therefore, while the Jedi deficient endothelial cells could be responsible for the altered neuronal activity, it is not due to enhanced vascular density or permeability.

In addition to satellite glia and endothelial cells, we also found that Jedi is a novel marker for perineurial glia. Although the perineurium has not been shown to directly influence neuronal function, we know that it has important developmental roles in myelination and formation of the NMJ[581,599]. Additionally, it plays a crucial role in regeneration of peripheral nerves because it is one of the first cell types to bridge the nerve gap after injury and participates in phagocytosis of myelin and axonal debris during Wallerian degeneration[460]. After injury, the permeability of the blood nerve barrier breaks down to allow infiltration of peripheral immune cells that often

contribute to neuropathic pain[175]. Our data show no statistically significant changes in Jedi KO perineurium morphology or permeability under basal conditions; however, it is possible that loss of Jedi from perineurial glia causes the release of soluble factors that alter neuronal activity in a paracrine signaling manner.

Our *in vitro* data demonstrating hypersensitivity of Jedi KO DRG neurons to a depolarizing current stimulus was performed in mixed neuron-glia co-cultures that contain several cell types. Since these cultures were dissociated into single cells and the data was acquired under a constant flow of extracellular solution within one to two days after the dissection, it is unlikely that acute cell-cell contact or paracrine signaling are responsible for the change we observed *in vitro*. Rather, the mechanism is more likely to be developmental, since our mouse is a global (constitutive) knock-out of Jedi.

One of the interesting changes that we found in Jedi KO DRG neurons was an increase in the number of cells that responded to capsaicin. Capsaicin is an agonist for the non-specific cation channel, TrpV1, which also responds to heat, acid, arachidonic acid derivatives (HETEs, AEA, etc.), mechanical, and osmotic pressure[600]. TrpV1 is expressed mostly in C fibers but also a subset of Aδ fibers[601]. A multitude of inflammatory chronic pain conditions including Irritable Bowel Syndrome, Rheumatoid Arthritis, and peripheral neuropathies have been shown to up-regulate TrpV1 activity through a number of different factors such as cytokines, prostaglandins, bradykinin, NGF, glutamine, and serotonin[602]. These molecules not only can be released by immune cells but also by satellite glial cells, Schwann cells, and endothelial cells when they become 'activated'[603,604]. Since DRG neurons isolated from Jedi KO mice are hyperactive and neuronal activity has also been shown to enhance TrpV1 activity, it is unclear whether TrpV1 underlies or is a by-product of neuronal activation. It is worth noting that 45% of Jedi KO neurons responded to capsaicin but only ~30% of the KO cells were positive for the TrpV1 immunostaining. We suggest this is likely due to non-specific binding of capsaicin to other

receptors and/or the relative insensitivity of antibody-based techniques.

Altered excitability of peripheral DRG neurons is associated with changes in nociception, raising the possibility that Jedi KO mice and humans with loss-of-function (LOF) Jedi SNPs such as rs12041331[373] may have altered pain responses. Consistent with this possibility, our patch clamp electrophysiology experiments show that small diameter DRG neurons isolated from Jedi KO animals exhibit enhanced excitability as demonstrated by the smaller rheobase and increase in the proportion of cells exhibiting a tonic rather than phasic firing pattern. Because our electrical recordings were from small diameter neurons, which are primarily nociceptors[605], and TrpV1+ cells are also mostly small in diameter (Figure 13E), and nociceptive[606], we hypothesize that the cells patched for whole cell current clamp and the cells exhibiting enhanced capsaicin sensitivity during calcium imaging are most likely an overlapping population of pain-sensing cells. However, we did not evaluate TrpV1 expression or capsaicin sensitivity directly in the neurons we patched, therefore we cannot say for certain that these are the same cells.

A variety of voltage-gated ion channels and calcium-activated ion channels contribute to the electrical excitability of DRG neurons. Among these, voltage-gated sodium channels (VGSCs) play crucial roles in determining action potential firing patterns. Several VGSCs are highly expressed in small diameter nociceptive neurons including tetrodotoxin (TTX) sensitive channels (primarily NaV1.7 along with NaV1.3 and NaV1.6) and TTX resistant channels (NaV1.8, and NaV1.9). Human and mouse mutations in these sodium channel subunits lead to hereditary changes in human pain sensitivity[607]. This prompted us to investigate if loss of Jedi affected sodium channel currents in small diameter DRG neurons. These whole cell voltage clamp experiments revealed changes to sodium channel function in neurons cultured from Jedi KO mice, thereby corroborating the changes in neuronal excitability observed in current clamp recordings. Specifically, we found the overall current density (amount of current normalized for

cell size) was not altered in the KO neurons compared to WT. However, we did find changes in the voltage-dependence of steady state inactivation which can serve as a biophysical fingerprint for the various sodium channel subtypes (Figure 15C). The fractional contribution of the more hyperpolarized component was doubled in KO neurons (Table 2). Jedi KO neurons also displayed a modest hyperpolarizing shift in activation, causing a larger and slightly hyperpolarized overlap of channel activation and inactivation, the so-called 'window current' (Figure 15C). We speculate that the relative contribution of TTX-sensitive sodium channels (perhaps NaV1.7) is greater in the KO neurons. These channels inactivate in the hyperpolarized voltage range that is increased in the KO neurons and the modest hyperpolarizing shift in activation (Figure 15B, C) is also consistent with an increased contribution from TTX-sensitive channels. Notably, the kinetics of closed-state inactivation are relatively slow for NaV1.7 channels[608,609]. This property means the channels can amplify subthreshold current inputs, thereby enhancing neuronal excitability[610], consistent with the decrease in rheobase for KO neurons that we report (Figure 14B). The shift from phasic to tonic evoked action potential firing in the KO neurons (Figure 14E) might also involve altered sodium channel expression and/or function, although contributions from potassium, calcium, or chloride channels are also possible. Overall, our electrophysiology data identified altered sodium channel function in the KO neurons, but determining the precise mechanism(s) leading to increased excitability will require more extensive biophysical characterization.

In conclusion, we observed that Jedi KO DRG neurons exhibited a change in neuronal excitability despite a lack of Jedi expression in the neurons; rather, we found high Jedi expression in perineurial glia and endothelial cells, and lower expression in a subset of satellite glia. We hypothesize that the change in neuronal activity is due to an indirect mechanism of intercellular interaction between these non-neuronal cells and the sensory neurons. It is interesting that all of the changes we found, capsaicin sensitivity, hyperactivity, and sodium

current changes, are also found in inflammatory pain states. Our findings, like others, indicate that indirectly targeting neurons through glia may be an alternative treatment for chronic pain.

Section 3.4: Materials and methods

Mice

All animal procedures were approved by the Vanderbilt University Medical Center's comprehensive Animal Care and Use Program (ACUP) in compliance with the NIH guidelines for the Care and Use of Laboratory Animals. Mice were housed under a controlled 12-hour light/dark cycle. Standard laboratory rodent diet (*LabDiet* catalog no. 5001) and water was available *ad libitum.* Jedi knock-out (KO) were Pear1$^{tm1a(KOMP)Wtsi}$ mice derived from embryonic stem cells provided by the International Mouse Phenotype Consortium (IMPC, catalog no. CSD31459_C05). Control mice were wild-type (WT) C57/BL6 mice obtained from Jackson Labs and then maintained by our laboratory (catalog no. 000664).

RT-PCR

RNA was isolated from flash frozen tissue using Trizol (ThermoFisher Scientific catalog no. 15596026) according to the manufacturer's directions. The RNA was treated with TURBO DNase (Lift Technologies catalog no. AM2238). cDNA was made using an Invitrogen RT kit with oligo dT primers and RNase included (Invitrogen catalog No 18080-051). PCR amplification was performed using the primers specified below.

Primers

The following primers were used to verify the orientation of the KOMP insert at the 5' end of the Jedi genomic DNA locus: All primer sequences listed 5' to 3': Forward,

TCTGACCTCCTCTTGTGCCTC and reverse, GGCTTCACTGAGTCTCTGGCA. The following primers were used to verify the orientation of the KOMP insert at the 3' end of the Jedi genomic DNA locus: Forward, CTGCCACTGTCATAGCATTA and reverse, CACTTAATGACACTCCTTTC. The following primers were used to amplify mouse GAPDH transcript for RT-PCR: Forward, TGCACCACCAACTGCTTAG and reverse, GATGCAGGGATGATGTTC. The following primers were used to amplify mouse Jedi transcript for RT-PCR: Forward, CCTGCAGCTGCCCACCGGGCTGGA and reverse, CCTGGCAGCCCGGGCCATGCGTGT.

Immunoprecipitation (IP) / Westerns

Mouse tissue was flash frozen for western blots and stored at -80° C. Tissue was ground into a fine powder then lysed and sonicated in RIPA buffer (1% NP-40, 0.5% deoxycholate, 0.1% SDS, 150 mM NaCl, 50 mM Tris-Cl pH 8.0) with protease and phosphatase inhibitors added according to the manufacturer's specifications (Roche catalog no. 04693159001 and Roche catalog no. 04906837001).

Two mg total protein per samples was pre-cleared with 1:1 mixture of Protein A/G sepharose beads (Invitrogen catalog no. 101041 and 101241, respectively). Anti-Jedi rabbit polyclonal antibody[359] (not commercially available) or control serum were incubated with the samples overnight at 4° C and pulled down with Protein A/G beads. After washing with lysis buffer, samples were denatured and run on an SDS-PAGE acrylamide gel, transferred to a nitrocellulose membrane, and blocked with 5% milk. IPs were immunoblotted with mouse anti-Jedi monoclonal[359] (not commercially available) or mouse anti-Tubulin (Calbiochem catalog no. CP06) primaries and anti-mouse secondaries (Promega catalog no. W402B) and developed on an Amersham Imager 600 version 1.2.0. Some western blots were developed on film in a dark

room. Similar to above but blotted with anti-Jedi1 (R&D catalog no. AF7607-SP) or anti-laminin (Millipore catalog no. AB2034).

DRG cultures

DRGs from adult or early postnatal animals, as indicated in each experiment, were pooled from all levels and digested at 37**°** C in 0.15% collagenase (Sigma catalog no. C5894), 0.05% trypsin (Worthington catalog no. LS003708), and 5 KU/mL DNase (Sigma catalog no. D5025) diluted in TESCA buffer (50 mM TES, 0.36 mM $CaCl_2$, pH 7.4) for 5-30 minutes, depending on the efficiency of the digest. After inactivating the digest with Hyclone serum, cells were triturated with a fire polished glass pipette, spun at 100 x g for 6 minutes, and resuspended in media. Media used for DRG cultures: 1 to 1 mixture of Neurobasal (Gibco catalog no. 21103-049) and UltraCulture (Lonza catalog no. 12-725F) media, 3% Hyclone serum (Hyclone catalog no. SH30088.03), 1% N2 (Gibco catalog no. 17502-048), 2% B27 (Gibco catalog no. 17504-044), 1% L-glutamine (Gibco catalog no. 25030-081), 1% Pen/Strep (Gibco catalog no. 15140-122), 50 ng/mL NGF (Harlan catalog no. B5017). Cells were plated on collagen (Sigma catalog no. C3867-1VL) coated glass coverslips and calcium imaging or patch clamping were completed within 24-48 hours after plating the cells.

HeLa cell cultures

HeLa cells overexpressing Jedi were used as a positive control for Jedi staining *in vitro* and as a positive control for western blot. HeLa cells were maintained in DMEM (Gibco catalog no. 11995-065) with 10% serum (Peak catalog no. PS-FB2) and were transfected with a Jedi-GFP fusion construct made within our lab[359] using Lipofectamine 2000 according to the manufacturer's instructions (Thermo Fisher Scientific catalog no. 11668030).

Immunohistochemistry (IHC)

Tissue was fixed in 10% neutral buffered formalin (NBF) for 2 hours for small tissue and overnight for larger tissues. Samples were then dehydrated and embedded in paraffin. Five micron sections were cut. Tissues were then rehydrated and antigen retrieval performed using one of the following three methods: (1) Proteinase K (Macherey Nagel/Clontech Laboratores catalog no. 740506) at a final concentration of 20 micrograms/mL for 30 minutes at room temperature according to the manufacturer's instructions. (2) Citrate buffer (10 mM citric acid, 0.05% Tween 20, pH 6.0) in pressure cooker for 12 minutes. (3) Tris-EDTA (10mM Tris Base, 1 mM EDTA, 0.05% Tween 20, pH 9.0) in pressure cooker for 12 minutes. All washes were done with PBS. All tissue was blocked in 5% BSA, 0.1% Tween-20 diluted in PBS. Slides were mounted in ProLong Gold with DAPI (Life Technologies, catalog no. P36931). Regular fluorescence microscopy was performed on a Nikon Eclipse Ti microscope with a DS-Qi2 camera using NIS Elements AR version 4.5 software. Confocal images were acquired on a Leica SP5 confocal microscope using LAS AP software version 2.7.3.9723.

Statistical analysis

All microscopy images were analyzed using the open source processing software ImageJ version 2.0.0-rc-69/1.52p. Unless stated otherwise, we stained a minimum of 5 sections of ganglia or sciatic nerve at least 60 microns apart per animal for each measurement. Data points represent an average of repeated measurements per animal. Each animal used as a single 'n' for statistical analysis. The number of animals used for each experiment varies for each experiment and is reported in the figure legend or text. Statistical tests and graphs were performed and generated using Prism8 software version 8.3.

Primary Antibodies used for IHC

PEAR1 (R&D catalog no. AF7607-SP), Laminin (Millipore catalog no. AB2034), Glut1 (Abcam catalog no. ab40084), BFABP (gift from Dr. Thomas Muller[611]), PGP9.5 (AbD Serotec catalog no. 7863-0504), GS (Santa Cruz catalog no. sc-6640-R), GFAP (Millipore catalog no. MAB360), HuC/D (Molecular Probes catalog no. A21272), ZO-1 (ThermoFisher Scientific, catalog no. 61-7300), Ki67 (Cell Signaling catalog no. 12202), TrpV1 (Alomone catalog no. ACC-030).

Immunocytochemistry (ICC)

Cells were fixed in 10% NBF for 25 minutes at room temperature, permeabilized in 0.5% Triton-X-100 diluted in PBS for 5 minutes at room temperature, and blocked in 10% horse serum, 10% goat serum, 0.1% Tween-20 diluted in PBS for 1 hour at room temperature. Primary antibodies were diluted in blocking buffer and incubated on the cells overnight at 4° C. Cells were washed with PBS and incubated with fluorescent secondary antibodies diluted in blocking buffer for 1 hour at room temperature. Cells were washed with PBS and mounted with 1 mm thick coverslips using ProLong Gold (Invitrogen catalog no. P36931) and imaged on a Leia SP5 confocal microscope at 100X magnification.

Primary antibodies used for ICC

anti-Jedi (R&D catalog no. AF7607), anti-Tuj1 (Covance catalog no. 801213), anti-TrpV1 (Alomone catalog no. ACC-030). *Secondary antibodies used for ICC:* anti-sheep secondary (Abcam catalog no. ab175712), anti-mouse secondary (Thermo Fisher Scientific catalog no. A11029), anti-rabbit secondary (Invitrogen catalog no. A11035).

TEM

Adult sciatic nerves were isolated and fixed in 0.1M sodium cacodylate (Electron Microscopy Sciences [EMS], catalog no. 11652), 2% paraformaldehyde (EMS catalog no. 15713-S), 3% glutaraldehyde (EMS catalog no. 16310) for 1 hour at room temperature then overnight at 4° C. Samples were washed three times in 0.1 M cacodylate buffer (wash buffer) and post-fixed in 1% osmium tetroxide (EMS catalog no. 19150) for 1 hour at room temperature then overnight at 0.5% osmium tetroxide. Samples were washed three times in wash buffer then gradually dehydrated with increasing concentrations of ethanol. Samples were then infiltrated in solutions with increasing ratios of Epon-812 (EMS catalog no. 14120) to propylene oxide (EMS catalog no. 20401) until reaching pure resin. Samples were embedded in Epon-812 and baked at 60° C for 48 hours. Thick sections were cut at 0.5 microns on a Leica UC7 ultramicrotome and counterstained with toluidine blue. Thin sections were cut at 70 – 80 nm, counterstained with 2.0% uranyl acetate and Reynolds lead citrate, and collected on a 300 mesh copper grid. TEM images were acquired on a Philips/FEI T-12 microscope using an AMT CCD camera and AMT Image Capture Engine software version 600.156.

Blood nerve barrier (BNB)

Sterile 2% Evan's blue dye (Sigma catalog no. E2129) dissolved in PBS was injected intravenously. Three hours after the injection, mice were perfused with PBS and organs collected and placed in formamide. The samples were baked at 55° C for 48 hours. Absorbance of the supernatant was measured at 610 nm and normalized to the weight of the tissue.

Calcium imaging

Methods for calcium imaging were previously published and summarized here[612,613]. The fluorescent calcium (Ca^{2+}) dye Fura-2 acetoxymethyl ester (AM) (Setarah Biotech catalog no.

6101) was used to measure cytosolic calcium concentration. Cells were washed twice with HEPES-buffered Hanks' balanced salt solution (HBSS) and incubated for 30 to 45 min with 3 μM Fura-2AMat 37°C and then washed in Fura-free HBSS solution for 30 to 60 min before recording. The coverslip with the cells attached was transferred to a recording chamber mounted on the stage of a Nikon TE2000 fluorescence microscope (Nikon Instruments Inc., Melville, NY). The total volume of the recording chamber was 300-400 uL and was constantly perfused from gravity-fed chambers at a rate of 4 mL/min with an NaCl-based extracellular solution containing 2 mM Ca^{2+} (145 mM NaCl, 2 mM KCl, 1 mM $MgCl_2$, 10 mM glucose, 10 mM HEPES, 2 mM $CaCl_2$, pH 7.3, ~305 mOsm). An InCyt IM2 fluorescence imaging system (Intracellular Imaging Inc., Cincinnati, OH) was used to monitor $[Ca^{2+}]_i$. Cells were alternately excited at wavelengths of 340 and 380 nm and emission at 510 nm detected using a PixelFly digital camera. Ratios were collected every 1 second throughout the experiment and converted to $[Ca^{2+}]_i$ using an i*n vitro* calibration curve, generated by adding 15.8 μM Fura-2 pentapotassium salt to solutions from a calibration kit containing 1 mM $MgCl_2$ and known concentrations of Ca^{2+} (0–1350 nM) (Invitrogen). Cells with an unstable baseline were excluded from the analysis. Cells were treated with the various drugs for 30 or 60 seconds, followed by washout with the NaCl-based solution for until calcium levels returned to baseline, except for capsaicin. Drugs used in the following order: 1 mM chloroquine (CQ) for 60 seconds, 100 uM histamine (HIST) for 60 seconds, 200 uM AITC for 60 seconds, and 500 nM CAP for 30 seconds. As a positive control, 90 mM KCl solution was added for 30 seconds to identify healthy neurons (57 mM NaCl, 90 mM KCl, 1 mM $MgCl_2$, 10 mM glucose, 10 mM HEPES, 2 mM $CaCl_2$, pH 7.3, ~305 mOsm). A cell was considered to respond to treatment if its intracellular calcium levels increased ≥15% above the baseline concentration in the 30 seconds prior to treatment. For cells that responded to capsaicin, their intracellular calcium concentrations remained high

even after washout. Therefore, they often did not respond to KCl. As long as all of the other requirements were met, these cells were included in the analysis.

Patch-clamp electrophysiology

All electrophysiology was performed on small diameter (< 25 micron diameter) neurons maintained in culture for 24-48 hours following plating. All experiments were performed at room temperature (23–25° C). Personnel performing patch clamp recording and initial data analysis were blinded to the genotype of the cells. Methods were similar to those we have previously described[612,614]. Patch pipette electrodes were pulled from borosilicate glass capillary tubes (World Precision Instruments, Sarasota, FL) using a Sutter P-97 pipette puller (Sutter Instrument, Novato, CA). Electrodes were coated close to the tip with dental wax (Electron Microscopy Sciences, Hatfield, PA) and fire-polished using a Narishige MF-830 microforge (Narishige, Amityville, NY) to a final resistance of ~2 MΩ when filled with patch-pipette solution. Cells were recorded in the conventional whole-cell configuration using a HEKA EPC10 amplifier and PatchMaster acquisition software (HEKA Instruments Inc., Holliston, MA, USA) or an Axopatch 200B amplifier, Digidata 1400A interface, and PClamp10 (Clampex) acquisition software (Molecular Devices, Sunnyvale, CA). Series resistance was partially compensated (~50 - 80%) and analog data were filtered at 10 kHz and digitized at 100 kHz for voltage-clamp recording of fast voltage-gated sodium channel currents, or filtered at 5 kHz and digitized at 20kHz for current clamp recording.

For current clamp recording, individual cells were first voltage-clamped and allowed to stabilize (patch solution equilibrate) for approximately 3-4 minutes. Membrane capacitance was determined using Patchmaster software as an objective measure of cell size (surface area). The recording mode was then switched to current clamp and spontaneous membrane potential was recorded for 1-2 minutes. Cells with an unstable resting membrane potential, or resting potential

more depolarized than -45mV were discarded. Membrane resistance was determined by applying small (5-10 pA, 100ms) hyperpolarizing and/or depolarizing current steps and recording the resulting change in membrane potential. Cells were stimulated with a series of 100 ms current steps of increasing magnitude (increment 5-10pA) to determine rheobase (the smallest current step that evoked an action potential). The cell was then stimulated with a 1 second step depolarization first to rheobase and then to twice rheobase to determine the number and pattern of evoked action potentials. Phasic firing was defined as a cell that fired one or two action potentials within the first 100 ms of stimulation and then remained silent for the remainder of the stimulus. Tonic firing was defined as 3 or more action potentials occurring throughout the duration of the stimulus. Action potential parameters were determined from the first evoked action potential and are summarized in table 1. The threshold potential was determined by calculating the 1st derivative of the action potential to better identify the onset of the upstroke of the action potential. Threshold potential was empirically set to be the potential at the time point when dV/dt reached 10% of its maximum value.

Voltage-clamp data for I_{Na} were subjected to linear capacitance and leak subtraction using P/N protocols (P/-4 or P/-8) with the leak pulses applied following the test pulses. The recording bath (volume ~300 uL) was continually perfused with fresh solution at a flow rate of ~3-4 ml/min from gravity-fed reservoirs. Standard extracellular recording solution (see below) was the same as that used for current clamp. In some cells extracellular NaCl was replaced with TEA-Cl to confirm the fast voltage-gated current was carried primarily by sodium channels. The voltage protocols are shown on the figures. Conductance was calculated from the peak inward current evoked by a voltage step as follows: $G = I / (V - E_{Na})$, where G = conductance, I = peak sodium current, V = membrane potential of the voltage step and E_{Na} = the reversal potential of sodium channel current).

Solutions used for electrophysiology were as follows: extracellular recording solution contained 145 mM NaCl, 2 mM KCl, 1 mM $MgCl_2$, 10 mM glucose, 10 mM HEPES, 2 mM $CaCl_2$, pH 7.3, ~315-320 mOsm adjusted with sucrose as needed. The intracellular patch pipette solution for current clamp contained 140 mM KCl, 0.5 mM EGTA, 5 mM HEPES, 3 mM Mg-ATP, pH 7.3, ~ 305-310 mOsm adjusted with sucrose as necessary. The intracellular patch pipette solution used for voltage-clamp recording of I_{Na} contained 140 mM CsCl, 10 mM NaCl, 2 mM EGTA, 10 mM HEPES, 2 mM $MgCl_2$, 2 mM Mg-ATP, pH 7.3, ~ 305-310 mOsm adjusted with sucrose as necessary. The calculated liquid junction potentials were ~5mV and were not corrected. All experiments were performed at room temperature (~23–25° C). Raw data were analyzed using PClamp10 (Clampfit) or HEKA FitMaster software. Graphing and statistical analyses were performed using OriginPro 2016

Section 3.5: Acknowledgements

We acknowledge the Translational Pathology Shared Resource supported by the NCI/NIH Cancer Center Support Grant 5P30 CA68485-19 and the Vanderbilt Mouse Metabolic Phenotyping Center Grant 2 U24 DK059637-16 for processing our tissues for paraffin embedding. We thank the Vanderbilt Cell Imaging Shared Resource (supported by NIH grants CA68485, DK20593, DK58404, DK59637 and EY08126) for processing and imaging our TEM samples. This work was supported by National Institute of Health grant R01 NS102365.

CHAPTER 4

MICE LACKING THE PHAGOCYTIC RECEPTOR JEDI DO NOT HAVE SOMATOSENSORY PHENOTYPES *IN VIVO*

Authors

Alexandra J. Trevisan, Angel Farinas, Phillip J. Kingsley, Lisa A. Poole, Lindsay N. Redman, Mary Katherine Morrice, Nikhil S. Kotharie, and Bruce D. Carter

Section 4.1: Introduction

DRG neurons detect a wide array of somatosensory modalities including pain, itch, touch, proprioception, and temperature[1]. Aberrant electrical activity of DRG neurons directly leads to chronic pain or itch, a common underlying mechanism in a multitude of pathological states including cancer, autoimmune diseases, diabetes, injury, and inflammation[615]. Our previous data showed that *in vitro*, DRG neurons isolated from mice lacking the phagocytic receptor Jedi were hyperactive. Therefore, we tested the hypothesis that Jedi KO mice would exhibit in vivo correlates of the enhanced DRG neuron excitability, including localized signs of inflammation, altered somatosensory responses, as well as impaired nerve regeneration.

The increase in AP firing that we previously observed in neurons from Jedi KO mice suggested that these mice would exhibit an increase in sensitivity to sensory neuron stimulation *in vivo*. The increase in neuronal firing occurred in small diameter neurons which are primarily nociceptors and pruriceptors. Typically, this leads to excessive nocifensive or scratching behavior in mice and humans[616–619].

Our prior characterization of Jedi expression in the peripheral nervous system showed that Jedi is not detectable in sensory neurons themselves; rather, it is expressed by perineurial glia, satellite glia, and endothelial cells. Therefore, the mechanism of DRG sensitization in Jedi KO animals is non-cell autonomous and probably occurs through a released soluble signal. Many secreted inflammatory molecules have been shown to instigate DRG neuron firing, including TNFα, IL6, IL-1β, and PGE2[620–623]. Levels of these pro-inflammatory and pain-inducing compounds are elevated in neuropathic pain states, rheumatoid arthritis, osteoarthritis, inflammatory bowel disease, multiple sclerosis, metabolic disorders, and nerve injury[615]. In chronic pain mouse models, immune cell infiltration occurs at the site of injury and pain, but also in the ganglia itself, leukocytes are believed to initiate action potentials at cell bodies as well as in the periphery through cytokines and lipid second messenger species[595,596,624]. The capsaicin receptor TrpV1 is an extremely important neuronal target of this 'inflammatory milieu' and increases in expression, phosphorylation levels, and localization[625]. Mice lacking the TrpV1 channel do not experience inflammatory-induced pain; therefore, TrpV1 is essential for this process[626,627]. We previously showed that a higher percentage of Jedi KO DRG neurons respond to the TrpV1 agonist capsaicin, consistent with *de novo* expression of TrpV1 in a normally non-nociceptive subtype of DRG neuron that becomes sensitized to pain under inflammatory conditions including nerve injury[628–630]. Although we previously showed a lack of global autoimmunity in Jedi KO mice, here, we hypothesized that the hyperactivity of Jedi KO sensory neurons is due to a local inflammatory mechanism mediated by TrpV1 in the DRG itself.

Our prior work utilized live calcium imaging and electrophysiology of cultured DRGs *in vitro* to demonstrate the hyperactivity of Jedi KO neurons. Because the process of culturing DRGs requires double axotomy, the behavior of the cells in a dish more closely resembles their behavior after an injury rather than at baseline[631,632]. Peripheral nerve injury is a common cause

of pain and inflammation that can persist long after regeneration is complete[633,634]. Relative to the CNS, the PNS has an amazing ability to re-grow damaged axons and restore function to the affected area[196,635]. An essential step that must occur prior to axonal regeneration is Wallerian degeneration, which involves the break-down and clearance of axonal and myelin debris distal to the injury site[636]. Several professional and non-professional phagocytes engulf this debris including perineurial cells and Schwann cells (albeit the contribution of these cells to Wallerian degeneration is minor compared to macrophages and neutrophils)[460,475,637]. Our prior data showed Jedi expression in perineurial glia, and a recent study showed that Schwann cells up-regulate Jedi post injury[475]. Since we previously characterized Jedi as a phagocytic receptor involved in clearance of dead cells during development, we hypothesized that Jedi may also play an important role in phagocytosis after injury[358–360]. Failure to efficiently clear axonal and myelin debris in the nerve inhibits re-growth of axons; therefore, impaired phagocytosis will in turn delay regeneration and functional outcome[389,638–640]. In the current study, we tested the role of Jedi in peripheral nerve injury repair by evaluating changes in its expression, phagocytosis, pain, and axonal regeneration.

Section 4.2: Results

Loss of Jedi does not result in systemic or local inflammation

Our previous data showed that sensory neurons isolated from Jedi KO mice were hyperactive despite Jedi not being expressed in the neurons themselves. We also found no changes to Jedi-expressing cells with known roles in the modulation of neuron function, namely satellite glia, endothelial cells, and perineurial cells. We alternatively hypothesized that neuron hypersensitivity would be associated with inflammation, another well-documented source of

DRG neuron hypersensitivity[641–643]. Data shown in Chapter 2 extensively characterizes a lack of systemic inflammation, so we looked more locally within the dorsal root ganglia itself.

We performed RNAseq analysis of flash frozen DRG tissue (Figure 16A) and cultured DRG cells *in vitro* (data not shown) to evaluate steady state changes in gene expression in the absence of Jedi. Overall, we found very few differentially expressed genes between genotypes both *in vivo* and *in vitro* under the same conditions used for electrophysiological analysis. Figure 16A shows no significant change in the number of normalized reads for inflammatory genes with greater than 10 TPM between genotypes. We conclude that the phenotypes observed previously must be due to a post-transcriptional mechanism.

Lipid second messengers, especially arachidonic acid derivatives, play a crucial role in inflammatory cell signaling[600,623,644]. We measured the levels of PGE2 in DRGs by mass spectrometry because it has specifically been shown to directly cause sensory neuron depolarization[644] (Figure 16B). Additionally, we measured prostaglandin D2 (PGD2), 12-hydroxyeicosatetraenoic acid (12-HETE), and 15-hydroxyeicosatetraenoic acid (15-HETE), all of which have pro-inflammatory effects[645] (data not shown). For each lipid species, we did not find significant differences when comparing Jedi WT and KO tissue samples. Jedi KO DRG neuron excitability is therefore independent of pro-inflammatory lipid signaling.

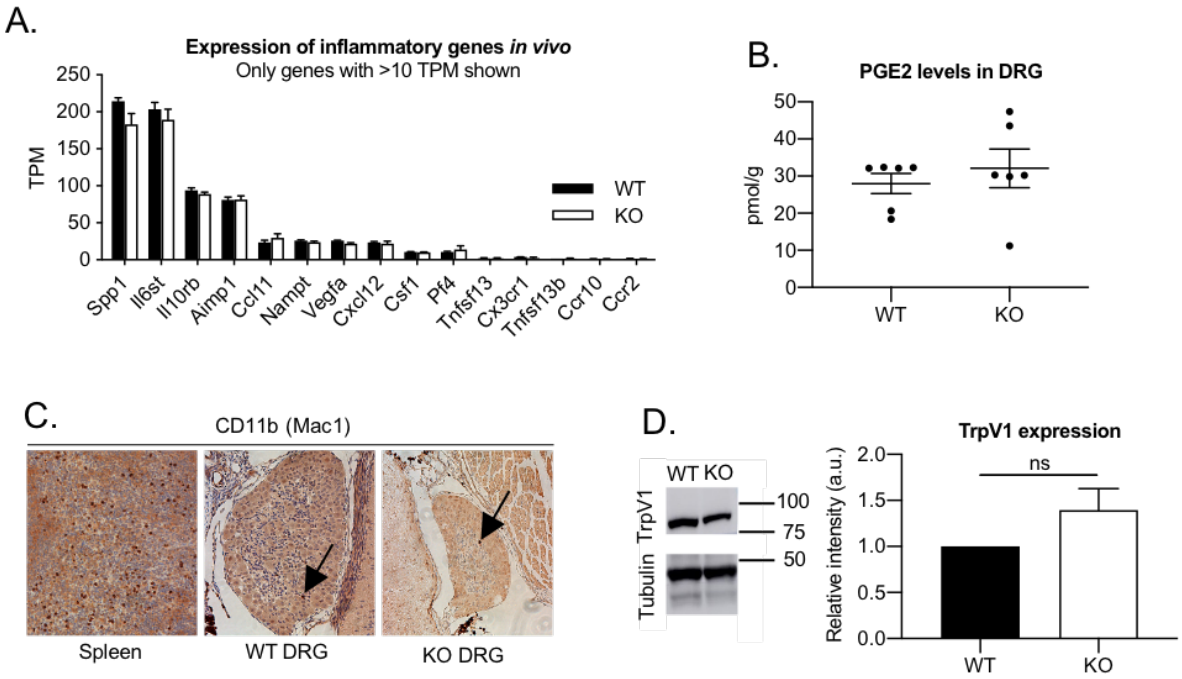

Figure 16: Sensory neuron hyperactivity is not due to inflammation. (A) RNAseq reads for selected inflammatory genes is shown for Jedi WT and KO flash frozen DRG samples aged 8-12 weeks (n=5 animals per genotype, both sexes). Only inflammatory genes with >10 TPMs is shown. No statistical change between genotypes using DEseq using a FDR < 0.05. (B) PGE2 levels shown for flash frozen DRG tissue samples. n=6 animals per genotype aged 8-12 weeks, 3 male and 3 female mice per genotype. No statistically significant change between genotypes using Student's t test. (C) IHC for CD11b in FFPE sections from spleen (positive control), WT DRG, and KO DRG. Arrows indicate resident CD11b+ macrophages in the ganglia. Age = P0. (D) Western blot for TrpV1 and Tubulin as a loading control. Ladder marks are in kDa. Quantification shown on right. Values reported relative to tubulin as KO/WT integrated density analysis with WT values set to 1 for each independent experiment. No statistical difference using one sample t and Wilcoxon test with an expected value of 1. n=10 samples per genotype aged 8-12 weeks old. Both sexes included in analysis.

In some inflammatory chronic pain models, immune cells infiltrate peripheral sensory ganglia and nerves and sensitize the neurons, thereby exacerbating pain sensation[595,596]. We immunostained DRGs at various developmental ages for CD11b+ macrophages, using spleen tissue as a positive control (Figure 16C). Although we did observe low levels of resident macrophages in Jedi WT and KO samples, we did not see an increase in the number of these cells in Jedi KO mice as predicted (Figure 16C). The DRGs did not exhibit hypercellularity or other histological signs of inflammation. Therefore, the increase DRG neuron activity is not associated with local recruitment of leukocytes.

As described earlier, TrpV1 is an essential mediator of inflammatory-induced pain[606,646]. Inflammatory signals increase TrpV1 levels and induce its phosphorylation thus potentiating its activity[629,647–650]. Previously, we found that more cultured KO DRG neurons respond to the TrpV1 agonist, capsaicin, compared to WT cells. We quantified the number of TrpV1-expressing cells both *in vivo* and *in vitro* and measured the intensity of the fluorescent signal in Chapter 3 but did not find any significant changes between genotypes in TrpV1 expression with microscopy-based techniques. Here, we validated these results by western-blotting for TrpV1, and again did not find a statistically significant increase in TrpV1 (Figure 16D). Based on this TrpV1 data, the RNAseq analysis *in vivo* and *in vitro*, mass spec for inflammatory lipid mediators, IHC for macrophages in the DRG, and all of the negative data for systemic immunity presented in Chapter 1, we conclude that the increase in TrpV1 neuron activity of Jedi KO mice is not due to an inflammatory mechanism.

Jedi KO mice do not exhibit altered somatosensory behavioral phenotypes as a result of hyperactive DRG neuron firing

Previously we found that a higher proportion of DRG neurons isolated from Jedi KO mice respond to capsaicin and that they fire more action potentials when stimulated with

depolarizing current (Figure 13). DRG neurons are responsible for detecting all bodily senses, including itch, pain, thermosensation, and touch, and the literature shows that alterations in DRG firing causes pain[651,652]. We therefore evaluated the somatosensory behavior of Jedi WT and KO mice to determine whether the *in vitro* sensitivity would be reflected in altered sensory responses *in vivo*.

Itch is the most common dermatological complaint in elderly patients and can be caused by dry, flaky skin and a thinning of the epidermal and dermal cutaneous layers[653–655]. Most pruriceptors are small diameter C fibers and a small population of Aδ neurons[656,657]. We therefore evaluated spontaneous scratching behavior in young adult (8-12 weeks old) and aged mice (greater than 1 year old) as a positive control. After habituating the animals for 4 days, we recorded the mice for 30 minutes and quantified the number of bouts and amount of time that the animals exhibited hind limb scratching or back biting behavior (Figure 17A). We consistently found that in both genotypes aged mice scratched more than young mice, but there was no significant difference in scratching bouts or time between genotypes (Figure 17A). Therefore, DRG neuron hypersensitivity in cultured cells did not manifest into pruritus in Jedi KO intact animals.

Due to the capsaicin hypersensitivity we observed in neurons isolated from Jedi KO mice *in vitro*, we treated animals with capsaicin injection into the foot *in vivo*. Capsaicin induces a painful reaction that includes lifting, shaking, and licking the hindfoot[658]. We categorically quantified these behaviors (Figure 17B) and measured the amount of time they spent doing them and the number of times we observed these behaviors within the first ten minutes after the injection. However, we did not observe an initial increase in nocifensive behavior in Jedi KO mice after capsaicin treatment (Figure 17B).

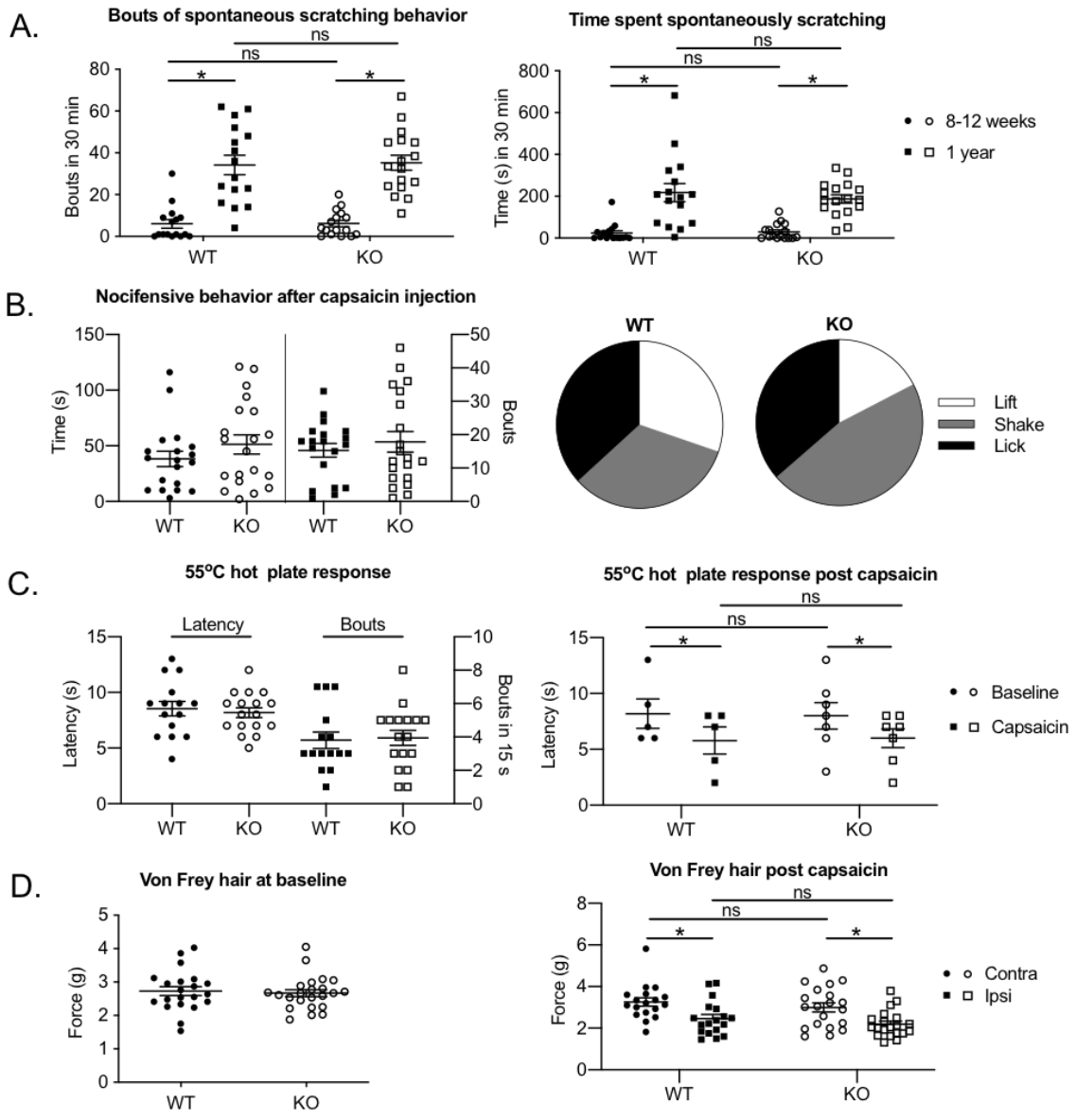

Figure 17: Jedi KO mice do not have behavioral somatosensory phenotypes before or after capsaicin administration. (A) The number of times and length of time that mice performed scratching behavior defined in Methods section in Jedi WT and KO mice at the indicated ages. n=16-17 animals in each group. Both sexes represented. 2 way ANOVA shows significance between ages but not between genotypes. (B) 1 microgram of capsaicin was injected into the rear footpad of mice and their immediate behavior within the first 10 minutes after injection was recorded. The amount of time and number of times they spent lifting, shaking, or licking the ipsilateral paw is recorded. The frequency of these behaviors is shown in pie charts on the right. n=19-20 animals per genotype with both sexes represented. No statistical change between genotypes using unpaired t test. (C) Hot plate test at baseline (left) and 1 hour after capsaicin injection (right). Latency and bouts of nocifensive behavior described in the methods section. Baseline: n=15-16 animals per genotype with both sexes represented. Capsaicin: n=5 animals per genotype. Age was 8-12 weeks old. No statistical change using unpaired t test. (D) Von Frey hair analysis at baseline and after capsaicin injection on the contralateral and ipsilateral side. Baseline n=21-23 animals per genotype. No change using unpaired t test. Capsaicin: n=16-18 animals per genotype. 2 way ANOVA shows significant changes between paws but not between genotypes.

We also measured thermosensation in Jedi KO mice by placing them on a hot or cold plate and measuring the latency and bouts of nocifensive behaviors (only data for hot plate shown in Figure 17C). Unfortunately, we again found no statistically significant change between genotypes. Since capsaicin sensitizes mice to heat, we performed the same assay one hour after the foot capsaicin treatment described above[659]. While the latency to hot plate response was significantly reduced as expected in both groups, there was no further decrease in Jedi KO animals (Figure 17C).

Another common assay for somatosensation is the Von Frey hair test, which measures non-noxious low threshold mechanosensation. We measured the amount of force required for mice to withdraw their feet from touch (Figure 17D). At baseline, there was no significant change in Jedi KO mice. Capsaicin is known to produce allodynia, or a painful response to non-noxious touch, such that the force required to elicit the withdraw response is decreased[659]. 90 minutes after the injection, we did observe allodynia in both WT and KO mice, but again, there was no significant difference between genotypes.

Overall, these behavioral assays do not reflect the hyperactivity of DRG neurons we observed *in vitro*, either under basal conditions or after the injection of capsaicin into the animals. The behavioral tests described here are not comprehensive of all somatosensation, so it is possible that alternative behavioral assays or other surgical, pharmacological, or genetic treatments may be required to produce an observable behavioral phenotype in these mice.

Jedi KO mice do not have altered responses to nerve injury

Because culturing DRG neurons requires double axotomy of the peripherally-extending and central projecting pseudounipolar axon, the behavior of these neurons *in vitro* more closely mimics their behavior after an injury rather than basal conditions[631,632]. We did not observe gross changes to somatosensory behavior in Jedi KO animals even after treatment with the alogen

capsaicin, despite their hyperactivity in electrophysiological recordings. Following a peripheral nerve injury, DRG neurons become hyperexcitable, TrpV1 levels increase, and chronic pain proceeds long after axonal regeneration is complete[634]. Additionally, previous work from our lab delineates the role of Jedi as a phagocytic receptor[358–360]. Phagocytosis is a critical step after nerve injury during the process of Wallerian degeneration, as axonal and myelin debris distal to the injury site must be removed by this process in order for regeneration to occur[636]. Therefore, we performed two separate peripheral nerve injuries in Jedi KO and control mice to mimic *in vivo* the culture conditions and test the role of Jedi as a phagocytic receptor post injury. We performed a sciatic nerve crush injury or sciatic nerve transection followed by epineurial sutures.

Previous work from Ben Barres' lab showed by RNAseq that Jedi expression increases following a nerve injury[475]. We immunostained for Jedi in nerve longitudinal sections and confirmed that in WT mice, Jedi expression increased distal to the injury, although there was an increase in background signal as well (Figure 18A). Schwann cells have been shown to be phagocytic following nerve injury, so we hypothesized that Jedi as up-regulated in these cells in order to facilitate engulfment of debris[475]. We tested this hypothesis by staining for myelin and axons and quantifying their disappearance after the injury at the distal side of the nerve (Figure 18B for myelin data, axonal data not shown). As expected, myelin and axonal debris was nearly cleared within one week of the injury, but the rate of clearance was not altered in the absence of Jedi. Similar to our analysis of efferocytosis in Chapter 2, we found that Jedi is dispensable for the clearance of cellular debris.

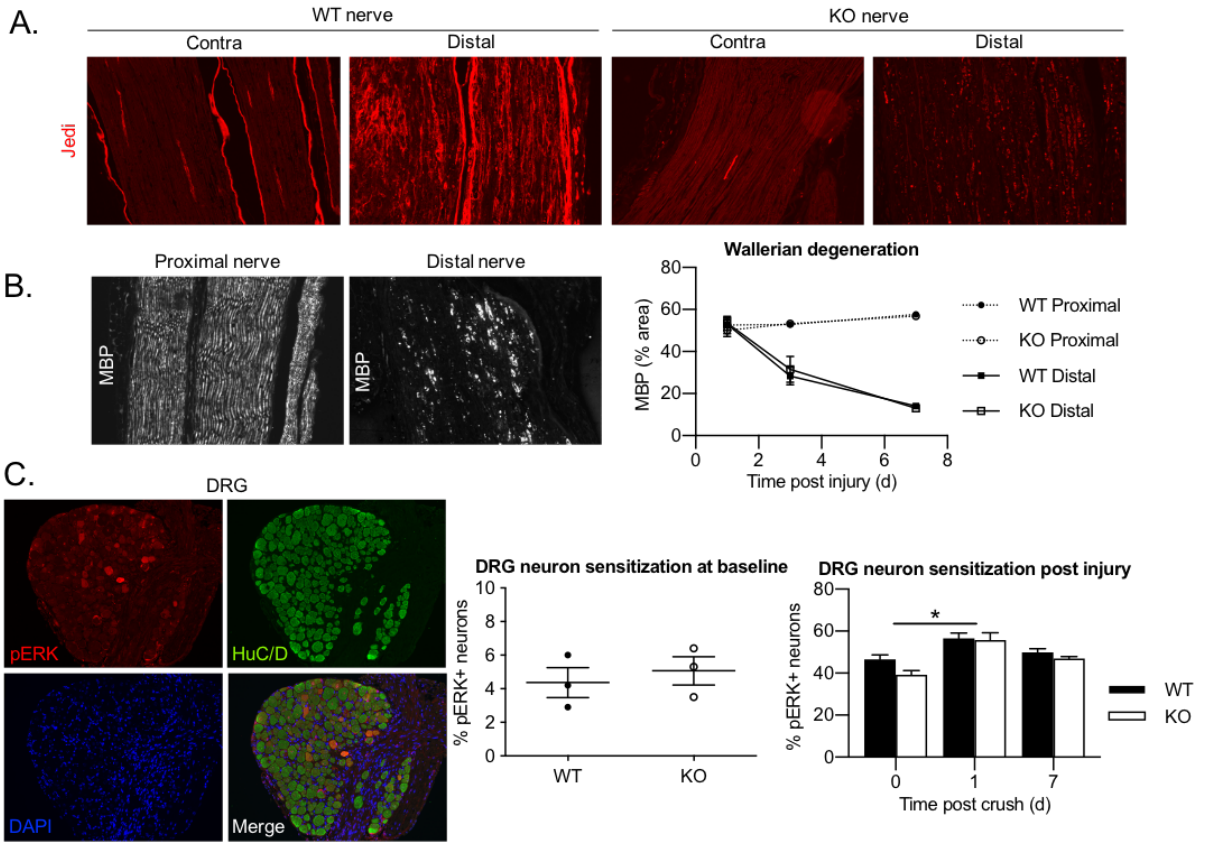

Figure 18: Jedi KO mice do not have altered responses to nerve injury. (A) Jedi IHC from 8-12 week old WT and KO mice 3 days post sciatic nerve crush in longitudinal nerve sections from the uninjured contralateral side or ipsilateral side distal to the crush site. Notice an increase in Jedi expression in the endoneurial space of the nerve in the WT mouse and that this signal is still above increased background that occurs with injury. (B) MBP IHC in mice 8-12 weeks old at 1, 3, and 7 days post sciatic nerve crush at the proximal and distal sides of the injury site. Representative staining shown on the left. n=3 animals per genotype. For each animal, nerves were serially sectioned at 5 microns and every 12th section stained, quantified, and then averaged such that a minimum of 5 measurements were made per animal. Error bars represent standard error of the mean. No statistical different between genotypes according to 2 way ANOVA analysis. (C) Representative IHC staining and quantification of phosphoERK in DRGs from adult 8-12 week old mice under basal conditions or at 0, 1, or 7 days post sciatic nerve crush. For each animal, DRGs were serially sectioned and every 12th section stained and quantified such that a minimum of 5 sections were analyzed per animal. Baseline: n=3 animals per genotype. No statistical change between genotypes according to an unpaired t test. Error bars represent SEM between animals. Post injury: n=1 animal per genotype. Error bars represent SEM within all sections analyzed per animal (this ranged from 8-16 sections per condition). 2 way ANOVA shows a statistically significant increase in the proportion of phosphoERK+ cells for both genotypes at 1 day post crush, which returns to normal by day 7. However, there were no significant changes between genotypes at any time point analyzed.

Following nerve injury, DRG neurons fire spontaneously and cause chronic pain. We used phosphoERK as a surrogate for neuronal activity at baseline and after injury in fixed sections of DRG tissue[438,660–662]. Under basal conditions, we did not find any change in phosphERK staining, which is consistent with the lack of behavioral phenotype (Figure 18C). Following nerve crush, we did observe a significant increase in phosphoERK staining in both genotypes after one day but this returned to baseline levels by one week (Figure 18C). At each time point, there was not a significant change between WT and KO mice, therefore we did not follow up with behavioral analysis. We conclude that Jedi does not play an essential role in sensitization of sensory neurons following a peripheral nerve injury.

The peripheral nervous system has an amazing ability to regenerate following Wallerian degeneration[663]. We tested for intrinsic changes in neurite outgrowth in Jedi KO mice *ex vivo* using whole DRG explants not subjected to enzymatic dissociation (Figure 19A). By day 5 after placing the explants in culture, there was exquisite outgrowth from both genotypes but there was no statistically significant change in the absence of Jedi. Therefore, neurite outgrowth is not intrinsically affected by loss of Jedi.

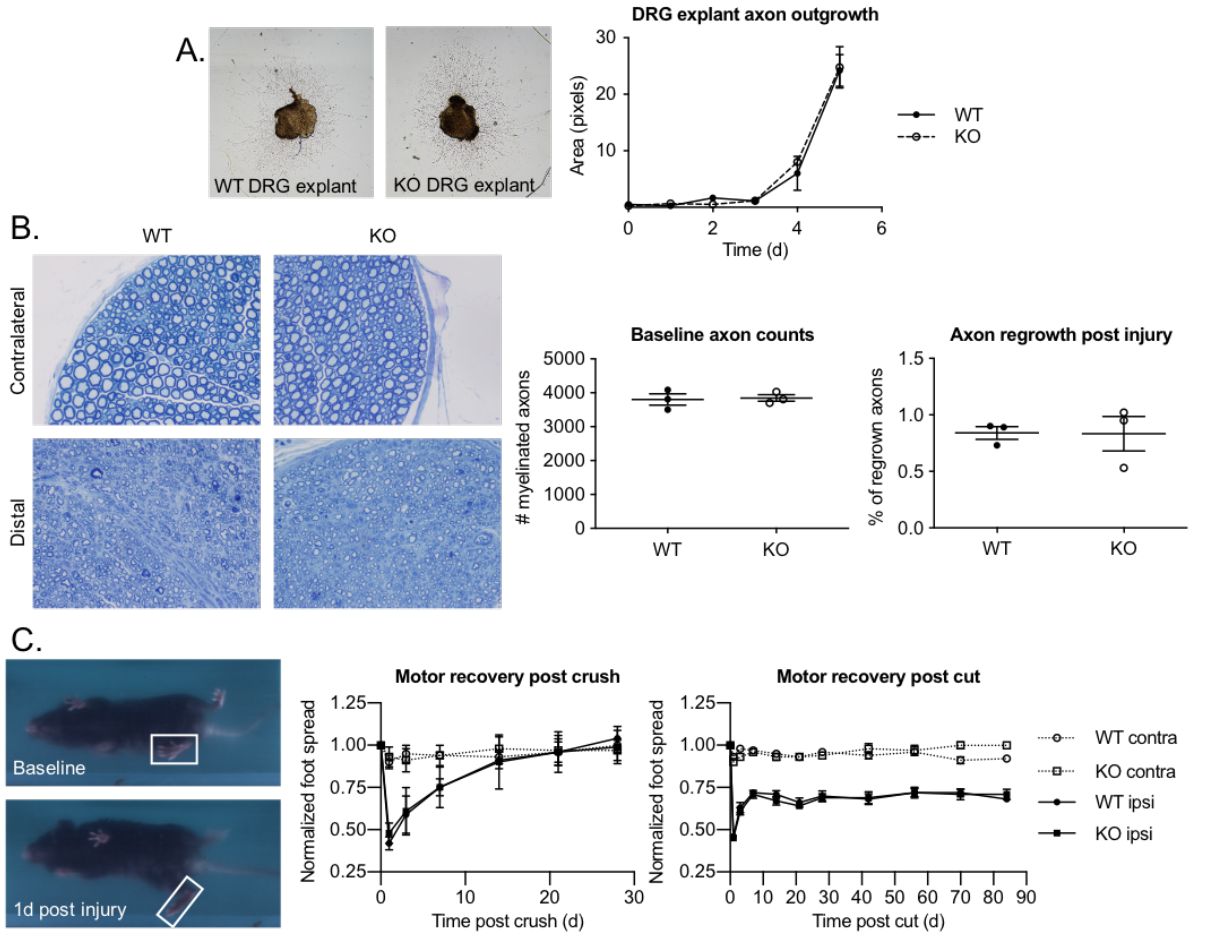

Figure 19: Axonal regeneration is unaltered in the absence of Jedi. (A) DRG explant cultures from naïve WT and KO adult mice aged 8-12 weeks old grown in a bed of Matrigel for up to 5 days. Neurite outgrowth was measured in area around the explant at 0, 1, 2, 3, 4, and 5 days in culture. n=3-5 ganglia per condition. 2 way ANOVA shows no statistical difference between genotypes at any time point measured. (B) Plastic embedded sciatic nerve cross sections were stained for toluidine blue 12 weeks post sciatic nerve transection in Jedi WT and KO animals that were 8-12 weeks old at time of surgery. Representative images shown for contralateral controls and the distal side of the ipsilateral injured nerve. Notice the morphology of myelin is thinner even 12 weeks after the injury. Axons were counted in contralateral controls to measure baseline axon counts. n=3 animals per genotype. No statistical change on the contralateral side using an unpaired student's t test. On the ipsilateral side, distal axon counts were normalized to proximal axon counts and represented as the percent of regrown axons across the injury site. n=3 animals per genotype with no statistical change between them using an unpaired student's t test. (C) Motor axon regeneration was inferred from motor activity on a clear-bottom treadmill recorded with a high speed camera. Length and toe with were measured and reported as a ratio from the contralateral and ipsilateral site of both sciatic nerve crush and transection. A minimum of 5 measurements per paw were averaged per animal. Crush: n=5-6 animals per condition with both sexes represented. Error bars represented SEM. No statistical change between genotypes at any time point using 2 way ANOVA. Transection: n=11-22 animals per condition with both sexes represented. Error bars represent SEM. No statistical change between genotypes using 2 way ANOVA.

To measure axon regeneration *in vivo*, we collected nerves and counted myelinated fibers at baseline and across the site of injury on the ipsilateral side using toluidine blue staining. We confirmed our data showing no difference in the number of DRG somas (Figure 12) by showing at baseline that there was no significant difference between axons (Figure 19B). In addition to sensory neurons, the sciatic nerve cross sections also includes motor and autonomic axons, which implies that there is also no change in the number of these other cell types[664]. Twelve weeks after the injury, we also did not find a significant change in newly grown axons across the site of injury between genotypes, indicating that Jedi does not play a significant role in axonal regeneration (Figure 19B). To validate these results, we assessed length and width of foot spread in live animals over time after either crush or transection. One day after the surgery, there was severe dysfunction of the injured foot (Figure 19C). After the crush injury, the animals fully recovered within 4 weeks, while the mice with transection only partially recovered even after 12 weeks. However, there was no difference in motor function recovery between genotypes, confirming that Jedi is not essential for axonal regeneration *in vivo*.

Section 4.3: Discussion

In summary, we did not find any in vivo correlates of the neuronal hyperexcitability detected in vitro from Jedi KO neurons. We have demonstrated this not only peripherally for systemic autoimmunity in Chapter 2, but we also did not find evidence of local inflammation within the peripheral somatosensory nervous system that could underlie the neuronal hyperactivity we discovered *in vitro*. Generally, an increase action potential firing of DRG neurons, as we observed with Jedi KO cultures, causes hypersensitivity to pain, itch, touch, temperature, or other bodily senses. However, we performed several common behavioral tests for somatosensation in Jedi WT and KO animals but did not find statistically significant differences between genotypes. In order to better mimic culture conditions *in vivo*, we performed

two different nerve injuries – sciatic nerve crush or transection – but again found no changes in phagocytosis, neuronal activity, or axonal regeneration in Jedi KO mice. These results do not necessarily mean that Jedi is not important; on the contrary, perhaps it is so important that its function is layered in redundancy making our current model inadequate to truly parse out its function.

Somatosensation is an incredibly complex system with a diversity of DRG neuronal subtypes responsible for detecting a wide range of stimuli. These neurons have been categorized over the years by a number of different attributes including their size, myelination status, conduction velocity, firing patterns, pattern of spinal cord innervation, and more recently, next generation single cell sequencing analysis[156]. Depending on which method used to organize them, there are up to 35 different types of DRG neurons, with the majority of these being nociceptors[665]. Our cell-by-cell analysis using electrophysiological methods only assayed 10-12 small-diameter neurons per genotype with unknown functional modalities. Many DRG neurons themselves are poly-modal, meaning that the same cell can detect, for example, heat and vibration. The combinations are dizzying and without further information it is hard to know which behavioral assays would be best to distinguish differences between Jedi WT and KO mice. Here, we performed the most common somatosensory behavioral assays – hot/cold plate, Von Frey hair, and capsaicin sensitivity, but there are many other possibilities we did not assess. Some of these include the Randall Selitto, acetone, dynamic temperature, texture discrimination, and tactile pre-pulse inhibition test among others[666–670]. Additionally, we performed surgical intervention in order discern a phenotype in the mice, but there are also a number of other challenges commonly used in the field to elicit responses, including Complete Freud's Adjuvant, chronic constriction model, histamine, or dry/aged skin models[671]. Additionally, our analysis solely focused on the glabrous skin of the paws, which have fundamentally different innervation patterns and specialized nerve ending receptors compared

to hairy skin. Exploring these other assays in the future may finally delineate a phenotype in the Jedi KO mice.

An alternative explanation for why we observed DRG neuron hyperexcitability *in vitro* but no behavior outcome for this *in vivo* is central compensation mechanisms in the spinal cord or even higher levels of processing in the CNS. A surprising amount of somatosensory information processing occurs locally in the spinal cord before being sent to higher brain regions via the posterior column-medial lemniscal system (DCMLS) or anterolateral pathways for fine touch and pain/temperature/crude touch, respectively[672]. The diversity of spinal cord interneurons is even greater than the DRG neurons themselves, and include both inhibitory and excitatory cells that utilize multiple neurotransmitters/peptides to integrate afferent sensory information[30]. The dorsal horn local circuitry is dynamically regulated; the best examples of this are demonstrated by chronic pain studies, which show that local spinal cord circuitry potentiates pain signals in a maladaptive manner[21,673,674]. One mechanism for potentiation of pain signals is the activation of central astrocytes, which become 'activated' in the dorsal horn of the spinal cord in chronic pain models[675]. We assessed astrocyte activation by staining for GFAP in the spinal cord in Jedi KO animals but did not find evidence for glial activation there (data not shown). Top-down regulation of somatosensory information can also come from higher brain regions including the periaqueductal grey matter (PAG) and rostroventral medulla (RVM), which send efferent projections to the dorsal horn that can modulate the excitatory or inhibitory tone of the region[676,677]. We did not further investigate the role of central modulation on incoming DRG signals in the Jedi KO mice, but if that were indeed the reason for lack of a somatosensory phenotype, it would be very interesting because increased DRG input to the spinal cord is usually further potentiated rather than down-regulated. If true, that finding would have profound implications for clinical treatment of chronic pain or itch patients.

Our mice are bred homozygously such that Jedi KO mice have never had Jedi protein even as gametes. This breeding regime gives the animals ample time to adapt to the absence of a protein. We recently created a floxed Jedi allele, allowing us to acutely remove the gene and measure responses in a mouse accustomed to having Jedi present. This could be accomplished by crossing with a global inducible Cre such as R26R-CreERT2 mice. Additionally, we can cross with tissue-specific promoters to create conditional KO in certain cell types like endothelial cells, perineurial glia, or satellite glia. Lastly, there are three mammalian family members closely related to Jedi (also known as MEGF12), MEGF10 and MEGF11. While relatively little is known about MEGF11, MEGF10 also functions as an engulfment receptor in the CNS and plays an important role in synapse pruning[554]. It is possible that MEGF10 compensates for loss of Jedi, therefore we also recently created double KO of both Jedi and MEGF10, but these mice have not yet been phenotyped. These alternative strategies may be a better approach to delineating a subtle phenotype of Jedi and its family members in an in vivo model.

Jedi is well-conserved as human and mouse Jedi share about 70% amino acid sequence identity. There is an intronic human single nucleotide polymorphism (SNP rs12041331) of Jedi that is highly prevalent in the African population that causes a decrease in human Jedi RNA and protein similar to our KO mouse model[363]. Prior GWAS studies have identified SNPs of Jedi to have irregularities in platelet clotting, but previous studies using the same mouse model described here indicate that Jedi KO mice do not recapitulate this phenotype[361–363,375]. Given our analysis of the DRGs, we wanted to specifically evaluate patients harboring rs12041331for neurological phenotypes using the de-identified genotype-medical record database BioVU. This analysis did not reveal any significant associations between rs12041331and any nervous system abnormality, which is in agreement with the *in vivo* analysis of the mouse presented here.

An interesting observation from the injury data presented here was the increase in Jedi expression following sciatic nerve crush, yet no discernable phenotype in regard to Wallerian degeneration, neuron activation, or axon regeneration. Why does Jedi expression increase if its function is inconsequential? It is common that genes expressed together will often be physically localized to similar regions of the chromosome, although this is obviously not always true[678]. However, it is extremely interesting that immediately upstream of the Jedi locus in both the human and mouse genomes is a gene that is of critical importance of DRG neuron survival, subtype specification, outgrowth, and function – TrkA[679,680]. This neurotrophin receptor not only plays a crucial role in development of the DRG but also in axon regeneration after nerve injury[681]. It is possible that Jedi up-regulation after injury is simply due to its close physical chromosomal position to TrkA and has no functional benefit at all to wound repair.

As previously mentioned, there are a number of transmembrane proteins that act as engulfment receptors in addition to Jedi. Our RNAseq data did not show transcriptional up-regulation of any of these receptors in the DRG (data not shown), although it is possible their activity is modulated through post-translational modifications not apparent in RNA analysis. Alternatively it is possible that a sufficient number of receptors are expressed such that loss on any single one does not lead to a deficiency in phagocytosis.

Following nerve injury, Schwann cells utilize the TAM family members Axl and MerTK to phagocytosis debris, although double KO mice of these receptors still show considerable clearance, indicating that still other engulfment receptors play a significant role here[475]. Although Brosius-Lutz et al. reported an increase in Jedi RNA, which we validated by immunostaining, we found no effect on myelin or axonal clearance post injury. Additionally, when we co-stained for Jedi and an axonal marker, we did not observe any debris surrounded by Jedi-positive cellular matter in the distal side of the axon (data not shown). This indicates that Jedi is dispensable for

Wallerian degeneration, although it may have more subtle effects on nerve repair that we did not assess.

Our results indicate that Jedi KO mice do not have overt somatosensory phenotypes despite *in vitro* hyperactivity of DRG neurons, even after challenges with the alogen capsaicin and two peripheral nerve injuries. We have posited several explanations for this discrepancy and suggestions for future studies. A more detailed and thorough analysis or the generation of alternative mouse models will be required to fully understand the role of Jedi in an animal.

Section 4.4: Materials and methods

Mice

All animal procedures were approved by the Vanderbilt University Medical Center's comprehensive Animal Care and Use Program (ACUP) in compliance with the NIH guidelines for the Care and Use of Laboratory Animals. Mice were housed under a controlled 12-hour light/dark cycle. Standard laboratory rodent diet (*LabDiet* catalog no. 5001) and water was available *ad libitum.* Jedi-1 knock-out (KO) were Pear1$^{tm1a(KOMP)Wtsi}$ mice derived from embryonic stem cells provided by the International Mouse Phenotype Consortium (IMPC, catalog no. CSD31459_C05). Control mice were wild-type (WT) C57/BL6 mice obtained from Jackson Labs and then maintained by our laboratory (catalog no. 000664).

RNAseq

Tissue: DRGs from five individual animals per genotype were pooled together and flash frozen. *Cells:* DRGs from a litter of mice per genotype were pooled for each sample, and a total of three samples was used per genotype. Cells were cultured for 24 hours before RNA isolation as follows: DRGs from postnatal animals were pooled from all levels and digested at 37° C in

0.15% collagenase (Sigma catalog no. C5894), 0.05% trypsin (Worthington catalog no. LS003708), and 5 KU/mL DNase (Sigma catalog no. D5025) diluted in TESCA buffer (50 mM TES, 0.36 mM $CaCl_2$, pH 7.4) for 5-30 minutes, depending on the efficiency of the digest. After inactivating the digest with Hyclone serum, cells were triturated with a fire polished glass pipette, spun at 100 x g for 6 minutes, and resuspended in media. Media used for DRG cultures: 1 to 1 mixture of Neurobasal (Gibco catalog no. 21103-049) and UltraCulture (Lonza catalog no. 12-725F) media, 3% Hyclone serum (Hyclone catalog no. SH30088.03), 1% N2 (Gibco catalog no. 17502-048), 2% B27 (Gibco catalog no. 17504-044), 1% L-glutamine (Gibco catalog no. 25030-081), 1% Pen/Strep (Gibco catalog no. 15140-122), 50 ng/mL NGF (Harlan catalog no. B5017). Cells were plated on collagen (Sigma catalog no. C3867-1VL) coated glass coverslips and calcium imaging or patch clamping were completed within 24-48 hours after plating the cells.

RNA was isolated using the RNeasy kit (Qiagen cat#74134). RNA quality control, library prep, and sequencing were performed by Vanderbilt University Medical Center Technologies for Advanced Genomics (VANTAGE) core facility. Briefly, RNA QC was determined using the Agilent Bioanalyzer (cat# G2939A) and processed using Illumina's TruSeq Stranded mRNA (polyA selected) library preparation. The Illumina HiSeq3000 was used for paired-end, 75 bp length reads targeting about 30 million reads per sample. Flexbar was used to trim the sequencing primers from the reads and the transcripts were aligned to the mouse transcriptome using HISAT2. Over 90% of the reads mapped to the mouse transcriptome. The results SAM files were converted to BAM files, sorted, and indexed using Samtools. Differential analysis of gene expression was performed in R using the DEseq package. Statistically significant differences had a FDR < 0.05.

LC/MS/MS

Murine DRGs were collected as described, frozen on dry ice and stored at -80°C prior to processing and analysis. Tissue was prepared for LC-MS/MS analysis as previously described. All LC-MS/MS analysis was performed on a Shimadzu Nexera system in-line with a SCIEX 6500 QTrap as previously described[682]. The QTrap was equipped with a TurboV Ionspray source and operated in both positive and negative ion mode. SCIEX Analyst software (ver 1.6.2) was used to control the instruments and acquire and process the data. The deuterated internal standards AEA-d4, 2-AG-d5, OEA-d4, AA-d8, PGE2-d4, PGD2-d4, PGF2α-d4, 6-keto-PGF2α-d4, TXB2-d4, PGE2-G-d5 and PGF2α-G-d5 were purchased from Cayman Chemicals (Ann Arbor, MI) OG-d5 was purchased from TRC (Toronto, ON, CA). Authentic standards of these analytes were purchased from Cayman.

For prostaglandin, endocannabinoid, and arachidonic acid analysis, the analytes were chromatographed on an Acquity UPLC BEH C18 reversed-phase column (5.0 x 0.21 cm; 1.7 μm) which was held at 40°C. A gradient elution profile was applied to each sample; %B was increased from 15% (initial conditions) to 99% over 4.0 min, and held at 99% for another minute. Then the column was returned to initial conditions for 1.5 min prior to the next injection. The flow rate was 330 μL/min and component A was water with 0.1% formic acid while component B was 2:1 acetonitrile:methanol (*v:v*) with 0.1% formic acid.

For PG-G analysis, the analytes were chromatographed on a Acquity BEH C18 column (10.0 x 0.21; 1.7 1.7 μm) which was held at 42°C. A gradient elution profile was applied to each sample; %B was increased from 6% (initial conditions) to 50% over 8.5 min, then increased to 99% over 0.5 min and held at 99% for another 2.2 min. Finally, the column was returned to initial conditions for 2.5 min prior to the next injection. The flow rate was 300 μL/min and component A

was 10 mM ammonium acetate (pH adjusted to approximately ≈ 3.3 with glacial acetic acid) while component B was acetonitrile with 5% component A.

All analytes were detected by the SCIEX 6500 QTrap via selected reaction monitoring (SRM). Table 1 gives the Q1 and Q3 *m/z* values, collision energy (CE), declustering potential (DP) and ionization mode for all analytes and their internal standards. Analytes were quantitated by stable isotope dilution against their deuterated internal standard. Data was normalized to tissue mass and is presented as either “pmol/g tissue” or “nmol/g tissue”.

Immunohistochemistry (IHC)

Tissue was fixed in 10% neutral buffered formalin (NBF) for 2 hours for DRG or nerve or overnight for larger organs such as spleen. Samples were then dehydrated and embedded in paraffin. Five micron sections were cut. Slides were placed on the Leica Bond Max IHC stainer. All steps besides dehydration, clearing and coverslipping were performed on the Bond Max. Slides were deparaffinized. Heat induced antigen retrieval was performed on the Bond Max using their Epitope Retrieval 2 solution for 20 minutes. Slides were placed in a Protein Block (Ref# x0909, DAKO, Carpinteria, CA) for 10 minutes. The sections were incubated with CD11b (Catalog #NB110-89474, Novus Biologicals LLC, Littleton, CO) diluted 1:15k for one hour. The Bond Refine Polymer detection system was used for visualization. Slides were the dehydrated, cleared and coverslipped. Slides were imaged on an Olympus BX41 microscope with CellSans Standard software.

Fluorescent IHC

Tissue was fixed in 10% neutral buffered formalin (NBF) for 2 hours for small tissue and overnight for larger tissues. Samples were then dehydrated and embedded in paraffin. Five micron sections were cut. Tissues were then rehydrated and antigen retrieval performed using

one of the following three methods: (1) Proteinase K (Macherey Nagel/Clontech Laboratores catalog no. 740506) at a final concentration of 20 micrograms/mL for 30 minutes at room temperature according to the manufacturer's instructions. (2) Citrate buffer (10 mM citric acid, 0.05% Tween 20, pH 6.0) in pressure cooker for 12 minutes. (3) Tris-EDTA (10mM Tris Base, 1 mM EDTA, 0.05% Tween 20, pH 9.0) in pressure cooker for 12 minutes. All washes were done with PBS. All tissue was blocked in 5% BSA, 0.1% Tween-20 diluted in PBS. Slides were mounted in ProLong Gold with DAPI (Life Technologies, catalog no. P36931). Regular fluorescence microscopy was performed on a Nikon Eclipse Ti microscope with a DS-Qi2 camera using NIS Elements AR version 4.5 software. Confocal images were acquired on a Leica SP5 confocal microscope using LAS AP software version 2.7.3.9723. *Primary Antibodies used for IHC:* PEAR1 (R&D catalog no. AF7607-SP), HuC/D (Molecular Probes catalog no. A21272), MBP (Biolegend catalog no. 836504), phosphoERK (Cell Signaling catalog no. 4376).

DRG explant cultures

DRGs were excised from early postnatal animals and placed in a bed of Matrigel (Corning catalog no. 356230) and incubated with the following media: 1 to 1 mixture of Neurobasal (Gibco catalog no. 21103-049) and UltraCulture (Lonza catalog no. 12-725F) media, 3% Hyclone serum (Hyclone catalog no. SH30088.03), 1% N2 (Gibco catalog no. 17502-048), 2% B27 (Gibco catalog no. 17504-044), 1% L-glutamine (Gibco catalog no. 25030-081), 1% Pen/Strep (Gibco catalog no. 15140-122). At each time point, 0-5 days, samples were fixed with 10% NBF overnight at room temperature. The next day, samples were washed with PBS and mounted in ProLong Gold + DAPI. Explants were imaged on an Olympus BX41 microscope with CellSans Standard software.

Westerns

Mouse tissue was flash frozen for western blots and stored at -80° C. Tissue was ground into a fine powder then lysed and sonicated in RIPA buffer (1% NP-40, 0.5% deoxycholate, 0.1% SDS, 150 mM NaCl, 50 mM Tris-Cl pH 8.0) with protease and phosphatase inhibitors added according to the manufacturer's specifications (Roche catalog no. 04693159001 and Roche catalog no. 04906837001). Samples were denatured and separated by SDS-PAGE acrylamide gel, transferred to a nitrocellulose membrane, and blocked with 5% milk. Membranes were immunoblotted with primary antibody (Alomone catalog no. ACC-030 rabbit polyclonal) 1:3,000 and with secondary anti-rabbit HRP 1:5,000 developed on an Amersham Imager 600 version 1.2.0 with ECL.

Scratching behavior

Scratching was analyzed as previously described[683–685]. Mice either 8-12 weeks old or over 1 year old were habituated to their recording chambers for 30 minutes a day every morning for 4 days. On the 5th day, the mice were recorded for 30 minutes. The observer analyzing the videos was blinded to genotype of the animal. Scratching behaviors consisted of scratching with the hind paw and biting of the back. Scratching with the hind paw was defined as the following: Scratching was only counted when performed with the hind paw, not the front paws. One bout of scratching constituted lifting of the hind leg, scratching, and then returning it to the floor regardless of how many scratches were made during that time. Back biting was defined as: One bout of biting constituted lowering the head to hairy skin only (not glaborous skin), biting, then returning the head to normal height, regardless of how many times the mouse bit itself during that time. Bouts were the number of times that one of these two actions were performed and time was the sum of how long each bout lasted.

Capsaicin injection

Mice 8-12 weeks old were habituated to the recording environment for 4 days prior to data collection on the fifth day. 1 ug capsaicin (Sigma catalog no. 12084-10MG-F) was injected into the top of the foot and the mouse was immediately recorded for their initial reaction for 10 minutes. The videos were analyzed for nocifensive behavior: Lifting of the injected paw, shaking of the injected paw, and licking the injected paw. The bouts and length of time spent doing these behaviors within the first 10 minutes was analyzed. One hour post-injection the mice were placed on a 55 degree hot plate and analyzed as described below. 90 minutes post injection Von Frey hair analysis was performed on the capsaicin injected mice as described below.

Thermosensation

Mice 8-12 weeks old were habituated to the recording environment at room temperature for 4 days prior to data collection. On the fifth day, the hot plate was set to the appropriate temperature (either 55, 47, 42, or 4 degrees C, only data for 55 degrees shown) and the mice were placed on the hot or cold plate for 15 seconds while recording their behavior. An observer blind to genotype analyzed the videos for the following nocifensive behaviors: Increased grooming with forepaws, increased ambulatory activity, rapidly repeated elevations of hind feet ('stomping'), licking of hind paws, agitated behavior, and jumping. The number of times and length of time spent doing these behaviors within 15 seconds was analyzed.

Von Frey hair

Mice 8-12 weeks old were habituated to the recording environment for 4 days prior to data collection. On the fifth day, mice were habituated in the wire mesh bottom cage for 15 minutes before experimentation. A pressure sensory was used to poke the center of the rear footpad until a fast withdraw response was observed. The maximum pressure required to elicit this response

was measured for a minimum of 10 times per mouse per foot (ipsilateral and contralateral foot for capsaicin injections). These values were averaged for each foot per animal.

Axon counting

Adult sciatic nerves were isolated and fixed in 0.1M sodium cacodylate (Electron Microscopy Sciences [EMS], catalog no. 11652), 2% paraformaldehyde (EMS catalog no. 15713-S), 3% glutaraldehyde (EMS catalog no. 16310) for 1 hour at room temperature then overnight at 4° C. Samples were washed three times in 0.1 M cacodylate buffer (wash buffer) and post-fixed in 1% osmium tetroxide (EMS catalog no. 19150) for 1 hour at room temperature then overnight at 0.5% osmium tetroxide. Samples were washed three times in wash buffer then gradually dehydrated with increasing concentrations of ethanol. Samples were then infiltrated in solutions with increasing ratios of Epon-812 (EMS catalog no. 14120) to propylene oxide (EMS catalog no. 20401) until reaching pure resin. Samples were embedded in Epon-812 and baked at 60° C for 48 hours. Thick sections were cut at 0.5 microns on a Leica UC7 ultramicrotome and counterstained with toluidine blue. Slides were imaged on an Olympus BX41 microscope with CellSans Standard software.

Sciatic nerve injury and motor function analysis

8-12 week old mice were anesthetized with isofluorane and placed on a heating pad. The surgical site was shaved and cleaned with providone iodide (Fisher catalog no. 19-02748). A small incision was made in the thigh parallel to the femur (less than 1 cm in length). Blunt force dissection was used to separate the gluteus maximus biceps femoris muscles to reveal the underlying nerve[686]. Sterile 0.9% saline was periodically administered to the injury site to keep the tissue moist. A small, homemade pin was used to expose the nerve. Number 5 forceps were used to crush the nerve for 30 seconds. The skin was then stapled and the mice allowed to

recover in separate cages on a heating pad with gel diet (Fisher catalog no. NC1216297) until the indicated time points.

Motor recovery was performed using TreadScan equipment and software from Clever Sys, Inc. Mice were placed on a clear-bottom treadmill moving at 12 cm/s and recorded with a high speed camera (120 frames per second) for 20 s. Hind feet length and width were measured manually in ImageJ software (see below) for both the contralateral and ipsilateral feet at minimum five times per animal per foot per time point. The ratio of length to width was averaged for each paw to obtain the final value per animal.

Statistical analysis

All microscopy images were analyzed using the open source processing software ImageJ version 2.0.0-rc-69/1.52p. Unless stated otherwise, we stained a minimum of 5 sections of ganglia or sciatic nerve at least 60 microns apart per animal for each measurement. Data points represent an average of repeated measurements per animal. Each animal used as a single ‘n’ for statistical analysis. The number of animals used for each experiment varies for each experiment and is reported in the figure legend or text. Statistical tests and graphs were performed and generated using Prism8 software version 8.3.

CHAPTER 5

DISCUSSION

Section 5.1: Summary of results

In the three data chapters presented here, the phenotypes of a mouse model lacking the phagocytic receptor Jedi were analyzed for autoimmune disease, abnormalities in somatosensation, and response to peripheral nerve injury. Overall, we did not find many phenotypes of the Jedi KO mouse, despite verifying at the DNA, RNA, and protein level that Jedi was in fact absent (note that some of this validation was not shown in this thesis). The few changes we observed were found using primary cell cultures obtained from WT and KO mice that were not recapitulated *in vivo*. Therefore, further investigations using different approaches are needed to understand the physiologic role of Jedi.

In Chapter 2, we collaborated with Dr. Amy Major, an immunologist, to evaluate whether Jedi KO mice exhibited signs of lupus-like autoimmune disease. We hypothesized that if Jedi were essential for the clearance of apoptotic cells, then in its absence, these cells would become necrotic, induce chronic inflammation, and eventually lead to loss of self-tolerance and autoimmune disease. Knock-outs of other phagocytic receptors have reported similar phenotypes[246,290,357,536,565,567]. However, mice lacking Jedi did not exhibit signs of defective phagocytosis, inflammation, expansion of any innate or adaptive immune cell populations, or altered signs of activation in any of these cell types. The results were similar when the mice were challenged with pristane and high fat diet (breeder chow) over many generations. We conclude from this data that Jedi is dispensable for professional phagocytosis, which is in agreement with

RNAseq databases showing little to no Jedi expression in macrophages, dendritic cells, monocytes, or neutrophils.

Chapter 3 evaluates where Jedi is expressed in the context of the peripheral somatosensory nervous system and what its potential role might be there under homeostatic conditions. We established that Jedi is expressed in blood vessels (confirming previous reports[371,379]), perineurial glia, and at low levels in satellite glia, but is not detected in sensory neurons or Schwann cells. There were no intrinsic changes to the glia or endothelial cells in the absence of Jedi. The neurons, however, appear hyperactivate *in vitro*, a phenotype that usually leads to chronic pain. We surmise that Jedi regulates neuronal function in a non-cell autonomous manner through a yet unknown mechanism. Most likely, this is a developmental change that persists throughout the process of culturing DRGs.

In the final data chapter, we performed several *in vivo* tests to determine whether DRG neuron hyperexcitability in culture ultimately translates to any changes in animal behavior. We do not find any changes in inflammation, a common cause for DRG neuron hyperexcitability, somatosensory tests at baseline conditions or after challenge with the allogenic compound capsaicin, or in response to two different peripheral nerve injuries. We propose that further studies are required to determine the specific conditions under which Jedi affects somatosensation *in vivo*.

Ultimately, these studies of the Jedi KO mouse led to a number of negative results. We propose a number of reasons for this throughout the text, including redundancy (Jedi belongs to a family of three structurally similar proteins) and compensation. Below, I will discuss alternative approaches that address these issues and the limitations of our interpretations.

Section 5.2: Alternative approaches to study the role of Jedi *in vivo*

Clearly, the current approach we are using to assess the role of Jedi in the somatosensory nervous system *in vivo* is not sufficient to delineate potential phenotypes. Somatosensation encompasses many different types of bodily sensations, including proprioception, mechanosensation, thermosensation, nociception, and itch. The data presented herein only tests non-nociceptive light touch (Von Frey hair), steady state thermosensation (hot or cold plate), and spontaneous scratching. There are a number of well-established alternative behavioral assays that could be performed such as the Randall-Selitto test for noxious mechanoperception[687], the dynamic cold/hot plate to assay temperature discrimination rather than absolute noxious temperature[688], the splay reflex test as a measure of proprioception[689], the acetone or dry ice test to measure cold sensitivity[667,690], the air puff test to evaluate non-nociceptive mechanical stimuli in hairy rather than glabrous skin[670], the texture discrimination task to gauge vibration sensitivity[669], and many others. However, these experiments are time-consuming and highly variable, requiring large numbers of mice to experiment on.

To challenge the mice, which thrive in a relatively stress free, clean environment, we have tried switching their diet, aging them, injecting pain-producing compound capsaicin, crushing, and transecting their sciatic nerves. These are only a few of the many possible pain or itch inducing tests one can perform. Popular alternative approaches are the chronic constriction model[691], complete Freud's adjuvant injection as a model for inflammatory pain[692], and the spinal nerve ligation as a neuropathy model[693] to name only a few. These are also time-consuming experiments that require large sample sizes due to high variability.

I would argue that the brute force approach described above is an exercise in futility. With no clear indications which behavioral assay or stimulus will elicit a phenotype in the Jedi KO mouse model, I would argue that the mouse model itself needs altering. As previously mentioned, our WT and KO colonies are separately bred homozygously and age/sex matched for all

experiments. So even from egg and sperm the mice lack Jedi protein and thus have ample time to adapt across many generations for its absence. Recently, I in combination with a previous graduate student in the lab, Dr. Francis E. Hickman, generated a floxed Jedi mouse that I confirmed deletes Jedi by crossing with a constitutively active and universally expressed Cre recombinase (Cre) mouse. If these floxed mice were crossed to an inducible Cre fused to mutant estrogen ligand-binding domain (CreERT2), then only after tamoxifen delivery would Jedi be acutely removed in the mice. The acute KO of Jedi prevents developmental compensation for its loss and may therefore reveal *in vivo* phenotypes not present in the constitutive KO. In addition, the floxed mouse will allow future students remove Jedi from specific cell types such as perineurial glia, satellite glia, or endothelial cells in order to elucidate mechanism.

Section 5.3: Critical assessment of results

The differences we did observe between WT and KO mice consist of electrophysiological studies assessing neuron activity and sodium currents, and live calcium imaging showing an increased proportion of neurons that respond to capsaicin. We interpret these results to indicate that Jedi KO neurons are hypersensitized, a phenotype indicative of chronic pain. While I stand by the technical validity of these results, the conclusions drawn from them should not be overstated.

Regarding the calcium imaging, we treated primary DRG cultures with a half maximal dose of capsaicin and quantified in a binary manner whether healthy, potassium chloride-responsive neurons increased intracellular calcium levels to 15% above baseline values. Under the conditions we utilized, we found that 35% of WT neurons and 45% of KO neurons responded to capsaicin. Over three independent experiments per genotype with a minimum of 100 cells analyzed each time (meaning that 300–500 cells in total were analyzed per condition), these numbers reached statistical significance. However, the biological significance of the absolute

value of the change, from 35% to 45%, a 1.3 fold increase, is unclear. The peak intracellular calcium levels were not statistically significant. The percent of cells and level of expression of the capsaicin receptor, TrpV1, both *in vitro* and *in vivo* was unchanged as measured by western blot and immunofluorescence. Upon capsaicin injection of mice *in vivo*, we found no change in initial nocifensive behavior, thermal hypersensitivity, or allodynia between genotypes. TrpV1 is an essential mediator of inflammatory pain, where its expression and activity increases[625–627]. For example, in the chronic constriction pain model, TrpV1 expression increases 1.5 fold and its activity increases 1.7 fold[694]. In a nerve transection model, TrpV1 expression and activity increased 3 fold[695]. Sometimes small molecular changes in can result in substantial physiological outcomes, but in the case of Jedi KO mice, the changes that we observed are less than the reported values that contribute to behavioral chronic pain. Therefore, the biological relevance of this finding remains unverified.

In collaboration with Kevin Currie's lab, we patched primary DRG neurons from acute cultures where we found hyperexcitability and changes in the voltage dependence of sodium channel function. We believe that most of the neurons we patched are nociceptors based on their size and shape of their AP, which is broad with a hump in the repolarization phase[696]. For each condition, we patched 10–12 cells due to the low throughput nature of these experiments. However, DRG neurons are an extremely heterogeneous population with up to 35 distinct subtypes, depending on the parameter used to distinguish them[156,578]. Different types of neurons have differences in firing patterns; for example, non-nociceptive cells tend to exhibit a phasic firing pattern, while nociceptors mostly display tonic responses to current stimulus[697]. Due to this heterogeneity, the few cells patched in these experiments may reflect subtle shifts in the populations of neurons or may not accurately represent the total population due to sampling error. To further explore the effects of loss of Jedi on these neurons, it would be beneficial to label the neurons along with electrophysiology. In addition, further exploration of the changes in the Na+

channels, particularly their sensitivity to tetrodotoxin should be performed in order to determine which specific class of channels are altered.

Section 5.4: Future studies

There are a number of unanswered questions in the somatosensory field. A better understanding of these processes may be relevant for a number of peripheral nerve diseases in addition to nerve injury. For example, peripheral neuropathy is the most common complication of both type I and type II diabetes that leads to pain, weakness, and numbness[698]. Chemotherapy and other drugs used in oncology commonly cause peripheral neuropathy with sensory neurons being the most affected and leads to long-term complications in patients even after they are in remission[699]. Guillain-Barre syndrome is a rare is autoimmune disease in which the immune system attacks peripheral axons and myelin often following infection. While 80% of patients spontaneously recover, Guillain Barre is fatal for the remaining cases[700]. The etiology of these diseases for the most part remain mysterious because we still do not understand many basic physiological principles of peripheral nervous system biology.

Perineurial glia

The developmental origin of perineurial glia is complex. Unlike sensory neurons, Schwann cells, and satellite glia, perineurial cells are not derived from the neural crest[701]. Sarah Kucenas' lab showed that ventral (motor) but not dorsal (sensory) root perineurial glia actually originate from NK transcription factor related, locus 2 (Nkx2.2)+ cells in the spinal cord and migrate to the periphery[599]. The Nkx2.2+ perineurial glia constitute the outer perineurial glia, while the inner layers of perineurium are still of unknown origin[581]. The functional differences between the inner and outer layers of perineurium also remain mysterious. In diabetes, the perineurial layer thickens, which is thought to contribute to an increase in endoneurial pressure and axon

degeneration[169,702,703]. Further characterization of the development of the perineurium may help elucidate whether the sensory or motor contributors of the perineurium are involved in neuropathy.

Neurons, Schwann cells, and perineurial glia rely on reciprocal intercellular signaling between each other for proper development and function[599,704–707]. Some of the signals between these cell types are known but are not fully characterized. In a Schwann cell-specific Dhh conditional KO mouse, the perineurial layer is patchy and disorganized, suggesting that Dhh plays a role in perineurial organization[708]. However, these mice have defects in other cell types including endoneurial fibroblasts and the epineurium and since no Dhh rescue experiment was performed, it is unclear whether the phenotype observed was directly due to Dhh. Zebrafish studies have shown that Notch signaling is important for proper perineurial cell migration along axons during embryogenesis, but the source of Notch ligand is unclear[704]. Schwann cells express Jagged1 while axons express Delta, so further studies are needed to investigate which is the endogenously relevant source of Notch ligands for perineurial glia[465,709]. TGF signaling also plays a role in perineurial cell migration and maturation during development and after nerve injury[706]. Axons regulate Schwann cell expression of TGFβ1 during development, but conditional KO and other experiments will be required to verify that this is the endogenous source of TGFβ for perineurial glia[710,711]. In zebrafish and mice where perineurial glia are genetically deleted, there are severe defects in motor axon exit from the spinal cord, problems with Schwann cell migration, lack of myelination, and morphological abnormalities in the NMJ[581,599]. While these studies hint at some of the molecules involved in intercellular signaling between various cell types in peripheral nerves, it is very preliminary. Future studies are needed to elucidate these mechanisms.

In *Chapter 1: Introduction, Section 1.6: Nerve injury repair*, I mentioned Dr. Sydney Sunderland and his contributions to modern surgical nerve injury repair. Prior to Dr. Sunderland's work, the complexity of perineurial fasciculation was not appreciated. There are two schools of thought on fascicular organization: The first is the cable model in which all of the fascicles run

parallel to one another with no mixing of the axons between them; The second is the plexiform model in which axons interchange between fascicles that separate and combine with one another[712]. Through meticulous dissection and serial cross-sectioning of human nerves, Dr. Sunderland found that both models co-existed even within the same nerve. Close to the midline, the fascicles resemble the plexiform model with significant intermingling of axons. As the nerves get closer to their peripheral targets however, the fascicles tend to follow the cable model[713]. One caveat to Dr. Sunderland's studies was that he did not track individual axons, for example using a retrograde tracer such as horseradish peroxidase (there are now more modern methods to do this such as fluorescent dyes or the use of viral vectors), so there has been some controversy in the field about the extent of cable versus plexiform nerve structure[714]. Another method to investigate the fascicular structure is to partially injure nerves and then track the location of Wallerian degeneration in distal nerves to assess whether axons are degenerating in multiple or fascicles or restricted to only the injured ones. These studies in various organisms have garnered conflicting results – most likely the structure of the fascicles depends on the species, the particular nerve being studied, and the proximo-distal location along the nerve[715,716]. Many peripheral nerves are mixed, meaning they contain sensory, motor, and autonomic fibers in varying ratios, but fascicles are not organized by fiber type, i.e. a single fascicle may contain any combination thereof. Rather, there seems to be a somatotopic organization of the fascicles in the distal-most regions of the nerve[717,718]. In other words, all of the fibers innervating the same finger will be in the same fascicle, a different finger, another fascicle. These fascicles, however, combine as the axons approach the spinal cord. To my knowledge, there have been virtually no papers investigating the molecular mechanisms involved in fascicular organization, although the somatotopic organization suggests that axonal activity may be involved i.e. axons that fire together may wire together. In data not reported in this thesis, I have found that the perineurium also fasciculates sensory ganglia, which is interesting considering reports that cell bodies are also

somatotopically organized within the DRG[719]. These studies will have very important impacts on nerve regeneration, as the perineurium is disorganized and leaky distal to the nerve injury for long periods of time[720].

Somatosensory neurons

It is widely accepted that there is significant local processing of somatosensory input at the level of the spinal cord before projection neurons reach higher level CNS neurons. More recently, however, accumulatiing data shows that sensory processing starts within the ganglia itself, prior to its delivery into the dorsal horn. This occurs through several mechanisms: T junction gate control, inhibitory gamma aminobutyric acid (GABA)ergic signaling, cross-activation of neurons, and the generation of ectopic action potentials within the soma. These studies provide new insights into the treatment of somatosensory-related diseases because they indicate that ganglia play an active (rather than passive) role in regulation of pain and itch.

As previously mentioned, DRG neurons have a pseudounipolar structure, meaning that the cell body is connected by an offshoot from a single axon that distally innervates peripheral organs and proximally synapses in the spinal cord. This structure where the soma offshoots from the main axon is called the “T branch” and some data indicate that it critically regulates the propagation of action potentials[721]. The T junction acts either as a complete barrier to AP transmission, a low-pass filter that dampens AP frequency and/or amplitude as it passes through, or in an opposing manner, amplifies AP signals[721,722]. Although there have been theoretical modeling studies that predict how the T junction affects neuronal activity, the actual molecular mechanisms in place and their regulation are almost completely unknown[723–725]. Two treatments for chronic pain that seem paradoxical are low dose capsaicin treatment (capsaicin cream is available at local drug stores) and electrical stimulation of DRG neurons[726–731]. Both treatments would logically lead to heightened pain, but in practice the opposite is observed. Although still

unproven, one hypothesis for the mechanisms of these treatments is that continuous, sub-threshold stimulation of these neurons enhances T junction blockade of impulses, thus leading to analgesic effects[732].

The pseudounipolar anatomy of DRG neurons also confers a unique ability of these cells to permit bi-directional electrical transmission[733]. DRGs lack the canonical dendrite-axon orientation of most neurons, as evidenced by the presence of neuropeptide/neurotransmitter vesicular-release machinery at both ends of the pseudounipolar axon. Efferent DRG activity was first illustrated in the late 1800s by electrically stimulating the dorsal roots, which led to cutaneous inflammation in the appropriate dermatome through a process now called 'neurogenic inflammation'[734]. In addition to its role in neuroinflammation, antidromic DRG signaling has also been shown to play a role in hyperalgesia, allodynia, bone growth, metabolism, migraine and fibromyalgia[21,735–738]. These sensory axon reflexes are only recently being appreciated – likely future research will elucidate further implications of this unusual phenomenon that causes both efferent and afferent signaling.

All DRG neurons are excitatory and utilize the neurotransmitter glutamate. Traditionally, glutamate is thought to be released pre-synaptically by DRGs in the spinal cord. A number of sensory neurons also release neuropeptides such as neuropeptide Y (NPY), CGRP, substance P, etc. However, it is becoming more and more appreciated that these factors are not only being released at synapses in the spinal cord and distal targets of innervation, but also at the cell bodies. This is a mysterious phenomenon since there are no known synapses in the ganglia, yet DRG neurons express receptors for these neuropeptides and neurotransmitters[739]. We do know, however, that glutamate release from cell bodies promotes satellite glia activation and leads to non-synaptic, cross-excitation of neurons, thus contributing to spontaneous DRG firing and chronic pain[117,129,740,741]. Cell body release of glutamate and cross excitation of other neurons in the ganglia implies that action potentials can be initiated at cell somas. This was first

demonstrated by Devor and Wall in 1983, who demonstrated that ectopic firing of DRG neurons resulting from a nerve injury were initiated both from the proximally injured nerve fibers and from the cell bodies[742]. Interestingly, they also showed that the cell body generated APs could travel in the orthodromic and antidromic direction (described above). DRG soma AP generation plays a significant role in pain, as transection of the dorsal root, which separates the cell body from the spinal cord, almost completely abrogates electrical transmission to the spinal cord[617].

If cell body glutamate is the metaphoric sword for DRG neuron cross-excitation, then DRG soma release of GABA is its shield. Since the 1970's and 80's GABA-ergic currents have been recorded from DRG neurons, and the expression of functional GABA receptors have also been observed for quite a while, but the functional role of GABA in DRGs was only recently elucidated[743,744]. Du et al. showed that GABA is released in the ganglia of sensory neurons and acts on other DRG neuron cell bodies (although central GABA release was also observed and probably contributed to the phenotype) and this activity alleviated both acute and chronic pain induced by several stimuli[745]. Together, the release of glutamate and GABA in the DRG indicates that there is pre-synaptic gate control of pain signals in the periphery prior to CNS transmission. This discovery has immense impact on potential pain treatments, as it indicates that targeting peripheral ganglia may be a viable target for pharmacological intervention for somatosensory diseases. The ganglia is not protected by the BBB or BNB making drug delivery to this region relatively simple compared to the brain. These discoveries are relatively recent, however, so future discoveries in this area of research will undoubtedly shed light on yet undiscovered mechanisms of pain control in the periphery.

The studies I have highlighted here challenge traditional views of how the neurons of the peripheral somatosensory nervous system operate. These experiments show evidence of peripheral gate control of pain, an unusual origin for AP generation at cell bodies, and bi-directional AP transmission. Future research in these areas will continue to challenge pre-existing

dogmas in the field, hopefully leading to improved clinical strategies for the treatment of chronic pain and itch.

Specialized DRG end terminal structures

I think it is worth mentioning some new and emerging ideas in the somatosensory field regarding specialized nerve endings in the skin. These are often very large cutaneous structures that consist of DRG sensory nerve endings, multiple non-neuronal cells, and ECM: Pacinian corpuscles are composed of a specialized type of Schwann cell that produces 20–60 layers lamellae around an Aβ fiber[746]; Meissner corpuscles also consist of both Aβ and C fiber terminals surrounded by specialized Schwann cell processes[746]; Merkel cells disks contain up to 150 individual epithelial-derived Merkel cells[747]; Aδ and C fiber 'free' nerve endings were recently shown to not be so 'free' (more on this below) and are actually surrounded by a specialized type of non-myelinating Schwann cell[748]. Despite our descriptive knowledge of these structures for over one hundred years, how these specialized nerve endings actually work, and especially the function of the non-neuronal accessory cells was underappreciated.

The prior dogma assumed that only the sensory neurons electrically responded directly to somatosensory stimuli such as force, temperature, and chemicals. Recent studies have definitively shown that non-neuronal cells are electrically excitable to somatosensory stimuli – Merkel disks are the best characterized example. *In vitro*, epithelial-derived Merkel cells respond directly to force application by whole cell patch clamping methods via the mechanosensitive channel Piezo2[749–751]. Genetic ablation specifically of Merkel cells causes insensitivity to light touch, in spite of functionally and morphologically intact neurons. These and other experiments indicate that Merkel cells themselves are mechanoresponsive cells that convey touch signals to afferent DRG fibers[752]. The currently accepted convention is that both Aβ fibers innervating Merkel cells and the Merkel cells themselves are activated by touch, the former is rapidly adapting and

the latter slowly adapting and together in a “two site” model that allows us to distinguish between rapid movement versus static pressure[752]. Unlike Merkel touch domes, the neuron-glia interactions that underlie Pacinian and Meissner corpuscles, which are important for conveying vibration and motion respectively, are virtually unknown. Further studies are needed to discern the mechanisms of these and other specialized cutaneous nerve endings.

Textbooks have taught for the past fifty or so years about free nerve endings in the epidermis of the skin that detect nociceptive input. However, recent work indicates that these ‘free’ nerve endings are not so free. Patrik Ernfors lab recently re-discovered and characterized a specialized type of Schwann cell that coats these nerve endings in the skin and themselves are excited by mechanical and other stimuli[748]. Through yet unknown mechanisms, the Schwann cells transmit this information to the neurons. Other groups have since shown that these special Schwann cells contribute to pain in neurofibromas, but their broader role in chronic pain is still unknown[753]. I am personally curious to know whether Jedi+ perineurial glia also extend into free nerve endings. To make things even more complicated, two groups also recently discovered that keratinocytes, are also directly depolarized by touch and temperature and communicate with neurons via ATP[754,755]. ‘Free’ nerve endings were previously thought to navigate between keratinocytes in the epidermis, but a new study using modern microscopy techniques shows that they actually may tunnel through the cytoplasm of keratinocytes[756]. This new research demonstrates that our knowledge of the morphology of cutaneous nerve endings was previous incorrect, and that the molecular underpinnings under which it operates are even less understood.

Section 5.5: Conclusions

Overall, the goal of this work was to determine the role of Jedi *in vivo* through the use of a constitutive, global KO mouse model. Despite the *in vitro* data extolling Jedi as an engulfment receptor when overexpressed in cell lines or when knocked down in primary DRG cultures, there

was no evidence to support this finding in the mouse model. We did however, identify Jedi as a novel marker for perineurial glia, but found that its loss had no intrinsic effect on the perineurium, satellite glia, or endothelial cells. Cultured DRGs from Jedi KO mice, however, did exhibit signs of hyperactivity, a trait often associated with chronic pain. Since Jed is not expressed by the neurons, our studies highlight the importance of intercellular communication between the peripheral glia, endothelium, and neurons. Despite these exciting *in vitro* results, the mouse did not display any behavioral readouts of pain under baseline conditions or after several treatments to exacerbate pain. Reasons for the lack of phenotypes have been delineated throughout the text. I do not believe that Jedi does nothing; rather, our experimental setup and/or conditions have not yet identified the circumstances under which its function becomes apparent.

Despite these negative results specifically regarding Jedi, I think there are a number of exciting avenues for future research in the field of somatosensation. The PNS is the critical communicator between the brain and spinal cord to the rest of the body, but research continues to focus heavily on CNS neurons and glia. Despite this bias, new data is challenging conventional views and expanding the role of DRG neurons to unprecedented avenues. For example, DRGs antidromic activity has a role in regulating the immune system, cancer metastasis, and wound healing[757–759]. Single cell biology is shedding new light on the diversity of cells within the PNS, and advanced microscopy techniques and genetic tools continue to discover new cell types within this system every day. Accepting these challenges to pre-existing dogmas can sometimes be difficult, but we must be open to new, quality data and ideas to revise our models of the molecular and cellular underpinnings of mother nature. When I first started grad school, I was told that we do not understand 99% of what is happening in the tip of our finger. This aptly applies to the contents of this dissertation, as the fingertips (particularly in humans) are one of the mostly highly innervated tissues in the body probably due to the evolutionary importance of tool handling and fine motor skills for the survival of our species. In the age of big data analysis and continual

automation of many experimental procedures, we hope to close gaps in our understanding of the molecular events that occur in the tips of our fingers. With all of this new technology, however, the most important tool is still innately human and irreplaceable by computers – new ideas of how the world works. I hope that we can have the courage to reconcile previous hypotheses with the data generated from these new ideas.

REFERENCES

1. Le Pichon, C. E. & Chesler, A. T. The functional and anatomical dissection of somatosensory subpopulations using mouse genetics. *Frontiers in Neuroanatomy* (2014). doi:10.3389/fnana.2014.00021
2. Dib-Hajj, S. D. & Waxman, S. G. Sodium Channels in Human Pain Disorders: Genetics and Pharmacogenomics. *Annu. Rev. Neurosci.* (2019). doi:10.1146/annurev-neuro-070918-050144
3. Indo, Y. *et al.* Mutations in the TRKA/NGF receptor gene in patients with congenital insensitivity to pain with anhidrosis. *Nat. Genet.* (1996). doi:10.1038/ng0896-485
4. Chen, Y. C. *et al.* Transcriptional regulator PRDM12 is essential for human pain perception. *Nat. Genet.* (2015). doi:10.1038/ng.3308
5. Mollanazar, N. K., Koch, S. D. & Yosipovitch, G. Epidemiology of Chronic Pruritus: Where Have We Been and Where Are We Going? *Current Dermatology Reports* (2015). doi:10.1007/s13671-014-0093-y
6. Skolnick, P. The Opioid Epidemic: Crisis and Solutions. *Annu. Rev. Pharmacol. Toxicol.* (2018). doi:10.1146/annurev-pharmtox-010617-052534
7. Edwards, L. L., King, E. M., Buetefisch, C. M. & Borich, M. R. Putting the “sensory” into sensorimotor control: The role of sensorimotor integration in goal-directed hand movements after stroke. *Frontiers in Integrative Neuroscience* (2019). doi:10.3389/fnint.2019.00016
8. Zeng, W. Z. *et al.* PIEZOs mediate neuronal sensing of blood pressure and the baroreceptor reflex. *Science (80-.).* (2018). doi:10.1126/science.aau6324
9. Lukacs, V. *et al.* Impaired PIEZO1 function in patients with a novel autosomal recessive congenital lymphatic dysplasia. *Nat. Commun.* **6**, 1–7 (2015).

10. De Groat, W. C. & Yoshimura, N. Afferent nerve regulation of bladder function in health and disease. *Handbook of Experimental Pharmacology* (2009). doi:10.1007/978-3-540-79090-7_4

11. Grider, J. R. & Jin, J. G. Distinct populations of sensory neurons mediate the peristaltic reflex elicited by muscle stretch and mucosal stimulation. *J. Neurosci.* (1994). doi:10.1523/jneurosci.14-05-02854.1994

12. Yamashita, H. *et al.* Impaired basal thermal homeostasis in rats lacking capsaicin-sensitive peripheral small sensory neurons. *J. Biochem.* (2008). doi:10.1093/jb/mvm233

13. Jenkins, B. A. & Lumpkin, E. A. Developing a sense of touch. *Dev.* (2017). doi:10.1242/dev.120402

14. Ardiel, E. L. & Rankin, C. H. The importance of touch in development. *Paediatr. Child Health (Oxford).* **15**, 153–156 (2010).

15. Blakemore, S. J. *et al.* Tactile sensitivity in Asperger syndrome. *Brain Cogn.* (2006). doi:10.1016/j.bandc.2005.12.013

16. Cascio, C. *et al.* Tactile perception in adults with autism: A multidimensional psychophysical study. *J. Autism Dev. Disord.* (2008). doi:10.1007/s10803-007-0370-8

17. Tomchek, S. D. & Dunn, W. Sensory processing in children with and without autism: a comparative study using the short sensory profile. *Am. J. Occup. Ther.* (2007). doi:10.5014/ajot.61.2.190

18. Maitre, N. L. *et al.* The Dual Nature of Early-Life Experience on Somatosensory Processing in the Human Infant Brain. *Curr. Biol.* (2017). doi:10.1016/j.cub.2017.02.036

19. Brauer, J., Xiao, Y., Poulain, T., Friederici, A. D. & Schirmer, A. Frequency of Maternal Touch Predicts Resting Activity and Connectivity of the Developing Social Brain. *Cereb. Cortex* (2016). doi:10.1093/cercor/bhw137

20. Peirs, C. & Seal, R. P. Neural circuits for pain: Recent advances and current views.

Science (2016). doi:10.1126/science.aaf8933

21. Basbaum, A. I., Bautista, D. M., Scherrer, G. & Julius, D. Cellular and Molecular Mechanisms of Pain. *Cell* **139**, 267–284 (2009).

22. Yam, M. F. *et al.* General pathways of pain sensation and the major neurotransmitters involved in pain regulation. *International Journal of Molecular Sciences* (2018). doi:10.3390/ijms19082164

23. Abraira, V. E. & Ginty, D. D. The sensory neurons of touch. *Neuron* (2013). doi:10.1016/j.neuron.2013.07.051

24. Dong, X. & Dong, X. Peripheral and Central Mechanisms of Itch. *Neuron* (2018). doi:10.1016/j.neuron.2018.03.023

25. Davidson, S. & Giesler, G. J. The multiple pathways for itch and their interactions with pain. *Trends in Neurosciences* (2010). doi:10.1016/j.tins.2010.09.002

26. Haberberger, R. V., Barry, C., Dominguez, N. & Matusica, D. Human dorsal root ganglia. *Front. Cell. Neurosci.* **13**, 1–17 (2019).

27. Farel, P. B. Trust, but verify: The necessity of empirical verification in quantitative neurobiology. *Anat. Rec.* (2002). doi:10.1002/ar.10111

28. West, C. A., McKay Hart, A., Terenghi, G. & Wiberg, M. Sensory neurons of the human brachial plexus: A quantitative study employing optical fractionation and in vivo volumetric magnetic resonance imaging. *Neurosurgery* (2012). doi:10.1227/NEU.0b013e318241ace1

29. Hendry, S. H. & Hsiao, S. S. Fundamentals of Sensory Systems. in *Fundamental Neuroscience: Fourth Edition* (2013). doi:10.1016/B978-0-12-385870-2.00022-6

30. Lai, H. C., Seal, R. P. & Johnson, J. E. Making sense out of spinal cord somatosensory development. *Dev.* **143**, 3434–3448 (2016).

31. Li, L. *et al.* The functional organization of cutaneous low-threshold mechanosensory

neurons. *Cell* (2011). doi:10.1016/j.cell.2011.11.027

32. Dubin, A. E. & Patapoutian, A. Nociceptors: The sensors of the pain pathway. *Journal of Clinical Investigation* (2010). doi:10.1172/JCI42843

33. Smith, D. H. Stretch growth of integrated axon tracts: Extremes and exploitations. *Progress in Neurobiology* (2009). doi:10.1016/j.pneurobio.2009.07.006

34. Oppenheim, R. Cell Death During Development Of The Nervous System. *Annu. Rev. Neurosci.* (1991). doi:10.1146/annurev.neuro.14.1.453

35. Marmigère, F. & Ernfors, P. Specification and connectivity of neuronal subtypes in the sensory lineage. *Nature Reviews Neuroscience* (2007). doi:10.1038/nrn2057

36. Tandrup, T. Unbiased estimates of number and size of rat dorsal root ganglion cells in studies of structure and cell survival. *Journal of Neurocytology* (2004). doi:10.1023/B:NEUR.0000030693.91881.53

37. Smith, E. S. J. & Lewin, G. R. Nociceptors: a phylogenetic view. *J. Comp. Physiol. A. Neuroethol. Sens. Neural. Behav. Physiol.* **195**, 1089–1106 (2009).

38. Park, T. J. *et al.* Selective inflammatory pain insensitivity in the African naked mole-rat (Heterocephalus glaber). *PLoS Biol.* **6**, 0156–0170 (2008).

39. Delmas, P., Hao, J. & Rodat-Despoix, L. Molecular mechanisms of mechanotransduction in mammalian sensory neurons. *Nature Reviews Neuroscience* (2011). doi:10.1038/nrn2993

40. Lechner, S. G., Frenzel, H., Wang, R. & Lewin, G. R. Developmental waves of mechanosensitivity acquisition in sensory neuron subtypes during embryonic development. *EMBO J.* **28**, 1479–1491 (2009).

41. Lewin, G. R. & Moshourab, R. Mechanosensation and pain. *Journal of Neurobiology* (2004). doi:10.1002/neu.20078

42. Li, C. L. *et al.* Somatosensory neuron types identified by high-coverage single-cell RNA-

sequencing and functional heterogeneity. *Cell Res.* (2016). doi:10.1038/cr.2015.149

43. Li, C., Wang, S., Chen, Y. & Zhang, X. Somatosensory Neuron Typing with High-Coverage Single-Cell RNA Sequencing and Functional Analysis. *Neuroscience Bulletin* (2018). doi:10.1007/s12264-017-0147-9

44. Usoskin, D. *et al.* Unbiased classification of sensory neuron types by large-scale single-cell RNA sequencing. *Nat. Neurosci.* (2015). doi:10.1038/nn.3881

45. Zeisel, A. *et al.* Molecular Architecture of the Mouse Nervous System. *Cell* (2018). doi:10.1016/j.cell.2018.06.021

46. Reid, G. & Flonta, M. L. Cold current in thermoreceptive neurons. *Nature* (2001). doi:10.1038/35097164

47. Bautista, D. M. *et al.* The menthol receptor TRPM8 is the principal detector of environmental cold. *Nature* (2007). doi:10.1038/nature05910

48. Knowlton, W. M. *et al.* A sensory-labeled line for cold: TRPM8-expressing sensory neurons define the cellular basis for cold, cold pain, and cooling-mediated analgesia. *J. Neurosci.* (2013). doi:10.1523/JNEUROSCI.1943-12.2013

49. Pogorzala, L. A., Mishra, S. K. & Hoon, M. A. The cellular code for mammalian thermosensation. *J. Neurosci.* (2013). doi:10.1523/JNEUROSCI.5788-12.2013

50. Yarmolinsky, D. A. *et al.* Coding and Plasticity in the Mammalian Thermosensory System. *Neuron* (2016). doi:10.1016/j.neuron.2016.10.021

51. Simone, D. A. & Kajander, K. C. Responses of cutaneous A-fiber nociceptors to noxious cold. *J. Neurophysiol.* (1997). doi:10.1152/jn.1997.77.4.2049

52. Nagy, I. & Rang, H. Noxious heat activates all capsaicin-sensitive and also a sub-population of capsaicin-insensitive dorsal root ganglion neurons. *Neuroscience* (1999). doi:10.1016/S0306-4522(98)00535-1

53. Treede, R. D., Meyer, R. A. & Campbell, J. N. Myelinated mechanically insensitive

afferents from monkey hairy skin: Heat-response properties. *J. Neurophysiol.* (1998). doi:10.1152/jn.1998.80.3.1082

54. Duggan, A. W., Hendry, I. A., Morton, C. R., Hutchinson, W. D. & Zhao, Z. Q. Cutaneous stimuli releasing immunoreactive substance P in the dorsal horn of the cat. *Brain Res.* (1988). doi:10.1016/0006-8993(88)90771-8

55. Lawson, S. N., Crepps, B. A. & Perl, E. R. Relationship of substance P to afferent characteristics of dorsal root ganglion neurones in guinea-pig. *J. Physiol.* (1997). doi:10.1111/j.1469-7793.1997.00177.x

56. Vandewauw, I. *et al.* A TRP channel trio mediates acute noxious heat sensing. *Nature* (2018). doi:10.1038/nature26137

57. Ranade, S. S. *et al.* Piezo2 is the major transducer of mechanical forces for touch sensation in mice. *Nature* (2014). doi:10.1038/nature13980

58. Murthy, S. E., Dubin, A. E. & Patapoutian, A. Piezos thrive under pressure: Mechanically activated ion channels in health and disease. *Nat. Rev. Mol. Cell Biol.* **18**, 771–783 (2017).

59. Ernfors, P., Lee, K. F., Kucera, J. & Jaenisch, R. Lack of neurotrophin-3 leads to deficiencies in the peripheral nervous system and loss of limb proprioceptive afferents. *Cell* (1994). doi:10.1016/0092-8674(94)90213-5

60. Lechner, S. G. & Lewin, G. R. Hairy sensation. *Physiology* (2013). doi:10.1152/physiol.00059.2012

61. Rutlin, M. *et al.* The cellular and molecular basis of direction selectivity of Aδ-LTMRs. *Cell* (2014). doi:10.1016/j.cell.2014.11.038

62. Wende, H. *et al.* The transcription factor c-Maf controls touch receptor development and function. *Science (80-.).* (2012). doi:10.1126/science.1214314

63. Zimmerman, A., Bai, L. & Ginty, D. D. The gentle touch receptors of mammalian skin.

Science (2014). doi:10.1126/science.1254229

64. Bai, L. *et al.* Genetic Identification of an Expansive Mechanoreceptor Sensitive to Skin Stroking. *Cell* (2015). doi:10.1016/j.cell.2015.11.060

65. Vallbo, Å., Olausson, H., Wessberg, J. & Norrsell, U. A system of unmyelinated afferents for innocuous mechanoreception in the human skin. *Brain Res.* (1993). doi:10.1016/0006-8993(93)90968-S

66. Seal, R. P. *et al.* Injury-induced mechanical hypersensitivity requires C-low threshold mechanoreceptors. *Nature* (2009). doi:10.1038/nature08505

67. Brumovsky, P. *et al.* Neuropeptide Y2 receptor protein is present in peptidergic and nonpeptidergic primary sensory neurons of the mouse. *J. Comp. Neurol.* (2005). doi:10.1002/cne.20639

68. Morton, C. R., Hutchison, W. D., Hendry, I. A. & Duggan, A. W. Somatostatin: evidence for a role in thermal nociception. *Brain Res.* (1989). doi:10.1016/0006-8993(89)90696-3

69. Dillon, S. R. *et al.* Interleukin 31, a cytokine produced by activated T cells, induces dermatitis in mice. *Nat. Immunol.* (2004). doi:10.1038/ni1084

70. Taylor-Clark, T. E., Nassenstein, C. & Undem, B. J. Leukotriene D 4 increases the excitability of capsaicin-sensitive nasal sensory nerves to electrical and chemical stimuli. *Br. J. Pharmacol.* (2008). doi:10.1038/bjp.2008.196

71. Huang, J. *et al.* Circuit dissection of the role of somatostatin in itch and pain. *Nat. Neurosci.* (2018). doi:10.1038/s41593-018-0119-z

72. Mishra, S. K. & Hoon, M. A. The Cells and Circuitry for Itch. *Science (80-.).* (2013).

73. Norrsell, U., Finger, S. & Lajonchere, C. Cutaneous sensory spots and the ‘law of specific nerve energies’: History and development of ideas. *Brain Res. Bull.* (1999). doi:10.1016/S0361-9230(98)00067-7

74. Craig, A. D. (Bud). Pain Mechanisms: Labeled Lines Versus Convergence in Central

Processing. *Annu. Rev. Neurosci.* (2003). doi:10.1146/annurev.neuro.26.041002.131022

75. Watanabe, M. *et al.* The Cellular and Synaptic Architecture of the Mechanosensory Dorsal Horn. *Cell* (2017). doi:10.1016/j.cell.2016.12.010

76. Nedergaard, M., Ransom, B. & Goldman, S. A. New roles for astrocytes: Redefining the functional architecture of the brain. *Trends in Neurosciences* (2003). doi:10.1016/j.tins.2003.08.008

77. Véga, C., Poitry-Yamate, C. L., Jirounek, P., Tsacopoulos, M. & Coles, J. A. Lactate Is Released and Taken Up by Isolated Rabbit Vagus Nerve During Aerobic Metabolism. *J. Neurochem.* (2002). doi:10.1046/j.1471-4159.1998.71010330.x

78. Véga, C., Martiel, J. L., Drouhault, D., Burckhart, M. F. & Coles, J. A. Uptake of locally applied deoxyglucose, glucose and lactate by axons and Schwann cells of rat vagus nerve. *Journal of Physiology* (2003). doi:10.1113/jphysiol.2002.029751

79. Peters, A. Golgi, Cajal, and the fine structure of the nervous system. *Brain Research Reviews* (2007). doi:10.1016/j.brainresrev.2006.12.002

80. Mei, L. & Xiong, W. C. Neuregulin 1 in neural development, synaptic plasticity and schizophrenia. *Nature Reviews Neuroscience* (2008). doi:10.1038/nrn2392

81. Newbern, J. & Birchmeier, C. Nrg1/ErbB signaling networks in Schwann cell development and myelination. *Seminars in Cell and Developmental Biology* (2010). doi:10.1016/j.semcdb.2010.08.008

82. Taveggia, C. *et al.* Neuregulin-1 type III determines the ensheathment fate of axons. *Neuron* (2005). doi:10.1016/j.neuron.2005.08.017

83. Michailov, G. V. *et al.* Axonal Neuregulin-1 Regulates Myelin Sheath Thickness. *Science (80-.).* (2004). doi:10.1126/science.1095862

84. Brinkmann, B. G. *et al.* Neuregulin-1/ErbB Signaling Serves Distinct Functions in Myelination of the Peripheral and Central Nervous System. *Neuron* (2008).

doi:10.1016/j.neuron.2008.06.028

85. Atanasoski, S. *et al.* ErbB2 signaling in Schwann cells is mostly dispensable for maintenance of myelinated peripheral nerves and proliferation of adult Schwann cells after injury. *J. Neurosci.* (2006). doi:10.1523/JNEUROSCI.4594-05.2006

86. Fricker, F. R. *et al.* Axonally derived neuregulin-1 is required for remyelination and regeneration after nerve injury in adulthood. *J. Neurosci.* (2011). doi:10.1523/JNEUROSCI.2568-10.2011

87. Topilko, P. *et al.* Krox-20 controls myelination in the peripheral nervous system. *Nature* (1994). doi:10.1038/371796a0

88. Nagarajan, R. *et al.* EGR2 mutations in inherited neuropathies dominant-negatively inhibit myelin gene expression. *Neuron* (2001). doi:10.1016/S0896-6273(01)00282-3

89. Parkinson, D. B. *et al.* Krox-20 inhibits Jun-NH2-terminal kinase/c-Jun to control Schwann cell proliferation and death. *J. Cell Biol.* (2004). doi:10.1083/jcb.200307132

90. Monuki, E. S., Kuhn, R., Weinmaster, G., Trapp, B. D. & Lemke, G. Expression and activity of the POU transcription factor SCIP. *Science (80-.).* (1990). doi:10.1126/science.1975954

91. Scherer, S. S. *et al.* Axons regulate Schwann cell expression of the POU transcription factor SCIP. *J. Neurosci.* (1994). doi:10.1523/jneurosci.14-04-01930.1994

92. Weinstein, D. E., Burrola, P. G. & Lemke, G. Premature Schwann cell differentiation and hypermyelination in mice expressing a targeted antagonist of the POU transcription factor SCIP. *Mol. Cell. Neurosci.* (1995). doi:10.1006/mcne.1995.1018

93. Jaegle, M. *et al.* The POU factor Oct-6 and Schwann cell differentiation. *Science (80-.).* (1996). doi:10.1126/science.273.5274.507

94. Zorick, T. S., Syroid, D. E., Brown, A., Gridley, T. & Lemke, G. Krox-20 controls SCIP expression, cell cycle exit and susceptibility to apoptosis in developing myelinating

Schwann cells. *Development* (1999).

95. Holland, N. R. *et al.* Small-fiber sensory neuropathies: Clinical course and neuropathology of idiopathic cases. *Ann. Neurol.* (1998). doi:10.1002/ana.410440111

96. Ochoa, J. & Mair, W. G. P. The normal sural nerve in man. *Acta Neuropathol.* (1969). doi:10.1007/bf00690643

97. Murinson, B. B. & Griffin, J. W. C-Fiber Structure Varies with Location in Peripheral Nerve. *J. Neuropathol. Exp. Neurol.* (2004). doi:10.1093/jnen/63.3.246

98. Wang, S. S. H. *et al.* Functional trade-offs in white matter axonal scaling. *J. Neurosci.* (2008). doi:10.1523/JNEUROSCI.5559-05.2008

99. Stierli, S., Imperatore, V. & Lloyd, A. C. Schwann cell plasticity-roles in tissue homeostasis, regeneration, and disease. *Glia* 2203–2215 (2019). doi:10.1002/glia.23643

100. Griffin, J. W. & Thompson, W. J. Biology and pathology of nonmyelinating schwann cells. *Glia* (2008). doi:10.1002/glia.20778

101. Boerboom, A., Dion, V., Chariot, A. & Franzen, R. Molecular mechanisms involved in schwann cell plasticity. *Frontiers in Molecular Neuroscience* (2017). doi:10.3389/fnmol.2017.00038

102. Salzer, J. L. Schwann cell myelination. *Cold Spring Harb. Perspect. Biol.* (2015). doi:10.1101/cshperspect.a020529

103. Kidd, G. J., Ohno, N. & Trapp, B. D. Biology of Schwann cells. in *Handbook of Clinical Neurology* (2013). doi:10.1016/B978-0-444-52902-2.00005-9

104. Jessen, K. R. & Mirsky, R. The repair Schwann cell and its function in regenerating nerves. *Journal of Physiology* (2016). doi:10.1113/JP270874

105. Hanani, M. Satellite glial cells in sensory ganglia: From form to function. *Brain Research Reviews* (2005). doi:10.1016/j.brainresrev.2004.09.001

106. Ledda, M., De Palo, S. & Pannese, E. Ratios between number of neuroglial cells and

number and volume of nerve cells in the spinal ganglia of two species of reptiles and three species of mammals. *Tissue Cell* (2004). doi:10.1016/j.tice.2003.09.001

107. Pannese, E. The satellite cells of the sensory ganglia. *Advances in anatomy, embryology, and cell biology* (1981). doi:10.1016/0306-3623(82)90041-6

108. Hanani, M., Huang, T. Y., Cherkas, P. S., Ledda, M. & Pannese, E. Glial cell plasticity in sensory ganglia induced by nerve damage. *Neuroscience* (2002). doi:10.1016/S0306-4522(02)00279-8

109. Pannese, E., Ledda, M., Cherkas, P. S., Huang, T. Y. & Hanani, M. Satellite cell reactions to axon injury of sensory ganglion neurons: Increase in number of gap junctions and formation of bridges connecting previously separate perineuronal sheaths. *Anat. Embryol. (Berl).* (2003). doi:10.1007/s00429-002-0301-6

110. Amir, R. & Devor, M. Chemically mediated cross-excitation in rat dorsal root ganglia. *J. Neurosci.* (1996). doi:10.1523/jneurosci.16-15-04733.1996

111. Amir, R. & Devor, M. Functional cross-excitation between afferent A- and C-neurons in dorsal root ganglia. *Neuroscience* (1999). doi:10.1016/S0306-4522(99)00388-7

112. Shinder, V. & Devor, M. Structural basis of neuron-to-neuron cross-excitation in dorsal root ganglia. *J. Neurocytol.* (1994). doi:10.1007/BF01262054

113. Allen, D. T. & Kiernan, J. A. Permeation of proteins from the blood into peripheral nerves and ganglia. *Neuroscience* (1994). doi:10.1016/0306-4522(94)90192-9

114. Arvidson, B. Distribution of intravenously injected protein tracers in peripheral ganglia of adult mice. *Exp. Neurol.* (1979). doi:10.1016/0014-4886(79)90134-1

115. Rosenbluth, J. THE DISTRIBUTION OF EXOGENOUS FERRITIN IN TOAD SPINAL GANGLIA AND THE MECHANISM OF ITS UPTAKE BY NEURONS. *J. Cell Biol.* (1964). doi:10.1083/jcb.23.2.307

116. Costa, F. A. L. & Neto, F. L. M. Satellite glial cells in sensory ganglia: its role in pain.

Brazilian J. Anesthesiol. (English Ed. (2015). doi:10.1016/j.bjane.2013.07.013

117. Ohara, P. T. *et al.* Gliopathic pain: When satellite glial cells go bad. *Neuroscientist* (2009). doi:10.1177/1073858409336094

118. Tagluk, M. E. & Tekin, R. The influence of ion concentrations on the dynamic behavior of the Hodgkin-Huxley model-based cortical network. *Cogn. Neurodyn.* (2014). doi:10.1007/s11571-014-9281-5

119. Vit, J. P., Jasmin, L., Bhargava, A. & Ohara, P. T. Satellite glial cells in the trigeminal ganglion as a determinant of orofacial neuropathic pain. *Neuron Glia Biol.* (2006). doi:10.1017/S1740925X07000427

120. Olsen, M. L. & Sontheimer, H. Functional implications for Kir4.1 channels in glial biology: From K + buffering to cell differentiation. *Journal of Neurochemistry* (2008). doi:10.1111/j.1471-4159.2008.05615.x

121. Vit, J. P., Ohara, P. T., Bhargava, A., Kelley, K. & Jasmin, L. Silencing the Kir4.1 potassium channel subunit in satellite glial cells of the rat trigeminal ganglion results in pain-like behavior in the absence of nerve injury. *J. Neurosci.* (2008). doi:10.1523/JNEUROSCI.5053-07.2008

122. Sato, K., Kiyama, H., Tae Park, H. & Tohyama, M. AMPA, KA and NMDA receptors are expressed in the rat DRG neurones. *Neuroreport* (1993). doi:10.1097/00001756-199309000-00013

123. Carlton, S. M. & Hargett, G. L. Colocalization of metabotropic glutamate receptors in rat dorsal root ganglion cells. *J. Comp. Neurol.* (2007). doi:10.1002/cne.21285

124. Willcockson, H. & Valtschanoff, J. AMPA and NMDA glutamate receptors are found in both peptidergic and non-peptidergic primary afferent neurons in the rat. *Cell Tissue Res.* (2008). doi:10.1007/s00441-008-0662-0

125. Miller, K. E. *et al.* Glutaminase immunoreactivity and enzyme activity is increased in the

rat dorsal root ganglion following peripheral inflammation. *Pain Res. Treat.* (2012). doi:10.1155/2012/414697

126. Cangro, C. B. *et al.* Localization of elevated glutaminase immunoreactivity in small DRG neurons. *Brain Res.* (1985). doi:10.1016/0006-8993(85)90428-7

127. Oliveira, A. L. R. *et al.* Cellular localization of three vesicular glutamate transporter mRNAs and proteins in rat spinal cord and dorsal root ganglia. *Synapse* (2003). doi:10.1002/syn.10249

128. Schousboe, A., Scafidi, S., Bak, L. K., Waagepetersen, H. S. & McKenna, M. C. Glutamate Metabolism in the Brain Focusing on Astrocytes. in (2014). doi:10.1007/978-3-319-08894-5_2

129. Jasmin, L., Vit, J. P., Bhargava, A. & Ohara, P. T. Can satellite glial cells be therapeutic targets for pain control? *Neuron Glia Biol.* (2010). doi:10.1017/S1740925X10000098

130. Boye Larsen, D. *et al.* Investigating the expression of metabotropic glutamate receptors in trigeminal ganglion neurons and satellite glial cells: Implications for craniofacial pain. *J. Recept. Signal Transduct.* (2014). doi:10.3109/10799893.2014.885049

131. Castillo, C. *et al.* Satellite glia cells in dorsal root ganglia express functional NMDA receptors. *Neuroscience* (2013). doi:10.1016/j.neuroscience.2013.02.031

132. Romão, L. F., De Sousa, V. O., Neto, V. M. & Gomes, F. C. A. Glutamate activates GFAP gene promoter from cultured astrocytes through TGF-β1 pathways. *J. Neurochem.* (2008). doi:10.1111/j.1471-4159.2008.05428.x

133. Sullivan, S. M. *et al.* Cytoskeletal anchoring of GLAST determines susceptibility to brain damage: An identified role for GFAP. *J. Biol. Chem.* (2007). doi:10.1074/jbc.M704152200

134. Gu, Y. *et al.* Neuronal soma-satellite glial cell interactions in sensory ganglia and the participation of purinergic receptors. *Neuron Glia Biology* (2010). doi:10.1017/S1740925X10000116

135. Suadicani, S. O. *et al.* Bidirectional calcium signaling between satellite glial cells and neurons in cultured mouse trigeminal ganglia. *Neuron Glia Biol.* (2010). doi:10.1017/S1740925X09990408

136. Li, J., Vause, C. V. & Durham, P. L. Calcitonin gene-related peptide stimulation of nitric oxide synthesis and release from trigeminal ganglion glial cells. *Brain Res.* (2008). doi:10.1016/j.brainres.2007.12.028

137. Kawasaki, Y. *et al.* Distinct roles of matrix metalloproteases in the early- and late-phase development of neuropathic pain. *Nat. Med.* (2008). doi:10.1038/nm1723

138. Thippeswamy, T. & Morris, R. The roles of nitric oxide in Dorsal Root Ganglion neurons. in *Annals of the New York Academy of Sciences* (2002). doi:10.1111/j.1749-6632.2002.tb04060.x

139. Belzer, V. & Hanani, M. Nitric oxide as a messenger between neurons and satellite glial cells in dorsal root ganglia. *Glia* (2019). doi:10.1002/glia.23603

140. Matsuka, Y., Neubert, J. K., Maidment, N. T. & Spigelman, I. Concurrent release of ATP and substance P within guinea pig trigeminal ganglia in vivo. *Brain Res.* (2001). doi:10.1016/S0006-8993(01)02888-8

141. Takeda, M. *et al.* Enhanced excitability of nociceptive trigeminal ganglion neurons by satellite glial cytokine following peripheral inflammation. *Pain* (2007). doi:10.1016/j.pain.2006.10.007

142. Takeda, M., Kitagawa, J., Takahashi, M. & Matsumoto, S. Activation of interleukin-1β receptor suppresses the voltage-gated potassium currents in the small-diameter trigeminal ganglion neurons following peripheral inflammation. *Pain* (2008). doi:10.1016/j.pain.2008.06.015

143. Ohtori, S., Takahashi, K., Moriya, H. & Myers, R. R. TNF-α and TNF-α receptor type 1 upregulation in glia and neurons after peripheral nerve injury: Studies in murine DRG and

spinal cord. *Spine (Phila. Pa. 1976).* (2004). doi:10.1097/00007632-200405150-00006

144. Retamal, M. A., Riquelme, M. A., Stehberg, J. & Alcayaga, J. Connexin43 hemichannels in satellite glial cells, can they influence sensory neuron activity? *Frontiers in Molecular Neuroscience* (2017). doi:10.3389/fnmol.2017.00374

145. Ji, R. R., Berta, T. & Nedergaard, M. Glia and pain: Is chronic pain a gliopathy? *Pain* **154**, (2013).

146. Huang, L. Y. M., Gu, Y. & Chen, Y. Communication between neuronal somata and satellite glial cells in sensory ganglia. *GLIA* (2013). doi:10.1002/glia.22541

147. Takeda, M., Takahashi, M. & Matsumoto, S. Contribution of the activation of satellite glia in sensory ganglia to pathological pain. *Neuroscience and Biobehavioral Reviews* (2009). doi:10.1016/j.neubiorev.2008.12.005

148. Shanthaveerappa, T. R. & Bourne, G. H. The perineural epithelium: Nature and significance. *Nature* (1963). doi:10.1038/199577a0

149. Mizisin, A. P. & Weerasuriya, A. Homeostatic regulation of the endoneurial microenvironment during development, aging and in response to trauma, disease and toxic insult. *Acta Neuropathologica* (2011). doi:10.1007/s00401-010-0783-x

150. Nelson, A. R., Sweeney, M. D., Sagare, A. P. & Zlokovic, B. V. Neurovascular dysfunction and neurodegeneration in dementia and Alzheimer's disease. *Biochim. Biophys. Acta - Mol. Basis Dis.* (2016). doi:10.1016/j.bbadis.2015.12.016

151. Sweeney, M. D., Sagare, A. P. & Zlokovic, B. V. Blood-brain barrier breakdown in Alzheimer disease and other neurodegenerative disorders. *Nature Reviews Neurology* (2018). doi:10.1038/nrneurol.2017.188

152. GAMBLE, H. J. & EAMES, R. A. AN ELECTRON MICROSCOPE STUDY OF THE CONNECTIVE TISSUES OF HUMAN PERIPHERAL NERVE. *J. Anat.* (1964).

153. OLDFORS, A. Permeability of the Perineurium of Small Nerve Fascicles: an

Ultrastructural Study Using Ferritin in Rats. *Neuropathol. Appl. Neurobiol.* **7**, 183–194 (1981).

154. Low, P. A., Dyck, P. J. & Schmelzer, J. D. Chronic elevation of endoneurial fluid pressure is associated with low-grade fiber pathology. *Muscle Nerve* (1982). doi:10.1002/mus.880050214

155. Low, P. A. & Dyck, P. J. Increased endoneurial fluid pressure in experimental lead neuropathy. *Nature* (1977). doi:10.1038/269427a0

156. Emery, E. C., Ernfors, P., Emery, E. C. & Ernfors, P. Dorsal Root Ganglion Neuron Types and Their Functional Specialization. *Oxford Handb. Neurobiol. Pain* 1–30 (2018). doi:10.1093/oxfordhb/9780190860509.013.4

157. Myers, R. R., Rydevik, B. L., Heckman, H. M. & Powell, H. C. Proximodistal gradient in endoneurial fluid pressure. *Exp. Neurol.* (1988). doi:10.1016/0014-4886(88)90233-6

158. Bush, M. S. & Allt, G. Blood-nerve barrier: distribution of anionic sites on the endothelial plasma membrane and basal lamina. *Brain Res.* (1990). doi:10.1016/0006-8993(90)91599-C

159. Shimizu, F. *et al.* Peripheral nerve pericytes modify the blood-nerve barrier function and tight junctional molecules through the secretion of various soluble factors. *J. Cell. Physiol.* (2011). doi:10.1002/jcp.22337

160. Shimizu, F. *et al.* Pericyte-derived glial cell line-derived neurotrophic factor increase the expression of claudin-5 in the blood-brain barrier and the blood-nerve barrier. *Neurochem. Res.* (2012). doi:10.1007/s11064-011-0626-8

161. Bell, M. A. & Weddell, A. G. M. A morphometric study of intrafascicular vessels of mammalian sciatic nerve. *Muscle Nerve* (1984). doi:10.1002/mus.880070703

162. Godel, T., Pham, M., Heiland, S., Bendszus, M. & Bäumer, P. Human dorsal-root-ganglion perfusion measured in-vivo by MRI. *Neuroimage* (2016).

doi:10.1016/j.neuroimage.2016.07.030

163. Jimenez-Andrade, J. M. *et al.* Vascularization of the dorsal root ganglia and peripheral nerve of the mouse: Implications for chemical-induced peripheral sensory neuropathies. *Mol. Pain* (2008). doi:10.1186/1744-8069-4-10

164. Arvidson, B. & Tjälve, H. Distribution of109Cd in the nervous system of rats after intravenous injection. *Acta Neuropathol.* (1986). doi:10.1007/BF00687046

165. Somjen, G. G. *et al.* The uptake of methyl mercury (203Hg) in different tissues related to its neurotoxic effects. *J. Pharmacol. Exp. Ther.* (1973).

166. McArthur, J. C., Brew, B. J. & Nath, A. Neurological complications of HIV infection. *Lancet Neurology* (2005). doi:10.1016/S1474-4422(05)70165-4

167. Fehrenbacher, J. C. Chemotherapy-induced peripheral neuropathy. in *Progress in Molecular Biology and Translational Science* (2015). doi:10.1016/bs.pmbts.2014.12.002

168. Rechthand, E. N., Smith, Q. R., Latker, C. H. & Rapoport, S. I. Altered blood-nerve barrier permeability to small molecules in experimental diabetes mellitus. *J. Neuropathol. Exp. Neurol.* (1987). doi:10.1097/00005072-198705000-00006

169. Richner, M. *et al.* Functional and structural changes of the blood-nerve-barrier in diabetic neuropathy. *Front. Neurosci.* (2019). doi:10.3389/fnins.2018.01038

170. Omura, K. *et al.* The recovery of blood-nerve barrier in crush nerve injury - A quantitative analysis utilizing immunohistochemistry. *Brain Res.* (2004). doi:10.1016/j.brainres.2003.10.067

171. Seitz, R. J. *et al.* The blood–nerve barrier in Wallerian degeneration: A sequential long-term study. *Muscle Nerve* (1989). doi:10.1002/mus.880120803

172. Mizisin, A. P., Kalichman, M. W., Myers, R. R. & Powell, H. C. Role of the blood-nerve barrier in experimental nerve edema. in *Toxicologic Pathology* (1990). doi:10.1177/019262339001800123

173. Kanda, T. Biology of the blood-nerve barrier and its alteration in immune mediated neuropathies. *J. Neurol. Neurosurg. Psychiatry* **84**, 208–212 (2013).

174. Willis, C. & Davis, T. Chronic Inflammatory Pain and the Neurovascular Unit: A Central Role for Glia in Maintaining BBB Integrity? *Curr. Pharm. Des.* (2008). doi:10.2174/138161208784705414

175. Lim, T. K. Y. *et al.* Blood-nerve barrier dysfunction contributes to the generation of neuropathic pain and allows targeting of injured nerves for pain relief. *Pain* (2014). doi:10.1016/j.pain.2014.01.026

176. Lim, T. K. Y. *et al.* Peripheral nerve injury induces persistent vascular dysfunction and endoneurial hypoxia, contributing to the genesis of neuropathic pain. *J. Neurosci.* (2015). doi:10.1523/JNEUROSCI.4040-14.2015

177. Fischer, S., Wobben, M., Marti, H. H., Renz, D. & Schaper, W. Hypoxia-induced hyperpermeability in brain microvessel endothelial cells involves VEGF-mediated changes in the expression of zonula occludens-1. *Microvasc. Res.* (2002). doi:10.1006/mvre.2001.2367

178. Liu, Q., Wang, X. & Yi, S. Pathophysiological changes of physical barriers of peripheral nerves after injury. *Front. Neurosci.* **12**, 1–8 (2018).

179. Kanda, T., Numata, Y. & Mizusawa, H. Chronic inflammatory demyelinating polyneuropathy: Decreased claudin-5 and relocated ZO-1. *J. Neurol. Neurosurg. Psychiatry* (2004). doi:10.1136/jnnp.2003.025692

180. Giannini, C. & Dyck, P. J. Basement membrane reduplication and pericyte degeneration precede development of diabetic polyneuropathy and are associated with its severity. *Ann. Neurol.* (1995). doi:10.1002/ana.410370412

181. Förstermann, U. & Münzel, T. Endothelial nitric oxide synthase in vascular disease: From marvel to menace. *Circulation* (2006). doi:10.1161/CIRCULATIONAHA.105.602532

182. Maiuolo, J. *et al.* The Role of Endothelial Dysfunction in Peripheral Blood Nerve Barrier: Molecular Mechanisms and Pathophysiological Implications. *Int. J. Mol. Sci.* **20**, 3022 (2019).

183. Buss, R. R., Sun, W. & Oppenheim, R. W. ADAPTIVE ROLES OF PROGRAMMED CELL DEATH DURING NERVOUS SYSTEM DEVELOPMENT. *Annu. Rev. Neurosci.* (2006). doi:10.1146/annurev.neuro.29.051605.112800

184. LEVI-MONTALCINI, R. Les conséquences de la destruction d'un territoire d'innervation périphérique sur le développement des centres nerveux correspondants dans l'embryon de Poulet. *Arch. Biol.* 537–545 (1942). doi:10.1142/9789812830319_0001

185. Hamburger, V. & Levi-Montalcini, R. Proliferation, differentiation and degeneration in the spinal ganglia of the chick embryo under normal and experimental conditions. *J. Exp. Zool.* (1949). doi:10.1002/jez.1401110308

186. Levi-Montalcini, R. The origin and development of the visceral in the spinal cord of the chick embryo. *J. Morphol.* (1950). doi:10.1002/jmor.1050860203

187. Levi-Montalcini, R. & Hamburger, V. Selective growth stimulating effects of mouse sarcoma on the sensory and sympathetic nervous system of the chick embryo. *J. Exp. Zool.* (1951). doi:10.1002/jez.1401160206

188. Hamburger, V. The effects of wing bud extirpation on the development of the central nervous system in chick embryos. *J. Exp. Zool.* (1934). doi:10.1002/jez.1400680305

189. Levi-Montalcini, R. & Cohen, S. IN VITRO AND IN VIVO EFFECTS OF A NERVE GROWTH-STIMULATING AGENT ISOLATED FROM SNAKE VENOM. *Proc. Natl. Acad. Sci.* (1956). doi:10.1073/pnas.42.9.695

190. Cohen, S., Levi-Montalcini, R. & Hamburger, V. A NERVE GROWTH-STIMULATING FACTOR ISOLATED FROM SARCOM AS 37 AND 180. *Proc. Natl. Acad. Sci.* (1954). doi:10.1073/pnas.40.10.1014

191. Levi-Montalcini, R. & Booker, B. EXCESSIVE GROWTH OF THE SYMPATHETIC GANGLIA EVOKED BY A PROTEIN ISOLATED FROM MOUSE SALIVARY GLANDS. *Proc. Natl. Acad. Sci.* (1960). doi:10.1073/pnas.46.3.373

192. Levi-Montalcini, R. Growth control of nerve cells by a protein factor and its antiserum. *Science (80-.).* (1964). doi:10.1126/science.143.3602.105

193. Cohen, S. PURIFICATION OF A NERVE-GROWTH PROMOTING PROTEIN FROM THE MOUSE SALIVARY GLAND AND ITS NEURO-CYTOTOXIC ANTISERUM. *Proc. Natl. Acad. Sci.* (1960). doi:10.1073/pnas.46.3.302

194. Hamburger, V., Brunso-Bechtold, J. K. & Yip, J. W. Neuronal death in the spinal ganglia of the chick embryo and its reduction by nerve growth factor. *J. Neurosci.* (1981). doi:10.1523/jneurosci.01-01-00060.1981

195. Huang, E. J. & Reichardt, L. F. Neurotrophins: Roles in Neuronal Development and Function. *Annu. Rev. Neurosci.* (2001). doi:10.1146/annurev.neuro.24.1.677

196. Ramón Y Cajal, S., DeFelipe, J., Jones, E. G. & May, R. M. *Cajal's Degeneration and Regeneration of the Nervous System*. *Cajal's Degeneration and Regeneration of the Nervous System* (2012). doi:10.1093/acprof:oso/9780195065169.001.0001

197. Dekkers, M. P. J., Nikoletopoulou, V. & Barde, Y. A. Death of developing neurons: New insights and implications for connectivity. *Journal of Cell Biology* (2013). doi:10.1083/jcb.201306136

198. Ribatti, D. The failed attribution of the Nobel Prize for Medicine or Physiology to Viktor Hamburger for the discovery of Nerve Growth Factor. *Brain Research Bulletin* (2016). doi:10.1016/j.brainresbull.2016.02.019

199. Arandjelovic, S. & Ravichandran, K. S. Phagocytosis of apoptotic cells in homeostasis. *Nat. Immunol.* **16**, 907–917 (2015).

200. Poon, I. K. H., Lucas, C. D., Rossi, A. G. & Ravichandran, K. S. Apoptotic cell clearance:

Basic biology and therapeutic potential. *Nature Reviews Immunology* (2014). doi:10.1038/nri3607

201. Flannagan, R. S., Jaumouillé, V. & Grinstein, S. The Cell Biology of Phagocytosis. *Annu. Rev. Pathol. Mech. Dis.* (2012). doi:10.1146/annurev-pathol-011811-132445
202. Kinchen, J. M. *et al.* Two pathways converge at CED-10 to mediate actin rearrangement and corpse removal in C. elegans. *Nature* (2005). doi:10.1038/nature03263
203. Hochreiter-Hufford, A. & Ravichandran, K. S. Clearing the dead: Apoptotic cell sensing, recognition, engulfment, and digestion. *Cold Spring Harb. Perspect. Biol.* (2013). doi:10.1101/cshperspect.a008748
204. Tauber, A. I. Immunity: How Elie Metchnikoff Changed the Course of Modern Medicine by Luba Vikhanski. *Bull. Hist. Med.* (2017). doi:10.1353/bhm.2017.0015
205. Vandivier, R. W., Henson, P. M. & Douglas, I. S. Burying the dead: The impact of failed apoptotic cell removal (efferocytosis) on chronic inflammatory lung disease. *Chest* (2006). doi:10.1378/chest.129.6.1673
206. Lauber, K. *et al.* Apoptotic cells induce migration of phagocytes via caspase-3-mediated release of a lipid attraction signal. *Cell* (2003). doi:10.1016/S0092-8674(03)00422-7
207. Gude, D. R. *et al.* Apoptosis induces expression of sphingosine kinase 1 to release sphingosine-1-phosphate as a ‘come-and-get-me’ signal. *FASEB J.* (2008). doi:10.1096/fj.08-107169
208. Truman, L. A. *et al.* CX3CL 1/fractalkine is released from apoptotic lymphocytes to stimulate macrophage chemotaxis. *Blood* (2008). doi:10.1182/blood-2008-06-162404
209. Elliott, M. R. *et al.* Nucleotides released by apoptotic cells act as a find-me signal to promote phagocytic clearance. *Nature* (2009). doi:10.1038/nature08296
210. Medina, C. B. & Ravichandran, K. S. Do not let death do us part: ‘Find-me’ signals in communication between dying cells and the phagocytes. *Cell Death and Differentiation*

(2016). doi:10.1038/cdd.2016.13

211. Chekeni, F. B. *et al.* Pannexin 1 channels mediate 'find-me' signal release and membrane permeability during apoptosis. *Nature* (2010). doi:10.1038/nature09413

212. Junger, W. G. Immune cell regulation by autocrine purinergic signalling. *Nature Reviews Immunology* (2011). doi:10.1038/nri2938

213. Qu, Y. *et al.* Pannexin-1 Is Required for ATP Release during Apoptosis but Not for Inflammasome Activation. *J. Immunol.* (2011). doi:10.4049/jimmunol.1100478

214. la Sala, A. *et al.* Extracellular ATP Induces a Distorted Maturation of Dendritic Cells and Inhibits Their Capacity to Initiate Th1 Responses. *J. Immunol.* (2001). doi:10.4049/jimmunol.166.3.1611

215. Haskó, G., Kuhel, D. G., Salzman, A. L. & Szabó, C. ATP suppression of interleukin-12 and tumour necrosis factor-α release from macrophages. *Br. J. Pharmacol.* (2000). doi:10.1038/sj.bjp.0703134

216. Savio, L. E. B., Mello, P. de A., da Silva, C. G. & Coutinho-Silva, R. The P2X7 receptor in inflammatory diseases: Angel or demon? *Frontiers in Pharmacology* (2018). doi:10.3389/fphar.2018.00052

217. Moffatt, O. D., Devitt, A., Bell, E. D., Simmons, D. L. & Gregory, C. D. Macrophage recognition of ICAM-3 on apoptotic leukocytes. *J. Immunol.* (1999).

218. Ucker, D. S. *et al.* Externalized glycolytic enzymes are novel, conserved, and early biomarkers of apoptosis. *J. Biol. Chem.* (2012). doi:10.1074/jbc.M111.314971

219. Leventis, P. A. & Grinstein, S. The Distribution and Function of Phosphatidylserine in Cellular Membranes. *Annu. Rev. Biophys.* (2010). doi:10.1146/annurev.biophys.093008.131234

220. Segawa, K. *et al.* Caspase-mediated cleavage of phospholipid flippase for apoptotic phosphatidylserine exposure. *Science (80-.).* (2014). doi:10.1126/science.1252809

221. Kornberg, R. D. & Mcconnell, H. M. Inside-Outside Transitions of Phospholipids in Vesicle Membranes. *Biochemistry* (1971). doi:10.1021/bi00783a003

222. Nakano, M. *et al.* Flip-flop of phospholipids in vesicles: kinetic analysis with time-resolved small-angle neutron scattering. *J. Phys. Chem. B* (2009). doi:10.1021/jp900913w

223. Suzuki, J., Denning, D. P., Imanishi, E., Horvitz, H. R. & Nagata, S. Xk-related protein 8 and CED-8 promote phosphatidylserine exposure in apoptotic cells. *Science (80-.).* (2013). doi:10.1126/science.1236758

224. Charras, G. T., Hu, C. K., Coughlin, M. & Mitchison, T. J. Reassembly of contractile actin cortex in cell blebs. *J. Cell Biol.* (2006). doi:10.1083/jcb.200602085

225. Croft, D. R. *et al.* Actin-myosin-based contraction is responsible for apoptotic nuclear disintegration. *J. Cell Biol.* (2005). doi:10.1083/jcb.200409049

226. Orlando, K. A., Stone, N. L. & Pittman, R. N. Rho kinase regulates fragmentation and phagocytosis of apoptotic cells. *Exp. Cell Res.* (2006). doi:10.1016/j.yexcr.2005.09.012

227. Coleman, M. L. *et al.* Membrane blebbing during apoptosis results from caspase-mediated activation of ROCK I. *Nat. Cell Biol.* (2001). doi:10.1038/35070009

228. Sebbagh, M. *et al.* Caspase-3-mediated cleavage of ROCK I induces MLC phosphorylation and apoptotic membrane blebbing. *Nat. Cell Biol.* (2001). doi:10.1038/35070019

229. Witasp, E. *et al.* Bridge over troubled water: Milk fat globule epidermal growth factor 8 promotes human monocyte-derived macrophage clearance of non-blebbing phosphatidylserine-positive target cells [2]. *Cell Death and Differentiation* (2007). doi:10.1038/sj.cdd.4402096

230. Wickman, G., Julian, L. & Olson, M. F. How apoptotic cells aid in the removal of their own cold dead bodies. *Cell Death and Differentiation* (2012). doi:10.1038/cdd.2012.25

231. Majeti, R. *et al.* CD47 Is an Adverse Prognostic Factor and Therapeutic Antibody Target

on Human Acute Myeloid Leukemia Stem Cells. *Cell* (2009). doi:10.1016/j.cell.2009.05.045

232. Barkal, A. A. *et al.* CD24 signalling through macrophage Siglec-10 is a target for cancer immunotherapy. *Nature* (2019). doi:10.1038/s41586-019-1456-0

233. Gordon, S. R. *et al.* PD-1 expression by tumour-associated macrophages inhibits phagocytosis and tumour immunity. *Nature* (2017). doi:10.1038/nature22396

234. Barkal, A. A. *et al.* Engagement of MHC class i by the inhibitory receptor LILRB1 suppresses macrophages and is a target of cancer immunotherapy article. *Nat. Immunol.* (2018). doi:10.1038/s41590-017-0004-z

235. Gardai, S. J. *et al.* Cell-surface calreticulin initiates clearance of viable or apoptotic cells through trans-activation of LRP on the phagocyte. *Cell* (2005). doi:10.1016/j.cell.2005.08.032

236. Oldenborg, P. A. *et al.* Role of CD47 as a marker of self on red blood cells. *Science (80-.).* (2000). doi:10.1126/science.288.5473.2051

237. Oldenborg, P. A., Gresham, H. D. & Lindberg, F. P. CD47-signal regulatory protein alpha (SIRPalpha) regulates Fcgamma and complement receptor-mediated phagocytosis. *J. Exp. Med.* (2001).

238. Lawrence, D. W., King, S. B., Frazier, W. A. & Koenig, J. M. Decreased CD47 expression during spontaneous apoptosis targets neutrophils for phagocytosis by monocyte-derived macrophages. *Early Hum. Dev.* (2009). doi:10.1016/j.earlhumdev.2009.09.005

239. Parnaik, R., Raff, M. C. & Scholes, J. Differences between the clearance of apoptotic cells by professional and non-professional phagocytes. *Curr. Biol.* (2000). doi:10.1016/S0960-9822(00)00598-4

240. Wood, W. *et al.* Mesenchymal cells engulf and clear apoptotic footplate cells in macrophageless PU.1 null mouse embryos. *Development* (2000).

241. Han, C. Z. *et al.* Macrophages redirect phagocytosis by non-professional phagocytes and influence inflammation. *Nature* (2016). doi:10.1038/nature20141

242. Kobayashi, N. *et al.* TIM-1 and TIM-4 Glycoproteins Bind Phosphatidylserine and Mediate Uptake of Apoptotic Cells. *Immunity* (2007). doi:10.1016/j.immuni.2007.11.011

243. Park, S. Y. & Kim, I. S. Stabilin receptors: Role as phosphatidylserine receptors. *Biomolecules* **9**, 1–16 (2019).

244. Hanayama, R. *et al.* Identification of a factor that links apoptotic cells to phagocytes. *Nature* (2002). doi:10.1038/417182a

245. Anderson, H. A. *et al.* Serum-derived protein S binds to phosphatidylserine and stimulates the phagocytosis of apoptotic cells. *Nature Immunology* (2003). doi:10.1038/ni871

246. Lemke, G. Biology of the TAM receptors. *Cold Spring Harb. Perspect. Biol.* (2013). doi:10.1101/cshperspect.a009076

247. Park, D. *et al.* BAI1 is an engulfment receptor for apoptotic cells upstream of the ELMO/Dock180/Rac module. *Nature* (2007). doi:10.1038/nature06329

248. Nagata, S., Hanayama, R. & Kawane, K. Autoimmunity and the Clearance of Dead Cells. *Cell* (2010). doi:10.1016/j.cell.2010.02.014

249. Miyanishi, M. *et al.* Identification of Tim4 as a phosphatidylserine receptor. *Nature* (2007). doi:10.1038/nature06307

250. Santiago, C. *et al.* Structures of T Cell Immunoglobulin Mucin Protein 4 Show a Metal-Ion-Dependent Ligand Binding Site where Phosphatidylserine Binds. *Immunity* (2007). doi:10.1016/j.immuni.2007.11.008

251. Park, S. Y. *et al.* Rapid cell corpse clearance by stabilin-2, a membrane phosphatidylserine receptor. *Cell Death Differ.* (2008). doi:10.1038/sj.cdd.4402242

252. Tollis, S., Dart, A. E., Tzircotis, G. & Endres, R. G. The zipper mechanism in

phagocytosis: Energetic requirements and variability in phagocytic cup shape. *BMC Syst. Biol.* (2010). doi:10.1186/1752-0509-4-149

253. Goodridge, H. S. *et al.* Activation of the innate immune receptor Dectin-1 upon formation of a ˜- Phagocytic synapse-™. *Nature* (2011). doi:10.1038/nature10071

254. Freeman, S. A. & Grinstein, S. Phagocytosis: Receptors, signal integration, and the cytoskeleton. *Immunol. Rev.* (2014). doi:10.1111/imr.12212

255. Gumienny, T. L. *et al.* CED-12/ELMO, a novel member of the CrkII/Dock180/Rac pathway, is required for phagocytosis and cell migration. *Cell* (2001). doi:10.1016/S0092-8674(01)00520-7

256. Leverrier, Y. & Ridley, A. J. Requirement for Rho GTPases and PI 3-kinases during apoptotic cell phagocytosis by macrophages. *Curr. Biol.* (2001). doi:10.1016/S0960-9822(01)00047-1

257. Nakaya, M., Tanaka, M., Okabe, Y., Hanayama, R. & Nagata, S. Opposite effects of Rho family GTPases on engulfment of apoptotic cells by macrophages. *J. Biol. Chem.* (2006). doi:10.1074/jbc.M510972200

258. Cannon, G. J. & Swanson, J. A. The macrophage capacity for phagocytosis. *J. Cell Sci.* (1992).

259. Lam, J., Herant, M., Dembo, M. & Heinrich, V. Baseline mechanical characterization of J774 macrophages. *Biophys. J.* (2009). doi:10.1529/biophysj.108.139154

260. Firdessa, R., Oelschlaeger, T. A. & Moll, H. Identification of multiple cellular uptake pathways of polystyrene nanoparticles and factors affecting the uptake: Relevance for drug delivery systems. *Eur. J. Cell Biol.* (2014). doi:10.1016/j.ejcb.2014.08.001

261. Morioka, S. *et al.* Efferocytosis induces a novel SLC program to promote glucose uptake and lactate release. *Nature* (2018). doi:10.1038/s41586-018-0735-5

262. Bajno, L. *et al.* Focal exocytosis of VAMP3-containing vesicles at sites of phagosome

formation. *J. Cell Biol.* (2000). doi:10.1083/jcb.149.3.697

263. Cox, D., Lee, D. J., Dale, B. M., Calafat, J. & Greenberg, S. A Rab11-containing rapidly recycling compartment in macrophages that promotes phagocytosis. *Proc. Natl. Acad. Sci. U. S. A.* (2000). doi:10.1073/pnas.97.2.680

264. Fairn, G. D. & Grinstein, S. How nascent phagosomes mature to become phagolysosomes. *Trends in Immunology* (2012). doi:10.1016/j.it.2012.03.003

265. Canton, J. Phagosome maturation in polarized macrophages. *J. Leukoc. Biol.* (2014). doi:10.1189/jlb.1mr0114-021r

266. Kawane, K. *et al.* Requirement of DNase II for definitive erythropoiesis in the mouse fetal liver. *Science (80-.).* (2001). doi:10.1126/science.292.5521.1546

267. Kawane, K. *et al.* Chronic polyarthritis caused by mammalian DNA that escapes from degradation in macrophages. *Nature* (2006). doi:10.1038/nature05245

268. Bellone, M. *et al.* Processing of Engulfed Apoptotic Bodies Yields T Cell Epitopes. *J. Immunol.* (1997).

269. Albert, M. L. *et al.* Immature dendritic cells phagocytose apoptotic cells via αvβ5 and CD36, and cross-present antigens to cytotoxic T lymphocytes. *J. Exp. Med.* (1998). doi:10.1084/jem.188.7.1359

270. Huang, F. P. *et al.* A discrete subpopulation of dendritic cells transports apoptotic intestinal epithelial cells to T cell areas of mesenteric lymph nodes. *J. Exp. Med.* (2000). doi:10.1084/jem.191.3.435

271. Magarian Blander, J. & Medzhitov, R. Toll-dependent selection of microbial antigens for presentation by dendritic cells. *Nature* (2006). doi:10.1038/nature04596

272. Henson, P. M. & Bratton, D. L. Antiinflammatory effects of apoptotic cells. *J. Clin. Invest.* (2013). doi:10.1172/JCI69344

273. Hoffmann, P. R. *et al.* Interaction between Phosphatidylserine and the Phosphatidylserine

Receptor Inhibits Immune Responses In Vivo. *J. Immunol.* (2005). doi:10.4049/jimmunol.174.3.1393

274. Huynh, M. L. N., Fadok, V. A. & Henson, P. M. Phosphatidylserine-dependent ingestion of apoptotic cells promotes TGF-β1 secretion and the resolution of inflammation. *J. Clin. Invest.* (2002). doi:10.1172/JCI0211638

275. Ramos, G. C. *et al.* Apoptotic mimicry: Phosphatidylserine liposomes reduce inflammation through activation of peroxisome proliferator-activated receptors (PPARs) in vivo. *Br. J. Pharmacol.* (2007). doi:10.1038/sj.bjp.0707302

276. Harel-Adar, T. *et al.* Modulation of cardiac macrophages by phosphatidylserine-presenting liposomes improves infarct repair. *Proc. Natl. Acad. Sci. U. S. A.* (2011). doi:10.1073/pnas.1015623108

277. Birge, R. B. *et al.* Phosphatidylserine is a global immunosuppressive signal in efferocytosis, infectious disease, and cancer. *Cell Death and Differentiation* (2016). doi:10.1038/cdd.2016.11

278. Kushwah, R. *et al.* Uptake of apoptotic DC converts immature DC into tolerogenic DC that induce differentiation of Foxp3+ Treg. *Eur. J. Immunol.* (2010). doi:10.1002/eji.200939782

279. Kushwah, R., Oliver, J. R., Zhang, J., Siminovitch, K. A. & Hu, J. Apoptotic Dendritic Cells Induce Tolerance in Mice through Suppression of Dendritic Cell Maturation and Induction of Antigen-Specific Regulatory T Cells. *J. Immunol.* (2009). doi:10.4049/jimmunol.0900824

280. Kondělková, K. *et al.* Regulatory T cells (TREG) and their roles in immune system with respect to immunopathological disorders. *Acta medica (Hradec Králové) / Universitas Carolina, Facultas Medica Hradec Králové* (2010). doi:10.14712/18059694.2016.63

281. Verbovetski, I. *et al.* Opsonization of apoptotic cells by autologous iC3b facilitates

clearance by immature dendritic cells, down-regulates DR and CD86, and up-regulates CC chemokine receptor 7. *J. Exp. Med.* (2002). doi:10.1084/jem.20020263

282. Stuart, L. M. *et al.* Inhibitory Effects of Apoptotic Cell Ingestion upon Endotoxin-Driven Myeloid Dendritic Cell Maturation. *J. Immunol.* (2002). doi:10.4049/jimmunol.168.4.1627

283. Croker, B. A. *et al.* Fas-mediated neutrophil apoptosis is accelerated by Bid, Bak,and Bax and inhibited by Bcl-2 and Mcl-1. *Proc. Natl. Acad. Sci. U. S. A.* (2011). doi:10.1073/pnas.1110358108

284. Poon, I. K. H. *et al.* Unexpected link between an antibiotic, pannexin channels and apoptosis. *Nature* (2014). doi:10.1038/nature13147

285. Elliott, M. R. & Ravichandran, K. S. The Dynamics of Apoptotic Cell Clearance. *Developmental Cell* (2016). doi:10.1016/j.devcel.2016.06.029

286. Steinman, R. M., Turley, S., Mellman, I. & Inaba, K. The induction of tolerance by dendritic cells that have captured apoptotic cells. *Journal of Experimental Medicine* (2000). doi:10.1084/jem.191.3.411

287. Henson, P. M. & Hume, D. A. Apoptotic cell removal in development and tissue homeostasis. *Trends in Immunology* (2006). doi:10.1016/j.it.2006.03.005

288. Burstyn-Cohen, T. *et al.* Genetic Dissection of TAM Receptor-Ligand Interaction in Retinal Pigment Epithelial Cell Phagocytosis. *Neuron* (2012). doi:10.1016/j.neuron.2012.10.015

289. Oka, K. *et al.* Lectin-like oxidized low-density lipoprotein receptor 1 mediates phagocytosis of aged/apoptotic cells in endothelial cells. *Proc. Natl. Acad. Sci. U. S. A.* (1998). doi:10.1073/pnas.95.16.9535

290. Morioka, S., Maueröder, C. & Ravichandran, K. S. Living on the Edge: Efferocytosis at the Interface of Homeostasis and Pathology. *Immunity* (2019). doi:10.1016/j.immuni.2019.04.018

291. Silva, M. T., Do Vale, A. & Dos Santos, N. M. N. Secondary necrosis in multicellular animals: An outcome of apoptosis with pathogenic implications. *Apoptosis* (2008). doi:10.1007/s10495-008-0187-8

292. Don, M. M. *et al.* Death of cells by apoptosis following attachment of specifically allergized lymphocytes in vitro. *Aust. J. Exp. Biol. Med. Sci.* (1977). doi:10.1038/icb.1977.38

293. Robertson, A. M. G., Bird, C. C., Waddell, A. W. & Currie, A. R. Morphological aspects of glucocorticoid-induced cell death in human lymphoblastoid cells. *J. Pathol.* (1978). doi:10.1002/path.1711260307

294. Artal-Sanz, M., Samara, C., Syntichaki, P. & Tavernarakis, N. Lysosomal biogenesis and function is critical for necrotic cell death in Caenorhabditis elegans. *J. Cell Biol.* (2006). doi:10.1083/jcb.200511103

295. Atlante, A. *et al.* An increase in the ATP levels occurs in cerebellar granule cells en route to apoptosis in which ATP derives from both oxidative phosphorylation and anaerobic glycolysis. *Biochim. Biophys. Acta - Bioenerg.* (2005). doi:10.1016/j.bbabio.2005.01.009

296. Zamaraeva, M. V., Sabirov, R. Z., Manabe, K. ichi & Okada, Y. Ca2+-dependent glycolysis activation mediates apoptotic ATP elevation in HeLa cells. *Biochem. Biophys. Res. Commun.* (2007). doi:10.1016/j.bbrc.2007.09.019

297. Bossy-Wetzel, E., Newmeyer, D. D. & Green, D. R. Mitochondrial cytochrome c release in apoptosis occurs upstream of DEVD-specific caspase activation and independently of mitochondrial transmembrane depolarization. *EMBO J.* (1998). doi:10.1093/emboj/17.1.37

298. Gleiss, B., Gogvadze, V., Orrenius, S. & Fadeel, B. Fas-triggered phosphatidylserine exposure is modulated by intracellular ATP. *FEBS Lett.* (2002). doi:10.1016/S0014-5793(02)02743-6

299. Syntichaki, P. & Tavernarakis, N. Death by necrosis. Uncontrollable catastrophe, or is there order behind the chaos? *EMBO Rep.* (2002). doi:10.1093/embo-reports/kvf138

300. Assefa, Z. *et al.* Caspase-3-induced truncation of type 1 inositol trisphosphate receptor accelerates apoptotic cell death and induces inositol trisphosphate-independent calcium release during apoptosis. *J. Biol. Chem.* (2004). doi:10.1074/jbc.M403872200

301. Neumar, R. W., Xu, Y. A., Gada, H., Guttmann, R. P. & Siman, R. Cross-talk between calpain and caspase proteolytic systems during neuronal apoptosis. *J. Biol. Chem.* (2003). doi:10.1074/jbc.M212255200

302. Ono, K., Kim, S. O. & Han, J. Susceptibility of Lysosomes to Rupture Is a Determinant for Plasma Membrane Disruption in Tumor Necrosis Factor Alpha-Induced Cell Death. *Mol. Cell. Biol.* (2003). doi:10.1128/mcb.23.2.665-676.2003

303. Liu, X. & Schnellmann, R. G. Calpain mediates progressive plasma membrane permeability and proteolysis of cytoskeleton-associated paxillin, talin, and vinculin during renal cell death. *J. Pharmacol. Exp. Ther.* (2003). doi:10.1124/jpet.102.043406

304. Honda, H., Kondo, T., Zhao, Q. L., Feril, L. B. & Kitagawa, H. Role of intracellular calcium ions and reactive oxygen species in apoptosis induced by ultrasound. *Ultrasound Med. Biol.* (2004). doi:10.1016/j.ultrasmedbio.2004.02.008

305. Bianchi, M. E. DAMPs, PAMPs and alarmins: all we need to know about danger. *J. Leukoc. Biol.* (2007). doi:10.1189/jlb.0306164

306. Wu, X., Molinaro, C., Johnson, N. & Casiano, C. A. Secondary necrosis is a source of proteolytically modified forms of specific intracellular autoantigens: Implications for systemic autoimmunity. *Arthritis Rheum.* (2001). doi:10.1002/1529-0131(200111)44:11<2642::AID-ART444>3.0.CO;2-8

307. Bell, C. W., Jiang, W., Reich, C. F. & Pisetsky, D. S. The extracellular release of HMGB1 during apoptotic cell death. *Am. J. Physiol. - Cell Physiol.* (2006).

doi:10.1152/ajpcell.00616.2005

308. Zitvogel, L., Kepp, O. & Kroemer, G. Decoding Cell Death Signals in Inflammation and Immunity. *Cell* (2010). doi:10.1016/j.cell.2010.02.015

309. Green, D. R., Ferguson, T., Zitvogel, L. & Kroemer, G. Immunogenic and tolerogenic cell death. *Nature Reviews Immunology* (2009). doi:10.1038/nri2545

310. Mũoz, L. E., Lauber, K., Schiller, M., Manfredi, A. A. & Herrmann, M. The role of defective clearance of apoptotic cells in systemic autoimmunity. *Nature Reviews Rheumatology* (2010). doi:10.1038/nrrheum.2010.46

311. Lövgren, T., Eloranta, M. L., Båve, U., Alm, G. V. & Rönnblom, L. Induction of interferon-α production in plasmacytoid dendritic cells by immune complexes containing nucleic acid released by necrotic or late apoptotic cells and lupus IgG. *Arthritis Rheum.* (2004). doi:10.1002/art.20254

312. Fransen, J. H. *et al.* Both early and late apoptotic blebs are taken up by DC and induce IL-6 production. *Autoimmunity* (2009). doi:10.1080/08916930902828049

313. Fadok, V. A., Bratton, D. L., Guthrie, L. & Henson, P. M. Differential Effects of Apoptotic Versus Lysed Cells on Macrophage Production of Cytokines: Role of Proteases. *J. Immunol.* (2001). doi:10.4049/jimmunol.166.11.6847

314. Takeuchi, O. & Akira, S. Pattern Recognition Receptors and Inflammation. *Cell* (2010). doi:10.1016/j.cell.2010.01.022

315. Iwasaki, A. & Medzhitov, R. Regulation of adaptive immunity by the innate immune system. *Science* (2010). doi:10.1126/science.1183021

316. Matzinger, P. The danger model: A renewed sense of self. *Science* (2002). doi:10.1126/science.1071059

317. Rittirsch, D. *et al.* Cross-talk between TLR4 and FcγReceptorIII (CD16) pathways. *PLoS Pathog.* (2009). doi:10.1371/journal.ppat.1000464

318. Krysko, O., De Ridder, L. & Cornelissen, M. Phosphatidylserine exposure during early primary necrosis (oncosis) in JB6 cells as evidenced by immunogold labeling technique. *Apoptosis* (2004). doi:10.1023/B:APPT.0000031452.75162.75

319. Hirt, U. A. & Leist, M. Rapid, noninflammatory and PS-dependent phagocytic clearance of necrotic cells. *Cell Death Differ.* (2003). doi:10.1038/sj.cdd.4401286

320. Böttcher, A. *et al.* Involvement of phosphatidylserine, αvβ3, CD14, CD36, and complement C1q in the phagocytosis of primary necrotic lymphocytes by macrophages. *Arthritis Rheum.* (2006). doi:10.1002/art.21660

321. Rennemeier, C. *et al.* Thrombospondin-1 promotes cellular adherence of Gram-positive pathogens via recognition of peptidoglycan . *FASEB J.* (2007). doi:10.1096/fj.06-7992com

322. Wang, A. V. T., Scholl, P. R. & Geha, R. S. Physical and functional association of the high affinity immunoglobulin G receptor (FcγRI) with the kinases Hck and Lyn. *J. Exp. Med.* (1994). doi:10.1084/jem.180.3.1165

323. Ghazizadeh, S., Bolen, J. B. & Fleit, H. B. Physical and functional association of Src-related protein tyrosine kinases with FcγRII in monocytic THP-1 cells. *J. Biol. Chem.* (1994).

324. Crowley, M. T. *et al.* A critical role for Syk in signal transduction and phagocytosis mediated by Fcγ receptors on macrophages. *J. Exp. Med.* (1997). doi:10.1084/jem.186.7.1027

325. Kiefer, F. *et al.* The Syk Protein Tyrosine Kinase Is Essential for Fcγ Receptor Signaling in Macrophages and Neutrophils. *Mol. Cell. Biol.* (1998). doi:10.1128/mcb.18.7.4209

326. Botelho, R. J. *et al.* Localized biphasic changes in phosphatidylinositol-4,5-bisphosphate at sites of phagocytosis. *J. Cell Biol.* (2000). doi:10.1083/jcb.151.7.1353

327. Hoppe, A. D. & Swanson, J. A. Cdc42, Rac1, and Rac2 display distinct patterns of

activation during phagocytosis. *Mol. Biol. Cell* (2004). doi:10.1091/mbc.E03-11-0847

328. Park, H. & Cox, D. Cdc42 regulates Fcγ receptor-mediated phagocytosis through the activation and phosphorylation of Wiskott-Aldrich syndrome protein (WASP) and neural-WASP. *Mol. Biol. Cell* (2009). doi:10.1091/mbc.E09-03-0230

329. Gaipl, U. S. *et al.* Complement binding is an early feature of necrotic and a rather late event during apoptotic cell death. *Cell Death Differ.* (2001). doi:10.1038/sj.cdd.4400826

330. Pinckard, R. N. *et al.* Consumption of classical complement components by heart subcellular membranes in vitro and in patients after acute myocardial infarction. *J. Clin. Invest.* (1975). doi:10.1172/JCI108145

331. Ogden, C. A., Kowalewski, R., Peng, Y., Montenegro, V. & Elkon, K. B. IGM is required for efficient complement mediated phagocytosis of apoptotic cells in vivo. *Autoimmunity* (2005). doi:10.1080/08916930500124452

332. Kim, S. J., Gershov, D., Ma, X., Brot, N. & Elkon, K. B. I-PLA2 activation during apoptosis promotes the exposure of membrane lysophosphatidylcholine leading to binding by natural immunoglobulin M antibodies and complement activation. *J. Exp. Med.* (2002). doi:10.1084/jem.20020542

333. Fu, M. *et al.* Identification of poly-reactive natural IgM antibody that recognizes late apoptotic cells and promotes phagocytosis of the cells. *Apoptosis* (2007). doi:10.1007/s10495-006-0581-z

334. Martin, M., Leffler, J. & Blom, A. M. Annexin A2 and A5 serve as new ligands for C1q on apoptotic cells. *J. Biol. Chem.* (2012). doi:10.1074/jbc.M112.341339

335. Ogden, C. A. *et al.* C1q and mannose binding lectin engagement of cell surface calreticulin and CD91 initiates macropinocytosis and uptake of apoptotic cells. *J. Exp. Med.* (2001). doi:10.1084/jem.194.6.781

336. Ciurana, C. L. F., Zwart, B., van Mierlo, G. & Hack, C. E. Complement activation by

necrotic cells in normal plasma environment compares to that by late apoptotic cells and involves predominantly IgM. *Eur. J. Immunol.* (2004). doi:10.1002/eji.200425045

337. Nauta, A. J. *et al.* Mannose-binding lectin engagement with late apoptotic and necrotic cells. *Eur. J. Immunol.* (2003). doi:10.1002/eji.200323888

338. Vives-Pi, M., Rodríguez-Fernández, S. & Pujol-Autonell, I. How apoptotic β-cells direct immune response to tolerance or to autoimmune diabetes: A review. *Apoptosis* (2015). doi:10.1007/s10495-015-1090-8

339. Turley, S. J. *et al.* Transport of peptide-MHC class II complexes in developing dendritic cells. *Science (80-.).* (2000). doi:10.1126/science.288.5465.522

340. Barker, R. N. *et al.* Antigen presentation by macrophages is enhanced by the uptake of necrotic, but not apoptotic, cells. *Clin. Exp. Immunol.* (2002). doi:10.1046/j.1365-2249.2002.01774.x

341. Shi, Y., Zheng, W. & Rock, K. L. Cell injury releases endogenous adjuvants that stimulate cytotoxic T cell responses. *Proc. Natl. Acad. Sci. U. S. A.* (2000). doi:10.1073/pnas.260497597

342. Gallucci, S., Lolkema, M. & Matzinger, P. Natural adjuvants: Endogenous activators of dendritic cells. *Nat. Med.* (1999). doi:10.1038/15200

343. Luis Muñoz-Carrillo, J. *et al.* Cytokine Profiling Plays a Crucial Role in Activating Immune System to Clear Infectious Pathogens. in *Immune Response Activation and Immunomodulation* (2019). doi:10.5772/intechopen.80843

344. Mantegazza, A. R., Magalhaes, J. G., Amigorena, S. & Marks, M. S. Presentation of Phagocytosed Antigens by MHC Class I and II. *Traffic* (2013). doi:10.1111/tra.12026

345. Trombetta, E. S., Ebersold, M., Garrett, W., Pypaert, M. & Mellman, I. Activation of lysosomal function during dendritic cell maturation. *Science (80-.).* (2003). doi:10.1126/science.1080106

346. Tsokos, G. C., Lo, M. S., Reis, P. C. & Sullivan, K. E. New insights into the immunopathogenesis of systemic lupus erythematosus. *Nature Reviews Rheumatology* (2016). doi:10.1038/nrrheum.2016.186

347. D'Cruz, D. P., Khamashta, M. A. & Hughes, G. R. Systemic lupus erythematosus. *Lancet* (2007). doi:10.1016/S0140-6736(07)60279-7

348. Yildirim-Toruner, C. & Diamond, B. Current and novel therapeutics in the treatment of systemic lupus erythematosus. *Journal of Allergy and Clinical Immunology* (2011). doi:10.1016/j.jaci.2010.12.1087

349. Munoz, L. E. *et al.* SLE - A disease of clearance deficiency? in *Rheumatology* (2005). doi:10.1093/rheumatology/keh693

350. Perniok, A., Wedekind, F., Herrmann, M., Specker, C. & Schneider, M. High levels of circulating early apoptic peripheral blood mononuclear cells in systemic lupus erythematosus. *Lupus* (1998). doi:10.1191/096120398678919804

351. Baumann, I. *et al.* Impaired uptake of apoptotic cells into tingible body macrophages in germinal centers of patients with systemic lupus erythematosus. *Arthritis Rheum.* (2002). doi:10.1002/1529-0131(200201)46:1<191::AID-ART10027>3.0.CO;2-K

352. Herrmann, M. *et al.* Impaired phagocytosis of apoptotic cell material by monocyte-derived macrophages from patients with systemic lupus erythematosus. *Arthritis Rheum.* (1998). doi:10.1002/1529-0131(199807)41:7<1241::AID-ART15>3.0.CO;2-H

353. Gaipl, U. S. *et al.* Clearance deficiency and systemic lupus erythematosus (SLE). *J. Autoimmun.* (2007). doi:10.1016/j.jaut.2007.02.005

354. Gaipl, U. S. *et al.* Clearance of apoptotic cells in human SLE. *Current directions in autoimmunity* (2006). doi:10.1159/000090781

355. Mevorach, D., Zhou, J. L., Song, X. & Elkon, K. B. Systemic exposure to irradiated apoptotic cells induces autoantibody production. *J. Exp. Med.* (1998).

doi:10.1084/jem.188.2.387

356. Asano, K. *et al.* Masking of phosphatidylserine inhibits apoptotic cell engulfment and induces autoantibody production in mice. *J. Exp. Med.* (2004). doi:10.1084/jem.20040342

357. Elliott, M. R. & Ravichandran, K. S. Clearance of apoptotic cells: Implications in health and disease. *Journal of Cell Biology* (2010). doi:10.1083/jcb.201004096

358. Wu, H. H. *et al.* Glial precursors clear sensory neuron corpses during development via Jedi-1, an engulfment receptor. *Nat. Neurosci.* (2009). doi:10.1038/nn.2446

359. Scheib, J. L., Sullivan, C. S. & Carter, B. D. Jedi-1 and MEGF10 Signal Engulfment of Apoptotic Neurons through the Tyrosine Kinase Syk. *J. Neurosci.* (2012). doi:10.1523/jneurosci.6350-11.2012

360. Sullivan, C. S. *et al.* The adaptor protein GULP promotes Jedi-1-mediated phagocytosis through a clathrin-dependent mechanism. *Mol. Biol. Cell* (2014). doi:10.1091/mbc.e13-11-0658

361. Jones, C. I. *et al.* A functional genomics approach reveals novel quantitative trait loci associated with platelet signaling pathways. *Blood* (2009). doi:10.1182/blood-2009-02-202614

362. Johnson, A. D. *et al.* Genome-wide meta-analyses identifies seven loci associated with platelet aggregation in response to agonists. *Nat. Genet.* (2010). doi:10.1038/ng.604

363. Faraday, N. *et al.* Identification of a specific intronic PEAR1 gene variant associated with greater platelet aggregability and protein expression. *Blood* (2011). doi:10.1182/blood-2010-11-320788

364. Lewis, J. P. *et al.* Genetic variation in PEAR1 is associated with platelet aggregation and cardiovascular outcomes. *Circ. Cardiovasc. Genet.* (2013). doi:10.1161/CIRCGENETICS.111.964627

365. Qayyum, R. *et al.* Genome-wide association study of platelet aggregation in African

Americans. *BMC Genet.* (2015). doi:10.1186/s12863-015-0217-9

366. Backman, J. D. *et al.* Prospective Evaluation of Genetic Variation in Platelet Endothelial Aggregation Receptor 1 Reveals Aspirin-Dependent Effects on Platelet Aggregation Pathways. *Clin. Transl. Sci.* (2017). doi:10.1111/cts.12438

367. Sokol, J., Skerenova, M., Ivankova, J., Simurda, T. & Stasko, J. Association of Genetic Variability in Selected Genes in Patients With Deep Vein Thrombosis and Platelet Hyperaggregability. *Clin. Appl. Thromb.* (2018). doi:10.1177/1076029618779136

368. Stimpfle, F. *et al.* Variants of PEAR1 are associated with outcome in patients with ACS and stable CAD undergoing PCI. *Front. Pharmacol.* (2018). doi:10.3389/fphar.2018.00490

369. Kim, Y. *et al.* Targeted Deep Resequencing Identifies Coding Variants in the PEAR1 Gene That Play a Role in Platelet Aggregation. *PLoS One* (2013). doi:10.1371/journal.pone.0064179

370. Keramati, A. R. *et al.* Targeted deep sequencing of the PEAR1 locus for platelet aggregation in European and African American families. *Platelets* (2019). doi:10.1080/09537104.2018.1447659

371. Nanda, N. *et al.* Platelet endothelial aggregation receptor 1 (PEAR1), a novel epidermal growth factor repeat-containing transmembrane receptor, participates in platelet contact-induced activation. *J. Biol. Chem.* (2005). doi:10.1074/jbc.M413411200

372. Jones, P. A. Functions of DNA methylation: Islands, start sites, gene bodies and beyond. *Nature Reviews Genetics* (2012). doi:10.1038/nrg3230

373. Izzi, B. *et al.* Allele-specific DNA methylation reinforces PEAR1 enhancer activity. *Blood* (2016). doi:10.1182/blood-2015-11-682153

374. Johnson, A. D. Pairing megakaryopoiesis methylation with PEAR1. *Blood* (2016). doi:10.1182/blood-2016-06-723940

375. Criel, M. *et al.* Absence of Pear1 does not affect murine platelet function in vivo. *Thromb. Res.* (2016). doi:10.1016/j.thromres.2016.08.026

376. Justice, M. J. & Dhillon, P. Using the mouse to model human disease: Increasing validity and reproducibility. *DMM Disease Models and Mechanisms* (2016). doi:10.1242/dmm.024547

377. Kauskot, A. *et al.* PEAR1 attenuates megakaryopoiesis via control of the PI3K/PTEN pathway. *Blood* (2013). doi:10.1182/blood-2012-10-462887

378. Krivtsov, A. V. *et al.* Jedi - A novel transmembrane protein expressed in early hematopoietic cells. *J. Cell. Biochem.* (2007). doi:10.1002/jcb.21232

379. Fisch, A. S. *et al.* Genetic variation in the platelet endothelial aggregation receptor 1 gene results in endothelial dysfunction. *PLoS One* (2015). doi:10.1371/journal.pone.0138795

380. Vandenbriele, C. *et al.* Platelet endothelial aggregation receptor-1: A novel modifier of neoangiogenesis. *Cardiovasc. Res.* (2015). doi:10.1093/cvr/cvv193

381. Grinsell, D. & Keating, C. P. Peripheral Nerve Reconstruction after Injury: A Review of Clinical and Experimental Therapies. *BioMed Research International* (2014). doi:10.1155/2014/698256

382. BrosiusLutz, A. & Barres, B. A. Contrasting the Glial Response to Axon Injury in the Central and Peripheral Nervous Systems. *Developmental Cell* (2014). doi:10.1016/j.devcel.2013.12.002

383. Scheib, J. & Höke, A. Advances in peripheral nerve regeneration. *Nature Reviews Neurology* (2013). doi:10.1038/nrneurol.2013.227

384. Witzel, C., Rohde, C. & Brushart, T. M. Pathway sampling by regenerating peripheral axons. *J. Comp. Neurol.* (2005). doi:10.1002/cne.20436

385. Siemionow, M. & Brzezicki, G. Chapter 8 Current Techniques and Concepts in Peripheral Nerve Repair. *International Review of Neurobiology* (2009). doi:10.1016/S0074-

7742(09)87008-6

386. Vickers, J. C. *et al.* Axonopathy and cytoskeletal disruption in degenerative diseases of the central nervous system. *Brain Research Bulletin* (2009). doi:10.1016/j.brainresbull.2009.08.004

387. Hill, C. S., Coleman, M. P. & Menon, D. K. Traumatic Axonal Injury: Mechanisms and Translational Opportunities. *Trends in Neurosciences* (2016). doi:10.1016/j.tins.2016.03.002

388. Waller, A. Experiments on the Section of the Glossopharyngeal and Hypoglossal Nerves of the Frog, and Observations of the Alterations Produced Thereby in the Structure of Their Primitive Fibres. *Proc. R. Soc. London* (1843). doi:10.1098/rspl.1843.0224

389. Freeman, M. R. Signaling mechanisms regulating Wallerian degeneration. *Current Opinion in Neurobiology* (2014). doi:10.1016/j.conb.2014.05.001

390. Lunn, E. R., Perry, V. H., Brown, M. C., Rosen, H. & Gordon, S. Absence of Wallerian Degeneration does not Hinder Regeneration in Peripheral Nerve. *Eur. J. Neurosci.* (1989). doi:10.1111/j.1460-9568.1989.tb00771.x

391. Perry, V. H., Brown, M. C. & Tsao, J. W. The Effectiveness of the Gene Which Slows the Rate of Wallerian Degeneration in C57BL/Ola Mice Declines With Age. *Eur. J. Neurosci.* (1992). doi:10.1111/j.1460-9568.1992.tb00126.x

392. Mack, T. G. A. *et al.* Wallerian degeneration of injured axons and synapses is delayed by a Ube4b/Nmnat chimeric gene. *Nat. Neurosci.* (2001). doi:10.1038/nn770

393. Laser, H. *et al.* The slow Wallerian degeneration protein, WldS, binds directly to VCP/p97 and partially redistributes it within the nucleus. *Mol. Biol. Cell* (2006). doi:10.1091/mbc.E05-04-0375

394. Sasaki, Y. & Milbrandt, J. Axonal degeneration is blocked by nicotinamide mononucleotide adenylyltransferase (Nmnat) protein transduction into transected axons.

J. Biol. Chem. (2010). doi:10.1074/jbc.C110.193904

395. Sasaki, Y. Metabolic aspects of neuronal degeneration: From a NAD + point of view. *Neuroscience Research* (2019). doi:10.1016/j.neures.2018.07.001

396. Avery, M. A., Sheehan, A. E., Kerr, K. S., Wang, J. & Freeman, M. R. Wld s requires Nmnatl enzymatic activity and N16- VCP interactions to suppress Wallerian degeneration. *J. Cell Biol.* (2009). doi:10.1083/jcb.200808042

397. Conforti, L. *et al.* Wld S protein requires Nmnat activity and a short N-terminal sequence to protect axons in mice. *J. Cell Biol.* (2009). doi:10.1083/jcb.200807175

398. Berger, F., Lau, C., Dahlmann, M. & Ziegler, M. Subcellular compartmentation and differential catalytic properties of the three human nicotinamide mononucleotide adenylyltransferase isoforms. *J. Biol. Chem.* (2005). doi:10.1074/jbc.M508660200

399. Ryu, K. W. *et al.* Metabolic regulation of transcription through compartmentalized NAD+ biosynthesis. *Science (80-.).* (2018). doi:10.1126/science.aan5780

400. Yan, T. *et al.* Nmnat2 delays axon degeneration in superior cervical ganglia dependent on its NAD synthesis activity. *Neurochem. Int.* (2010). doi:10.1016/j.neuint.2009.09.007

401. Araki, T., Sasaki, Y. & Milbrandt, J. Increased nuclear NAD biosynthesis and SIRT1 activation prevent axonal degeneration. *Science (80-.).* (2004). doi:10.1126/science.1098014

402. Loreto, A., Di Stefano, M., Gering, M. & Conforti, L. Wallerian Degeneration Is Executed by an NMN-SARM1-Dependent Late Ca2+ Influx but Only Modestly Influenced by Mitochondria. *Cell Rep.* (2015). doi:10.1016/j.celrep.2015.11.032

403. Rosell, A. L. & Neukomm, L. J. Axon death signalling in Wallerian degeneration among species and in disease. *Open Biology* (2019). doi:10.1098/rsob.190118

404. Gilley, J. & Coleman, M. P. Endogenous Nmnat2 Is an Essential Survival Factor for Maintenance of Healthy Axons. *PLoS Biol.* (2010). doi:10.1371/journal.pbio.1000300

405. Conforti, L., Gilley, J. & Coleman, M. P. Wallerian degeneration: An emerging axon death pathway linking injury and disease. *Nature Reviews Neuroscience* (2014). doi:10.1038/nrn3680

406. Hoopfer, E. D. *et al.* Wlds Protection Distinguishes Axon Degeneration following Injury from Naturally Occurring Developmental Pruning. *Neuron* (2006). doi:10.1016/j.neuron.2006.05.013

407. Simon, D. J. *et al.* A caspase cascade regulating developmental axon degeneration. *J. Neurosci.* (2012). doi:10.1523/JNEUROSCI.3012-12.2012

408. Osterloh, J. M. *et al.* dSarm/Sarm1 is required for activation of an injury-induced axon death pathway. *Science (80-.).* (2012). doi:10.1126/science.1223899

409. Büki, A., Siman, R., Trojanowski, J. Q. & Povlishock, J. T. The role of calpain-mediated spectrin proteolysis in traumatically induced axonal injury. *J. Neuropathol. Exp. Neurol.* (1999). doi:10.1097/00005072-199904000-00007

410. Adalbert, R. *et al.* Intra-axonal calcium changes after axotomy in wild-type and slow Wallerian degeneration axons. *Neuroscience* (2012). doi:10.1016/j.neuroscience.2012.08.056

411. Avery, M. A. *et al.* Wld S prevents axon degeneration through increased mitochondrial flux and enhanced mitochondrial Ca 2+ buffering. *Curr. Biol.* (2012). doi:10.1016/j.cub.2012.02.043

412. Vargas, M. E., Yamagishi, Y., Tessier-Lavigne, M. & Sagasti, A. Live imaging of calcium dynamics during axon degeneration reveals two functionally distinct phases of calcium influx. *J. Neurosci.* (2015). doi:10.1523/JNEUROSCI.2484-15.2015

413. Gerdts, J., Brace, E. J., Sasaki, Y., DiAntonio, A. & Milbrandt, J. SARM1 activation triggers axon degeneration locally via NAD+ destruction. *Science (80-.).* (2015). doi:10.1126/science.1258366

414. Gerdts, J., Summers, D. W., Sasaki, Y., DiAntonio, A. & Milbrandt, J. Sarm1-mediated axon degeneration requires both SAM and TIR interactions. *J. Neurosci.* (2013). doi:10.1523/JNEUROSCI.1197-13.2013

415. Gilley, J., Orsomando, G., Nascimento-Ferreira, I. & Coleman, M. P. Absence of SARM1 rescues development and survival of NMNAT2-Deficient axons. *Cell Rep.* (2015). doi:10.1016/j.celrep.2015.02.060

416. Essuman, K. *et al.* The SARM1 Toll/Interleukin-1 Receptor Domain Possesses Intrinsic NAD+ Cleavage Activity that Promotes Pathological Axonal Degeneration. *Neuron* (2017). doi:10.1016/j.neuron.2017.02.022

417. Sasaki, Y., Nakagawa, T., Mao, X., DiAntonio, A. & Milbrandt, J. NMNAT1 inhibits axon degeneration via blockade of SARM1-mediated NAD+depletion. *Elife* (2016). doi:10.7554/eLife.19749

418. Xiong, X. *et al.* The Highwire Ubiquitin Ligase Promotes Axonal Degeneration by Tuning Levels of Nmnat Protein. *PLoS Biol.* (2012). doi:10.1371/journal.pbio.1001440

419. Neukomm, L. J., Burdett, T. C., Gonzalez, M. A., Züchner, S. & Freeman, M. R. Rapid in vivo forward genetic approach for identifying axon death genes in Drosophila. *Proc. Natl. Acad. Sci. U. S. A.* (2014). doi:10.1073/pnas.1406230111

420. Babetto, E., Beirowski, B., Russler, E. V., Milbrandt, J. & DiAntonio, A. The Phr1 Ubiquitin Ligase Promotes Injury-Induced Axon Self-Destruction. *Cell Rep.* (2013). doi:10.1016/j.celrep.2013.04.013

421. Jessen, K. R. & Mirsky, R. The origin and development of glial cells in peripheral nerves. *Nature Reviews Neuroscience* (2005). doi:10.1038/nrn1746

422. Chen, Z.-L., Yu, W.-M. & Strickland, S. Peripheral Regeneration. *Annu. Rev. Neurosci.* (2007). doi:10.1146/annurev.neuro.30.051606.094337

423. Jessen, K. R. & Mirsky, R. Negative regulation of myelination: Relevance for

development, injury, and demyelinating disease. *Glia* (2008). doi:10.1002/glia.20761

424. Arthur-Farraj, P. J. *et al.* Changes in the Coding and Non-coding Transcriptome and DNA Methylome that Define the Schwann Cell Repair Phenotype after Nerve Injury. *Cell Rep.* (2017). doi:10.1016/j.celrep.2017.08.064

425. Grigoryan, T. & Birchmeier, W. Molecular signaling mechanisms of axon-glia communication in the peripheral nervous system. *BioEssays* (2015). doi:10.1002/bies.201400172

426. Willem, M. Proteolytic processing of Neuregulin-1. *Brain Research Bulletin* (2016). doi:10.1016/j.brainresbull.2016.07.003

427. Fricker, F. R. *et al.* Axonal neuregulin 1 is a rate limiting but not essential factor for nerve remyelination. *Brain* (2013). doi:10.1093/brain/awt148

428. Stassart, R. M. *et al.* A role for Schwann cell-derived neuregulin-1 in remyelination. *Nat. Neurosci.* (2013). doi:10.1038/nn.3281

429. Chen, L. E. *et al.* Recombinant human glial growth factor 2 (rhGGF 2) improves functional recovery of crushed peripheral nerve (a double-blind study). *Neurochem. Int.* (1998). doi:10.1016/S0197-0186(98)00037-0

430. Joung, I. *et al.* Secretion of EGF-like domain of heregulinβ promotes axonal growth and functional recovery of injured sciatic nerve. *Mol. Cells* (2010). doi:10.1007/s10059-010-0137-5

431. Yildiz, M. *et al.* Efficacy of glial growth factor and nerve growth factor on the recovery of traumatic facial paralysis. *Eur. Arch. Oto-Rhino-Laryngology* (2011). doi:10.1007/s00405-011-1492-3

432. Duregotti, E. *et al.* Mitochondrial alarmins released by degenerating motor axon terminals activate perisynaptic schwann cells. *Proc. Natl. Acad. Sci. U. S. A.* (2015). doi:10.1073/pnas.1417108112

433. Goethals, S., Ydens, E., Timmerman, V. & Janssens, S. Toll-like receptor expression in the peripheral nerve. *Glia* (2010). doi:10.1002/glia.21041

434. Boivin, A. *et al.* Toll-like receptor signaling is critical for Wallerian degeneration and functional recovery after peripheral nerve injury. *J. Neurosci.* (2007). doi:10.1523/JNEUROSCI.3027-07.2007

435. Lee, H. *et al.* Necrotic neuronal cells induce inflammatory Schwann cell activation via TLR2 and TLR3: Implication in Wallerian degeneration. *Biochem. Biophys. Res. Commun.* (2006). doi:10.1016/j.bbrc.2006.09.108

436. Takada, H., Yuasa, S. & Araki, T. Demyelination can proceed independently of axonal degradation during Wallerian degeneration in wlds mice. *Eur. J. Neurosci.* (2011). doi:10.1111/j.1460-9568.2011.07783.x

437. Gamage, K. K. *et al.* Death Receptor 6 Promotes Wallerian Degeneration in Peripheral Axons Current Biology Report Death Receptor 6 Promotes Wallerian Degeneration in Peripheral Axons. *Curr. Biol.* (2017). doi:10.1016/j.cub.2017.01.062

438. Agthong, S., Kaewsema, A., Tanomsridejchai, N. & Chentanez, V. Activation of MAPK ERK in peripheral nerve after injury. *BMC Neurosci.* (2006). doi:10.1186/1471-2202-7-45

439. Woodhoo, A. *et al.* Notch controls embryonic Schwann cell differentiation, postnatal myelination and adult plasticity. *Nat. Neurosci.* (2009). doi:10.1038/nn.2323

440. Arthur-Farraj, P. J. *et al.* c-Jun Reprograms Schwann Cells of Injured Nerves to Generate a Repair Cell Essential for Regeneration. *Neuron* (2012). doi:10.1016/j.neuron.2012.06.021

441. Parkinson, D. B. *et al.* c-Jun is a negative regulator of myelination. *J. Cell Biol.* (2008). doi:10.1083/jcb.200803013

442. Fontana, X. *et al.* C-Jun in Schwann cells promotes axonal regeneration and motoneuron survival via paracrine signaling. *J. Cell Biol.* (2012). doi:10.1083/jcb.201205025

443. Stoll, G., Jander, S. & Myers, R. R. Degeneration and regeneration of the peripheral nervous system: From Augustus Waller's observations to neuroinflammation. in *Journal of the Peripheral Nervous System* (2002). doi:10.1046/j.1529-8027.2002.02002.x

444. Gaudet, A. D., Popovich, P. G. & Ramer, M. S. Wallerian degeneration: Gaining perspective on inflammatory events after peripheral nerve injury. *Journal of Neuroinflammation* (2011). doi:10.1186/1742-2094-8-110

445. Fazal, S. V. *et al.* Graded elevation of c-Jun in Schwann cells in vivo: Gene dosage determines effects on development, remyelination, tumorigenesis, and hypomyelination. *J. Neurosci.* (2017). doi:10.1523/JNEUROSCI.0986-17.2017

446. Jessen, K. R. & Mirsky, R. The success and failure of the schwann cell response to nerve injury. *Frontiers in Cellular Neuroscience* (2019). doi:10.3389/fncel.2019.00033

447. McKerracher, L. *et al.* Identification of myelin-associated glycoprotein as a major myelin-derived inhibitor of neurite growth. *Neuron* (1994). doi:10.1016/0896-6273(94)90247-X

448. Mukhopadhyay, G., Doherty, P., Walsh, F. S., Crocker, P. R. & Filbin, M. T. A novel role for myelin-associated glycoprotein as an inhibitor of axonal regeneration. *Neuron* (1994). doi:10.1016/0896-6273(94)90042-6

449. Shen, Y. J., DeBellard, M. E., Salzer, J. L., Roder, J. & Filbin, M. T. Myelin-associated glycoprotein in myelin and expressed by Schwann cells inhibits axonal regeneration and branching. *Mol. Cell. Neurosci.* (1998). doi:10.1006/mcne.1998.0700

450. Kang, H. & Lichtman, J. W. Motor axon regeneration and muscle reinnervation in young adult and aged animals. *J. Neurosci.* (2013). doi:10.1523/JNEUROSCI.4067-13.2013

451. Painter, M. W. *et al.* Diminished Schwann cell repair responses underlie age-associated impaired axonal regeneration. *Neuron* (2014). doi:10.1016/j.neuron.2014.06.016

452. Brown, M. C., Perry, V. H., Hunt, S. P. & Lapper, S. R. Further Studies on Motor and Sensory Nerve Regeneration in Mice With Delayed Wallerian Degeneration. *Eur. J.*

Neurosci. (1994). doi:10.1111/j.1460-9568.1994.tb00285.x

453. Chen, S. & Bisby, M. A. Imparied motor axon regeneration in the C57BL/Ola mouse. *J. Comp. Neurol.* (1993). doi:10.1002/cne.903330310

454. Caroni, P. & Schwab, M. E. Two membrane protein fractions from rat central myelin with inhibitory properties for neurite growth and fibroblast spreading. *J. Cell Biol.* (1988). doi:10.1083/jcb.106.4.1281

455. Perry, V. H., Tsao, J. W., Feam, S. & Brown, M. C. Radiation-induced Reductions in Macrophage Recruitment Have Only Slight Effects on Myelin Degeneration in Sectioned Peripheral Nerves of Mice. *Eur. J. Neurosci.* (1995). doi:10.1111/j.1460-9568.1995.tb01063.x

456. De, S., Trigueros, M. A., Kalyvas, A. & David, S. Phospholipase A2 plays an important role in myelin breakdown and phagocytosis during wallerian degeneration. *Mol. Cell. Neurosci.* (2003). doi:10.1016/S1044-7431(03)00241-0

457. Jung, J. *et al.* Actin polymerization is essential for myelin sheath fragmentation during Wallerian degeneration. *J. Neurosci.* (2011). doi:10.1523/JNEUROSCI.4537-10.2011

458. Martini, R., Fischer, S., López-Vales, R. & David, S. Interactions between schwann cells and macrophages in injury and inherited demyelinating disease. *Glia* (2008). doi:10.1002/glia.20766

459. Gomez-Sanchez, J. A. *et al.* Schwann cell autophagy, myelinophagy, initiates myelin clearance from injured nerves. *J. Cell Biol.* (2015). doi:10.1083/jcb.201503019

460. Lewis, G. M. & Kucenas, S. Perineurial Glia Are Essential for Motor Axon Regrowth following Nerve Injury. *J. Neurosci.* (2014). doi:10.1523/jneurosci.1906-14.2014

461. Mueller, M. *et al.* Rapid response of identified resident endoneurial macrophages to nerve injury. *Am. J. Pathol.* (2001). doi:10.1016/S0002-9440(10)63070-2

462. Mueller, M. *et al.* Macrophage response to peripheral nerve injury: The quantitative

contribution of resident and hematogenous macrophages. *Lab. Investig.* (2003). doi:10.1097/01.LAB.0000056993.28149.BF

463. Perry, V. H., Brown, M. C. & Gordon, S. The macrophage response to central and peripheral nerve injury: A possible role for macrophages in regeneration. *J. Exp. Med.* (1987). doi:10.1084/jem.165.4.1218

464. Vass, K., Hickey, W. F., Schmidt, R. E. & Lassmann, H. Bone marrow-derived elements in the peripheral nervous system: An immunohistochemical and ultrastructural investigation in chimeric rats. *Lab. Investig.* (1993).

465. Napoli, I. *et al.* A Central Role for the ERK-Signaling Pathway in Controlling Schwann Cell Plasticity and Peripheral Nerve Regeneration In Vivo. *Neuron* (2012). doi:10.1016/j.neuron.2011.11.031

466. Gray, M., Palispis, W., Popovich, P. G., Van Rooijen, N. & Gupta, R. Macrophage depletion alters the blood-nerve barrier without affecting Schwann cell function after neural injury. *J. Neurosci. Res.* (2007). doi:10.1002/jnr.21166

467. Weerasuriya, A. & Hockman, C. H. Perineurial permeability to sodium during Wallerian degeneration in rat sciatic nerve. *Brain Res.* (1992). doi:10.1016/0006-8993(92)90727-Q

468. Wekerle, H., Schwab, M., Linington, C. & Meyermann, R. Antigen presentation in the peripheral nervous system: Schwann cells present endogenous myelin autoantigens to lymphocytes. *Eur. J. Immunol.* (1986). doi:10.1002/eji.1830161214

469. Rotshenker, S. Wallerian degeneration: The innate-immune response to traumatic nerve injury. *J. Neuroinflammation* **8**, 109 (2011).

470. Boven, L. A. *et al.* Myelin-laden macrophages are anti-inflammatory, consistent with foam cells in multiple sclerosis. *Brain* (2006). doi:10.1093/brain/awh707

471. Ydens, E. *et al.* Acute injury in the peripheral nervous system triggers an alternative macrophage response. *J. Neuroinflammation* (2012). doi:10.1186/1742-2094-9-176

472. Komori, T., Morikawa, Y., Inada, T., Hisaoka, T. & Senba, E. Site-specific subtypes of macrophages recruited after peripheral nerve injury. *Neuroreport* (2011). doi:10.1097/WNR.0b013e32834cd76a

473. Shacham-Silverberg, V. *et al.* Phosphatidylserine is a marker for axonal debris engulfment but its exposure can be decoupled from degeneration. *Cell Death Dis.* (2018). doi:10.1038/s41419-018-1155-z

474. Wakatsuki, S. & Araki, T. Specific phospholipid scramblases are involved in exposure of phosphatidylserine, an “eat-me” signal for phagocytes, on degenerating axons. *Commun. Integr. Biol.* (2017). doi:10.1080/19420889.2017.1296615

475. Lutz, A. B. *et al.* Schwann cells use TAM receptor-mediated phagocytosis in addition to autophagy to clear myelin in a mouse model of nerve injury. *Proc. Natl. Acad. Sci. U. S. A.* (2017). doi:10.1073/pnas.1710566114

476. Narciso, M. S. *et al.* Sciatic nerve regeneration is accelerated in galectin-3 knockout mice. *Exp. Neurol.* (2009). doi:10.1016/j.expneurol.2009.01.008

477. Mietto, B. S. *et al.* Lack of galectin-3 speeds Wallerian degeneration by altering TLR and pro-inflammatory cytokine expressions in injured sciatic nerve. *Eur. J. Neurosci.* (2013). doi:10.1111/ejn.12161

478. Vogelbaum, M. A., Long, J. X. & Rich, K. M. Developmental regulation of apoptosis in dorsal root ganglion neurons. *J. Neurosci.* (1998). doi:10.1523/jneurosci.18-21-08928.1998

479. Hyman, C. *et al.* BDNF is a neurotrophic factor for dopaminergic neurons of the substantia nigra. *Nature* (1991). doi:10.1038/350230a0

480. Lindsay, R. M. Nerve growth factors (NGF, BDNF) enhance axonal regeneration but are not required for survival of adult sensory neurons. *J. Neurosci.* (1988). doi:10.1523/jneurosci.08-07-02394.1988

481. Aguayo, A. J., Peyronnard, J. M. & Bray, G. M. A quantitative ulthastructural study of regeneration from isolated proximal stumps of transected unmyelinated nerves. *J. Neuropathol. Exp. Neurol.* (1973). doi:10.1097/00005072-197304000-00006

482. Fu, S. Y. & Gordon, T. The cellular and molecular basis of peripheral nerve regeneration. *Mol. Neurobiol.* (1997). doi:10.1007/BF02740621

483. Himes, B. T. & Tessler, A. Death of some dorsal root ganglion neurons and plasticity of others following sciatic nerve section in adult and neonatal rats. *J. Comp. Neurol.* (1989). doi:10.1002/cne.902840206

484. Snider, W. D., Elliott, J. L. & Yan, Q. Axotomy-induced neuronal death during development. *J. Neurobiol.* (1992). doi:10.1002/neu.480230913

485. Hart, A. M., Terenghi, G. & Wiberg, M. Neuronal death after peripheral nerve injury and experimental strategies for neuroprotection. *Neurological Research* (2008). doi:10.1179/174313208X362479

486. Terenghi, G., Hart, A. & Wiberg, M. The nerve injury and the dying neurons: Diagnosis and prevention. *J. Hand Surg. Eur. Vol.* (2011). doi:10.1177/1753193411422202

487. Hu, P. & McLachlan, E. M. Selective Reactions of Cutaneous and Muscle Afferent Neurons to Peripheral Nerve Transection in Rats. *J. Neurosci.* (2003). doi:10.1523/jneurosci.23-33-10559.2003

488. Kole, A. J., Annis, R. P. & Deshmukh, M. Mature neurons: equipped for survival. *Cell death & disease* (2013). doi:10.1038/cddis.2013.220

489. Walsh, G. S., Orike, N., Kaplan, D. R. & Miller, F. D. The invulnerability of adult neurons: A critical role for p73. *J. Neurosci.* (2004). doi:10.1523/JNEUROSCI.1299-04.2004

490. Krajewska, M. *et al.* Dynamics of expression of apoptosis-regulatory proteins Bid, Bcl-2, Bcl-X, Bax and Bak during development of murine nervous system. *Cell Death Differ.* (2002). doi:10.1038/sj.cdd.4400934

491. Kole, A. J., Swahari, V., Hammond, S. M. & Deshmukh, M. miR-29b is activated during neuronal maturation and targets BH3-only genes to restrict apoptosis. *Genes Dev.* (2011). doi:10.1101/gad.1975411

492. Wright, K. M., Smith, M. I., Farrag, L. & Deshmukh, M. Chromatin modification of Apaf-1 restricts the apoptotic pathway in mature neurons. *J. Cell Biol.* (2007). doi:10.1083/jcb.200708086

493. Tedeschi, A. & Bradke, F. Spatial and temporal arrangement of neuronal intrinsic and extrinsic mechanisms controlling axon regeneration. *Current Opinion in Neurobiology* (2017). doi:10.1016/j.conb.2016.12.005

494. Quadrato, G. & Di Giovanni, S. Waking up the sleepers: Shared transcriptional pathways in axonal regeneration and neurogenesis. *Cellular and Molecular Life Sciences* (2013). doi:10.1007/s00018-012-1099-x

495. Wolf, J. A., Stys, P. K., Lusardi, T., Meaney, D. & Smith, D. H. Traumatic axonal injury induces calcium influx modulated by tetrodotoxin-sensitive sodium channels. *J. Neurosci.* (2001). doi:10.1523/jneurosci.21-06-01923.2001

496. Cho, Y., Sloutsky, R., Naegle, K. M. & Cavalli, V. Injury-Induced HDAC5 nuclear export is essential for axon regeneration. *Cell* **155**, 894 (2013).

497. Stirling, D. P. & Stys, P. K. Mechanisms of axonal injury: internodal nanocomplexes and calcium deregulation. *Trends in Molecular Medicine* (2010). doi:10.1016/j.molmed.2010.02.002

498. Gaub, P. *et al.* HDAC inhibition promotes neuronal outgrowth and counteracts growth cone collapse through CBP/p300 and P/CAF-dependent p53 acetylation. *Cell Death Differ.* (2010). doi:10.1038/cdd.2009.216

499. Cho, Y. & Cavalli, V. HDAC5 is a novel injury-regulated tubulin deacetylase controlling axon regeneration. *EMBO J.* (2012). doi:10.1038/emboj.2012.160

500. Hao, Y. *et al.* An evolutionarily conserved mechanism for cAMP elicited axonal regeneration involves direct activation of the dual leucine zipper kinase DLK. *Elife* (2016). doi:10.7554/eLife.14048

501. Shin, J. E. *et al.* Dual Leucine Zipper Kinase Is Required for Retrograde Injury Signaling and Axonal Regeneration. *Neuron* (2012). doi:10.1016/j.neuron.2012.04.028

502. Nix, P., Hisamoto, N., Matsumoto, K. & Bastiani, M. Axon regeneration requires coordinate activation of p38 and JNK MAPK pathways. *Proc. Natl. Acad. Sci. U. S. A.* (2011). doi:10.1073/pnas.1104830108

503. Lindwall, C. & Kanje, M. Retrograde axonal transport of JNK signaling molecules influence injury induced nuclear changes in p-c-Jun and ATF3 in adult rat sensory neurons. *Mol. Cell. Neurosci.* (2005). doi:10.1016/j.mcn.2005.03.002

504. Seijffers, R., Mills, C. D. & Woolf, C. J. ATF3 increases the intrinsic growth state of DRG neurons to enhance peripheral nerve regeneration. *J. Neurosci.* (2007). doi:10.1523/JNEUROSCI.5313-06.2007

505. Gey, M. *et al.* Atf3 mutant mice show reduced axon regeneration and impaired regeneration-associated gene induction after peripheral nerve injury. *Open Biol.* (2016). doi:10.1098/rsob.160091

506. Hammarlund, M., Nix, P., Hauth, L., Jorgensen, E. M. & Bastiani, M. Axon regeneration requires a conserved MAP kinase pathway. *Science (80-.).* (2009). doi:10.1126/science.1165527

507. Willis, D. *et al.* Differential transport and local translation of cytoskeletal, injury-response, and neurodegeneration protein mRNAs in axons. *J. Neurosci.* (2005). doi:10.1523/JNEUROSCI.4235-04.2005

508. Verma, P. *et al.* Axonal protein synthesis and degradation are necessary for efficient growth cone regeneration. *J. Neurosci.* (2005). doi:10.1523/JNEUROSCI.3073-04.2005

509. Perlson, E. *et al.* Vimentin-dependent spatial translocation of an activated MAP kinase in injured nerve. *Neuron* (2005). doi:10.1016/j.neuron.2005.01.023

510. Reynolds, A. J., Hendry, I. A. & Bartlett, S. E. Anterograde and retrograde transport of active extracellular signal-related kinase 1 (ERK1) in the ligated rat sciatic nerve. *Neuroscience* (2001). doi:10.1016/S0306-4522(01)00235-4

511. Blackmore, M. G. Molecular Control of Axon Growth: Insights from Comparative Gene Profiling and High-Throughput Screening. in *International Review of Neurobiology* (2012). doi:10.1016/B978-0-12-398309-1.00004-4

512. Hu, G. *et al.* Single-cell RNA-seq reveals distinct injury responses in different types of DRG sensory neurons. *Sci. Rep.* (2016). doi:10.1038/srep31851

513. Raivich, G. *et al.* The AP-1 transcription factor c-Jun is required for efficient axonal regeneration. *Neuron* (2004). doi:10.1016/j.neuron.2004.06.005

514. Schweizer, U. *et al.* Conditional gene ablation of Stat3 reveals differential signaling requirements for survival of motoneurons during development and after nerve injury in the adult. *J. Cell Biol.* (2002). doi:10.1083/jcb.200107009

515. Sun, K. L. W., Correia, J. P. & Kennedy, T. E. Netrins: Versatile extracellular cues with diverse functions. *Development* (2011). doi:10.1242/dev.044529

516. Ishii, N., Wadsworth, W. G., Stern, B. D., Culotti, J. G. & Hedgecock, E. M. UNC-6, a laminin-related protein, guides cell and pioneer axon migrations in C. elegans. *Neuron* (1992). doi:10.1016/0896-6273(92)90240-E

517. Dun, X. P. & Parkinson, D. B. Role of Netrin-1 signaling in nerve regeneration. *International Journal of Molecular Sciences* (2017). doi:10.3390/ijms18030491

518. Park, J. I. *et al.* Netrin inhibits regenerative axon growth of adult dorsal root ganglion neurons in vitro. *J. Korean Med. Sci.* (2007). doi:10.3346/jkms.2007.22.4.641

519. Webber, C. A. *et al.* Schwann cells direct peripheral nerve regeneration through the

Netrin-1 receptors, DCC and Unc5H2. *Glia* (2011). doi:10.1002/glia.21194

520. Madison, R. D., Zomorodi, A. & Robinson, G. A. Netrin-1 and peripheral nerve regeneration in the adult rat. *Exp. Neurol.* (2000). doi:10.1006/exnr.1999.7292

521. Lee, H. K. *et al.* Netrin-1 induces proliferation of Schwann cells through Unc5b receptor. *Biochem. Biophys. Res. Commun.* (2007). doi:10.1016/j.bbrc.2007.08.143

522. Jaminet, P. *et al.* Evaluating the role of Netrin-1 during the early phase of peripheral nerve regeneration using the mouse median nerve model. *Restor. Neurol. Neurosci.* (2013). doi:10.3233/RNN-120277

523. Brunet, I. *et al.* Netrin-1 controls sympathetic arterial innervation. *J. Clin. Invest.* (2014). doi:10.1172/JCI75181

524. Rishal, I. & Fainzilber, M. Axon-soma communication in neuronal injury. *Nature Reviews Neuroscience* (2014). doi:10.1038/nrn3609

525. Liu, K., Tedeschi, A., Park, K. K. & He, Z. Neuronal Intrinsic Mechanisms of Axon Regeneration. *Annu. Rev. Neurosci.* (2011). doi:10.1146/annurev-neuro-061010-113723

526. Siqueira, M. G. & Kline, D. G. Sir Sydney Sunderland and the Sunderland society. *J. Neurosurg.* (2018). doi:10.3171/2017.7.JNS171110

527. Cattin, A. L. *et al.* Macrophage-Induced Blood Vessels Guide Schwann Cell-Mediated Regeneration of Peripheral Nerves. *Cell* (2015). doi:10.1016/j.cell.2015.07.021

528. Gregory, C. D. & Devitt, A. The macrophage and the apoptotic cell: An innate immune interaction viewed simplistically? *Immunology* (2004). doi:10.1111/j.1365-2567.2004.01959.x

529. Green, D. R., Oguin, T. H. & Martinez, J. The clearance of dying cells: Table for two. *Cell Death and Differentiation* (2016). doi:10.1038/cdd.2015.172

530. Silva, M. T. Secondary necrosis: The natural outcome of the complete apoptotic program. *FEBS Letters* (2010). doi:10.1016/j.febslet.2010.10.046

531. Ravichandran, K. S. Find-me and eat-me signals in apoptotic cell clearance: Progress and conundrums. *Journal of Experimental Medicine* (2010). doi:10.1084/jem.20101157

532. Jaiswal, S. *et al.* CD47 Is Upregulated on Circulating Hematopoietic Stem Cells and Leukemia Cells to Avoid Phagocytosis. *Cell* (2009). doi:10.1016/j.cell.2009.05.046

533. Kauskot, A. *et al.* A novel mechanism of sustained platelet α IIbβ 3 activation via PEAR1. *Blood* (2012). doi:10.1182/blood-2011-11-392787

534. Sonmez, O. & Sonmez, M. Role of platelets in immune system and inflammation. *Porto Biomed. J.* (2017). doi:10.1016/j.pbj.2017.05.005

535. Duffau, P. *et al.* Platelet CD154 potentiates interferon-α secretion by plasmacytoid dendritic cells in systemic lupus erythematosus. *Sci. Transl. Med.* (2010). doi:10.1126/scitranslmed.3001001

536. Ramirez-Ortiz, Z. G. *et al.* The scavenger receptor SCARF1 mediates the clearance of apoptotic cells and prevents autoimmunity. *Nat. Immunol.* (2013). doi:10.1038/ni.2670

537. Fang, X. Y., Xu, W. D., Pan, H. F., Leng, R. X. & Ye, D. Q. Novel insights into Tim-4 function in autoimmune diseases. *Autoimmunity* (2015). doi:10.3109/08916934.2014.983266

538. Wium, M., Paccez, J. & Zerbini, L. The Dual Role of TAM Receptors in Autoimmune Diseases and Cancer: An Overview. *Cells* (2018). doi:10.3390/cells7100166

539. Wilhelm, A. J., Rhoads, J. P., Wade, N. S. & Major, A. S. Dysregulated CD4+ T cells from SLE-susceptible mice are sufficient to accelerate atherosclerosis in LDLr-/- mice. *Ann. Rheum. Dis.* **74**, 778–785 (2015).

540. Sullivan, C. The Mechanisms by which apoptotic neurons in the developing dorsal root ganglia are cleared. (Vanderbilt University, 2014).

541. Lu, R. *et al.* Dysregulation of innate and adaptive serum mediators precedes systemic lupus erythematosus classification and improves prognostic accuracy of autoantibodies.

J. Autoimmun. (2016). doi:10.1016/j.jaut.2016.06.001

542. Munroe, M. E. *et al.* Altered type II interferon precedes autoantibody accrual and elevated type i interferon activity prior to systemic lupus erythematosus classification. *Ann. Rheum. Dis.* (2016). doi:10.1136/annrheumdis-2015-208140

543. Cascalho, M. *et al.* A B220-, CD19- population of B cells in the peripheral blood of quasimonoclonal mice. *Int. Immunol.* (2000). doi:10.1093/intimm/12.1.29

544. Katikaneni, D. S. & Jin, L. B cell MHC class II signaling: A story of life and death. *Human Immunology* (2019). doi:10.1016/j.humimm.2018.04.013

545. Folzenlogen, D., Hofer, M. F., Leung, D. Y. M., Freed, J. H. & Newell, M. K. Analysis of CD80 and CD86 expression on peripheral blood B lymphocytes reveals increased expression of CD86 in lupus patients. *Clin. Immunol. Immunopathol.* (1997). doi:10.1006/clin.1997.4353

546. Suárez-Fueyo, A., Bradley, S. J. & Tsokos, G. C. T cells in Systemic Lupus Erythematosus. *Current Opinion in Immunology* (2016). doi:10.1016/j.coi.2016.09.001

547. Li, W., Deng, C., Yang, H. & Wang, G. The regulatory T cell in active systemic lupus erythematosus patients: A systemic review and meta-analysis. *Front. Immunol.* (2019). doi:10.3389/fimmu.2019.00159

548. Richard, M. L. & Gilkeson, G. Mouse models of lupus: What they tell us and what they don't. *Lupus Sci. Med.* **5**, (2018).

549. Yumura, W. *et al.* Dietary fat and immune function. II. Effects on immune complex nephritis in (NZB x NZW)F1mice. *J. Immunol.* (1985).

550. Morrow, W. J. W. *et al.* Dietary fat and immune function. I. Antibody responses, lymphocyte and accessory cell function in (NZB x NZW)F1mice. *J. Immunol.* (1985).

551. Morrow, W. J. W. *et al.* Dietary fat influences the expression of autoimmune disease in MRL/lpr/lpr mice. *Immunology* (1986).

552. Iin, B.-F., Huang, C.-C., Chiang, B.-L. & Jeng, S.-J. Dietary fat influences Ia antigen expression, cytokines and prostaglandin E 2 production of immune cells in autoimmune-prone NZB x NZW F1 mice . *Br. J. Nutr.* (1996). doi:10.1079/bjn19960175

553. Abdolmaleki, F. *et al.* The role of efferocytosis in autoimmune diseases. *Frontiers in Immunology* (2018). doi:10.3389/fimmu.2018.01645

554. Chung, W. S. *et al.* Astrocytes mediate synapse elimination through MEGF10 and MERTK pathways. *Nature* (2013). doi:10.1038/nature12776

555. Morel, L., Perry, D., Sang, A., Yin, Y. & Zheng, Y. Y. Murine models of systemic lupus erythematosus. *Journal of Biomedicine and Biotechnology* (2011). doi:10.1155/2011/271694

556. Li, J. *et al.* Meningothelial cells as part of the central nervous system host defence. *Biol. Cell* (2013). doi:10.1111/boc.201300013

557. Garfield, R. E., Chacko, S. & Blose, S. Phagocytosis by muscle cells. *Lab. Investig.* (1975).

558. Ichimura, T. *et al.* Kidney injury molecule-1 is a phosphatidylserine receptor that confers a phagocytic phenotype on epithelial cells. *J. Clin. Invest.* (2008). doi:10.1172/JCI34487

559. Davies, S. P., Reynolds, G. M. & Stamataki, Z. Clearance of apoptotic cells by tissue epithelia: A putative role for hepatocytes in liver efferocytosis. *Frontiers in Immunology* (2018). doi:10.3389/fimmu.2018.00044

560. Juncadella, I. J. *et al.* Apoptotic cell clearance by bronchial epithelial cells critically influences airway inflammation. *Nature* (2013). doi:10.1038/nature11714

561. Han, C. Z. *et al.* Macrophages redirect phagocytosis by non-professional phagocytes and influence inflammation. *Nature* **539**, 570–574 (2016).

562. Seeberg, J. C. *et al.* Non-professional phagocytosis: a general feature of normal tissue cells. *Sci. Rep.* **9**, 1–8 (2019).

563. Rodriguez-Manzanet, R. *et al.* T and B cell hyperactivity and autoimmunity associated with niche-specific defects in apoptotic body clearance in TIM-4-deficient mice. *Proc. Natl. Acad. Sci. U. S. A.* (2010). doi:10.1073/pnas.0910359107

564. Wong, K. *et al.* Phosphatidylserine receptor Tim-4 is essential for the maintenance of the homeostatic state of resident peritoneal macrophages. *Proc. Natl. Acad. Sci. U. S. A.* (2010). doi:10.1073/pnas.0910929107

565. Miyanishi, M., Segawa, K. & Nagata, S. Synergistic effect of TIM4 and MFG-E8 null mutations on the development of autoimmunity. *Int. Immunol.* (2012). doi:10.1093/intimm/dxs064

566. Duncan, J. L. *et al.* An RCS-like retinal dystrophy phenotype in Mer knockout mice. *Investig. Ophthalmol. Vis. Sci.* (2003). doi:10.1167/iovs.02-0438

567. Devitt, A. *et al.* Persistence of apoptotic cells without autoimmune disease or inflammation in CD 14-/- mice. *J. Cell Biol.* (2004). doi:10.1083/jcb.200410057

568. Chen, X. *et al.* Apoptotic engulfment pathway and schizophrenia. *PLoS One* (2009). doi:10.1371/journal.pone.0006875

569. Vandenbriele, C. *et al.* Dextran sulfate triggers platelet aggregation via direct activation of PEAR1. *Platelets* (2016). doi:10.3109/09537104.2015.1111321

570. Sun, Y. *et al.* A human platelet receptor protein microarray identifies the high affinity immunoglobulin e receptor subunit α (FcεR1α) as an activating platelet endothelium aggregation receptor 1 (PEAR1) ligand. *Mol. Cell. Proteomics* (2015). doi:10.1074/mcp.M114.046946

571. Hakimi, J. *et al.* The α subunit of the human IgE receptor (FcERI) is sufficient for high affinity IgE binding. *J. Biol. Chem.* (1990).

572. Maurer, M. *et al.* Immunoglobulin E-mediated autoimmunity. *Frontiers in Immunology* (2018). doi:10.3389/fimmu.2018.00689

573. Barth, N. D., Marwick, J. A., Vendrell, M., Rossi, A. G. & Dransfield, I. The 'Phagocytic synapse' and clearance of apoptotic cells. *Frontiers in Immunology* (2017). doi:10.3389/fimmu.2017.01708

574. Gabriel, C. L. *et al.* Autoimmune-mediated glucose intolerance in a mouse model of systemic lupus erythematosus. *Am. J. Physiol. - Endocrinol. Metab.* (2012). doi:10.1152/ajpendo.00665.2011

575. Covarrubias, R., Wilhelm, A. J. & Major, A. S. Specific deletion of LDL receptor-related protein on macrophages has skewed in Vivo effects on cytokine production by invariant natural killer T cells. *PLoS One* (2014). doi:10.1371/journal.pone.0102236

576. Wilhelm, A. J., Rhoads, J. P., Wade, N. S. & Major, A. S. Dysregulated CD4+ T cells from SLE-susceptible mice are sufficient to accelerate atherosclerosis in LDLr-/- mice. *Ann. Rheum. Dis.* (2015). doi:10.1136/annrheumdis-2013-203759

577. Amann, J. M. *et al.* Mtgr1 Is a Transcriptional Corepressor That Is Required for Maintenance of the Secretory Cell Lineage in the Small Intestine. *Mol. Cell. Biol.* (2005). doi:10.1128/mcb.25.21.9576-9585.2005

578. Lallemend, F. & Ernfors, P. Molecular interactions underlying the specification of sensory neurons. *Trends in Neurosciences* (2012). doi:10.1016/j.tins.2012.03.006

579. Kucenas, S. Perineurial glia. *Cold Spring Harb. Perspect. Biol.* (2015). doi:10.1101/cshperspect.a020511

580. Weerasuriya, A. & Mizisin, A. P. The Blood-Nerve Barrier: Structure and Functional Significance. in *The Blood-Brain and Other Neural Barriers* 149–173 (2010). doi:10.1007/978-1-60761-938-3_6

581. Clark, J. K. *et al.* Mammalian Nkx2.2+ perineurial glia are essential for motor nerve development. *Dev. Dyn.* (2014). doi:10.1002/dvdy.24158

582. Weis, J., May, R. & Schröder, J. M. Fine structural and immunohistochemical

identification of perineurial cells connecting proximal and distal stumps of transected peripheral nerves at early stages of regeneration in silicone tubes. *Acta Neuropathol.* (1994). doi:10.1007/BF00294509

583. Muona, P., Sollberg, S., Peltonen, J. & Uitto, J. Glucose transporters of rat peripheral nerve: Differential expression of GLUT1 gene by Schwann cells and perineurial cells in vivo and in vitro. *Diabetes* (1992). doi:10.2337/diab.41.12.1587

584. Pummi, K. P., Heape, A. M., Grénman, R. A., Peltonen, J. T. K. & Peltonen, S. A. Tight junction proteins ZO-1, occludin, and claudins in developing and adult human perineurium. *J. Histochem. Cytochem.* (2004). doi:10.1369/jhc.3A6217.2004

585. Weerasuriya, A. & Mizisin, A. P. The Blood-Nerve Barrier: Structure and Functional Significance. in (2010). doi:10.1007/978-1-60761-938-3_6

586. White, F. A., Keller-Peck, C. R., Michael Knudson, C., Korsmeyer, S. J. & Snider, W. D. Widespread elimination of naturally occurring neuronal death in Bax- deficient mice. *J. Neurosci.* (1998).

587. Etchegaray, J. I. *et al.* Defective Phagocytic Corpse Processing Results in Neurodegeneration and Can Be Rescued by TORC1 Activation. *J. Neurosci.* (2016). doi:10.1523/jneurosci.1912-15.2016

588. Marrone, M. C. *et al.* TRPV1 channels are critical brain inflammation detectors and neuropathic pain biomarkers in mice. *Nat. Commun.* (2017). doi:10.1038/ncomms15292

589. Voolstra, O. & Huber, A. Post-Translational Modifications of TRP Channels. *Cells* (2014). doi:10.3390/cells3020258

590. Dahlhamer, J. M. *et al.* Prevalence of chronic pain and high-impact chronic pain among adults — United States, 2016. *Morbidity and Mortality Weekly Report* (2018).

591. J.N., P., F., L., M., D. & P., G. Primary culture of trigeminal satellite glial cells: A cell-based platform to study morphology and function of peripheral glia. *Int. J. Physiol.*

Pathophysiol. Pharmacol. (2014).

592. Dubový, P., Jančálek, R., Klusáková, I., Svíženská, I. & Pejchalová, K. Intra- and extraneuronal changes of immunofluorescence staining for TNF- and TNFR1 in the dorsal root ganglia of rat peripheral neuropathic pain models. *Cell. Mol. Neurobiol.* (2006). doi:10.1007/s10571-006-9006-3

593. George, D., Ahrens, P. & Lambert, S. Satellite glial cells represent a population of developmentally arrested Schwann cells. *Glia* (2018). doi:10.1002/glia.23320

594. Ohara, P. T. *et al.* Gliopathic pain: when satellite glial cells go bad. (2009).

595. Hu, P., Bembrick, A. L., Keay, K. A. & McLachlan, E. M. Immune cell involvement in dorsal root ganglia and spinal cord after chronic constriction or transection of the rat sciatic nerve. *Brain. Behav. Immun.* (2007). doi:10.1016/j.bbi.2006.10.013

596. Kim, D., You, B., Lim, H. & Lee, S. J. Toll-like receptor 2 contributes to chemokine gene expression and macrophage infiltration in the dorsal root ganglia after peripheral nerve injury. *Mol. Pain* (2011). doi:10.1186/1744-8069-7-74

597. Moreau, N. *et al.* Early alterations of Hedgehog signaling pathway in vascular endothelial cells after peripheral nerve injury elicit blood-nerve barrier disruption, nerve inflammation, and neuropathic pain development. *Pain* (2016). doi:10.1097/j.pain.0000000000000444

598. Beazley-Long, N. *et al.* VEGFR2 promotes central endothelial activation and the spread of pain in inflammatory arthritis. *Brain. Behav. Immun.* (2018). doi:10.1016/j.bbi.2018.03.012

599. Kucenas, S. *et al.* CNS-derived glia ensheath peripheral nerves and mediate motor root development. *Nat. Neurosci.* (2008). doi:10.1038/nn2025

600. Rosenbaum, T. & Simon, S. TRPV1 Receptors and Signal Transduction. in *TRP Ion Channel Function in Sensory Transduction and Cellular Signaling Cascades* (eds. Liedtke, W. & Heller, S.) (2007). doi:10.1201/9781420005844.ch5

601. Guo, A., Vulchanova, L., Wang, J., Li, X. & Elde, R. Immunocytochemical localization of the vanilloid receptor 1 (VR1): relationship to neuropeptides, the P2X $_3$ purinoceptor and IB4 binding sites. *Eur. J. Neurosci.* (1999). doi:10.1046/j.1460-9568.1999.00503.x

602. Brandt, M. R., Beyer, C. E. & Stahl, S. M. TRPV1 antagonists and chronic pain: Beyond thermal perception. *Pharmaceuticals* (2012). doi:10.3390/ph5020114

603. Kevil, C. G. Endothelial cell activation in inflammation: Lessons from mutant mouse models. *Pathophysiology* (2003). doi:10.1016/S0928468002000834

604. Hunt, B. J. & Jurd, K. M. Endothelial cell activation. A central pathophysiological process. *BMJ* (1998).

605. Julius, D. & Basbaum, A. *Molecular mechanisms of nociception. Nature* (2001). doi:10.1038/35093019

606. Caterina, M. J. *et al.* The capsaicin receptor: A heat-activated ion channel in the pain pathway. *Nature* (1997). doi:10.1038/39807

607. Cummins, T. R., Sheets, P. L. & Waxman, S. G. The roles of sodium channels in nociception: Implications for mechanisms of pain. *Pain* (2007). doi:10.1016/j.pain.2007.07.026

608. Cummins, T. R., Howe, J. R. & Waxman, S. G. Slow closed-state inactivation: A novel mechanism underlying ramp currents in cells expressing the hNE/PN1 sodium channel. *J. Neurosci.* (1998). doi:10.1523/jneurosci.18-23-09607.1998

609. Herzog, R. I., Cummins, T. R., Ghassemi, F., Dib-Hajj, S. D. & Waxman, S. G. Distinct repriming and closed-state inactivation kinetics of Nav1.6 and Nav1.7 sodium channels in mouse spinal sensory neurons. *J. Physiol.* (2003). doi:10.1113/jphysiol.2003.047357

610. Rush, A. M., Cummins, T. R. & Waxman, S. G. Multiple sodium channels and their roles in electrogenesis within dorsal root ganglion neurons. *Journal of Physiology* (2007). doi:10.1113/jphysiol.2006.121483

611. Kurtz, A. *et al.* The expression pattern of a novel gene encoding brain-fatty acid binding protein correlates with neuronal and glial cell development. *Development* (1994).

612. McDavid, S., Bauer, M. B., Brindley, R. L., Jewell, M. L. & Currie, K. P. M. Butanol isomers exert distinct effects on voltage-gated calcium channel currents and thus catecholamine secretion in adrenal chromaffin cells. *PLoS One* (2014). doi:10.1371/journal.pone.0109203

613. Jewell, M. L., Breyer, R. M. & Currie, K. P. M. Regulation of calcium channels and exocytosis in mouse adrenal chromaffin cells by prostaglandin EP3 receptors. *Mol. Pharmacol.* (2011). doi:10.1124/mol.110.068569

614. Brindley, R. L., Bauer, M. B., Blakely, R. D. & Currie, K. P. M. An interplay between the serotonin transporter (SERT) and 5-HT receptors controls stimulus-secretion coupling in sympathoadrenal chromaffin cells. *Neuropharmacology* (2016). doi:10.1016/j.neuropharm.2016.08.015

615. Krames, E. S. The role of the dorsal root ganglion in the development of neuropathic pain. *Pain Med. (United States)* **15**, 1669–1685 (2014).

616. Liu, X., Chung, K. & Chung, J. M. Ectopic discharges and adrenergic sensitivity of sensory neurons after spinal nerve injury. *Brain Res.* (1999). doi:10.1016/S0006-8993(99)02165-4

617. Liu, C. N. *et al.* Tactile allodynia in the absence of C-fiber activation: Altered firing properties of DRG neurons following spinal nerve injury. *Pain* (2000). doi:10.1016/S0304-3959(00)00251-7

618. Sukhotinsky, I., Ben-Dor, E., Raber, P. & Devor, M. Key role of the dorsal root ganglion in neuropathic tactile hypersensibility. *Eur. J. Pain* (2004). doi:10.1016/S1090-3801(03)00086-7

619. Devor, M. Ectopic discharge in Aβ afferents as a source of neuropathic pain.

Experimental Brain Research (2009). doi:10.1007/s00221-009-1724-6

620. Leung, L. & Cahill, C. M. TNF-α and neuropathic pain - a review. *Journal of Neuroinflammation* (2010). doi:10.1186/1742-2094-7-27

621. Zhou, Y. Q. *et al.* Interleukin-6: An emerging regulator of pathological pain. *Journal of Neuroinflammation* (2016). doi:10.1186/s12974-016-0607-6

622. Ren, K. & Torres, R. Role of interleukin-1β during pain and inflammation. *Brain Research Reviews* (2009). doi:10.1016/j.brainresrev.2008.12.020

623. Kawabata, A. Prostaglandin E2 and pain - An update. *Biological and Pharmaceutical Bulletin* (2011). doi:10.1248/bpb.34.1170

624. Kobayashi, Y. *et al.* Macrophage-T cell interactions mediate neuropathic pain through the glucocorticoid-induced tumor necrosis factor ligand system. *J. Biol. Chem.* (2015). doi:10.1074/jbc.M115.636506

625. Brain, S. D. TRPV1 and TRPA1 channels in inflammatory pain: Elucidating mechanisms. *Ann. N. Y. Acad. Sci.* (2011). doi:10.1111/j.1749-6632.2011.06326.x

626. Caterina, M. J. *et al.* Impaired nociception and pain sensation in mice lacking the capsaicin receptor. *Science (80-.).* (2000). doi:10.1126/science.288.5464.306

627. Davis, J. B. *et al.* Vanilloid receptor-1 is essential for inflammatory thermal hyperalgesia. *Nature* (2000). doi:10.1038/35012076

628. Biggs, J. E. *et al.* Changes in vanilloid receptor 1 (TRPV1) expression following lingual nerve injury. *Eur. J. Pain* (2007). doi:10.1016/j.ejpain.2006.02.004

629. Hudson, L. J. *et al.* VR1 protein expression increases in undamaged DRG neurons after partial nerve injury. *Eur. J. Neurosci.* (2001). doi:10.1046/j.0953-816X.2001.01591.x

630. Kim, H. Y. *et al.* Differential Changes in TRPV1 Expression After Trigeminal Sensory Nerve Injury. *J. Pain* (2008). doi:10.1016/j.jpain.2007.11.013

631. Saijilafu *et al.* PI3K-GSK3 signalling regulates mammalian axon regeneration by inducing

the expression of Smad1. *Nat. Commun.* (2013). doi:10.1038/ncomms3690

632. Zou, H., Ho, C., Wong, K. & Tessier-Lavigne, M. Axotomy-induced smad1 activation promotes axonal growth in adult sensory neurons. *J. Neurosci.* (2009). doi:10.1523/JNEUROSCI.5397-08.2009

633. Xie, W., Strong, J. A. & Zhang, J. M. Active nerve regeneration with failed target reinnervation drives persistent neuropathic pain. *eNeuro* (2017). doi:10.1523/ENEURO.0008-17.2017

634. Costigan, M., Scholz, J. & Woolf, C. J. Neuropathic Pain: A Maladaptive Response of the Nervous System to Damage. *Annu. Rev. Neurosci.* (2009). doi:10.1146/annurev.neuro.051508.135531

635. Abe, N. & Cavalli, V. Nerve injury signaling. *Current Opinion in Neurobiology* (2008). doi:10.1016/j.conb.2008.06.005

636. Rotshenker, S. Wallerian degeneration: The innate-immune response to traumatic nerve injury. *Journal of Neuroinflammation* (2011). doi:10.1186/1742-2094-8-109

637. Lindborg, J. A., Mack, M. & Zigmond, R. E. Neutrophils are critical for myelin removal in a peripheral nerve injury model of wallerian degeneration. *J. Neurosci.* (2017). doi:10.1523/JNEUROSCI.2085-17.2017

638. Huang, J. K. *et al.* Neurscience: Glial membranes at the node of ranvier prevent neurite outgrowth. *Science (80-.).* (2005). doi:10.1126/science.1118313

639. Shen, Z. L. *et al.* Cellular activity of resident macrophages during Wallerian degeneration. *Microsurgery* (2000). doi:10.1002/1098-2752(2000)20:5<255::AID-MICR6>3.0.CO;2-A

640. Barrette, B. *et al.* Requirement of myeloid cells for axon regeneration. *J. Neurosci.* (2008). doi:10.1523/JNEUROSCI.1447-08.2008

641. Guan, Z., Hellman, J. & Schumacher, M. Contemporary views on inflammatory pain mechanisms: TRPing over innate and microglial pathways. *F1000Research* (2016).

doi:10.12688/f1000research.8710.1

642. Kidd, B. L. & Urban, L. A. Mechanisms of inflammatory pain. *Br. J. Anaesth.* (2001). doi:10.1093/bja/87.1.3

643. Cook, A. D., Christensen, A. D., Tewari, D., McMahon, S. B. & Hamilton, J. A. Immune Cytokines and Their Receptors in Inflammatory Pain. *Trends in Immunology* (2018). doi:10.1016/j.it.2017.12.003

644. England, S., Bevan, S. & Docherty, R. J. PGE2 modulates the tetrodotoxin-resistant sodium current in neonatal rat dorsal root ganglion neurones via the cyclic AMP-protein kinase A cascade. *J. Physiol.* (1996). doi:10.1113/jphysiol.1996.sp021604

645. Sullivan, L. C., Chavera, T. A., Gao, X., Pando, M. M. & Berg, K. A. Regulation of δ opioid receptor-mediated signaling and antinociception in peripheral sensory neurons by arachidonic acid-dependent 12/15-lipoxygenase metabolites. *J. Pharmacol. Exp. Ther.* (2017). doi:10.1124/jpet.117.241604

646. Schumacher, M. A. Transient receptor potential channels in pain and inflammation: Therapeutic opportunities. *Pain Practice* (2010). doi:10.1111/j.1533-2500.2010.00358.x

647. Fukuoka, T. *et al.* VR1, but not P2X3, increases in the spared L4 DRG in rats with L5 spinal nerve ligation. *Pain* (2002). doi:10.1016/S0304-3959(02)00067-2

648. Amaya, F. *et al.* Local inflammation increases vanilloid receptor 1 expression within distinct subgroups of DRG neurons. *Brain Res.* (2003). doi:10.1016/S0006-8993(02)03972-0

649. Amaya, F. *et al.* NGF and GDNF differentially regulate TRPV1 expression that contributes to development of inflammatory thermal hyperalgesia. *Eur. J. Neurosci.* (2004). doi:10.1111/j.1460-9568.2004.03701.x

650. Premkumar, L. S. & Ahern, G. P. Induction of vanilloid receptor channel activity by protein kinase C. *Nature* (2000). doi:10.1038/35050121

651. Djouhri, L., Koutsikou, S., Fang, X., McMullan, S. & Lawson, S. N. Spontaneous pain, both neuropathic and inflammatory, is related to frequency of spontaneous firing in intact C-fiber nociceptors. *J. Neurosci.* (2006). doi:10.1523/JNEUROSCI.3388-05.2006

652. North, R. Y., Lazaro, T. T. & Dougherty, P. M. Ectopic spontaneous afferent activity and neuropathic pain. in *Clinical Neurosurgery* (2018). doi:10.1093/neuros/nyy119

653. Berger, T. G., Shive, M. & Harper, G. M. Pruritus in the older patient: A clinical review. *JAMA - Journal of the American Medical Association* (2013). doi:10.1001/jama.2013.282023

654. Akiyama, T. *et al.* Mouse model of touch-evoked itch (alloknesis). *J. Invest. Dermatol.* (2012). doi:10.1038/jid.2012.52

655. Miyamoto, T., Nojima, H., Shinkado, T., Nakahashi, T. & Kuraishi, Y. Itch-associated response induced by experimental dry skin in mice. *Jpn. J. Pharmacol.* (2002). doi:10.1254/jjp.88.285

656. Lamotte, R. H., Dong, X. & Ringkamp, M. Sensory neurons and circuits mediating itch. *Nature Reviews Neuroscience* (2014). doi:10.1038/nrn3641

657. Ringkamp, M. *et al.* A role for nociceptive, myelinated nerve fibers in itch sensation. *J. Neurosci.* (2011). doi:10.1523/JNEUROSCI.3005-11.2011

658. Sawynok, J., Reid, A. & Meisner, J. Pain behaviors produced by capsaicin: Influence of inflammatory mediators and nerve injury. *J. Pain* (2006). doi:10.1016/j.jpain.2005.09.013

659. Sang, C. N., Gracely, R. H., Max, M. B. & Bennett, G. J. Capsaicin-evoked mechanical allodynia and hyperalgesia cross nerve territories: Evidence for a central mechanism. *Anesthesiology* (1996). doi:10.1097/00000542-199609000-00007

660. Gao, Y.-J. & Ji, R.-R. c-Fos or pERK, Which is a Better Marker for Neuronal Activation and Central Sensitization After Noxious Stimulation and Tissue Injury? *Open Pain J.* (2009). doi:10.2174/1876386300902010011

661. Obata, K. *et al.* Differential activation of extracellular signal-regulated protein kinase in primary afferent neurons regulates brain-derived neurotrophic factor expression after peripheral inflammation and nerve injury. *J. Neurosci.* (2003). doi:10.1523/jneurosci.23-10-04117.2003

662. Doya, H. *et al.* Extracellular signal-regulated kinase mitogen-activated protein kinase activation in the dorsal root ganglion (DRG) and spinal cord after DRG injury in rats. *Spine (Phila. Pa. 1976).* (2005). doi:10.1097/01.brs.0000182091.53834.08

663. Huebner, E. A. & Strittmatter, S. M. Axon regeneration in the peripheral and central nervous systems. *Results Probl. Cell Differ.* (2009). doi:10.1007/400_2009_19

664. Schmalbruch, H. Fiber composition of the rat sciatic nerve. *Anat. Rec.* (1986). doi:10.1002/ar.1092150111

665. Teichert, R. W. *et al.* Functional profiling of neurons through cellular neuropharmacology. *Proc. Natl. Acad. Sci. U. S. A.* (2012). doi:10.1073/pnas.1118833109

666. Santos-Nogueira, E., Redondo Castro, E., Mancuso, R. & Navarro, X. Randall-selitto test: A new approach for the detection of neuropathic pain after spinal cord injury. *J. Neurotrauma* (2012). doi:10.1089/neu.2010.1700

667. Brenner, D. S., Golden, J. P. & Gereau IV, R. W. A novel behavioral assay for measuring cold sensation in mice. *PLoS One* (2012). doi:10.1371/journal.pone.0039765

668. Lolignier, S. *et al.* The Nav1.9 Channel Is a Key Determinant of Cold Pain Sensation and Cold Allodynia. *Cell Rep.* (2015). doi:10.1016/j.celrep.2015.04.027

669. Wetzel, C. *et al.* A stomatin-domain protein essential for touch sensation in the mouse. *Nature* (2007). doi:10.1038/nature05394

670. Orefice, L. L. L. *et al.* Peripheral Mechanosensory Neuron Dysfunction Underlies Tactile and Behavioral Deficits in Mouse Models of ASDs. *Cell* **166**, 299–313 (2016).

671. LaMotte, R. H., Shimada, S. G. & Sikand, P. Mouse models of acute, chemical itch and

pain in humans. *Experimental Dermatology* (2011). doi:10.1111/j.1600-0625.2011.01367.x

672. Wall, P. D. & Dubner, R. Somatosensory Pathways. *Annu. Rev. Physiol.* (1972). doi:10.1146/annurev.ph.34.030172.001531

673. Drdla, R. & Sandkühler, J. Long-term potentiation in superficial spinal dorsal horn: A pain amplifier. in *Synaptic Plasticity in Pain* (2009). doi:10.1007/978-1-4419-0226-9_9

674. Latremoliere, A. & Woolf, C. J. Central Sensitization: A Generator of Pain Hypersensitivity by Central Neural Plasticity. *Journal of Pain* (2009). doi:10.1016/j.jpain.2009.06.012

675. Ren, K. & Dubner, R. Neuron-glia crosstalk gets serious: Role in pain hypersensitivity. *Current Opinion in Anaesthesiology* (2008). doi:10.1097/ACO.0b013e32830edbdf

676. Behbehani, M. M. Functional characteristics of the midbrain periaqueductal gray. *Progress in Neurobiology* (1995). doi:10.1016/0301-0082(95)00009-K

677. Lei, J., Sun, T., Lumb, B. M. & You, H. J. Roles of the periaqueductal gray in descending facilitatory and inhibitory controls of intramuscular hypertonic saline induced muscle nociception. *Exp. Neurol.* (2014). doi:10.1016/j.expneurol.2014.04.019

678. Thévenin, A., Ein-Dor, L., Ozery-Flato, M. & Shamir, R. Functional gene groups are concentrated within chromosomes, among chromosomes and in the nuclear space of the human genome. *Nucleic Acids Res.* (2014). doi:10.1093/nar/gku667

679. Ernsberger, U. Role of neurotrophin signalling in the differentiation of neurons from dorsal root ganglia and sympathetic ganglia. *Cell and Tissue Research* (2009). doi:10.1007/s00441-009-0784-z

680. Mitre, M., Mariga, A. & Chao, M. V. Neurotrophin signalling: Novel insights into mechanisms and pathophysiology. *Clinical Science* (2017). doi:10.1042/CS20160044

681. Mantyh, P. W., Koltzenburg, M., Mendell, L. M., Tive, L. & Shelton, D. L. Antagonism of nerve growth factor-TrkA signaling and the relief of pain. *Anesthesiology* (2011).

doi:10.1097/ALN.0b013e31821b1ac5

682. Bedse, G. *et al.* Functional Redundancy Between Canonical Endocannabinoid Signaling Systems in the Modulation of Anxiety. *Biol. Psychiatry* (2017). doi:10.1016/j.biopsych.2017.03.002

683. Inagaki, N. *et al.* Scratching behavior in various strains of mice. *Skin Pharmacol. Appl. Skin Physiol.* (2001). doi:10.1159/000056338

684. Kuraishi, Y., Nagasawa, T., Hayashi, K. & Satoh, M. Scratching behavior induced by pruritogenic but not algesiogenic agents in mice. *Eur. J. Pharmacol.* (1995). doi:10.1016/0014-2999(94)00780-B

685. Shimada, S. G., Shimada, K. A. & Collins, J. G. Scratching behavior in mice induced by the proteinase-activated receptor-2 agonist, SLIGRL-NH2. *Eur. J. Pharmacol.* (2006). doi:10.1016/j.ejphar.2005.11.012

686. Bauder, A. R. & Ferguson, T. A. Reproducible mouse sciatic nerve crush and subsequent assessment of regeneration by whole mount muscle analysis. *J. Vis. Exp.* (2012). doi:10.3791/3606

687. RANDALL, L. O. & SELITTO, J. J. A method for measurement of analgesic activity on inflamed tissue. *Arch. Int. Pharmacodyn. thérapie* (1957).

688. Yalcin, I., Charlet, A., Freund-Mercier, M. J., Barrot, M. & Poisbeau, P. Differentiating Thermal Allodynia and Hyperalgesia Using Dynamic Hot and Cold Plate in Rodents. *J. Pain* (2009). doi:10.1016/j.jpain.2009.01.325

689. Hatzipetros, T. *et al.* A quick phenotypic neurological scoring system for evaluating disease progression in the SOD1-G93A mouse model of ALS. *J. Vis. Exp.* (2015). doi:10.3791/53257

690. Yoon, C., Young Wook, Y., Heung Sik, N., Sun Ho, K. & Jin Mo, C. Behavioral signs of ongoing pain and cold allodynia in a rat model of neuropathic pain. *Pain* (1994).

doi:10.1016/0304-3959(94)90023-X

691. Austin, P. J., Wu, A. & Moalem-Taylor, G. Chronic constriction of the sciatic nerve and pain hypersensitivity testing in rats. *J. Vis. Exp.* (2012). doi:10.3791/3393

692. McCarson, K. E. Models of Inflammation: Carrageenan- or Complete Freund's Adjuvant (CFA)–Induced Edema and Hypersensitivity in the Rat. *Curr. Protoc. Pharmacol.* (2015). doi:10.1002/0471141755.ph0504s70

693. Kim, S. H. & Chung, J. M. An experimental model for peripheral neuropathy produced by segmental spinal nerve ligation in the rat. *Pain* (1992).

694. Kanai, Y., Nakazato, E., Fujiuchi, A., Hara, T. & Imai, A. Involvement of an increased spinal TRPV1 sensitization through its up-regulation in mechanical allodynia of CCI rats. *Neuropharmacology* (2005). doi:10.1016/j.neuropharm.2005.05.003

695. Wang, T. *et al.* Phenotypic switching of nonpeptidergic cutaneous sensory neurons following peripheral nerve injury. *PLoS One* (2011). doi:10.1371/journal.pone.0028908

696. Lechner, S. G., Frenzel, H., Wang, R. & Lewin, G. R. Developmental waves of mechanosensitivity acquisition in sensory neuron subtypes during embryonic development. *EMBO J.* (2009). doi:10.1038/emboj.2009.73

697. Viatchenko-Karpinski, V. & Gu, J. G. Mechanical sensitivity and electrophysiological properties of acutely dissociated dorsal root ganglion neurons of rats. *Neurosci. Lett.* (2016). doi:10.1016/j.neulet.2016.10.011

698. O'Brien, P. D., Sakowski, S. A. & Feldman, E. L. Mouse models of diabetic neuropathy. *ILAR J.* **54**, 259–272 (2014).

699. Zajaczkowską, R. *et al.* Mechanisms of chemotherapy-induced peripheral neuropathy. *International Journal of Molecular Sciences* (2019). doi:10.3390/ijms20061451

700. Willison, H. J., Jacobs, B. C. & van Doorn, P. A. Guillain-Barré syndrome. *The Lancet* (2016). doi:10.1016/S0140-6736(16)00339-1

701. Joseph, N. M. *et al.* Neural crest stem cells undergo multilineage differentiation in developing peripheral nerves to generate endoneurial fibroblasts in addition to Schwann cells. *Development* (2004). doi:10.1242/dev.01429

702. Hill, R. E. & Williams, P. E. Perineurial cell basement membrane thickening and myelinated nerve fibre loss in diabetic and nondiabetic peripheral nerve. *J. Neurol. Sci.* (2004). doi:10.1016/j.jns.2003.09.011

703. Johnson, P. C., Brendel, K. & Meezan, E. Human diabetic perineurial cell basement membrane thickening. *Lab. Investig.* (1981).

704. Binari, L. A., Lewis, G. M. & Kucenas, S. Perineurial glia require notch signaling during motor nerve development but not regeneration. *J. Neurosci.* (2013). doi:10.1523/JNEUROSCI.4893-12.2013

705. Kucenas, S., Wang, W. Der, Knapik, E. W. & Appel, B. A selective glial barrier at motor axon exit points prevents oligodendrocyte migration from the spinal cord. *J. Neurosci.* (2009). doi:10.1523/JNEUROSCI.4193-09.2009

706. Morris, A. D., Lewis, G. M. & Kucenas, S. Perineurial glial plasticity and the role of TGF-β in the development of the blood-nerve barrier. *J. Neurosci.* (2017). doi:10.1523/JNEUROSCI.2875-16.2017

707. Birchmeier, C. ErbB receptors and the development of the nervous system. *Experimental Cell Research* (2009). doi:10.1016/j.yexcr.2008.10.035

708. Parmantier, E. *et al.* Schwann cell-derived desert hedgehog controls the development of peripheral nerve sheaths. *Neuron* (1999). doi:10.1016/S0896-6273(01)80030-1

709. Kim, H. *et al.* Notch-regulated oligodendrocyte specification from radial glia in the spinal cord of zebrafish embryos. *Dev. Dyn.* (2008). doi:10.1002/dvdy.21620

710. Feng, Z. & Ko, C. P. Schwann cells promote synaptogenesis at the neuromuscular junction via transforming growth factor-β1. *J. Neurosci.* (2008).

doi:10.1523/JNEUROSCI.2589-08.2008

711. Scherer, S. S., Kamholz, J. & Jakowlew, S. B. Axons modulate the expression of transforming growth factor-betas in Schwann cells. *Glia* (1993). doi:10.1002/glia.440080407

712. Valle, M. & Zamorani, M. P. Nerve and Blood Vessels. in *Ultrasound of the Musculoskeletal System* (2007). doi:10.1007/978-3-540-28163-4_4

713. Sunderland, S. S. The anatomy and physiology of nerve injury. *Muscle Nerve* (1990). doi:10.1002/mus.880130903

714. Kumar, P. Retrograde Tracing. *Mater. Methods* (2019). doi:10.13070/mm.en.9.2713

715. Dyer, K. R. & Duncan, I. D. The intraneural distribution of myelinated fibres in the equine recurrent laryngeal nerve. *Brain* (1987). doi:10.1093/brain/110.6.1531

716. Ueyama, T. The topography of root fibres within the sciatic nerve trunk of the dog. *J. Anat.* (1978).

717. Stewart, J. D. Peripheral nerve fascicles: Anatomy and clinical relevance. *Muscle and Nerve* (2003). doi:10.1002/mus.10454

718. Bäumer, P., Weiler, M., Bendszus, M. & Pham, M. Somatotopic fascicular organization of the human sciatic nerve demonstrated by MR neurography. *Neurology* (2015). doi:10.1212/WNL.0000000000001526

719. Puigdellívol-Sánchez, A., Prats-Galino, A., Ruano-Gil, D. & Molander, C. Sciatic and femoral nerve sensory neurones occupy different regions of the L4 dorsal root ganglion in the adult rat. *Neurosci. Lett.* (1998). doi:10.1016/S0304-3940(98)00518-7

720. Bradley, J. L., Abernethy, D. A., King, R. H. M., Muddle, J. R. & Thomas, P. K. Neural architecture in transected rabbit sciatic nerve after prolonged nonreinnervation. *J. Anat.* (1998). doi:10.1017/S0021878298003550

721. Krames, E. S. The role of the dorsal root ganglion in the development of neuropathic

pain. *Pain Medicine (United States)* (2014). doi:10.1111/pme.12413

722. Gemes, G. *et al.* Failure of action potential propagation in sensory neurons: Mechanisms and loss of afferent filtering in C-type units after painful nerve injury. *J. Physiol.* (2013). doi:10.1113/jphysiol.2012.242750

723. Sundt, D., Gamper, N. & Jaffe, D. B. Spike propagation through the dorsal root ganglia in an unmyelinated sensory neuron: A modeling study. *J. Neurophysiol.* (2015). doi:10.1152/jn.00226.2015

724. Lei, Z. & Chiu, S. Y. Computer model for action potential propagation through branch point in myelinated nerves. *J. Neurophysiol.* (2001). doi:10.1152/jn.2001.85.1.197

725. Amir, R. & Devor, M. Electrical excitability of the soma of sensory neurons is required for spike invasion of the soma, but not for through-conduction. *Biophys. J.* (2003). doi:10.1016/S0006-3495(03)75024-3

726. Deer, T. R., Grigsby, E., Weiner, R. L., Wilcosky, B. & Kramer, J. M. A prospective study of dorsal root ganglion stimulation for the relief of chronic pain. *Neuromodulation* (2013). doi:10.1111/ner.12013

727. Van Buyten, J. P., Smet, I., Liem, L., Russo, M. & Huygen, F. Stimulation of Dorsal Root Ganglia for the Management of Complex Regional Pain Syndrome: A Prospective Case Series. *Pain Pract.* (2015). doi:10.1111/papr.12170

728. Liem, L. *et al.* A multicenter, prospective trial to assess the safety and performance of the spinal modulation dorsal root ganglion neurostimulator system in the treatment of chronic pain. *Neuromodulation* (2013). doi:10.1111/ner.12072

729. Liem, L. *et al.* One-year outcomes of spinal cord stimulation of the dorsal root ganglion in the treatment of chronic neuropathic pain. *Neuromodulation* (2015). doi:10.1111/ner.12228

730. Anand, P. & Bley, K. Topical capsaicin for pain management: Therapeutic potential and

mechanisms of action of the new high-concentration capsaicin 8 patch. *British Journal of Anaesthesia* (2011). doi:10.1093/bja/aer260

731. Fattori, V., Hohmann, M. S. N., Rossaneis, A. C., Pinho-Ribeiro, F. A. & Verri, W. A. Capsaicin: Current understanding of its mechanisms and therapy of pain and other pre-clinical and clinical uses. *Molecules* (2016). doi:10.3390/molecules21070844
732. Esposito, M. F., Malayil, R., Hanes, M. & Deer, T. Unique Characteristics of the Dorsal Root Ganglion as a Target for Neuromodulation. *Pain Med.* (2019). doi:10.1093/pm/pnz012
733. Chiu, I. M., Von Hehn, C. A. & Woolf, C. J. Neurogenic inflammation and the peripheral nervous system in host defense and immunopathology. *Nature Neuroscience* (2012). doi:10.1038/nn.3144
734. Sorkin, L. S., Eddinger, K. A., Woller, S. A. & Yaksh, T. L. Origins of antidromic activity in sensory afferent fibers and neurogenic inflammation. *Seminars in Immunopathology* (2018). doi:10.1007/s00281-017-0669-2
735. Kodama, D., Hirai, T., Kondo, H., Hamamura, K. & Togari, A. Bidirectional communication between sensory neurons and osteoblasts in an in vitro coculture system. *FEBS Letters* (2017). doi:10.1002/1873-3468.12561
736. Kozlova, E. N. & Jansson, L. In vitro interactions between insulin-producing β cells and embryonic dorsal root ganglia. *Pancreas* (2005). doi:10.1097/01.mpa.0000181489.35022.4a
737. Geppetti, P., Rossi, E., Chiarugi, A. & Benemei, S. Antidromic vasodilatation and the migraine mechanism. *Journal of Headache and Pain* (2012). doi:10.1007/s10194-011-0408-3
738. Pearce, J. M. S. Myofascial pain, fibromyalgia or fibrositis? *European Neurology* (2004). doi:10.1159/000079748

739. Kung, L. H. *et al.* Evidence for Glutamate as a Neuroglial Transmitter within Sensory Ganglia. *PLoS One* (2013). doi:10.1371/journal.pone.0068312

740. McRoberts, J. A. *et al.* Selective knockdown of NMDA receptors in primary afferent neurons decreases pain during phase 2 of the formalin test. *Neuroscience* (2011). doi:10.1016/j.neuroscience.2010.10.045

741. Yang, C. Q. *et al.* Vesicular glutamate transporter-3 contributes to visceral hyperalgesia induced by trichinella spiralis infection in rats. *Dig. Dis. Sci.* (2012). doi:10.1007/s10620-011-1970-x

742. Wall, P. D. & Devor, M. Sensory afferent impulses originate from dorsal root ganglia as well as from the periphery in normal and nerve injured rats. *Pain* (1983). doi:10.1016/0304-3959(83)90164-1

743. Gallagher, J. P., Higashi, H. & Nishi, S. Characterization and ionic basis of GABA-induced depolarizations recorded in vitro from cat primary afferent neurones. *J. Physiol.* (1978). doi:10.1113/jphysiol.1978.sp012189

744. Akaike, N., Inoue, M. & Krishtal, O. A. 'Concentration-clamp' study of gamma-aminobutyric-acid-induced chloride current kinetics in frog sensory neurones. *J. Physiol.* (1986). doi:10.1113/jphysiol.1986.sp016246

745. Du, X. *et al.* Local GABAergic signaling within sensory ganglia controls peripheral nociceptive transmission. *J. Clin. Invest.* (2017). doi:10.1172/JCI86812

746. Oaklander, A. L. & Siegel, S. M. Cutaneous innervation: Form and function. *Journal of the American Academy of Dermatology* (2005). doi:10.1016/j.jaad.2005.08.049

747. Paré, M., Elde, R., Mazurkiewicz, J. E., Smith, A. M. & Rice, F. L. The Meissner corpuscle revised: A multiafferented mechanoreceptor with nociceptor immunochemical properties. *J. Neurosci.* (2001). doi:10.1523/jneurosci.21-18-07236.2001

748. Abdo, H. *et al.* Specialized cutaneous schwann cells initiate pain sensation. *Science (80-.*

). (2019). doi:10.1126/science.aax6452

749. Woo, S. H. *et al.* Piezo2 is required for Merkel-cell mechanotransduction. *Nature* (2014). doi:10.1038/nature13251

750. Maksimovic, S. *et al.* Epidermal Merkel cells are mechanosensory cells that tune mammalian touch receptors. *Nature* (2014). doi:10.1038/nature13250

751. Ikeda, R. *et al.* Merkel cells transduce and encode tactile stimuli to drive aβ-Afferent impulses. *Cell* (2014). doi:10.1016/j.cell.2014.02.026

752. Woo, S. H., Lumpkin, E. A. & Patapoutian, A. Merkel cells and neurons keep in touch. *Trends Cell Biol.* **25**, 74–81 (2015).

753. Rice, F. L. *et al.* The evolution and multi-molecular properties of NF1 cutaneous neurofibromas originating from C-fiber sensory endings and terminal Schwann cells at normal sites of sensory terminations in the skin. *PLoS One* (2019). doi:10.1371/journal.pone.0216527

754. Moehring, F., Halder, P., Seal, R. P. & Stucky, C. L. Uncovering the Cells and Circuits of Touch in Normal and Pathological Settings. *Neuron* (2018). doi:10.1016/j.neuron.2018.10.019

755. Baumbauer, K. M. *et al.* Keratinocytes can modulate and directly initiate nociceptive responses. *Elife* (2015). doi:10.7554/eLife.09674

756. Talagas, M. *et al.* Intra-epidermal nerve endings progress within keratinocyte cytoplasmic tunnels in normal human skin. *Exp. Dermatol.* (2020). doi:10.1111/exd.14081

757. Baral, P., Udit, S. & Chiu, I. M. Pain and immunity: implications for host defence. *Nature Reviews Immunology* (2019). doi:10.1038/s41577-019-0147-2

758. Gwathmey, K. G. Plexus and peripheral nerve metastasis. in *Handbook of Clinical Neurology* (2018). doi:10.1016/B978-0-12-811161-1.00017-7

759. Emmerson, E. Efficient Healing Takes Some Nerve: Electrical Stimulation Enhances

Innervation in Cutaneous Human Wounds. *Journal of Investigative Dermatology* (2017). doi:10.1016/j.jid.2016.10.018